2019

Application of Agent-Based Modeling to Complex Systems

Robert J. Zupko II
Michigan Technological University, rzupko@mtu.edu

APPLICATION OF AGENT-BASED MODELING TO COMPLEX SYSTEMS

By

Robert J. Zupko II

A DISSERTATION

Submitted in partial fulfillment of the requirements for the degree of

DOCTOR OF PHILOSOPHY

In Computational Science and Engineering

MICHIGAN TECHNOLOGICAL UNIVERSITY

2019

This dissertation has been approved in partial fulfillment of the requirements for the Degree of DOCTOR OF PHILOSOPHY in Computational Science and Engineering.

Department of Social Sciences

Dissertation Advisor:	*Dr. Mark Rouleau*
Committee Member:	*Dr. Donald Lafreniere*
Committee Member:	*Dr. Audrey Mayer*
Committee Member:	*Dr. Daisuke Minakata*
Committee Member:	*Dr. Thomas Oommen*
Department Chair:	*Dr. Hugh Gorman*

Contents

List of Figures

List of Tables

Preface

This dissertation is a collection of four manuscripts that have been prepared for publication. They have been formatted to conform to a single style, but otherwise appear as published or as prepared for submission. Publication status is recorded as a footnote on the first page for each relevant chapter. Supplementary information is included as a chapter appendix when possible, otherwise it is described in Appendix B.

The first manuscript, Chapter 2 of this dissertation "ForestSim: Spatially Explicit Agent-Based Modeling of Non-Industrial Forest Owner Policies," appears in *SoftwareX*. The article concerns the development of an agent-based modeling tool to evaluate forest policies. I am the primary author of the article and developed the ForestSim agent- based modeling platform. Dr. Mark Rouleau assisted in the preparation and editing of the manuscript that appears in this dissertation.

I am the sole author of the second manuscript (Chapter 3), "Life Cycle Assessment of the Production of Gasoline and Diesel from Forest Residues Using Integrated Hydropyrolysis and Hydroconversion" The manuscript has been published by the *International Journal of Life Cycle Assessment*. The article describes a life cycle assessment of a proposed biorefinary in Ontonagon, Michigan.

Chapter 4 contains the third manuscript, "Integration of Agent-Based Modeling and Life Cycle Sustainability Assessment for the Comprehensive Assessment of Biofuels." This paper is in preparation for submission to *Journal of Cleaner Production*. I am the sole author of the manuscript, which argues for the broader integration of agent-based modeling and life cycle sustainability assessment, as well as containing a case study that builds upon Chapters 2 and 3.

The fourth manuscript (Chapter 5), "Development of an Agent-Based Model to Predict the Fate of Organic Contaminants Degradation in Aqueous-Phase Advanced

Oxidation Processes," is in preparation for submission to *Environmental Modeling & Software*. This article concerns the development and testing of an agent-based model to study advanced oxidation processes. I am the sole developer of the program described as well as all algorithms that are not otherwise attributed. Divya Kamath and Dr. Daisuke Minakata conducted all the laboratory experiments described, while I was responsible for the computational modeling. Dr. Minakata led the development of the acetone reaction pathways used in the model. The version of the manuscript that appears in this dissertation was prepared by myself. The chapter incorporates material submitted to the National Science Foundation and a chapter of Erica Coscarelli's Masters thesis [1], which was attributed to myself, Divya Kamath, Erica Coscarelli, Dr. Rouleau and Dr. Minakata. Some of the funding for this project came from the National Science Foundation grant CBET-1435926 and a student research grant from the Great Lakes Research Center.

Also included in this dissertation is "Forest Ownership Patterns in the Western Upper Peninsula of Michigan, USA," which appears as Appendix A. I am the sole author of the work which is based upon the data processing conducted in part for Chapters 3 and 4. I am also the sole author of the descriptive information about the Western Upper Peninsula region, contained therin, that may be of interest to other scholars. The material contained in Appendix A is intended for submission to *Landscape & Urban Planning* as a research note.

Acknowledgments

A book is rarely written in isolation and a dissertation is no exception. This work owes its existence to a long list of individuals, some of whom my failiable memory will forget. First, I would like to extend my gratitude to my advisor, Mark Rouleau, as well as all of those that have played a role in my doctoral committee: Timothy Havens, Donald Lafreniere, Audrey Mayer, Daisuke Minakata, and Thomas Oommen. Beyond the committee, I would also like to thank Melissa Baird, Hugh Gorman, Warren Perger, and Chelsea Shelley for helping to address some of the issues that have come up along the way. As an interdisciplinary dissertation, it is inevitable that consulting with others was a necessary part of the process and I would like to thank Brett Butler, Robert Handler, Matthew Kelly, David Shonnard, and Stas Zinchik for their assistance at various points in my research. I would also like to extend a special thanks to Christine Flood, Seán Gohman, Jennifer Rachels, and Amy Spahn for patiently listening to me navigate some of the tricker bits of the process.

Beyond the scope of research, the list of those that have provided moral support and encouragement over the years - decades - of my education pursues is long. To begin, I would like to thank my parents, grandparents, and extended family for their help and support over the years. Next, I would like to thank the following, whose names I attempt to remember in no particular order: Kaitlin Andersen, Apurva Baruah, Michael Bleddynn, Katie Bristo, Erin Burkett, Raven Cooper-Lee, Ann Dubs, Bailey Duxbury, Erin Eberhard, Dean Enjo, Alicia Gallagher, Eric Gieseke, Amanda Girard, Laura Grotjan, Kris Gurksnis, Jay Hennessey, Peter Henstock, Bryan Higgs, Gideon Hoekstra, Lauren Knop, Apostolos Koutropoulos, Bobby LeBrasseur, Amanda Lee, William Lytle, Kelley Mascharka, Heather McGee, James Mertens, Dwight Neves, Michael Noble, Martha Rozsi McRoy, Gary Nagel, Kai Orion, Nam Pho, Jason Plum,

Tess Peterson, Daniel Redding, Stephanie Austin Redding, Vladimir Riabov, Guilherme Aramizo Ribeiro, Marie Richards, McCall Sayen, Mihaela Sabin, Jacob Slattery, Gina Stevens, Pamela Tan, Hakan Uras, Sam Verbanac, Angela Walczyk, Allida Warn, and Sunflower Wilson. Plus to all of those whose names I forgot, and my cat who sat by my desk for most of this, thanks!

Finally, this dissertation was partly supported by National Science Foundation grant CBET-1435926, a student research grant from the Great Lakes Research Center, and a doctoral finishing fellowship from Michigan Technological University.

Abstract

This dissertation examines the application of agent-based modeling (ABM) to complex systems with the intent of developing a means of overcoming limitations present in existing tools. This is done though the development of two ABMs intended to address complex systems present in the fields of sustainability studies and chemistry.

After introductory information, Chapters 2 - 4 of this dissertation address the limitations of tools intended to project the environmental, economic, and social impacts of woody biomass based biofuels. Chapter 2 begins by discussing the limitations in tools to study timber harvest decision making and its impact upon the landscape, and develops an ABM platform to address this gap. Next, Chapter 3 presents a life cycle assessment (LCA) of a proposed biorefinery in Ontonagon, Michigan is conducted. This study acts as a benchmark benchmark for the case study presented in Chapter 4, where an argument for the integration of ABM and life cycle sustainability assessment (agent-based LCSA) is presented. The argument is followed by a case study demonstrating the applicability of the technique. The case study finds that while Ontonagon is a promising site for a biorefinery, there are concerns regarding the quantity of woody biomass that may be delivered as a feedstock and potential impacts upon regional wetlands.

Chapter 5 of this dissertation addresses the limitations of models of advanced oxidation processes (AOPs) using ordinary differential equations (ODEs). We argue that these limitations can be addressed by modeling the AOP as a complex system, including the complete elementary reaction pathway using ABM. To demonstrate the applicability of this novel approach, an ABM is developed and two in silico studies of acetone degradation induced by hydroxyl radicals are performed. We found that when using a comprehensive list of elementary reaction pathways, the ABM was able to replicate concentration curves for major chemical species in our laboratory

study. As a novel application of ABM to AOPs we conclude that the technique shows considerable promise.

Chapter 1

Introduction

1.1 Introduction

Complex systems are prevalent throughout all fields of scientific inquiry and are limiting factors in current models used for projecting future states in the systems. These limitations typically manifest as a result of the tools that are unable to properly model the system, which is necessary when studying current or future system level behavior (e.g., greenhouse gas emissions, or changes in chemical concentrations). One means of overcoming this limitation is through the application of agent-based modeling (ABM), a computational technique in which software "agents" represent heterogeneous actors in a system. By using ABM it is possible to allow a system to be studied as interactions of its constituent parts. This dissertation examines two complex systems in service of a broader question: "How can ABM be used to address the limitations in existing tools used to study complex systems?"

In addressing the first complex system, this dissertation asks: "How can the limitations of existing sustainability assessment tools be addressed when projecting the environmental, economic, and social impacts of woody biomass based biofuels?" Biofuels are a useful case study since they have the potential to act as one part of a renewable energy portfolio to sustainably address renewable energy goals [2]. At the

same time it remains unclear if a sufficient supply of woody biomass feedstocks for biofuel can be acquired [3], without excessive negative impacts (e.g., loss of ecosystem services, habitat loss, etc.) [4]. As sustainable biofuels are a result of complex interactions between humans and the environment, it is necessary to model future states of these interactions to determine if the biofuels are indeed sustainable.

For the second complex system considered, this dissertation asks: "How advanced oxidation processes (AOPs) can be modeled to address the limitations of existing techniques?" Developing better tools to study AOPs is critical, since improving the understanding of intermediate by-products in AOPs would have immediate applications in the design of water treatment processes [5]. The study of AOPs requires a means of projecting future states of the AOP treatment process so that the concentrations of intermediate by-products can be measured. As a result, addressing this question impacts the field of chemistry, but also relates to the long-term sustainability of the existing environment as a result of the use of AOPs in water treatment.

1.2 Background

1.2.1 Complex Systems and Agent-Based Modeling

In order to understand the limitations of tools used to study complex systems, it is necessary to review why complex systems are studied and what makes them difficult to model. Nature is fundamentally a collection of complex systems constructed by interactions between entities such as energies, atoms, and molecules. A definition of complex systems begins with complexity: studying elements of the system does not necessarily give rise to an understanding of how the system will behave over time [6]. As succinctly stated by Thurner et al. [7, p. 22], "complex systems are co-evolving multilayer networks." Complexity may be described quantitatively via the amount information needed to describe the current state of the system [8], but it may also be possible to describe the fundamental behavior of the system using a very short list

of rules. This is beautifully illustrated by Conway's Game of Life [9]: a system that can be described using four rules and an initial pattern of cells, but whose long-term behavior may be that of a universal Turing machine [10]. Finally, an important class of complex systems is complex adaptive systems, in which members of the system exhibit the ability to learn and adapt over time in response to stimuli [11]. These are of particular note to sustainability science, since individuals and societies may alter their behavior over time in response to prior events.

Complex systems are characterized by a number of key features, namely: nonlinearity, feedback loops, and emergence [6, 8, 12–14]. These features can be broken down as follows. First, *nonlinearity* means that the behavior of the system is not proportional to the inputs and, although unlikely, small changes may result in impacts up to and including collapse of the system as a whole (i.e., the classic Butterfly Effect). Second, *feedback loops* reinforce behaviors of the system, meaning that components such as variables may be amplified (positive feedback) or dampened (negative feedback) in response to the inputs. Finally, *emergence* may be defined as "stable macroscopic patterns arising from [local interactions]" [15, p. 35]. Defining emergence in this manner is important since it offers insight into how these emergent patterns can be studied, namely by examining the local interactions that occur. With these definitions in mind, complex systems become more apparent. The relationships between predators and prey are one of the classic examples since both populations are interdependent, but reductions in land may reduce the total population for both [16].

The complexity associated with complex systems, and complex adaptive systems, makes modeling them difficult and it is only through computing that we are able to simulate them directly [7]. While equations have been used to describe complex systems, these are simplifications that prevent a complete understanding of the system [17]. For example, equation-based models are incapable of explaining emergent properties of a system, such a flocking patterns [18]. Agent-based modeling addresses these limitations by simulating complex systems through the description of agents'

interactions with the environment and amongst themselves [15, 19]. This allows study of the emergent behavior since it will manifest at the system level when agent interactions are correctly described [15, 20]. This is of particular relevance when attempting to project possible outcomes for a system when the results are not known (e.g., market response to a new product), but individual decision making can be described beforehand.

The ability of ABM to study complex systems has been demonstrated by prior scholarship, typically focused on studying interactions between humans and the environment, or social patterns that result from social interactions. One of the seminal arguments for the use of ABM in the study of social patterns was written by [6] who draw linkages between ABM, complexity theory, and organization science. A similar argument for social simulation was written by [21], who noted that the behaviors of societies are emergent, necessitating the use of ABM. Expanding beyond social interactions, [22] discuss human-environment interactions as a complex adaptive system and argue for the application of ABM, before demonstrating its application in studying how panda habitat degradation. In a later work, [23] reviews the application of ABM in the context of coupled human and natural systems (CHANS), noting a connection to complexity theory and how various ABMs capture elements of a complex system. A similar connection to complex systems is made by [24] who note that consideration of spatio-temporal relationships in forest management can be evaluated using complex systems theory, necessitating the use of ABM to study the relationships. This is similar to an earlier argument made by [25] in a review of simulations for ecosystem management. Another application of ABM is land-use/land-cover change (LUCC), where [26] note the linkages to complex systems and use ABM to study the roles that households have in driving LUCC. Finally, in a later work, [27] argue that ABM has an advantage in studying LUCC over pattern-mimicking models since land transfers that may impact decision making can be incorporated, echoing connections to nonlinearity in feedback loops in complex systems. Underscoring all of

the aforementioned works is the argument that ABM is the appropriate technique to be applied to a complex system; although as noted by [28], ABM may face technical barriers in its application (e.g., processing of data generated).

1.2.2 Modeling Complex Systems for Sustainability Science

Agent-based modeling is of particular relevance to the field of sustainability science since human-environmental regimes are fundamentally complex systems. As noted by [29], two of the characteristics of sustainable regimes are resilience and desirability to human societies, which can be described as properties, or products, of complex systems. Resilience is defined as "the degree to which the system can adjust to disturbances without shifting to a new regime" [29, p. 278], and is a product of the nonlinearity and feedback loops associated with a complex system. Likewise, the desirability of the regime refers to how desirable the system is to humans (e.g., local access to forests, or overall pleasing atmospheric temperatures). Since this desirability is based upon the collective attitudes of the occupants of the system (i.e., humans), it is an inherently emergent property of the regime. Thus, while human-environmental regimes are complex systems, a common shortcoming of existing sustainability assessment tools is that they typically work with snapshot and aggregate data [30–32]. Recalling that an important aspect of complex systems are emergent behaviors that manifest over time, the problem with snapshots and aggregate data is that may fail to appropriately account for changes over time or localized impacts [33]. This is of particular concern when attempting to discover "tipping points" in which a system may accelerate into an unrecoverable state [34] or, into a new human-environmental regime that is habitable, but not as desirable (e.g., warmer global temperatures). These limitations are incorporated into one of the core questions of sustainability science by [35] who stated,

> How can the dynamic interactions between nature and society - including lags and inertia - be better incorporated into emerging models and

> conceptualizations that integrate the Earth system, human development, and sustainability? [35, p. 641]

One means of addressing the limitations of snapshot and aggregate data is through the incorporation of ABM to project possible system states, or to generate data for assessment tools. This is the approach taken by scholars looking to incorporate ABM and LCA [36, 37]. Life cycle assessment (LCA) is a tool for holistically assessing the environmental impacts of a product's entire life cycle, and it can be expanded out into life cycle sustainability assessment (LCSA) by incorporating social and economic indicators [30]. An early example of this is Davis et al. [38] who combined ABM with LCA to evaluate how actors respond to changing circumstances when confronted with different sources of energy. The authors offered a proof-of-principle demonstration of a Dutch energy marketplace, with agents adjusting their choice of energy production based upon source global warming potential. Similarly, [39] developed a proof-of-concept ABM that fed land-use data into an LCA of switchgrass biofuel feedstocks. A more recent example was given by [40], who used an ABM to develop the life cycle inventory of an LCSA. Their synthetic proof-of-concept example of the technique focused on green building development, but failed to make use of spatial data generated by the model. While these and other studies (see [41–43]) demonstrate that scholarly interest is developing to combine ABM and LCA or LCSA, there still is considerable work to be done.

1.2.3 Modeling Complex Systems for Chemistry

While chemistry is described as "the science of equilibria" [7, p. 9], this approach becomes problematic when attempting to gain a greater insight into reactions and reflects a history of abstracting inherently complex systems away [44]. This is especially relevant with AOPs, a chemical treatment processes in which organic contaminants are removed through the use of hydroxyl radicals [45, 46]. The ability of AOPs to eliminate contaminants makes them highly attractive for water treatment,

but the complexity of the reactions elude laboratory understanding and intermediate by-products can be more toxic than parent contaminates [47]. These challenges are further compounded by the hundreds of thousands of chemicals in commercial use. Therefore, modeling is an attractive means of studying AOPs, and mechanistic models have been developed (see [48–50]). These approaches have been limited in that they can be time-intensive to solve and produce unstable numerical solutions (i.e., concentration profiles) that are highly sensitive to initial conditions. These issues are a byproduct of the complex system manifest in the chemistry of the AOPs. ABM may address these limitations since it offers the ability to completely describe AOP reaction pathways at the molecular (i.e., individual) level and allows for concentration profiles to be produced as an emergent product of the system. Despite the benefits associated with studying AOPs in this fashion, ABM has remained relatively unexplored in the study of AOPs and in the broader field of chemistry, with some limited work done in biochemistry to explore the applications of ABM in the context of intracellular reactions (see [51–53]).

1.3 Structure of Dissertation

Chapters 2 through 4 address the research question,"How can the limitations of existing sustainability assessment tools be addressed when evaluating the environmental, economic, and social impacts of woody biomass based biofuels?" This question is ultimately answered in Chapter 4 with the development and application of agent-based LCSA. However, doing so required an appropriate platform upon which to develop the ABM, and a means of validating the results of the case study.These tasks are acomplished in Chapters 2 and 3, respectively. Furthermore, while the research question concerns woody biomass based biofuels, a specific case study involving the proposed development of an integrated hydropyrolysis and hydroconversion (IH^2) biorefinery in Ontonagon, Michigan was used to frame the question.

In Chapter 2 the need for an appropriate platform is addressed through the development of ForestSim, a spatially-explicit ABM platform intended for bioenergy sustainability assessment and forest management policy analysis. This chapter also briefly argues that existing ABM tools (e.g., MASON [54] and NetLogo [55]) are limited and a tailored ABM platform is more appropriate for practitioners since it reduces the programming necessary for model development.

Chapter 3 conducts a life cycle assessment (LCA) to validate the results of the agent-based LCSA against, and asks the question: "What are the potential environmental impacts and energy return on investment (EROI) of IH^2 fuels manufactured in Ontonagon, Michigan?" This work is necessary since a common question and critique of ABM is if the results are an accurate representation of real-world processes (see [56, 57]). The LCA described in the chapter is conducted using inventory data derived from a geographic information systems analysis of the region surrounding Ontonagon as well as previously published studies of relevant industries. The study also makes extensive use of a prior survey of logging and transportation operations in the Upper Peninsula region of Michigan along with adjacent counties in Wisconsin to inform the life cycle inventory [58, 59]. The results of the LCA suggest that fuels would have a favorable environmental impact and EROI, but there were concerns that the site selected may have insufficient feedstocks.

Chapter 4 develops an agent-based LCSA as a solution to the limitations in evaluating the environmental, economic, and social impacts of woody biomass-based biofuels. The chapter begins with the argument that the integration of ABM and LCSA is necessary, citing the known issues in assessment due to complex systems, as well as the scholarly discourse calling for improvements in tools. A methodological approach to agent-based LCSA is then presented using the theoretical underpinnings from ISO 14040 [60]. Finally, the chapter returns to the proposed IH^2 biorefinery in Ontonagon as a case study implementation of the technique. The case study found that environmental impacts were in line with the LCA, supporting the results, but sufficient

feedstocks are a continued concern. As a methodological approach to the integration of ABM and LCSA, this chapter contributes to the broader research agenda through the advancement of the discourse and development of the technique.

Chapter 5 completes the collection of manuscripts and addresses the research question, "How can AOPs be modeled that addresses the limitations of existing techniques?" Existing mathematical approaches are limited by the complex chemistry involved, which is attributable to the underlying complex system. By developing an ABM approach to studying AOPs, the chapter argues that a more comprehensive - if not complete - model of the chemistry can be constructed. The chapter explores the key components of an ABM that was developed to study AOPs highlighting the molecular simulation and algorithms necessary to support the simulation. Validation of the model is then explored along with results from a case study of UV/H_2O_2 treatment of acetone.

Chapter 2

ForestSim: Spatially Explicit Agent-Based Modeling of Non-Industrial Forest Owner Policies

Robert Zupko and Mark Rouleau[1]

[1] The material contained in this chapter has been adapted for publication in *SoftwareX*

Abstract

Bioenergy from woody biomass is an important part of a sustainable energy portfolio. However, sustainable portfolios are complicated when non-industrial private forest (NIPF) owners own much of the biomass in a given region. Success and sustainability of bioenergy often depends on policies to encourage biomass harvesting without negatively impacting socio-environmental relations. We present ForestSim, an extension to MASON for bioenergy policy analysis using agent-based simulation to assess the sustainability of alternative forest management policies. Spatially-explicit models of NIPF agents embedded within forested landscapes and respond to forest management policies. The modifiable computational framework allows policy makers to conduct "thought experiments" to assess the feasibility of alternative forest management policies at little to no cost prior to implementation. ForestSim enables policy-makers and policy researchers to design and conduct highly tailored computational experiments to produce results that non-technical audiences, such as the general public and fellow policy-makers/researchers, can easily interpret and understand.

Keywords: Agent-Based Modeling - Policy Modeling - Forest Modeling - Environmental Impacts - Land-Use Change

2.1 Introduction and Background

THE sustainable production of bioenergy from woody biomass requires forest management policies that can anticipate complex social, environmental, and economic impacts [61]. This is particularly true in regions with forests divided among

many non-industrial private forest (NIPF) owners because their highly decentralized land-use decision-making has major consequences for the sustainability of bioenergy. Various policies and incentives exist to encourage sustainable forest management practices on NIPF owner lands [62, 63]. Policy instruments that attempt to encourage biomass harvesting are critical to bioenergy sustainability because they influence not only the availability and reliability of biomass feedstocks, but also regional land-use and land-cover change patterns. This is why such instruments must be carefully crafted to avoid unintended conflicts with the environment and other social values while ensuring economically feasible bioenergy production. This paper describes ForestSim, an extension to MASON [54] that enables researchers and policy makers to simulate and assess the broad sustainability impacts of alternative forest management policies for NIPF owner biomass harvesting.

At its core, ForestSim is a spatially-explicit agent-based model (ABM) platform designed for NIPF owner policy experimentation. ForestSim simulates the decentralized biomass harvesting activities of thousands of individual NIPF agents, embedded within real landscapes, and the forest growth dynamics that result from NIPF owner land use change. ForestSim uses Geographic Information Systems (GIS) based parcel boundary and land cover maps to define a regional forest landscape. It then uses information obtained from NIPF owner harvesting literature and regional forest management surveys to design the agent decision making schema for the individual agents occupying actual forested properties. Within this ABM environment, ForestSim allows users to design and experiment with alternative forest management policies to assess and compare the sustainability impacts of NIPF agents reacting to alternative harvesting incentives (or disincentives) and the socio-natural feedback that occurs over the course of a simulation. The end product is a sustainability assessment scorecard used to compare the long-run effectiveness of competing forest management policies across the social, environmental, and economic sectors of a given region.

ForestSim was developed in response to the lack of a platform for bioenergy policy experimentation. Specifically, ForestSim integrates tools and techniques from three primary areas: biomass estimation, forest growth modeling, and ABM simulation for land use change. ForestSim development begins with biomass estimation, a critical starting point for any bioenergy development project, because it determines the feasibility of maintaining a bioenergy industry in a given region (i.e., the region either possesses sufficient biomass or not). ForestSim applies forest growth modeling to ensure that agents are able to respond to a realistic environment with forest growth and regrowth patterns impacting their decision making. Finally, by building ForestSim as an extension to MASON we are able to leverage it as a robust platform for ABM already in use for land use, land-use change (LULUC) models.

ForestSim's design goals were to:

- Provide a flexible and modifiable platform for policy analysis, specifically in the areas of: forest management, bioenergy development, and conservation;
- Provide a basic forest growth model with the means for it to be replaced with other researcher specified, or region specific models;
- Provide a flexible and modifiable means of modeling forest owner (i.e., agent) land use decision making;
- Provide a flexible and modifiable means of capturing time-series and geographic model data for the purposes of sustainability assessment; and
- Provide an extension that does not diminish the computationally efficient operation of MASON.

Unlike MASON [54] and NetLogo [55], ForestSim is a simplified modeling environment that provides a preconstructed model that can be adjusted to address specific research questions. This prebuilt environment eliminates much of the time needed to develop a MASON model, reducing the time spent on software development and allowing more time for productive research activities. However, a limited degree of programming is

needed for specific details such as agent (e.g., a NIPF owner) decision making and forest growth models. Additionally, to ensure that models are geographically relevant, appropriate GIS data need to be provided to the model. An example of how ForestSim is modified appears later in this paper. ForestSim is a unique contribution to the forest modeling community because it helps streamline the process for developing policy simulations.

Next, we will discuss how ForestSim relates to other tools and techniques that apply for forest policy modeling. That is followed by an overview of the software architecture and a proof-of-concept model.

2.2 Relation to Existing Tools and Techniques

Biomass availability is commonly estimated in the literature using multi-criteria GIS analyses [64, 65], which has largely superseded aerial photography analysis of the past [66]. Multi-criteria GIS analysis evaluates forest cover conditions with respect to access to transportation networks and other quality indicators (i.e., species type, slope, soil quality, etc.) int order to estimate a volume of economically harvestable biomass [67–69], or useable wood fuel [70], in a given region. This approach typically assumes that all non-protected forested land (i.e. any forest that is not withdrawn from harvesting for conservation purposes) is "available" for harvest. The problem with this approach is that it produces over-inflated biomass estimates for regions with high numbers of NIPF owners because, although all estimated biomass is "available" in theory, the actual amount of "available" biomass depends on the varied willingness-to-harvest of diverse NIPF owners [71]. To overcome this problem, ForestSim uses information on the willingness to harvest of NIPF owners within the region to adjust its biomass estimates in accordance with social reality.

ForestSim also integrates forest growth models. Forest growth modeling is necessary for ForestSim to project biomass estimates into the future, capturing the change

over time that occurs when forests respond to NIPF owner harvesting and vice-versa. Two methods of forest growth modeling exist in the literature today: individual tree and whole-stand modeling [72, 73]. ForestSim adopts the whole-stand modeling approach because the overarching policy analysis goal is to assess the regional sustainability impacts of bioenergy development (e.g., aggregate biomass volumes, habitat disconnectivity, acres of open-access land, etc.) not the impacts of harvesting on individual forest parcels. It is important to note that existing tools, such as the US Forest Service's Forest Vegetation Simulator (FVS), are already available to conduct some similar analysis tasks [e.g. 74–77]. However, none of these existing tools have the ability to incorporate heterogeneous harvest decision-making or adaptive management (e.g. agents changing harvest behaviors in response to social, environmental, or economic stimuli). This is because most forest growth models rely on systems dynamic modeling [78], which makes it impossible to model individual-level NIPF owner dynamics. ForestSim, on the other hand, uses the ABM simulation environment to conduct its analysis, which eliminates the need to assume forest growth takes place under a homogeneous regional forest management regime. ForestSim is also agnostic about its underlying forest growth model, making it possible for researchers and policymakers to "plug-and-play" with any forest growth model of interest while conducting policy experiments.

Finally, ForestSim leverages the ABM aspects of MASON as a simulation for land-use change. ABM simulation is becoming an increasingly popular method for investigating the complex interactions of humans and the natural environment [e.g. 24, 79–82]. Unlike traditional analytical methods, ABM simulation makes it possible to model the interactions of spatially-explicit, heterogeneous, and adaptive individuals [17]. This is critical for modeling land-use change because most large-scale land-use patterns emerge from the localized decisions of highly diverse actors [27, 83, 84]. This is also important for sustainability assessment because it permits a more realistic representation of sustainability than the simplistic balance-sheet approach of

traditional techniques like Life Cycle Analysis [i.e. 39]. Sustainability in an ABM is the emergent product of localized interactions across space, time, and various sectors of society and nature [23, 85] rather than a simple tally of individual sustainability indicators.

These are the reasons why the ABM approach is becoming increasingly attractive in bioenergy research [86, 87]. However, up to this point, most bioenergy ABMs have focused solely on modeling the land-use impacts of bioenergy development (also most have focused entirely on bioenergy crops as opposed to woody biomass) while overlooking broader sustainability concerns, such as value conflicts that cross environmental, social, and economic boundaries [88]. ForestSim advances this existing work by providing researchers and policymakers a modifiable platform for policy experimentation that can assess broad bioenergy sustainability concerns.

2.3 ForestSim Architecture and Execution

2.3.1 Overview

ForestSim was written in Java using - and as an extension to - the open-source multi-agent simulation library MASON [54] and its GIS library extension GeoMASON [89]. MASON provides basic simulation functionality for ForestSim, such as a graphical user interface to control the simulation and modify experimental parameters, charting features to track key simulation outcomes, a GIS shapefile display to depict land-use change, and a scheduler to coordinate agent activation.

Architecturally, the two major software classes are the simulation agents and the agent environment. The primary agents in ForestSim represent spatially embedded private forest owners (NIPF agents). Each agent is assigned a forested parcel (a GIS polygon) with a specified forest cover using digitized property and land cover maps. The agent environment then consists of a set of forest stands (a GIS raster grid built upon National Land Cover Data from the USGS) assigned to each forested

parcel that indicates current forest growth. Throughout the course of the simulation, forest stands grow in accordance with natural tree growth dynamics and regrow in response to harvesting. During each simulation round, NIPF agents can manipulate (i.e. harvest) all or some of the individual forest stands that lie within the property boundaries of their assigned parcel. Harvest decisions are made based upon one of two NIPF owner decision-making schemas prominent in the literature: economic optimizers (i.e., timber harvesters) or multi-objective owners (MOOs) [see 90, 91]. Economic optimizing agents seek to increase the market value of their forest with the goal of maximizing harvest profits, while MOO agents attempt to balance economic gains against potential losses to alternative ecosystem services due to harvesting. Finally, three global agents are included in the simulation to provide support services that represent various aspects of a regional forest products or bioenergy supply chain: logging agents to harvest parcels, trucking agents to transport raw materials to processing facilities, and refinery agents to purchase and process raw materials into bioenergy. These major classes are all outlined in greater detail in the next section.

2.3.2 ForestSim Architecture

As mentioned above and shown in Figure 2.1, the two major classes of ForestSim are the abstract `ParcelAgent` class and the concrete `Environment` class. The `ParcelAgent` class is an abstract class that provides users with a basic template for designing NIPF agents. This template includes the general attributes that all NIPF agents share in common (e.g. property size, neighbors, owner type, etc.) and a standard framework for agent decision-making with abstract methods for voluntary incentive programs (VIP) enrollment and harvesting. When an NIPF agent is activated, the simulation scheduler invokes the agent's `step` method which first calls the `doPolicyOperation` method (see Listing 2.1) to determine whether or not to enroll in a VIP designed to encourage biomass harvesting. The general `doPolicyOperation`

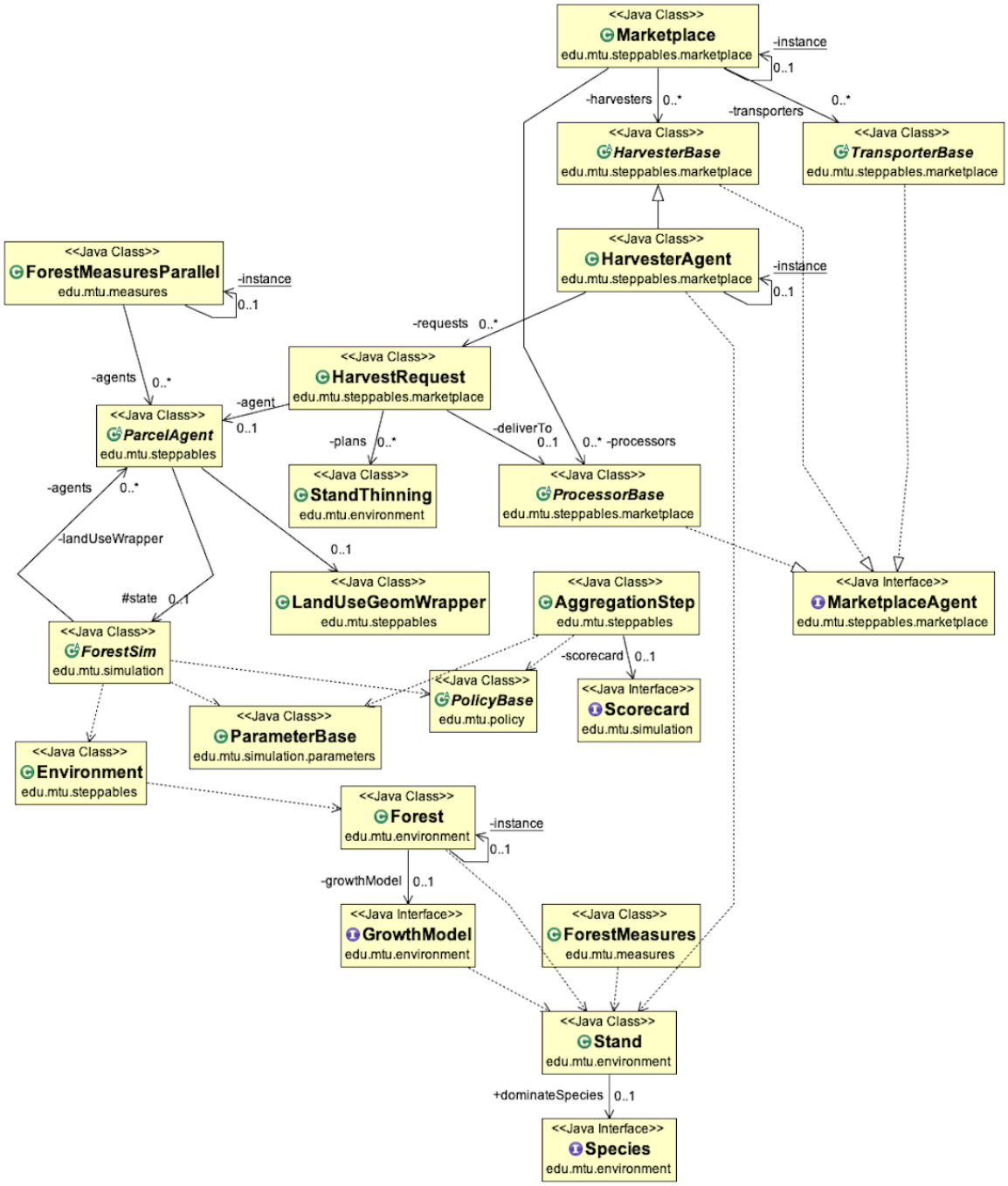

Figure 2.1: Basic overview of ForestSim architecture

method provided in the `ParcelAgent` class first checks to see if a VIP is active, then determines if the agent meets the participation requirements (e.g., minimum acreage, minimum stocking levels, minimum land tenure, etc.). If so, then enrolls the agent's

Listing 2.1: An example of a doPolicyOperation function for a parcel agent

```
function doPolicyOperation()
1. Is a policy active?
  1.1. No, return
2. Do I qualify for the policy?
  2.1. Do I do I have enough acres?
    2.1.1. No, return
  2.2. Is my current stocking high enough?
    2.2.1. No, return
  2.3. Have I owned the land long enough?
    2.3.1. No, return
3. Should I enroll in the policy?
  3.1. Does the policy conflict with my values?
    3.1.1. Yes, return
  3.2. Does this policy make economic sense to me?
    3.2.1. No, return
4. Enroll in the policy
```

Listing 2.2: An example of a doHarvestOperation function for a parcel agent

```
function doHarvestOperation()
1. Do I have enough harvestable stands?
  1.1. No, return
2. Am I enrolled in a VIP?
  2.1. Am I completed to harvest?
    2.1.1. Yes, request the harvest
    2.1.2. Investigate harvest consequences
    2.1.3. Return
3. Request a bid from a logging company
4. Does the bid meet my financial goals?
  4.1 No, return
5. Request the harvest
6. Investigate harvest consequences
```

property in the VIP so long as biomass harvesting is both economically viable and does not conflict with the agent's ownership values. Once the `doPolicyOperation` method is complete, the agent's step method then calls the `doHarvestOperation` method to determine whether or not to harvest (this occurs regardless of the agent's status in a VIP). The general `doHarvestOperation` method (see Listing 2.2) first

checks to see if there are any stands on the agent's property with sufficient stocking levels to be harvested and, if so, the agent harvests if required by a VIP (the financial consequences of this decision also impact future VIP enrollments) or harvests if expected timber profits exceed costs. It should be noted that this general framework is intended to serve as a template only. Users are encouraged to design child `ParcelAgent` classes with more specific behaviors for VIP enrollment and harvesting tailored to various ownership types active in their study region (we provide a demonstration of this agent customization feature in our case study below).

When an NIPF agent decides to harvest, ForestSim uses a number of global support agents to coordinate various aspects of the biomass supply chain beyond the forest owner. The NIPF agent simply registers a request to harvest a specified number of stands with a `Harvester` agent whose role is similar to that of a logging company. By default, the `Harvester` agent uses a first-in-first-out priority queue to process harvest requests and stores the results for later use. The `Harvester` agent is only able to execute a limited (user-specified) number of harvests in a given round (all harvests unexecuted are shifted to the next simulation round). Once again, users are free to modify the `Harvester` decision-making schema to accommodate more complex harvest scheduling algorithms based upon their own needs. ForestSim also provides users with modifiable class interfaces to model more complex scenarios beyond the harvest stage, if needed. These include a transporter agent that plays the role of a trucking company moving the harvest to market, and a processor agent that plays the role of the final consumer who purchases biomass to generate bioenergy.

After all NIPF and support agents have been activated in a given round, the MASON scheduler then calls the `Environment` class. This class updates the status of individual forest stands throughout the region. The `Environment` class is linked to the `Forest` class, which contains an array of `Stand` objects. Each `Stand` represents a patch of forest cover that is tied to a single pixel in a raster-based GIS land-cover map (the dimensions of each `Stand` depend on the GIS data provided by the user).

The `Forest` class uses its `GrowthModel` interface to determine how much each "undisturbed" stand will grow in a given round. By default, ForestSim provides a generic model (i.e., `GenericGrowthModel` class) of even-aged whole stands with incremental annual growth [72]. Users are free to implement any growth model that suits their local forest conditions or to make use of the default generic forest growth model of ForestSim. The `GenericGrowthModel` uses Perlin noise [92] to generate initial growth levels that resemble natural forests (see `calculateInitialStands`), and then `growStand` to apply annual periodic growth to the forest.

2.3.3 Model Inputs

ForestSim requires users to provide four inputs in order to run a simulation. First, users must provide spatial information to define their geographic location of interest. ForestSim requires polygon-based GIS parcel maps to define property boundaries for the NIPF agents and raster-based GIS land cover type data (e.g., USGS National Land Cover Data) to determine where forest growth is possible within the region as well as current forest growth at specified locations. Second, users must specify an appropriate tree growth model to be used in the `GrowthModel` interface to simulate stand growth during a model run. ForestSim does not provide a "generic" growth model due to the variation that exists between regional environments. This approach ensures that the underlying growth model is the best representation possible of the environment and goals of the end-user. Third, users must decide how many links in the biomass supply chain they would like to simulate. The default setting is to simulate only up to the point of harvest but not beyond. Finally, users can also extend the `ParcelAgent` abstract class if necessary to tailor the `doPolicyOperation` and `doHarvestOperation` methods to better represent the local decision-making rules of different NIPF owner types in their study region.

2.3.4 Model Execution

Two major processes make up the overall ForestSim operation flow. The first is the model initialization process, which is shown in Figure 2.2. The process:

1. Geographic information system land cover and parcel information is loaded from the paths indicated in the model configuration.
2. The abstract `initialize` method is invoked to allow for any additional GIS data to be loaded into the model.
3. The environment is initialized by calculating the initial forest stands through the `GrowthModel` interface via the `calculateInitialStands` method.

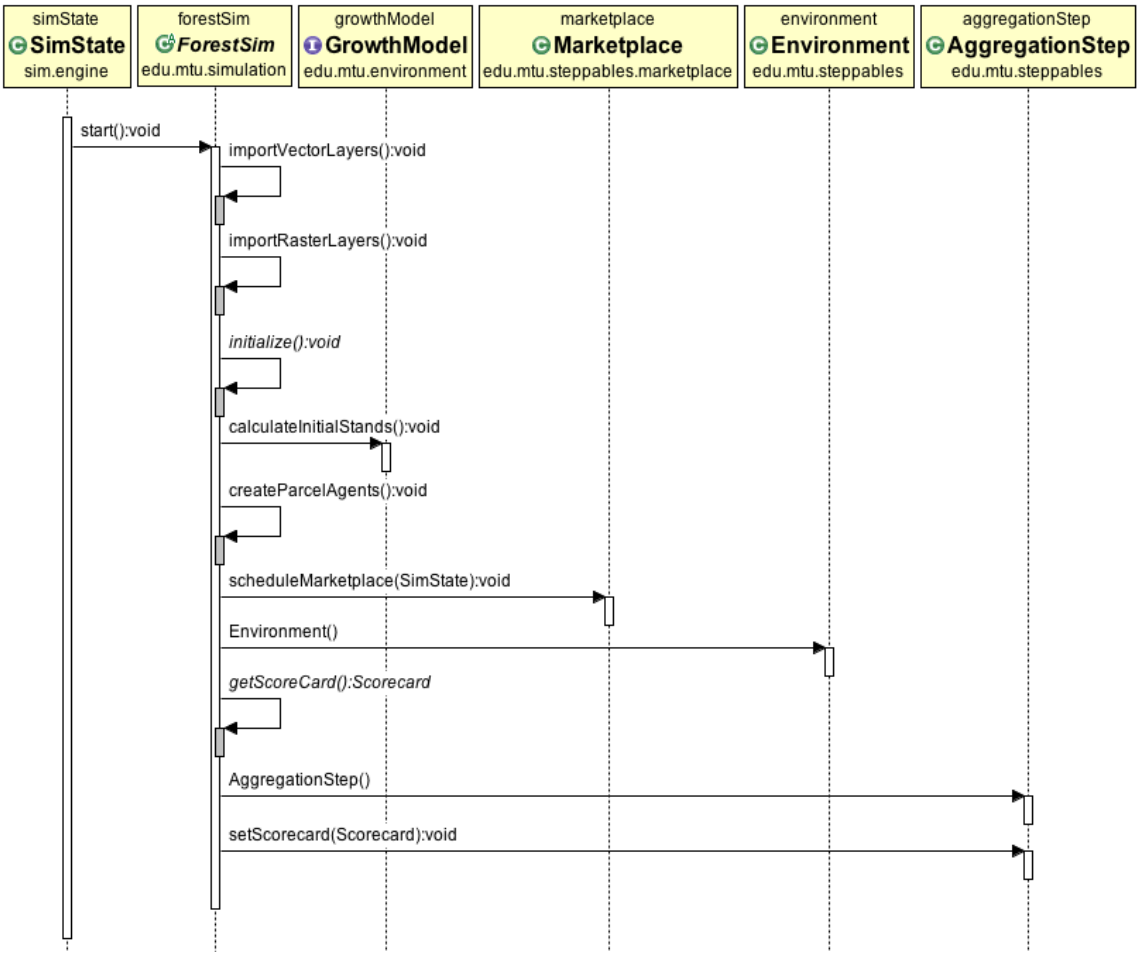

Figure 2.2: Sequence diagram of model initialization

4. NIPF agents are sequentially initialized in proportions supplied by the user and randomly assigned a parcel in the landscape and assigned to a parcel with the probabilities being determined by model configuration.
5. The marketplace is initialized and agents added to the schedule as needed.
    5.1. The order of the agents in the marketplace is randomized before scheduling with a Fisher-Yates shuffle [93].
6. The environment agent is added to the schedule.
7. If a `Scorecard` can be generated, it is added to the schedule via the `AggregationStep` agent.

The initialization process is followed by the main simulation loop. This may take the form of either an aggregate simulation (Figure 2.3) or a marketplace simulation (Figure 2.4). An aggregate simulation proceeds as follows:

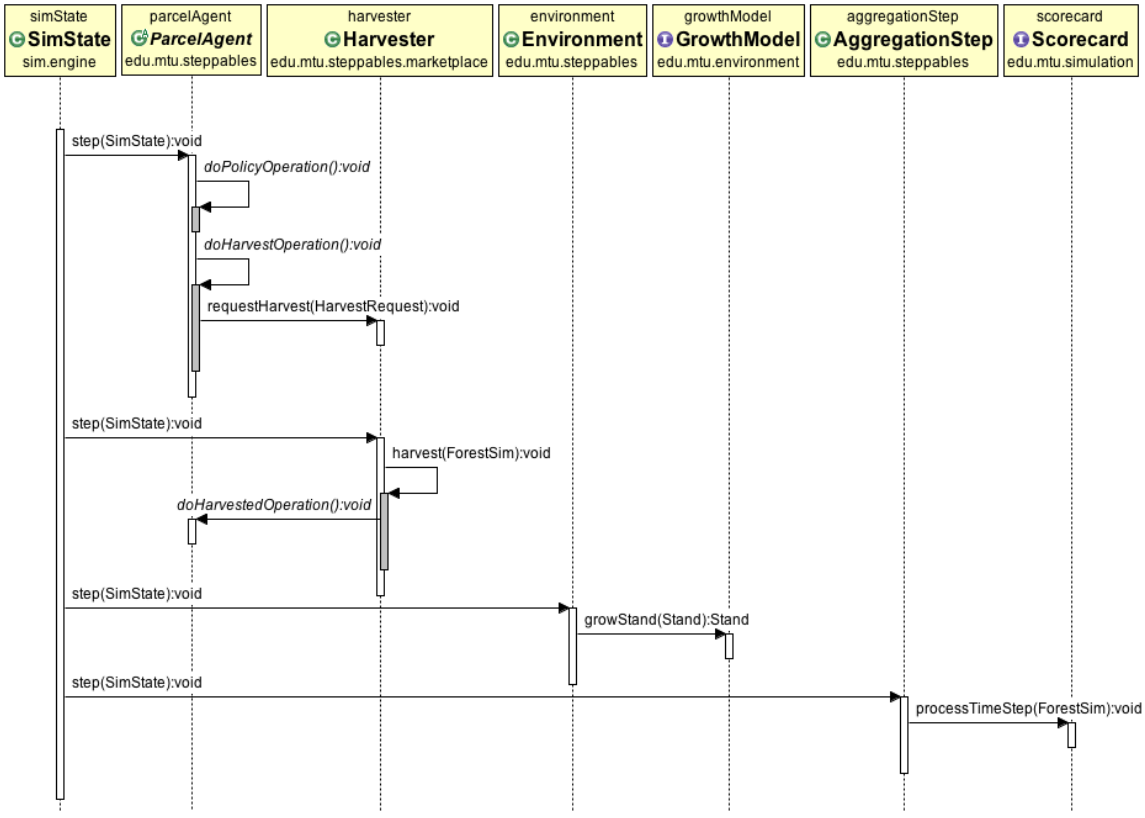

Figure 2.3: Aggregate Simulation Loop

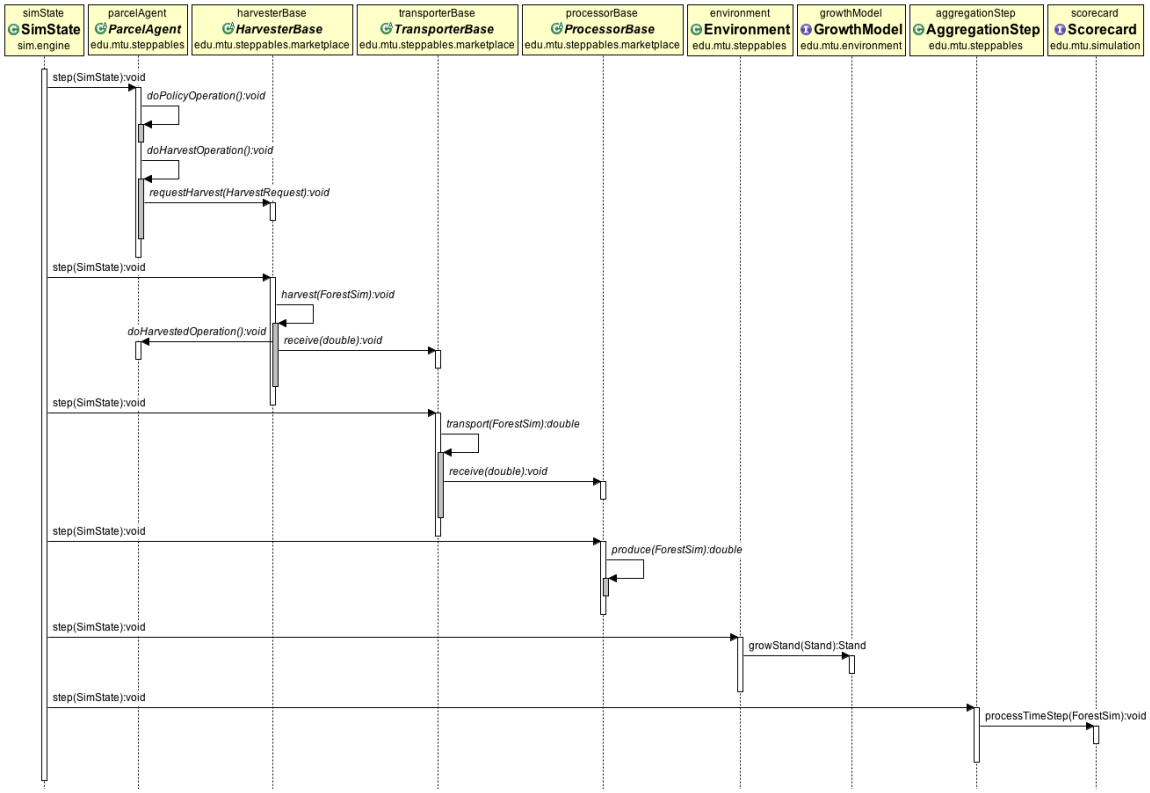

Figure 2.4: Marketplace Simulation Loop

1. `ParcelAgent` objects are sequentially activated by MASON. Agents that elect to harvest their parcel pass the request to the `Harvester` agent.
2. The `Harvester` agent is then invoked, which then processes the requests for harvests, up to the user imposed limit. For parcels the agent is able to harvest, woody biomass is removed, the forest stand attributes are updated to reflect the harvest, and woody biomass is reported.
3. When the parcel is harvested, the NIPF agent is informed that it took place.
4. The `Environment` agent is invoked, which ensures that the forest stands are updated to reflect the growth that occurred in the simulation timestep.
5. The object that implements the `Scorecard` interface is invoked to allow the simulation to collect any data that is needed to prepare a sustainability scorecard.

A marketplace simulation is similar, but differs in that before the `Environment` agent is invoked, the agents that are part of the market place are first invoked in the following order shown in Figure 2.4.

2.3.5 Model Outputs

ForestSim uses a scorecard concept to drive analytical outputs during a simulation. At the end of each time step, ForestSim first calls the `Scorecard` and then checks to see if the model has run to completion. The `Scorecard` provides end-users with a way of collecting information from the model's state (e.g., woody biomass harvested, carbon sequestration, etc.) with the intent of developing a sustainability assessment (or policy assessment) scorecard tailored to the management interests of the user. After the `Scorecard` has been called, ForestSim either proceeds to the next time step or terminates the model.

2.4 Model Demonstration

2.4.1 Motivation

The current section uses a proof-of-concept case study to demonstrate how ForestSim can be used for policy experimentation. In this example, we explore the sustainability impacts of using VIPs to encourage biomass harvesting [see 94, 95]. The policy analysis goal is to determine the different impacts that alternative VIP incentive mechanisms have on the three classic pillars of sustainability: the economic, the environmental, and the social (more on these below).

We chose this example to demonstrate ForestSim's capabilities for two reasons. First, the decentralized nature of VIP regulation warrants a methodological tool that can adequately model the interactions of heterogeneous and adaptive actors. This is

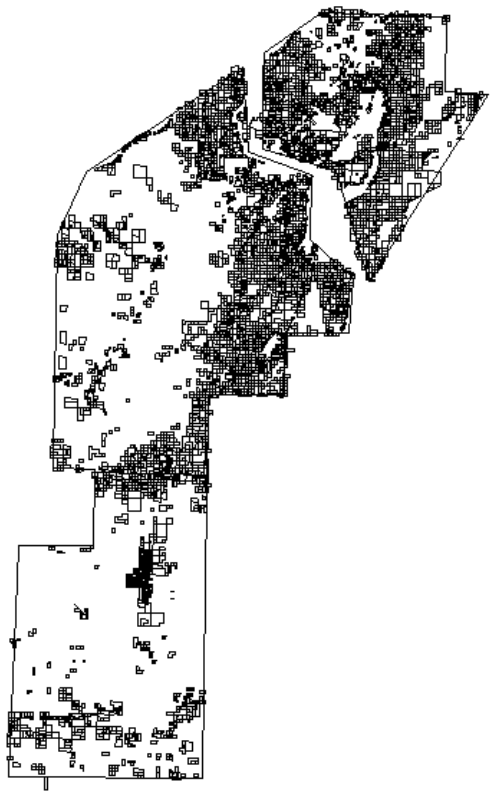

Figure 2.5: Map of Houghton County and NIPF owner parcels

due to individual forest owners voluntarily agreeing to adhere to certain forest management practices in exchange for a financial or other rewards. Second, this example allows us to illustrate why the bottom-up ABM approach to modeling emergent phenomenon is significantly better at analyzing sustainability impacts than alternative policy analysis methods.

One of the fundamental problems with establishing a bioenergy system is ensuring a sufficient and reliable supply of biomass. Additionally, many forested regions throughout the world divide forest ownership among a multitude of individual private forest owners, further complicating matters. This means that biomass supply greatly depends upon the highly decentralized decision making of heterogeneous and adaptive actors. In situations such as these, policymakers often use VIPs to encourage actors

to adopt their preferred management practice, and to achieve coordinated regional outcomes [96]. In our proof-of-concept example, we compare the sustainability impacts of no-VIP incentivization to two alternative VIP incentivization mechanisms: individual-based rewards or an agglomeration bonus. Traditional VIPs often reward landowners individually for their own program participation, yet current research suggests that adding an agglomeration bonus to reward landowners for the participation of their neighbors can increase enrollment rates and produce even better management outcomes at the regional level [97]. Our case study explores this issue through a proof-of-concept demonstration of ForestSim that shows how alternative incentive mechanisms impact regional sustainability indicators beyond the simple metric of program enrollment rates and the specific indicators targeted by the VIP itself.

For demonstration purposes, we chose to conduct our policy experiments in the context of Houghton County, in the Upper Peninsula of Michigan (USA). It is approximately 80% forested, with a mix of hardwood species that are generally fully stocked, with low annual removal rates [98]. Houghton County also faces one of the highest utility rates in the country, making it a prime candidate for bioenergy conversion. Forest ownership in the region is nearly evenly distributed among industrial (35%), public (30%), and private (33%) (or, NIPF) owners [99]. This makes Houghton County a good test case for the effectiveness of VIPs designed to encourage biomass harvesting.

This case study tracks the following sustainability indicators with relevance to stakeholders in the Houghton County region, and to illustrate how different dimensions of sustainability can be assessed. These indicators are:

- Economic: The primary economic sustainability concern in this example centers on biomass supply. We consider our bioenergy system economically sustainable so long as a steady and reliable supply of biomass is available to fuel a hypothetical 10 megawatt (MW) power plant. We assume a feedstock 613,000 bone

dry tons of woody biomass is required annually based upon prior case studies [100–102].

- Social: Whitetail deer hunting is an extremely popular recreation activity in Houghton County that relies heavily on use of the region's forests [90]. Access to public and private lands for hunting is critical to the sustainability of this activity. That is why VIPs in the region often require program participants to provide open access to their land to the general public, which is replicated in our model. Therefore, we assume our bioenergy system is more sustainable the greater the amount of open access land that is available.
- Environmental: Finally, biomass harvesting can cause obvious harm to the environment if done irresponsibly. Forests provide a number of ecosystem services that are critical to environmental regulatory functions, such as carbon sequestration. Therefore, the final sustainability indicator that we track is the carbon sequestration capability of the region's forests as it changes over time due to harvesting and new growth. We consider our bioenergy system to be sustainable so long as there is no major net loss of carbon sequestration levels across the region.

2.4.2 Preparation

As stated above, ForestSim requires two GIS-based user inputs to begin policy experimentation: parcel boundaries and land cover data. For our demonstration, we use a a digitized parcel boundary map obtained from the Houghton County Tax Equalization department for the year 2012. We also used the latest National Land Cover Database GIS raster file from the year 2011 [103] to depict current forest cover. Finally, we overlaid our parcel boundary map on top of our NLCD land cover map to identify privately owned forested properties of greater than 10 acres in size. We then filtered out all other properties for the purposes of this demonstration because these other

parcels would be ineligible for the biomass VIP of interest in our case study. Characteristic species were selected for the region based upon U.S. Forest Service data [98] and assigned based on NLCD codes (i.e., Red Maple (*Acre rubrum*) for deciduous forests and woody wetlands, Eastern White Pine (*Pinus strobus*) for evergreen forests.

Since this is a proof-of-concept model, we elected to implement a minimalist schema, shown in Table 2.1, and to only track the biomass that is harvested. We designed our economic optimizer agents to be perfectly rational with respect to harvest profits (i.e., *homo economicus*). For the model 30% of the parcels are allocated to these economic optimizers. The remaining 70% of the parcels are allocated to MOOs, who are designed to be economically naive in that they often pass up profitable harvest opportunities under the assumption that they prefer to manage for some other non-financial goal at these times. In both cases, the agent is provided with a parcel of land that has at least ten acres of forest. Economic agents prefer to harvest a minimum of 40 acres, unless enrolled in a VIP upon which they will harvest smaller parcels. Harvester agents were limited to harvesting 2500 parcels per year, effectively ensuring it did not represent a barrier to NIPF owner activity.

Table 2.1
Decision Making Schema of Non-Industrial Private Forest Owner Agents

Economic Optimizer Agent	Multi-Objective Owner Agent
Always harvest when minimal harvest conditions are met and profitable	May harvest when minimal harvest conditions are met and profitable
Harvest when the highest net present value can be achieved	Harvest when the bid exceeds the minimum they are willing to accept
Join voluntary incentive program when economically advantageous	May join voluntary incentive program if economically advantageous and they are willing to harvest
Entire parcel is harvested	

When agents in the model wish to harvest, they request a stumpage bid. This stumpage bid is based upon the expected quantity of harvested woody biomass and the value of the given species present in the parcel. The stumpage value for Red Maple (*Acre rubrum*) was set at the rate of $479.75 which is based upon the 2016 stumpage rate by volume for Baraga Forest Management Unit which contains Houghton County [104]. Likewise, the stumpage value for White Pine (*Pinus strobus*) was set at the rate of $100 which is based upon the stumpage rate by volume for Gwinn Forest Management Unit which is located in the Central Upper Peninsula region. Economic agents project the growth of the forest in their parcel and schedule a harvest for the timestep with the highest net present value. In contrast, MOOs will solicit a bid and harvest if the bid exceeds the minimum they are willing to accept. The minimum is set when the agent is created and is randomly drawn from a normal distribution with a mean of $523.23 and a standard deviation of $123.12 [71].

The VIPs in the model are intentionally simple. Both VIPs incentivize harvesting through a tax incentive (i.e., a millage bonus). However, the agglomeration bonus offers a higher incentive if any of the neighboring properties are also enrolled. Both VIPs require that the NIPF owner harvest their property before they can withdraw from the VIP. This approximates a tax clawback or property lien intended to prevent free-riders [94].

2.4.3 Execution and Results

For our proof-of-concept model we allowed the model to run for two hundred years. The VIP was introduced at the sixty year mark to allow for model burn-in and initial NIPF owner harvesting to take place. The model was repeated a total of two hundred times for each of the three policies prior to analysis.

Figure 2.6 shows the mean harvested biomass in metric tons (MT) dry weight under each of the three policy scenarios. The above-ground biomass is calculated

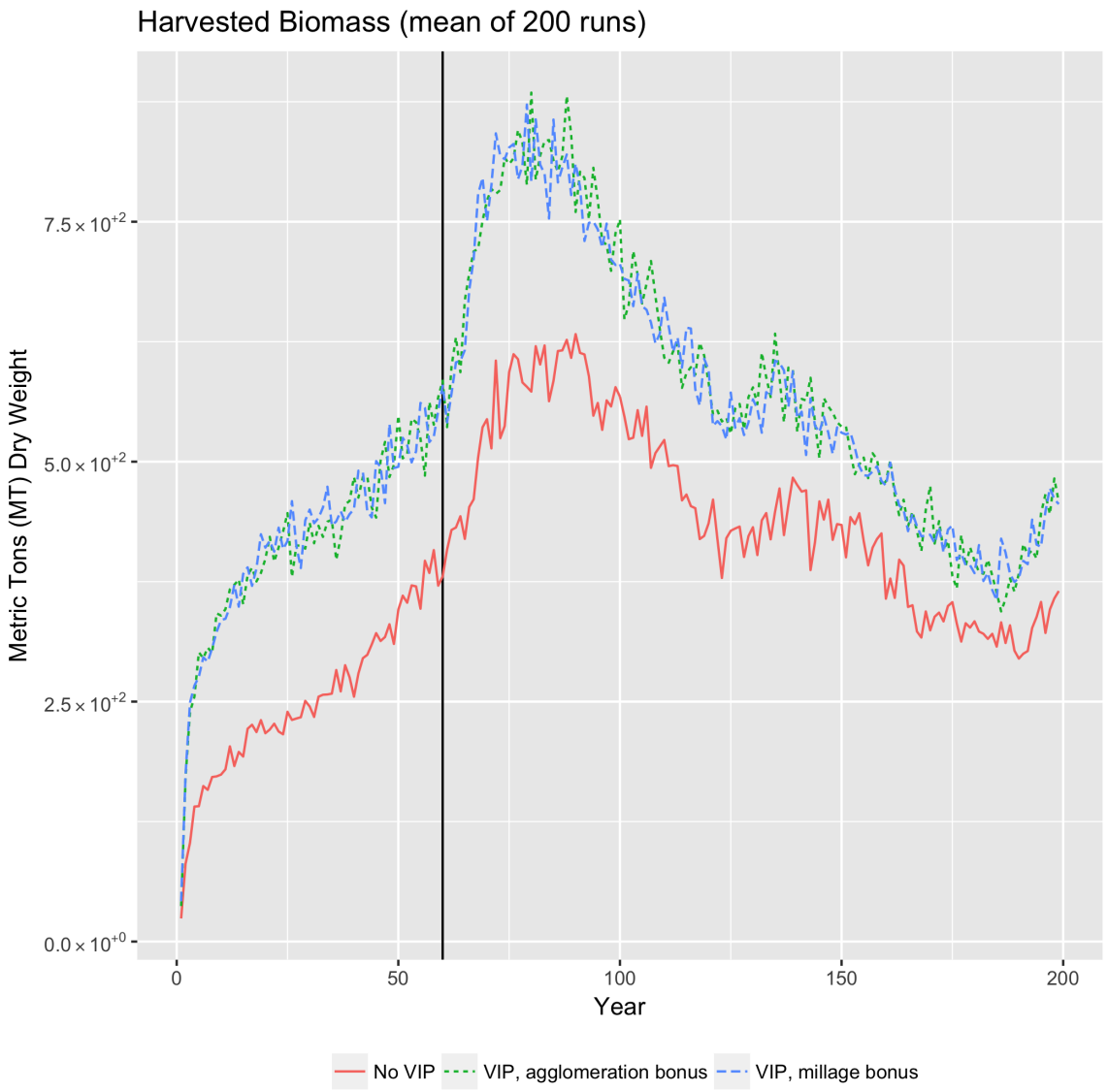

Figure 2.6: Harvested biomass in metric tons (MT) dry weight

using a generalized equation for trees in the United States [105]. Biomass volumes in all three scenarios oscillate with changes in natural forest growth as expected. Also as expected, both VIP scenarios generate greater biomass volumes than the no-VIP scenario. Nevertheless, the amount of biomass harvested in all three scenarios is insufficient to meet the annual needs of a hypothetical 10 MW woody biomass plant and the agglomeration bonus appears not to be noticeably different than the millage bonus in this regard. From this we can conclude that financial incentivization alone

is insufficient to ensure the economic feasibility of bioenergy production in Houghton County.

Figure 2.7 shows the mean forest carbon sequestration on the basis of the carbon content of vegetation [106] for all three policy scenarios. As expected, both VIP scenarios result in a lower aggregate carbon sequestration capacity than the no-VIP scenario. This result is not surprising given that both VIP scenarios were also

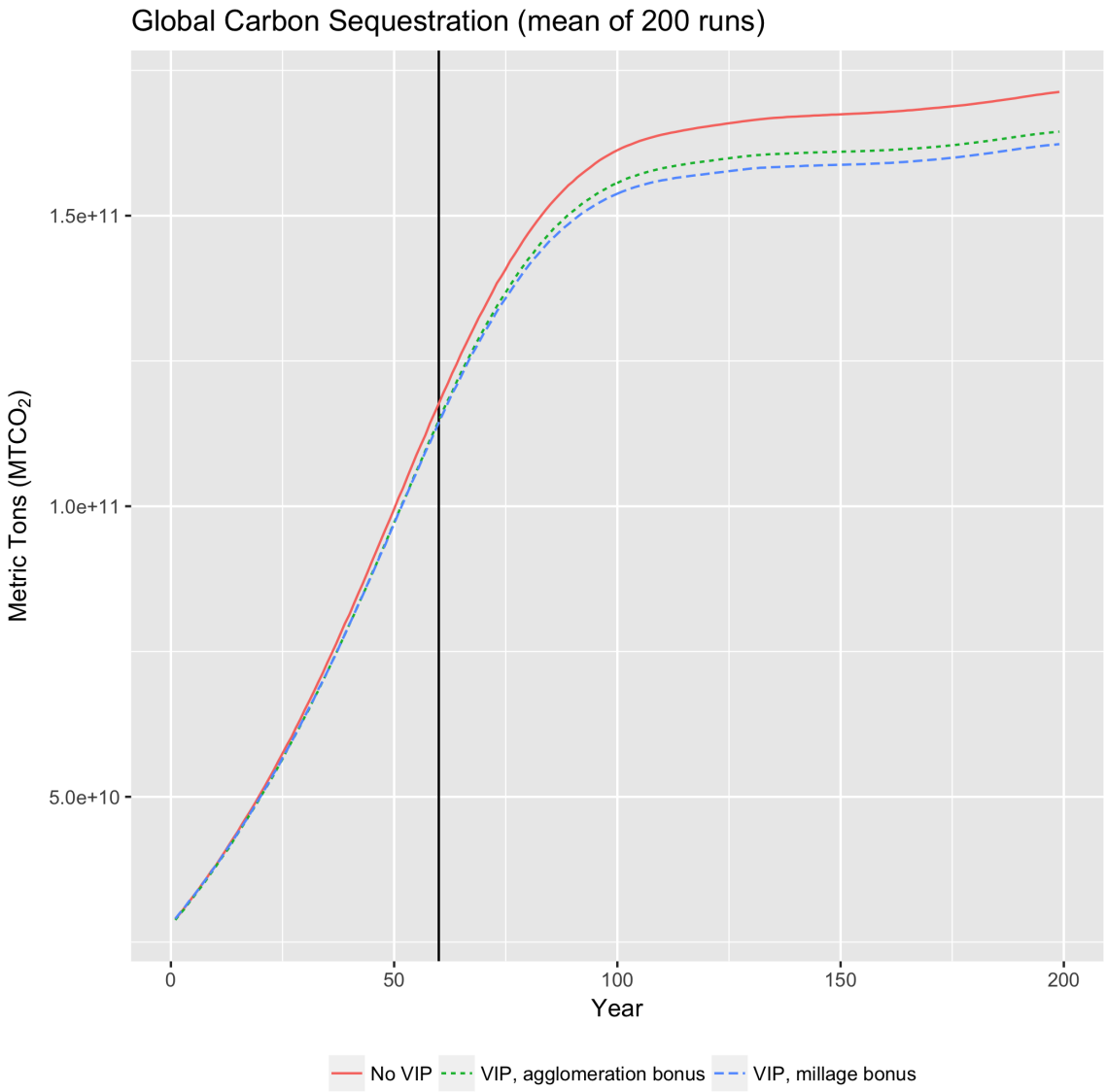

Figure 2.7: Forest carbon sequestration in metric tons of CO_2 ($MTCO_2$)

producing more biomass and, hence, inducing greater harvesting rates that reduce carbon sequestration capacity. It is, however, interesting to note that carbon sequestration capacity remains slightly higher under the agglomeration bonus than under the millage bonus regime. From this we can conclude that VIP incentivization does in fact have negative consequences for carbon sequestration capacity. Yet, one should not read too much into this conclusion because determining whether the benefits of bioenergy outweigh the costs in this setting requires that a calculation of the total carbon impact of the entire biomass life cycle, which is beyond the scope of this simple demonstration.

Finally, Figure 2.8 shows the impact on the availability of public access to recreational lands through open access acreage to forested land under all three policy scenarios. The impact of no-VIP incentivization is somewhat trivial in this case because our simple demonstration assumes that NIPF agents must enroll in a VIP to make their forested land available to the public (more accurately, open access is a requirement of VIP enrollment). Therefore, the no-VIP scenario produces zero acres of open access forested land.

Under the two VIP scenarios, however, we see that significantly more open access acreage is made available under the agglomeration bonus than the millage bonus regime, particularly after the first generation of harvesting (approximately 40 years). This result is likely due to the greater attractiveness of the financial incentive available through the agglomeration bonus to neighbors enrolled in the same program that is not available to enrollees of the millage bonus program, as current VIP literature supports [91].

From this, we can conclude that the agglomeration bonus is the most sustainable policy alternative based on our rather simplified sustainability assessment example. Both VIP scenarios are more economically sustainable than the no-VIP scenario (albeit insufficient to power a 10 MW plant) but the agglomeration bonus is able to

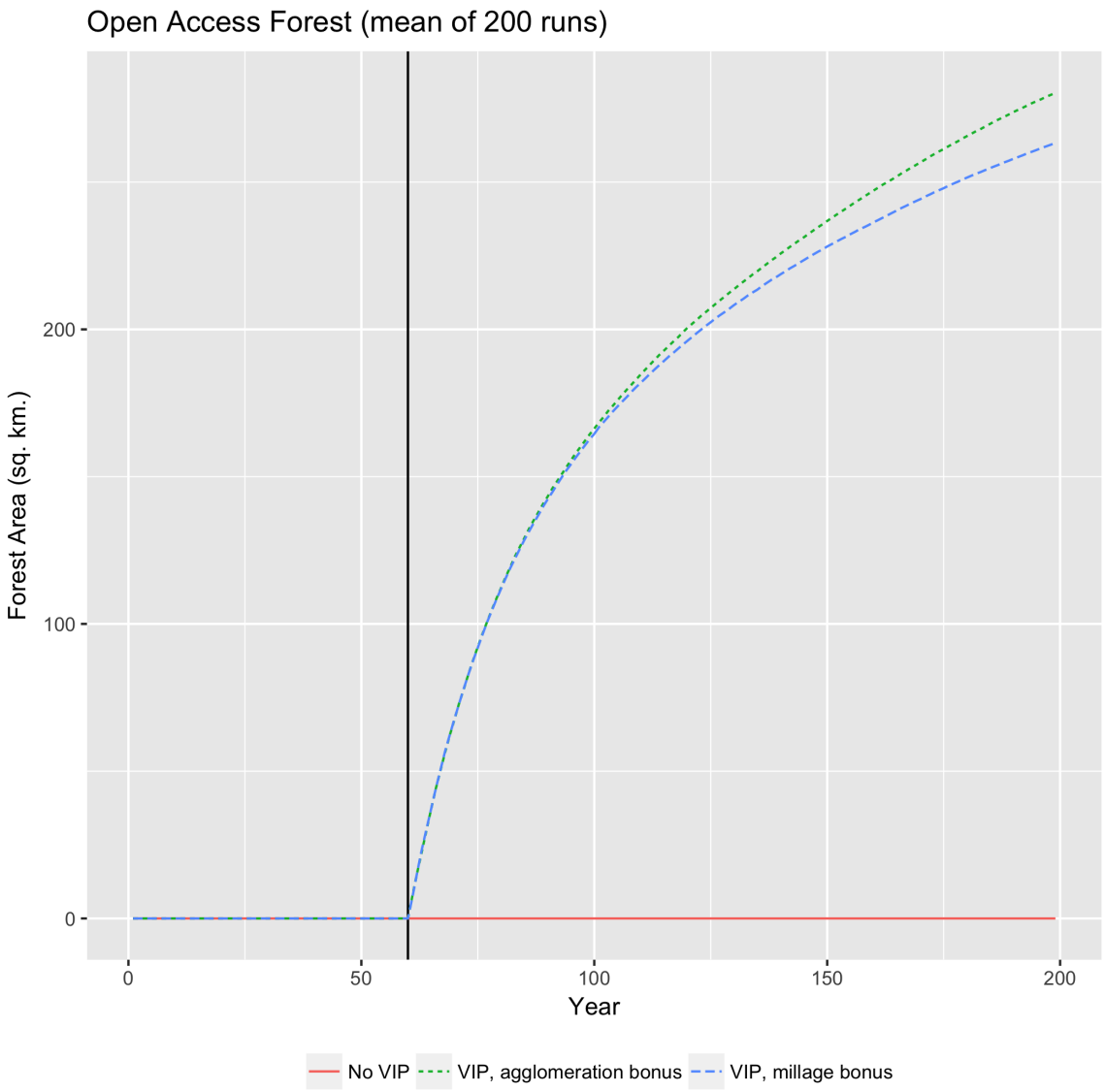

Figure 2.8: Open access to forest

generate comparable biomass volumes with a lower negative impact on environmental sustainability (carbon sequestration capacity) and a greater positive impact on social sustainability (open access acreage).

2.5 Discussion

The case study presented in the previous section was intended for demonstration purposes only. The goal was to simply demonstrate the policy analysis and sustainability assessment capabilities of ForestSim. Through this demonstration it was possible to see how ForestSim can be used to track sustainability assessment criteria that fall into each of the three classic pillars of sustainability so as to compare the impacts of alternative policy scenarios on NIPF owner harvesting. New users should be able to easily replicate this demonstration for any case study region of interest without modifications to ForestSim using only the required regional data (land cover and property boundaries) necessary to geolocate their simulation. This exercise will give new users a chance to orient themselves to the software while also providing a code structure that is easily modifiable for more sophisticated model runs once user are familiar with the ForestSim environment.

One of the most valuable features of ForestSim is its flexible architecture. ForestSim enables user to develop highly complex policy analysis experiments incrementally and over time. This development approach allows users to validate the underlying mechanisms of various sub-models in isolation of each other prior to integrating these sub-models and increasing the level of simulation complexity. For example, to avoid unnecessarily overcomplicating the demonstration above, the case study example was conducted with the default Harvester agent settings using a simplified First-In-First-Out harvest priority queue and no transportation or bioenergy production agents. This made it possible to validate the role of VIP incentivization on NIPF owner biomass harvesting without the additional complicating factor of harvest bidding, harvest scheduling, transportation logistics, or biomass purchasing. The flexibility of the ForestSim architecture also allows users to experimentally control various aspects of their policy design, social setting, environmental conditions, and economic relations to perform complex thought experiments that would be impossible in real

life. Users can also modify any or all aspects of the agent decision-making schema across all agent types to determine how such changes impact biomass harvesting rates or any other sustainability assessment criteria. This flexibility also means that users can tailor ForestSim to the unique features of their study region without having to design and implement their own model from scratch. Such a tool is invaluable to interdisciplinary research teams that possess some level of computational capability but are more interested in the policy or sustainability outcomes ForestSim permits them to generate with little to no computational effort. By helping to reduce some of the programmatic burden that is needed to develop complex models, ForestSim can occupy a useful place in the forest management policy community and ignite future innovative research endeavors.

2.6 Conclusion

In this paper we presented ForestSim, an agent-based simulation for bioenergy policy analysis and sustainability assessment. We used a simple case study to demonstrate the main features of ForestSim in an effort to determine which voluntary incentive program would be the most sustainable for encouraging biomass harvesting in Houghton County, Michigan, USA. We also discussed how and why ForestSim could be a valuable tool for the forest management policy and research communities. ForestSim is a free open source project under an MIT license and is available at https://github.com/forestsim-mtu/forestsim.

Chapter 3

Life Cycle Assessment of the Production of Gasoline and Diesel from Forest Residues Using Integrated Hydropyrolysis and Hydroconversion

Robert Zupko[1]

[1] Reprinted by permission from Springer Nature Customer Service Centre GmbH: Springer Berlin Heidelberg *The International Journal of Life Cycle Assessment* (Life cycle assessment of the production of gasoline and diesel from forest residues using integrated hydropyrolysis and hydroconversion, Robert Zupko), ©2019, advance online publication, 29 March 2019 (doi: 10.1007/s11367-019-01616-8)

Abstract

Purpose: Renewable gasoline and diesel can be produced through integrated hydropyrolysis and hydroconversion (IH^2) using renewable feedstocks such as woody biomass from logging residues. This study assesses the potential environmental impacts of IH^2 process fuels manufactured in Ontonagon, Michigan to determine their environmental impacts and if these manufactured fuels will meet regulatory requirements. The energy return on investment (EROI) is also calculated for comparison to other renewable fuels.

Methods: A cradle-to-grave life cycle assessment was conducted using regional forestry, timber harvest, and transportation data from the region. Regional geographic data was used to determine service areas that may provide woody biomass. The service areas were then developed into inventory data based upon the type and distribution of potential woody biomass feedstocks. Survey data from loggers in the region were used to ensure that harvest types were allocated in accordance with regional activity. Remaining inventory items were derived from existing data in the literature, or existing life cycle inventory databases. This study uses a functional unit of one megajoule of gasoline or diesel produced using the IH^2 process and assessed several environmental indicators as well as EROI.

Results and discussion: Fuels produced generate approximately 88% less greenhouse gas (GHG) emissions when compared to petroleum gasoline and diesel, allowing the fuels to meet regulatory requirements. Electricity used in preparation of feedstock and manufacturing, along with fuels used in transport of feedstocks, account for 92.19% of the energy used in production of IH^2 gasoline and diesel. This results in a calculated EROI 4.19 and 4.31 per kilogram of diesel and gasoline, respectively; which compares favorably to previous assessments of cellulosic ethanol that use similar feedstocks. This study demonstrates that while environmental impacts and EROI are sensitive to site selection, there is a sufficient GHG emission reduction

such that IH^2 fuels are capable of meeting regulatory requirements.

Conclusions: Fuels produced at the facility result in a reduction in GHG emissions, but better site selection may result in less fuel being used in transportation. Reducing the quantity of electricity needed in n-th generation facilities would also reduce environmental impacts while improving the EROI. The energy mix used to supply IH^2 facilities should also be considered during the planning process. Finally, future research may be needed to ensure feedstocks recovered from logging operations match expectations.

Keywords: Carbon Footprint - Biofuels - Woody Biomass - Energy Return on Investment - Hydropyrolysis - Gasoline - Diesel

3.1 Introduction

Gasoline and diesel fuels produced using the integrated hydropyrolysis and hydroconversion (IH^2) process from renewable feedstocks have the potential to address a number of existing concerns (see [107, 108]) with first generation biofuels as well as meeting regulatory goals. The Renewable Fuel Standard (RFS) as well as the Energy Independence and Security Act (EISA) of 2007 have mandated that approximately 80 billion liters of second generation or higher renewable fuels, with a life cycle greenhouse gas (GHG) emissions at least 50% lower than than petroleum counterparts, be blended with transportation fuels by 2022 [109]. IH^2 process fuels are categorized as second generation biofuels since they rely upon feedstocks such as woody biomass (e.g., logging residues, short rotation crops, etc.), corn stover, or algae [110]. Additionally, while ethanol blends can be used to meet regulatory targets, IH^2 process gasoline and diesel are inherently compatible with their petroleum counterparts [111] making them an attractive means of meeting these regulatory goals.

While there is a growing body of literature evaluating the impacts of biofuels (see [108, 112, 113]), work focused on assessing the IH^2 process or other broader catalytic hydropyrolysis techniques has been limited. This is likely attributable to the recent development of the process with [111] acting as the seminal publication followed by a comprehensive technical report by [114]. While the technical report includes a carbon footprint assessment, feedstocks are assumed to be a mix of forest materials (e.g., wood chips, underutilized roundwood, etc.) and mill residues from northern Wisconsin limiting its applicability. Following these early publications, [115] conducted the first preliminary life cycle assessment (LCA) of the diesel and gasoline products from the IH^2 process. Their study evaluated the greenhouse gas (GHG) emissions of four possible feedstocks: microalgae, bagasse, corn stover, and timber products from existing logging. The results of the study were encouraging with the authors noting a 30 to 96% GHG savings depending upon the selection of feedstock. The work was followed by [116] who conducted a carbon footprint analysis to evaluate the impact of integration with a petroleum refinery in Memphis, Tennessee along with the role that feedstock selection plays. In their case study, the refinery would supply the H_2 needed for hydropyrolysis and hydroconversion as opposed to internal production using C1-C3 coproducts. Possible biomass feedstocks include corn stover and forest residues which are broadly defined to include logging residues, unmerchantable roundwood, and mill residues. [116] also produced encouraging results showing a 67 to 90% GHG reduction when compared to petroleum fuels. However, the site selection required that forest residues be transported between 113 and 132 km. As such, the results are difficult to evaluate in the context of a facility that is closer to the harvests.

From a broader standpoint, [117] conducted an evaluation of the current state-of-the-art in the conversion of lignocellulosic biomass and included catalytic processes in the evaluation. The report noted that more work was needed in the development of catalysts, and their techno-economic evaluation projected n-th generation

plant economics of approximately $0.92/liter gasoline equivalent ($3.50/gallon gasoline equivalent) by 2022. [118] evaluated catalytic hydropyrolysis in the context of plant designs that incorporate carbon capture and storage technologies and found that carbon negative outcomes were possible in some scenarios. However, the authors noted that there are a number of key issues that need to be addressed before the evaluated technologies would be in use.

To date there has been no systematic assessment of the environmental impacts, or energy return on investment (EROI) of a first generation facility and its regionally-specific supply chain. As a result of this lack of systematic assessments, it also remains unclear if IH^2 facilities will meet RFS requirements once sited. This is a regulatory concern since prior work has shown that biofuels are sensitive to their supply chain, and excessive environmental impacts and negative EROIs can apply to specific facilities [108, 113, 119]. One means of alleviating these concerns are to ensure that facilities are located close to their primary source of feedstocks, although this may increase the distance that products must travel to a blending terminal. This is the approach taken in the case of the proposed IH^2 biorefinery in Ontonagon, Michigan by SynSel Energy Incorporated [120–122]. Ontonagon is a rural community in a heavily forested part of Michigan. The location was selected in part to allow the facility to be close to existing logging activity which will supply wood waste as a feedstock. While there is considerable interest from the local community, the environmental impacts remain uncertain. Furthermore, it is not known if the facility will produce fuels that meet regulatory requirements.

In this study, a cradle-to-grave LCA is conducted to evaluate the environmental impacts and EROI of the Ontonagon IH^2 biorefinery using a systematic accounting of the collection, chipping, and transport of logging residues as a woody biomass feedstock. Regional transportation networks, land cover data, and property ownership data is used to determine the likely sources of feedstocks, offering greater insight into their impact. This study evaluates the environmental impact of manufactured fuels,

cumulative energy demand of key manufacturing stages, and the overall EROI. The results are evaluated in the context of the RFS to determine if fuels produced will meet the regulatory requirements. Additionally, insights into facility placement are possible and suggestions for improvements to future n-th generation facilities are provided.

3.2 Methodology

3.2.1 Goal and scope definition

The goal of this study is to conduct a cradle-to-grave assessment of an IH^2 biofuels facility based in Ontonagon, Michigan using the LCA methodology outlined in ISO 14040 [60]. The system boundary includes feedstock collection (chipped woody biomass), transport, processing (size reduction and drying), fuel production, waste treatment, transport, and consumption of manufactured fuels (see Figure 3.1). The functional unit is one megajoule (MJ) of gasoline or diesel produced through the IH^2 process. Ammonia/Ammonia Sulfate produced is accounted for as a co-product, but credits were not assigned due to the lack of clarity regarding a consumer of the product or the transportation logistics that would be involved. Likewise, woody biomass generated is treated as a co-product of timber operations with allocations

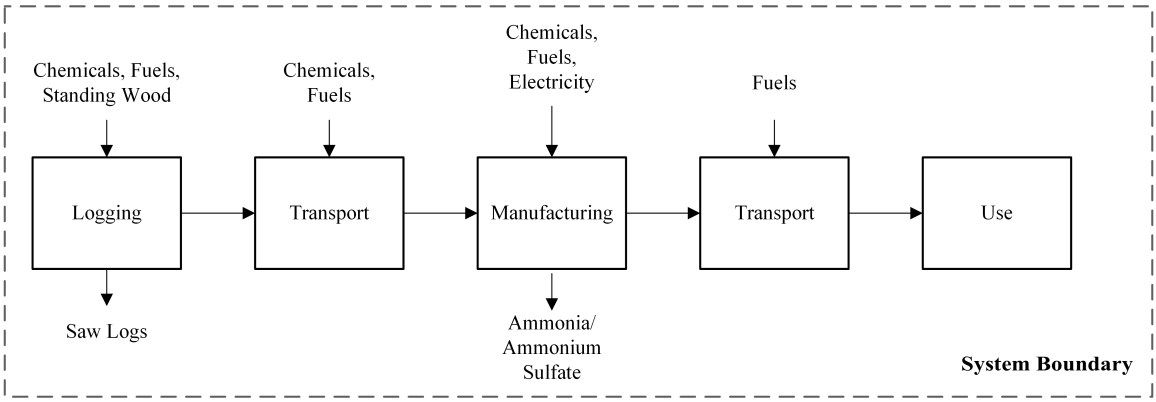

Figure 3.1: System boundary of the IH^2 process

assigned based upon the forest type. All input data was collected and entered into SimaPro 8.5 [123] for simulation (see Electronic Supplementary Material 3 for comprehensive inputs)[2], along with inventory data for the US from the DATASMART Life Cycle Inventory Package [124] and the U.S. Life-Cycle Inventory [125], as well as the TRACI 2.1 V1.04, IPCC GWP 1.03, Cumulative Energy Demand 1.10; and Greenhouse Gas Protocol 1.02 [126] packages were used to conduct the assessment.

3.2.2 IH^2 Description

Integrated hydropyrolysis and hydroconversion (IH^2) is a form of catalytic hydropyrolysis and produces hydrocarbon fuels (e.g. gasoline and diesel) from sources such as woody biomass (i.e., forest residues, logging residues, or slash) from timber harvests [111, 115, 116]. Fuels from the IH^2 process are a direct substitution for petroleum-based fuels and may be incorporated into existing distribution networks, although blending is generally expected due to higher octane ratings for IH^2 fuels [114]. The process is briefly described as follows: following aggregation, drying, and resizing of feedstocks, they are introduced via feedstock hopper into a hydropyrolysis reactor based upon a fluidized bed reactor (see Figure 3.2). During the reaction

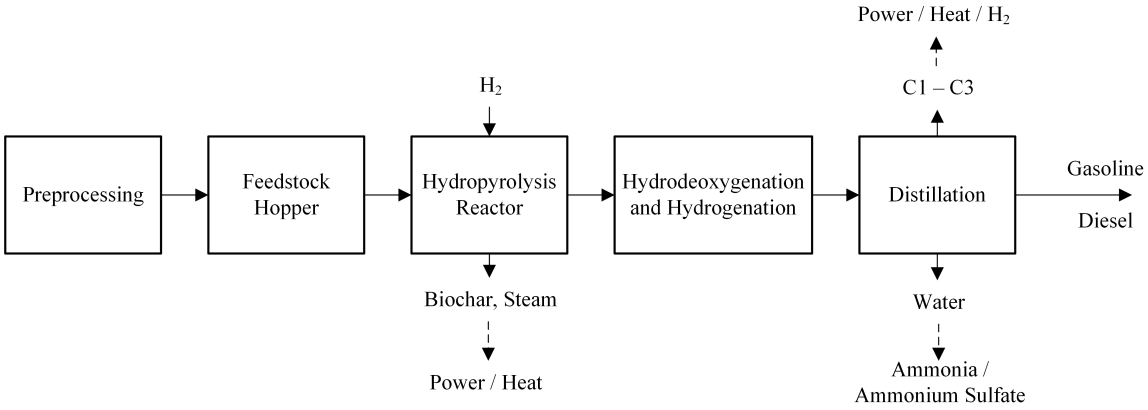

Figure 3.2: Simplified overview of the IH^2 process

[2] See Appendix B

the feedstocks are devolatized and a light hydrocarbon vapor product is produced along with C1-C3 gases, H_2O, COx, and biochar. The reactor is pressurized to 20-35 bar to induce the reactions; and hydrogen is introduced to reduce the oxide content of the final fuel. Biochar is continuously removed from the reactor to quench reactions. Hydropyrolysis vapors are then directed to the hydroconversion reactor with a catalyst that induces additional hydrodeoxygenation and hydrogenation to take place. Condensation is used to recover hydrocarbon vapors through the use of a distillation column to separate gasoline and diesel fuels. The C1-C3 gases can either be burned as fuel to generate electricity, or used in the generation of H_2 gas for circulation back into the hydropyrolysis reactor. In the case of woody biomass feedstocks, ammonia/ammonium sulfate can be recovered as a coproduct which has possible applications as a fertilizer or as an industrial chemical feedstock [115]. Finally, the highly endothermic nature of the IH^2 process results in significant amounts of steam that can be redirected to drive compressors, generators, or assist in feedstock drying.

3.2.3 Regional Description

Ontonagon is a rural village in the Western Upper Peninsula (WUP) region of Michigan. The WUP region consists of the counties of Gogebic, Ontonagon, Houghton, Keweenaw, Baraga, and Iron. The village receives power from the Upper Peninsula Power Company (UPPCO), whose energy mix is a combination of owned facilities and power purchased from the regional grid of Michigan, Illinois, Indiana, Ohio and Wisconsin (Tables S1 and S2, Electronic Supplementary Material 2).[3] The region borders Lake Superior and is heavily forested, with approximately 13,343 sq.km of forested land and includes approximately 2,722 sq.km of woody wetlands that may be unsuitable for commercial logging (see Section 3.7). Ownership of forested land is divided between state, federal, and private lands. Approximately 4,898 sq.km of

[3] See Appendix B

private lands have been registered as commercial forests with the State of Michigan. These commercial forests contain approximately 4,544 sq.km of actual forested land (i.e., land that is characterized by tree cover) and account for about 34% of the total forested land in the region. Owners of these lands receive a tax incentive from the state with the stipulation to have a at least forty contiguous acres of forest as well as a forest management plan with intent to conduct commercial harvests [127]. Since commercial harvests are conducted on these lands they can be assumed to have forest roads that service them, although such roads may be privately owned and not appear on regional maps. The region contains nine sawmills and one veneer mill that serve as the primary consumers of merchantable timber [128] while the IH^2 facility would be the primary consumer of woody biomass produced during timber harvests.

The first step in this study was to determine the extent of the region that would supply woody biomass to the IH^2 facility by conducting a GIS analysis using ArcGIS 10.3.1 [129]. This involved a network analysis using state road network data [130] to identify service areas from zero to 165 km in 33 km steps. The selection of the 165 km extent of the analysis compares favorably to responses from loggers regarding their travel distance and captures the approximately 73% of responses for distances between zero and 144.84 km (120 mi) [58, 59]. Approximately 15% of respondents reported traveling 144.84 to 193.121 km (90 to 120 mi) and is partially captured by the

Table 3.1
Summary of the maximum potential harvestable biomass (excluding woody wetlands) along with transportation inventory and service area allocations

Service Area	**Total Biomass** (dry t)	**Inputs**			
		Fuel Use (L/load)	Lubricants (L/load)	Grease (kg/load)	Allocation
0 - 33 km	6,570,839	37.08	0.05	0.02	7.45%
34 - 66 km	17,380,859	74.16	0.11	0.03	19.72%
67 - 99 km	34,811,538	111.24	0.16	0.05	39.50%
100 - 132 km	17,122,830	148.31	0.21	0.07	19.43%
133 - 165 km	12,254,466	185.39	0.26	0.09	13.90%

upper bounds of 165 km. Parcels registered as commercial forests were then selected based upon their geographic distance from the facility using the same zero to 165 km pattern. The service area and commercial forests were merged, and state parks were removed due to the lack of logging on them (see Figure 3.3). The identified service areas were then used to clip land cover data from the National Land Cover Database [103]. A count of forested land pixels (i.e., deciduous forest, evergreen forests, and mixed forest) was then taken for each zone. Woody wetlands were excluded from the analysis on the assumption that complications associated with harvesting [131] would significantly limit their impact. Finally, the data was aggregated and estimates for the distribution of feedstocks calculated, which acts as the basis of woody biomass production as well as transportation distances (see Table 3.1).

3.2.4 Energy Return on Investment

The energy return on investment (EROI), sometimes referred to as the energy return on energy invested (ERoEI), is the ratio between the total energy returned by a fuel versus the total energy needed to manufacture and deliver the fuel to consumers [132]. In this study the extended EROI approach outlined by [133] is used in which the energy delivered to society is divided by the total energy required to manufacture, transport, and use the energy. Formally this is defined as,

$$EROI = \frac{Energy_{out}}{Energy_{in}} \tag{3.1}$$

Where $Energy_{out}$ is the potential energy of one kilogram of the fuel and $Energy_{in}$ is the total energy input from the system boundary. For the potential energy the values of 46.536 MJ/kg and 45.575 MJ/kg where used for conventional gasoline and low-sulfur diesel, respectively [134]. As EROI has been used in studies of petroleum-based transportation fuels as well as biofuels (see [113, 132, 135], this approach allows the IH^2 fuels to be properly compared to prior work as well as assessing their potential environmental impact.

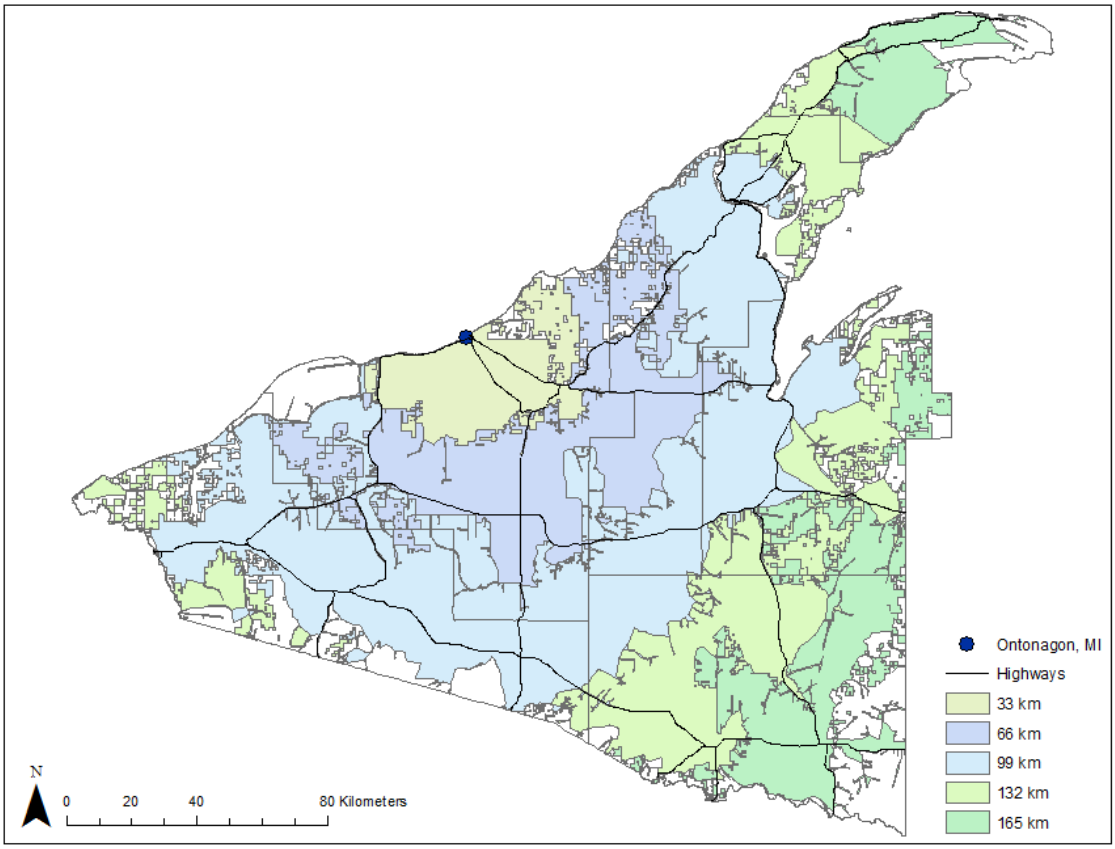

Figure 3.3: Map of the study region depicting the major highways leading from Ontonagon along with the service area boundaries used to determine the distribution of woody biomass sources

3.3 Life Cycle Inventory

3.3.1 Feedstock Production

While the IH^2 process can use a variety of biomass feedstocks as an input, plans for the Ontonagon facility call for woody biomass as the feedstock. Woody biomass is generated during timber operations and consists of the non-merchantable portion of the stem, branches, and roots. Woody biomass is also distinct from coarse woody debris (or coarse woody material) which is deadwood from natural processes [131]. Typically woody biomass is left on site to act as a soil abatement to prevent erosion,

or used during harvesting operations to prevent soil compaction [136]. To be used as a biomass feedstock it must be first collected and chipped to reduce its bulk before transport. Good forestry practice guidelines and state laws can limit the amount that can be collected by mandating that a percentage, typically between 10 and 45%, be retained on site [131]. Currently Michigan's Department of Natural Resources does not specify a precise figure [137], so a baseline of 30% was selected based upon good forestry practice guidelines.

The quantity of woody biomass that is generated during timber operations is dependent upon both the species of tree being harvested as well as the productivity of harvesting operations. In order to estimate the quantity of above-ground woody biomass that a single tree could produce, equations from [105] were used to derive the ratio between merchantable biomass (mbm) and woody biomass (bm) (Equations 3.3 - 3.4).

$$bm = Exp(\beta_0 + \beta_1 ln(dbh)) \tag{3.2}$$

$$mbm = bm * Exp(\alpha_0 + \frac{\alpha_1}{dbh}) + Exp(\gamma_0 + \frac{\gamma_1}{dbh}) \tag{3.3}$$

$$ratio = \frac{bm - mbm}{mbm} \tag{3.4}$$

Where β_0 and β_1 are the parameters for the appropriate species group, α_0 and α_1 are the parameters for the species group stem wood, and γ_0 and γ_1 are the parameters for the stem bark as listed in [105]. This ratio is then applied to the harvest productivity on the basis of merchantable biomass in tonnes per system hour to determine woody biomass production in tonnes per system hour.

Harvesting is assumed to follow patterns established by a survey of Michigan loggers that intended to study the potential for a cellulosic ethanol facility in the Upper Peninsula of Michigan [58, 59]. The analysis focused on cut-to-length and

feller buncher harvester operations which accounted for the majority of treatments applied (i.e., 30% selective cut, 70% shelterwood cut, and clear cutting). Feller buncher harvester operations involve whole tree harvesting and result in slash being aggregated at a landing where trees are delimited, topped, and bucked [136]. In contrast, cut-to-length operations involve the tree being delimited and cut into specified log lengths immediately after being felled. Residues can then either be piled in front of the harvester as a mat to protect the soil, or alongside, for later collection. In the case of either operation, woody biomass would be chipped prior to being loaded into a chip van. Since the survey by Abbas et al. [58] indicates that chipping rarely occurs, this study assumes that loggers will respond to the demand and begin chipping woody biomass to supply the IH^2 facility. As a proxy for usage data, a survey by Spinelli and Magagnotti [138] was used to estimate materials used in chipping. Based upon the distribution of harvester operations, it was estimated that 315 L/day of diesel along with 0.494 kg/day of blades would be consumed (Table S6, Electronic Supplementary Material 2).[4] In order to simplify this study, logger productivity and woody biomass generation was calculated on the basis of the operation, treatment, and forest types found within the zones delimited by the network analysis (Table S5, Electronic Supplementary Material 2).[5] This data was then aggregated into a single inventory item using the distribution of harvest operations and treatment types (see Table 3.2) and standing wood was used as the input from nature. This study continues the assumption set forth by [59] that harvesters will work an eight hour day with a steady rate of production and fuel use throughout the day. Finally, impacts and credits associated with replanting are not accounted for since the majority of harvesting is focused on stands grown through natural processes [59].

[4] See Appendix B
[5] ibid.

Table 3.2
Allocation of woody biomass sources based upon the harvesting process and expected daily production

		Productivity (t system h)		Allocation
		Timber	Woody Biomass	
Cut-to-length	30% cut	7.48	2.71	28%
	70% cut	9.04	3.28	23%
	Clearcut	11.96	4.34	25%
Feller-buncher	30% cut	7.81	2.84	8%
	70% cut	10.13	3.68	9%
	Clearcut	14.33	5.21	7%

3.3.2 Feedstock Transportation

Following chipping of woody biomass during timber operations, chip vans are used to transport them to the receiving facility. Transportation of green wood chips was allocated on the basis of the biomass distributions in the regional service areas. The inputs are outlined in Table 3.1 based upon the chip vans profile developed for Michigan by [59].

3.3.3 IH^2 Production

IH^2 production has two major steps. First, feedstocks are prepared, requiring on-site transport of materials, drying, and size reduction prior to being fed into the IH^2 process (see Table 3.5). In accordance with previous studies (see [115, 116]), combustion of biochar from the IH^2 process along with energy from the regional grid is used to reduce the moisture content of feedstocks to 20% prior to further size reduction. Following preparation, the feedstocks are introduced to the IH^2 process which involves the materials and energy flows previously outlined in the literature [115, 116]. Table 3.3 outlines these inputs with the assumption that waste streams are assumed to be directed to municipal sanitary landfills or water treatment facilities.

Table 3.3
Inventory for feedstock preparation and IH^2 fuel manufacturing

Item				Total
Feedstock Preparation	Inputs	Yard equipment	Diesel, low-sulphur	1376 L/d
			Lubricants	121 L/d
			Grease	163 kg/d
		Feedstock processing and drying	Electricity (size reduction)	29840 kWh
			Electricity (drying)	25513 kWh
		Green Woodchips, on site		1816 t
	Output	Processed Feedstock		908 t
Manufacturing	Inputs	Processed Feedstock		1000 t
		Electricity		60 MWh
		Cooling Water		3085 t
		Boiler Feedwater		5630 t
		Inerting Gas (N_2)		120 kg
	Outputs	Renewable Gasoline		169040 kg
		Renewable Diesel		80420 kg
		Ammonia/Ammonia Sulfate		2000 kg
		Sour Water		538 t
		Cooling Tower Blowdown		1329 t
		Ash		3840 kg

3.3.4 Product Transport and Use

While it is possible that gasoline and diesel produced will be consumed close to the Ontonagon facility, the majority is likely to be transported to a larger market. Green Bay and Superior, Wisconsin were selected as candidate locations due to existing blending terminals and proximity to rail and water based transport. Following selection the relevant distances calculated and inventory proxies for regional rail and Great Lakes Barges were selected (see Appendix 3.7). Following delivery at

the terminal, delivery to the pump follows GREET [139] model assumptions. Once received by one of the markets it is assumed that usage patterns will be consistent with patterns typically found in the United States [140].

3.3.5 Life Cycle Impact Assessment

Previous work within the WUP region has identified a robust set of sustainability criteria and indicators of interest to local residents [141, 142]. These criteria and indicators compare favorably with criteria that are generally selected for bioenergy systems [143] and form the basis of the life cycle impact methods selected. The Intergovernmental Panel on Climate Change (IPCC) Fifth Assessment Report Global Warming Potential (GWP) for both 20- and 100-year time spans were selected in recognition of local concerns about GHG emissions and to allow a baseline comparison to other fuels [144]. To allow a direct comparison to prior work by [116] the GHG emissions were also captured, allowing the GHG reduction compared to petroleum gasoline and diesel to be evaluated. The Tool for the Reduction and Assessment of Chemical and Other Environmental Impacts (TRACI) was developed by the U.S. Environmental Protection Agency (EPA) and allows for broader pollution categories such as ozone depletion, global warming, human health criteria, smog formation, acidification, and eutrophication [145]. This study uses the updated 2.1 version which incorporates additional impact assessments and aligns with local concerns regarding air and water quality [146]. Finally, the cumulative energy demand (CED) necessary to produce the gasoline and diesel was calculated so the total energy return on investment (EROI) could be compared to other fuels as well as addressing a local economic concern.

Table 3.4
Results of the TRACI assessment per MJ of IH^2 process gasoline and diesel

		Diesel		Gasoline	
Impact category	**Unit**	Mean	SD	Mean	SD
Ozone depletion	g CFC-11 eq	1.40E-06	4.35E-08	1.36E-06	4.14E-08
Global warming	g CO_2 eq	1.05E+01	2.96E-01	1.02E+01	2.52E-01
Smog	g O_3 eq	8.02E-01	8.10E-02	7.80E-01	7.73E-02
Acidification	g SO_2 eq	8.11E-02	2.72E-03	7.89E-02	2.52E-03
Eutrophication	g N eq	2.64E-02	3.93E-04	2.56E-02	3.51E-04
Carcinogenics	CTUh	2.23E-09	2.21E-11	2.16E-09	3.02E-11
Non carcinogenics	CTUh	3.50E-09	3.16E-11	3.39E-09	4.08E-11
Respiratory effects	g PM2.5 eq	3.22E-03	1.34E-04	3.11E-03	1.06E-04

3.4 Results

The IPCC GWP of IH^2 process gasoline and diesel was found to be similar when evaluated along 20- and 100-year time frames with the delivery site and method accounting for much of the variation. Gasoline showed a 20 year potential of 13.23 $\pm$ 0.27 g CO_2 equiv/MJ and a 100 year potential of 10.44 $\pm$ 0.25 CO_2 equiv/MJ. Diesel showed a 20 year potential of 13.65 $\pm$ 0.31 g CO_2 equiv/MJ and a 100 year potential of 10.78 $\pm$ 0.3 g CO_2 equiv/MJ. This pattern continued for the results of the TRACI assessment (see Table 3.4) in which the environmental and human impacts of the fuels are similar and largely attributable to the diesel fuels and energy mix used in feedstock processing and manufacturing. Generally the impacts are low enough that they are unlikely to be of concern; however, since logging residues are not currently used in the region [59] the impact of smog, acidification, and eutrophication due to their collection and transport may represent a long term concern for residents of the region that would be directly attributable to the IH^2 facility.

In accordance with the RFS, the consumption of fuels was assumed to be carbon neutral due to carbon sequestration during regrowth of biomass when compared to petroleum fuels [147]. As a result, the GHG emissions calculated using Greenhouse

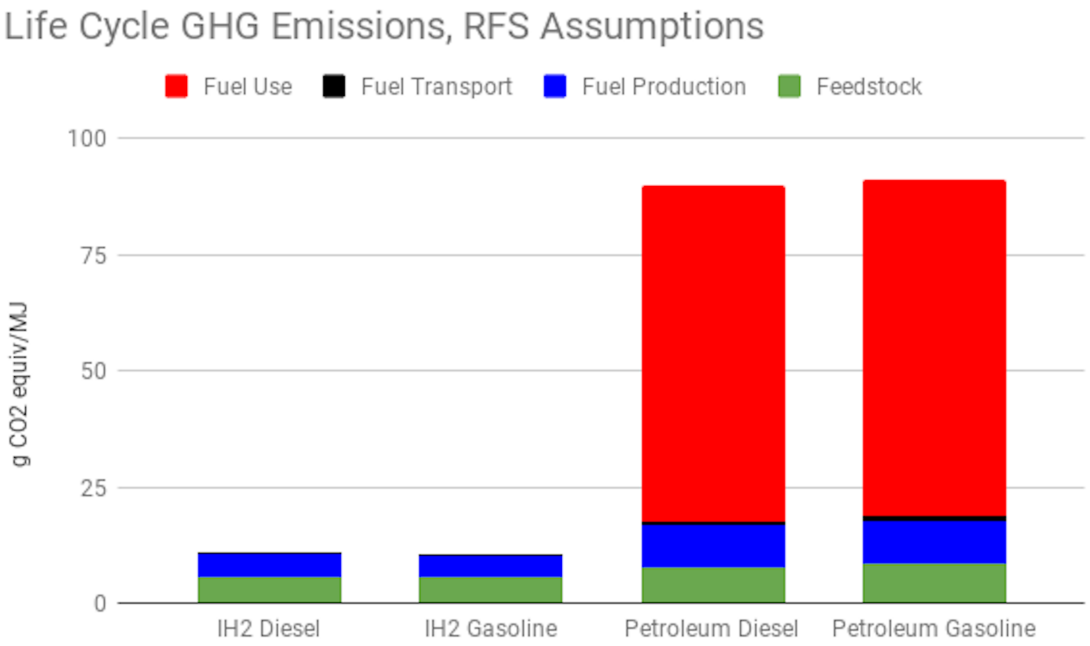

Figure 3.4: Comparison of life cycle GHG emissions between petroleum fuels and IH^2 fuels

Table 3.5
Life Cycle GHG Emissions comparison with petroleum fuels

	IH^2 Fuels[1]				**Petroleum Fuels[2]**	
g CO_2 equiv/MJ	Diesel	Gasoline	Diesel	Gasoline	Diesel	Gasoline
Feedstock	5.68	5.54	10.38	10.14	7.54	8.3
Fuel Production	4.69	4.57	4.69	4.57	9.05	9.27
Fuel Transport	0.71	0.62	0.71	0.62	0.85	1.03
Fuel Use					72.7	72.6
Total	11.08	10.73	15.78	15.33	90.14	91.2
1:1 Displacement GHG Reduction	87.71%	88.23%	82.49%	83.19%		
1:0.5 Displacement GHG Reduction	75.42%	76.47%	64.99%	66.38%		

1. Fuel transport mean based upon on regional blending terminals, see Table 3.7
2. Data source: NTEL DOE/NETL-2009/1346 [140]

Gas Protocol 1.02 [126] was quite low (see Figure 3.4 and Table 3.5) and the results were in line with the results of the IPCC GWP over 100-year timeframes. Since standing wood is used as the input from nature, a basic estimate of the impact of land-use change is incorporated along with CO_2 uptake. Land-use change was estimated to account for $3.41 \times 10^{-5} \pm 1.29 \times 10^{-6}$ g CO_2 equiv/MJ for diesel and $3.27 \times 10^{-5} \pm 1.14 \times 10^{-6}$ g CO_2 equiv/MJ for gasoline. The results also incorporate an estimated CO_2 uptake of -0.39 g/MJ for diesel and -0.38 g/MJ for gasoline. One of the biggest sources of variability was due to transportation of the products to a blending facility. In the case of diesel, 0.53 and 0.89 g CO_2 equiv/MJ were produced for transport by rail to Green Bay and Superior respectively, while 1.02 and 0.39 g CO_2 equiv/MJ was produced when transported by water. Gasoline resulted in slightly lower impacts with 0.52 and 0.87 g CO_2 equiv/MJ produced when transported by rail to Green Bay and Superior respectively and 0.78 and 0.31 g CO_2 equiv/MJ when transported by water. When compared to baseline scenarios for petroleum fuels [140] the GHG emissions represent an approximately 88% GHG reduction. While these results assume a one-to-one comparison per the RFS, this may not be a realistic comparison since the actual displacement may only be 1:0.5 [148]. In the case of IH2 fuels, a 1:0.5 displacement would result in a 75.42% and 76.47% reduction in GHG emissions for diesel and gasoline, respectively, when applying the same assumptions as Table 3.5.

Two variables examined in the context of GHG emissions were the impact of soil carbon loss due to harvesting and the regional energy grid mixture versus the national average. While a full accounting of the impact that timber harvests would have upon soil carbon loss is beyond the scope of this study, an estimate was done using the biomass distributions from the U.S. Forest Service [149] for Northern Lake States species (see Table S7, Electronic Supplementary Information 2).[6] Assuming that an 8% loss of soil carbon due to harvesting [150], which is emitted to the atmosphere as CO_2, GHG emissions increased by 4.7 g CO_2 equiv/MJ for diesel and 4.6 g CO_2

[6] See Appendix B

equiv/MJ for gasoline. This would result in the GHG reduction being approximately 83% for the fuels. However, these figures likely represent a high estimate of the soil carbon loss since only data from clear-cut impacts was used and re-sequestration of soil carbon during forest regrowth is not considered. Likewise, when the national grid mix for the United States is substituted for the regional grid mix, the GHG emissions fall by 2.11 g CO_2 equiv/MJ for diesel and 2.05 g CO_2 equiv/MJ for gasoline. This implies that an energy grid mixture closer to the national average would result in a 90% GHG reduction when compared to petroleum fuels.

As with previous indicators, the CED of the fuels are heavily influenced by transportation fuels and the regional energy grid. To produce one kilogram of diesel 10.88 ± 0.19 MJ was consumed and similarly gasoline required 10.8 ± 0.17 MJ. For both fuels only 0.31 MJ of the energy required came from renewable sources. Likewise, for both fuels approximately 35.7% of the CED is due to feedstock collection and

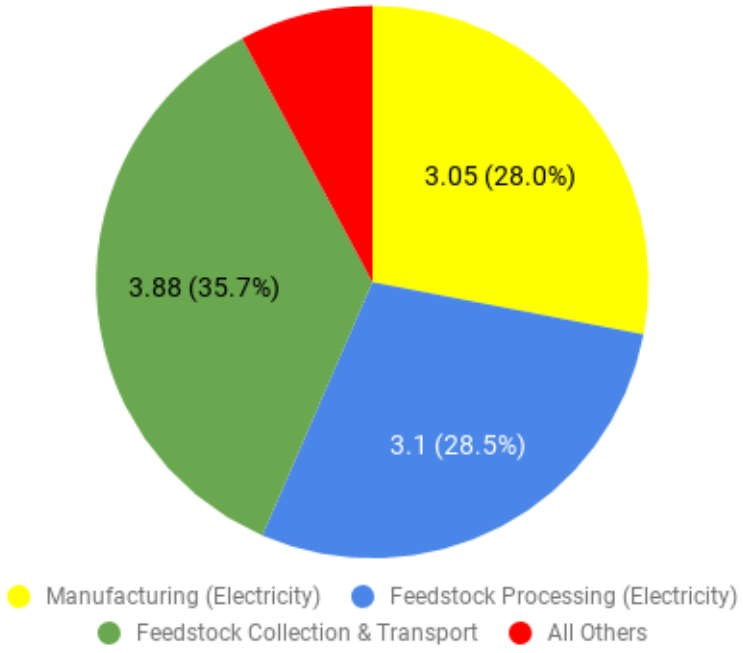

Figure 3.5: Distribution of CED involved with production of one kg of IH[2] gasoline or diesel including component CED and percentage

transport, 28.5% is electricity used during feedstock processing, 28.0% is electricity used during manufacturing (see Figure 3.5). The calculated EROI for the fuels was 4.19 ± 0.07 for diesel and 4.31 ± 0.07 for gasoline with the variation attributable to delivery location and method.

3.5 Discussion

As a first-generation facility, it is expected that there are process inefficiencies that result in a higher environmental impact than would be seen in an n-*th* generation facility. The EROI of the fuels is just outside the low-end estimate for cellulosic ethanol ranges of 4.4 to 6.6 [108] and quite competitive when compared to corn ethanol whose EROI may not exceed one [151]. Given that approximately 56.5% of the CED is due to electricity consumed during feedstock processing and manufacturing, process improvements to n-*th* generation facilities could result in the EROI being competitive with cellulosic ethanol. Additionally, a significant amount of the energy invested is due to the collection of feedstocks. A best case scenario would be to have access to feedstocks in the entire 165 km service area resulting in about 86,000 sq.km of potentially harvestable land. However, only approximately 9,250 sq.km of harvestable land was identified (Table S4, Electronic Supplementary Material 2).[7] While this would increase to 11,500 sq.km if woody wetlands are included, it only represents about 13% of the theoretical maximum due to the presence of Lake Superior. Better site selection allowing for more woody biomass to be harvested in the area around the facility would reduce the amount of fuel needed to transport feedstocks resulting in a better EROI as well as reducing the GWP and GHG emissions. This would also help to address the impacts identified by the TRACI assessment since diesel consumed during the transport of feedstocks is a contributing factor.

While biochar from the IH^2 process can be used as an energy source for feedstock drying, the process still has significant energy demands. As a result, the major source

[7] See Appendix B

of GHG emissions and GWP of the fuels comes from fossil fuels consumed during manufacturing processes since coal and natural gas are significant components of a regional energy mix that is supplemented by oil fired facilities as needed (Table S1, Electronic Supplementary Material 2).[8] Previous studies have assigned credits for ammonia/ammonium sulfate on the assumption that it could be sold as a synthetic nitrogen fertilizer which would offset some of the grid's impact [115, 116]. However, Fan et al. [116] only reported a -0.31 to -0.32 g CO_2 equiv/MJ indicating that the offset may not be that significant and process improvements reducing electricity use or development of renewable energy sources in the region may result in greater GHG and GWP reductions. Despite these concerns, fuels produced by the facility still exceed the 50% reduction in GHG emissions target set by the RFS. When the estimated 88% reduction for the site is considered along with the 86 to 95% reduction from previous studies [115, 116], there is some evidence to suggest that the IH^2 process using woody biomass as a feedstock may have a significant GHG reduction inherent to the process. While further research is needed to confirm this, such a reduction would imply other factors of site selection (e.g., local infrastructure, markets, tax incentives, etc.) may be more significant as long as sufficient woody biomass is present as a feedstock.

One potential limitation of this study is the assumption that 70% of the woody biomass generated during logging operations would be recoverable. While this study assumes that 36% of the woody biomass consumed would be from selective harvests, use of slash during logging operations might result in little to none being available as feedstock. However, that loss might be offset by non-merchantable saw logs being chipped as a feedstock during shelterwood and clearcut harvesting. This represents an area of future work since regional harvesting patterns as a whole may change in response to the demand for woody biomass.

Another possible source of error in GHG and GWP reductions is the role that land-use change would play due to timber harvesting along with the harvesting in and of

[8] See Appendix B

itself [152]. While the estimate conducted as part of this study shows that there may be as much as a 30% difference due to the effects of soil carbon loss, quantifying the effect of timber harvests on soil carbon is difficult. Meta-analyses have shown anywhere from a negligible effect on soil carbon [153] to an average loss of 8% soil carbon [150], which can be expected to recover over 50 to 70 years. The recovery is consistent with the Covington Curve [154] which describes soil organic carbon dynamics and finds that after approximately 65 years the total carbon may be higher than at the time of harvest depending on local conditions. Further complicating the issue is the uncertainty in soil recovery following timber harvests, the possibility of soil carbon migrating into mineral soils, and careful harvesting negating soil impacts [155]. Dependency on local conditions is a consistent theme in the literature since the actual impacts on the soil are likely site specific (see [156, 157]). As such, this study assumed the standard forest ecosystem estimates by the U.S. Forest Service [149] which shows no impact on soil organic carbon following clear-cut treatment or stand regrowth on forest land in the Northern Lake States. Additionally, it should also be noted that no land-use changes are expected as a result of this operation (i.e., harvested land returns to forest after regrowth); supporting the assumption that soils will recover from any short term losses. This assumption is also consistent with carbon neutrality due to sequestration during regrowth of biomass [147]. However, the validity of this assumption may represent an avenue for future research and possible critique of the RFS.

While the RFS conducts a one-to-one comparison (i.e., replacement) of biofuels to their petroleum counter parts, this assumption may be erroneous due to increases in market consumption of fuels (i.e., rebounding) (see [148, 158]). In the event of rebounding, overall energy demand increases, reducing the impact that renewable fuels would have. While this study is consistent with the RFS guidelines in evaluating the life cycle GHG emissions, changes to the policy may be necessary to address these assumptions. The effects of rebounding may also be quite significant since conventional

biofuels (i.e., corn ethanol) may only result in a 50% displacement of the petroleum-equivalent fuel [148]. As such, future studies should account for rebounding in order to make a robust assessment of the life cycle impacts. However, since IH^2 fuels are a direct substitution of petroleum counterparts, ethanol fuels may not be an appropriate proxy for rebounding effects and additional research as they are introduced into the marketplace may be needed.

3.6 Conclusions

The primary goal of this study was to assess the environmental impacts of IH^2 fuels manufactured in Ontonagon, Michigan to see if they met RFS requirements, as well as determining the EROI so it can be contextualized against other renewable fuels. While this study shows that IH^2 fuels show considerable promise in addressing RFS requirements, considerable opportunities still exist for improvements. The manufacturing process is quite energy intensive and represent a possible area of improvement in n-th generation facilities. Considerations for the sources of electricity supplying facilities also need to be made since energy grid mixtures have a significant impact upon GWP and GHG emissions during manufacturing. While this study shows that delivery of the fuels to blending terminals does introduce some variability in the impacts, the Ontonagon location compares favorably with the baseline values for the transport of petroleum fuels. When siting facilities, planners need to be ensure that regional feedstocks are maximized while at the same time minimizing the distance feedstocks must travel. This also implies that future work is needed to ensure that quantity and source of woody biomass feedstocks delivered meet the expectations drawn from existing logging operations.

3.7 Acknowledgements

The author would like to acknowledge Robert Handler and David Shonnard (Michigan Technological University, Sustainable Futures Institute) for their feedback and providing access to SimaPro, Matthew Kelly (Michigan Technological University) for feedback in preparing the woody biomass estimates, and Stas Zinchik (Michigan Technological University) for assistance in preparing the explanation of the IH^2 process. The author would also like to thank the reviewers and editor for their kind feedback on this manuscript.

Supplementary Material

3.A Regional Description

Summary information for the Western Upper Peninsula (WUP) was calculated using ArcGIS 10.3.1 using data from the National Land Cover Database (NLCD) [103], Michigan County Maps [159], and Michigan Commercial Forest Maps [160]. The area and total potential biomass in the region was calculated as follows. First, the NLCD was clipped to the counties that make up the region. The count of pixels for deciduous forest, evergreen forest, mixed first, and woody wetlands was taken and the regional biomass estimate per acre [98] was applied (see Table 3.6).

Table 3.6
Summary of Region and its Commercial Forests

	Region		**Commercial Forests**	
	Area (sq.km)	Biomass (dry t)	Area (sq.km)	Biomass (dry t)
Deciduous Forest	7,018.84	66,871,404.95	2,819.34	26,860,998.25
Evergreen Forest	1,467.83	13,984,607.43	269.14	2,564,213.41
Mixed Forest	2,134.44	20,335,654.14	626.97	5,973,375.19
Woody Wetlands	2,721.79	25,931,657.93	828.63	7,894,685.26
Total	13,342.90	127,123,324.45	4,544.08	43,293,272.11

Commercial forests data for the WUP was determined by first clipping the statewide commercial forests to just those in the WUP counties. A sum of the registered acreage was then taken to arrive at the estimate of 4,898 sq.km. The forest area and biomass estimate was then calculated using the same process as was applied to the region.

3.B Transportation Analysis

Following manufacturing, IH^2 fuels need to be delivered to a blending terminal before it can ultimately be delivered to end users. The November 2018 Terminal Control Locations Directory [161] was used to identify possible sites. Green Bay and Superior, Wisconsin were selected due to their proximity to Ontonagon, Michigan as well as their rail and waterway access. Green Bay hosts a terminal operated by U.S. Oil along with the Port of Green Bay. The terminal is equipped with facilities to products via pipeline, rail, truck, and Great Lakes Barges [162]. Superior, WI hosts

Table 3.7
Distance that IH^2 fuels travel to a blending terminal from Ontonagon, Michigan

Operation	**Transport Method**	**Distance (km)**	**Inventory Items**
To Green Bay	Rail	341.35	Transport, freight, rail, diesel, with particle filter US* US-EI U
	Water	929.22	Transport, barge tanker/US- US-EI U
To Superior	Rail	636.2	Transport, freight, rail, diesel, with particle filter US* US-EI U
	Water	278.25	Transport, barge tanker/US- US-EI U
To Pump	Road	48.28	Transport, combination truck, short haul, diesel powered, East North Central/tkm/RNA

the Superior Terminal which is operated by Enbridge Energy and is adjacent to Duluth, Minnesota which hosts the Port of Duluth-Superior. The Superior Terminal is part of the Enbridge Northern Gateway Pipelines and the Husky Superior Refinery is located nearby. While Superior is focused on pipeline transport and delivery, the concentration of services in the area makes it a contender for deliveries in the event of future upgrades.

To determine the transportation distance of finished products from Ontonagon to targeted terminals, the Network Analysis tool from ArcGIS 10.3.1 was used. First, US State Boundaries [163] where used as a base map and limited to the states of Michigan, Minnesota, and Wisconsin. Transportation data from USA Railroads [164]

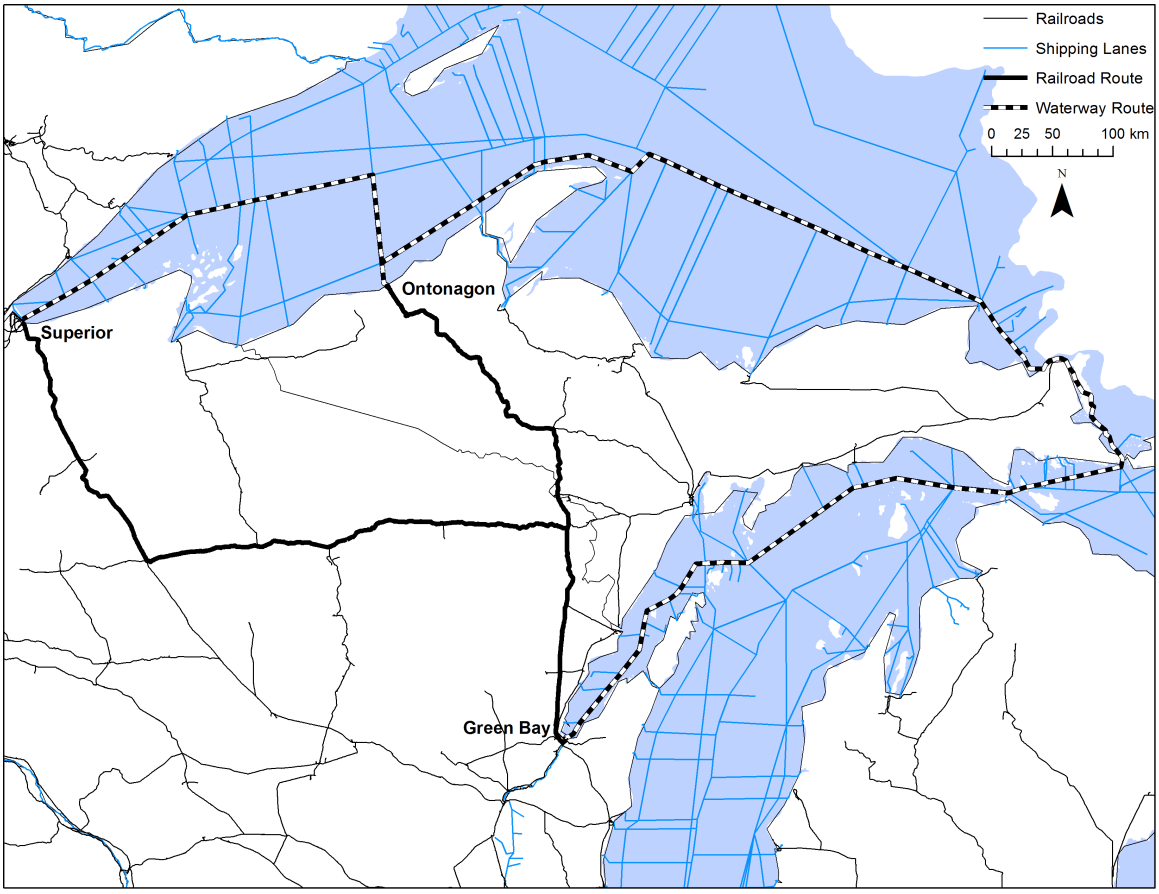

Figure 3.6: Shortest rail and shipping routes from Ontonagon to major blending facilities

and the Commercial Waterway data for the Great Lakes Basin [165], which is derived from National Waterway Network data [166], was used after being clipped to the relevant region. The shortest network was then calculated to each location following both railroad and shipping lanes (Figure 3.6) and is summarized in Table 3.7.

Chapter 4

Integration of Agent-Based Modeling and Life Cycle Sustainability Assessment for the Comprehensive Assessment of Biofuels

Robert Zupko[1]

[1] The material in this chapter has been prepared for submission to *Journal of Cleaner Production*

Abstract

Biofuels, such as those derived from woody biomass, are being developed as one part of a renewable energy portfolio; however, it remains unclear if they can be sustainably developed. Limitations in existing tools to project the impacts of biofuels projects not only limits considering the sustainability of the projects, but determining the quantity of woody biomass feedstocks that may be delivered to a biorefinery or bioenergy facility that is dependent upon the marketplace for supply. This manuscript argues that the integration of agent-based modeling (ABM) and life cycle sustainability assessment (LCSA) to form agent-based LCSA addresses these concerns. To demonstrate the applicability of the method, a case study of a proposed biorefinery in Ontonagon, Michigan, USA is conducted. The case study uses an ABM to model the expected harvest decision making of forest owners and the decision making of loggers to determine if they were willing to supply woody biomass to the biorefinery under a number of different price points. The results from the ABM were used to inform inventory data for projections of environmental impacts, and also projected sustainable impacts for economic and social concerns. The results of the case study show that while Ontonagon is a promising site for a biorefinery, the quantity of woody biomass delivered is a concern along with potential impacts to wetlands in the region. Ultimately, the case study demonstrates the applicability of the method and its application in future research.

Highlights

- Argument for combining agent-based modeling and life cycle sustainability assessment.
- Presentation of an approach to agent-based life cycle sustainability assessment.
- Case study of woody biomass based biofuels using integrated approach presented.

- Case study supports previous LCA findings, projects economic impacts for region.
- Supply of feedstocks may not meet requirements for facility operations.

Keywords: Agent-Based Modeling - Life Cycle Assessment - Life Cycle Sustainability Assessment - Biofuels - Forests

4.1 Introduction

Anthropogenic climate change is an "unprecedented slow-motion global emergency" [167] that requires new thinking, approaches, and policies to avoid adverse outcomes in the future. One climate mitigation strategy that continues to develop is a transition from nonrenewable fossil fuels to renewable energy sources, such as woody biomass. Projections show that woody biomass, and biofuels manufactured using woody biomass, may meet 14% to 18% of the world's energy needs by 2050 [2]. However, it remains unclear if a sufficient supply of woody biomass feedstocks for biofuel can be acquired [3] without excessive negative impacts (e.g., loss of ecosystem services, habitat loss, reduced carbon sequestration, etc.) [4]. These concerns are further compounded by limitations of existing sustainability assessment tools that make it difficult to project the impacts of biofuel projects before they are implemented.

The purpose of this manuscript is to demonstrate how the integration of agent-based modeling (ABM) and life cycle sustainability assessment (LCSA) allows sustainably projections to be made for biorefineries in development. Incorporation of ABM and LCSA into a single method, agent-based LCSA is necessary, since it allows for limitations in both ABM and LCSA to be overcome. Fundamentally LCSA is limited by its inability to properly project the interactions between humans and nature as part of a complex system. This results in data that is not available when evaluating regional potential for the development of biofuels, or though the application

of aggregate (i.e., national scale inventory data) that that neglects localized impacts. While ABM allows the generation of appropriate data by projecting the interactions between humans and nature, it is limited through the lack of a clear approach to sustainability assessment. Thus, the development of agent-based LCSA allows these limitations to be overcome, resulting in a valuable method for evaluating regional potential for woody biomass based biofuels.

This paper is structured primarily in two parts. Part one begins with a justification for the development of agent-based LCSA in Section 4.2, drawing upon the relevant literature. This is followed by a description of the generic methodological approach to agent-based LCSA, in Section 4.3. Part two of this paper concerns a case study application of agent-based LCSA examining a proposed biorefinery in Ontonagon, Michigan, in Section 4.4. The results of this case study are discussed in Section 4.5, along with some broader implications, followed by concluding remarks.

4.2 Agent-Based LCSA

4.2.1 Justification

The objective of sustainability assessment is to evaluate a system to determine if it can continue to operate in its current capacity or if changes to the system are needed [168]. One significant complication in conducting sustainablity assessments is the complexity of the systems being assessed with many biological, ecological systems, and actors operating at different scales [169]. Thus, landscapes are complex mosaics of inter-connected ecosystem services that impact human well-being and vice-versa in multiple ways [170]. The possibility of a "catastrophic shift" in the system due to unsustainable practices or self-reinforcing loops could be exacerbated by the demands upon the ecosystem for bioenergy feedstocks [171, 172]. Similarly, [173] discusses complex systems from the standpoint of "runaway sociocultural niche construction," in which societies and ecosystems form reinforcing feedback loops that directly impact

each other. They argue that agent-based virtual laboratories are needed to apply generative social science techniques (see [20]) to study these feedback loops. Taken together, these concerns may be seen as fundamental issues in assessing the resilience of the system. Resilience, in this context, is defined as "...the degree to which the system can adjust to disturbances without shifting to a new regime" [29, p. 278] (which is a product of the nonlinearity and feedback loops intrinsic to complex systems). Ultimately a tool intended for use by decision makers must evaluate biofuels as part of a complex system, including as much of the product life cycle as possible to ensure that an accurate determination of long and short-term consequences for sustainability can be made.

One means of assessing the impact of biofuels is LCSA, which builds upon existing environmentally-focused life cycle assessments (LCAs) by incorporating life cycle costing (LCC) and social LCA (s-LCA) [30]. In applying LCSA, environmental indicators (e.g., GHG emissions) are evaluated alongside economic (e.g., energy return on investment, or EROI) and social indicators (e.g., protection of heritage sites). These indicators are evaluated for the entire lifecycle, such as cradle-to-gate or cradle-to-grave. As a result, LCSA allows for sustainability assessments to evaluate the "triple bottom line" of environmental, economic, and social concerns [174]. While the triple bottom line may not be truly inclusive of all sustainability concerns related to biofuels [175], it is sufficient to ensure that practitioners are assessing multiple aspects of the impacts of biofuel development and not just a single concern from a global perspective with a social component. As such, LCSA encourages a more participatory approach to the development of sustainability indicators used (see [141, 142, 176]). This participatory approach also has the potential to mitigate environmental and social justice concerns.

Complicating the application of LCSA to the assessment of biofuels is their dependence upon feedstocks (e.g., woody biomass) that is the result of diverse interactions

between landowners and ecosystems. These diverse interactions necessitate incorporation of not only spatial information, but a representation of social diversity. First, localized spatial information offers greater accuracy and regionality (not only for predictive assessments but also for existing product cycles) [33]. Second, actors within a landscape have heterogeneous behavior that alter not only material flows or demands for goods, but also generats "hot spots" of disproportionate negative impacts based upon the location of actors within the landscape (see [177–179]). Both of these factors contribute to impacts, as well as the life cycle inventory (LCI) data to be used in the LCSA (where the LCI is the inventory of flows to and from nature as a result of a product's life cycle). However, unless the LCI data is generated using a regionally appropriate approach, the results of the LCSA may be misleading or incorrect.

One means of generating this LCI data is through the use of ABM to project how humans and nature interact, and to capture these interactions as inventory data. ABM is a computational technique in which software "agents" represent heterogeneous actors in a system. It allows complex systems (i.e., human and environment interactions) to be modeled from the "bottom up" [15, 19]. Recalling the need for landowners to supply feedstocks, the ABM allows diverse decision making to be included (e.g., conservation goals, economic goals, etc.) as well responses to local conditions (e.g., distance to a biorefinery, or the presence of wetlands) to ensure that LCI data is appropriate to the region. This argument is shared by [40] who aruge that as a result of the top-down and aggregate nature of LCSAs, spatial, temporal, and emergent dynamics of a system may not be accounted for, a deficiency that can be addressed by using an ABM to generate LCI data. Finally, while the application of ABM and LCA has been limited, recent critical reviews have noted that their combination allows for more robust LCI data when complex systems are considered [36, 37].

One key limitation to ABM is that sustainability assessment and life cycle thinking is not intrinsic to ABM. Thus, while models can incorporate sustainability indicators,

ABM does not require it. This is a result of ABM being developed as a methodological approach to study complex systems, with a particular emphasis on complex social systems [15], and not in the context of sustainability assessment. One means of addressing this limitation is through the grounding of LCA in formalities such as ISO 14040 [60], which draws upon life cycle thinking. Life cycle thinking is valuable aspect of LCA since it mandates identification of the full scope (i.e., life cycle) of products impacts, which has secondary effects such as helping to mitigate "burden shifting" [180]. Likewise, the framework to LCA provided by ISO 14040 is flexible enough to incorporate ABM. However, LCA in and of itself is narrow (i.e., environmental focus) compared to the broader view of LCSA. As a result, LCSA is preferred in the development of agent-based LCSA since the practitioner is encouraged to take a holistic view of the system being modeled (i.e., incorporation of an agent's actions, the life cycle of the product being evaluated, and interplay inherent between the two). This holistic view is particularly compelling when evaluating the impacts of biofuels projects which can have societal and ecosystems impacts [181, 182].

4.2.2 Prior Approaches

One of the first attempts at developing an agent-based LCSA was by [38] who studied evolving energy infrastructure systems and the role taxes play in energy markets. In their proof-of-concept, agents adjusted decision making based upon a carbon dioxide tax that was, in turn, calculated based upon a simplified LCA of energy sources. The authors found that ABM and LCA could be effectively combined to give insights into how a dynamic system could evolve over time. However, one limitation is that this model failed to integrate spatial information. In a similar study, [42] incorporated ABM and LCA to study mobility policies and electric vehicles. The authors noted that the micro-scale simulation of an ABM helped to avoid bias introduced due to aggregate macroscale LCI data. In the context of biofuels, [41] developed an ABM in which agents representing farmers fed into an LCA to study the adoption of switchgrass as a biofuel feedstock. The authors demonstrated that the ABM could be a

proxy source for social and economic indicators (i.e., crop adoption and profitability) while also projecting environmental impacts using LCA using ABM data.

4.3 Generic Methodological Approach

ISO 14040 [60] offers a means of operationalizing agent-based LCSA as a methodology and calls for connected phases of goal and scope definition, inventory analysis, and impact assessment. (all of which are subject to interpretation intended to improve quality of the LCA) (see Figure 4.1). To illustrate this for agent-based LCSA, the modeler must consider how the ABM will be coupled to the LCSA. As noted by [36], an ABM can feed data into an LCA, the LCA can feed information into the ABM, or data can flow in both directions. However, the modeler must also consider the landscape they are studying. For example, in the case of a biorefinery, multiple actors may ultimately drive the quantity of feedstocks delivered to a facility. While commercial forest owners may be primarily concerned with the economics of a harvest, non-industrial private forest (NIPF) owners may consider economics as well as social perceptions of a harvest (see Figure 4.2). These social perceptions are driven in part

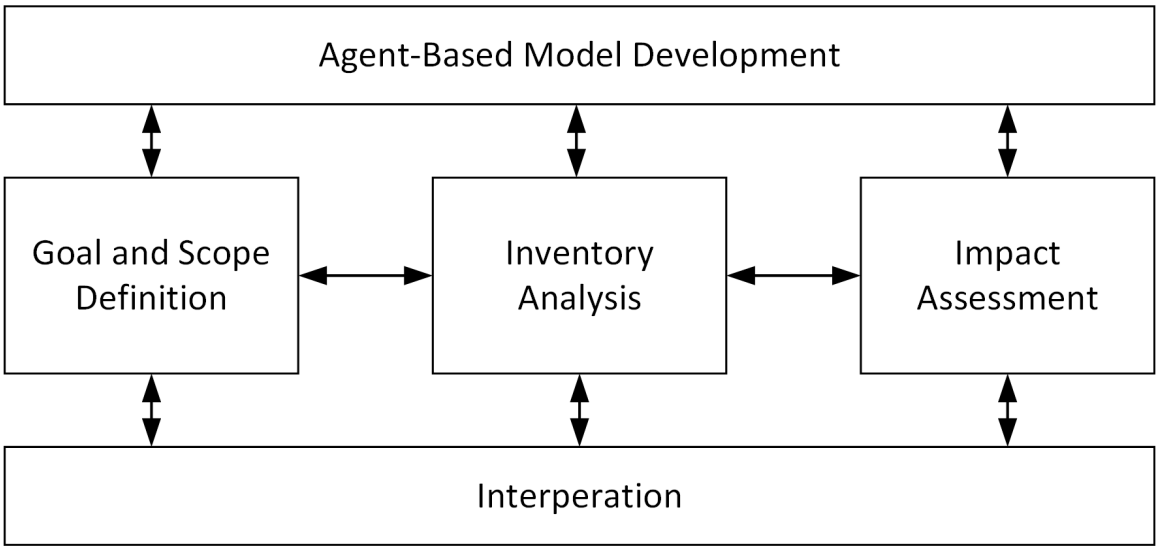

Figure 4.1: Summary of agent-based life cycle assessment phases

by observing previous harvests that took place and result in NIPF owners being less likely to harvest. Thus, while feedstocks produced may be used as part of the LCI, the impacts of the actors upon the landscape also result in feedback loops which may influence the outcome of the study over time. Identifying these feedback loops and landscape impacts helps to refine the scope of the LCSA. Ultimately this means that actors and landscapes that are appropriate for inclusion in the ABM must be incorporated into the LCSA. Furthermore, as development of agent decision making is critical to ABM development [183]; metrics relevant to agent decision making (e.g., profitability of harvests) also play a role in indicator selection. Where possible, the ABM may actually be the source for these results when the impact assessment is conducted, since agents may be queried for model development and execution.

Thus, the development of the agent-based LCSA may follow the same phases as the prototypical LCA. First, the product life cycle defines the broad system boundary

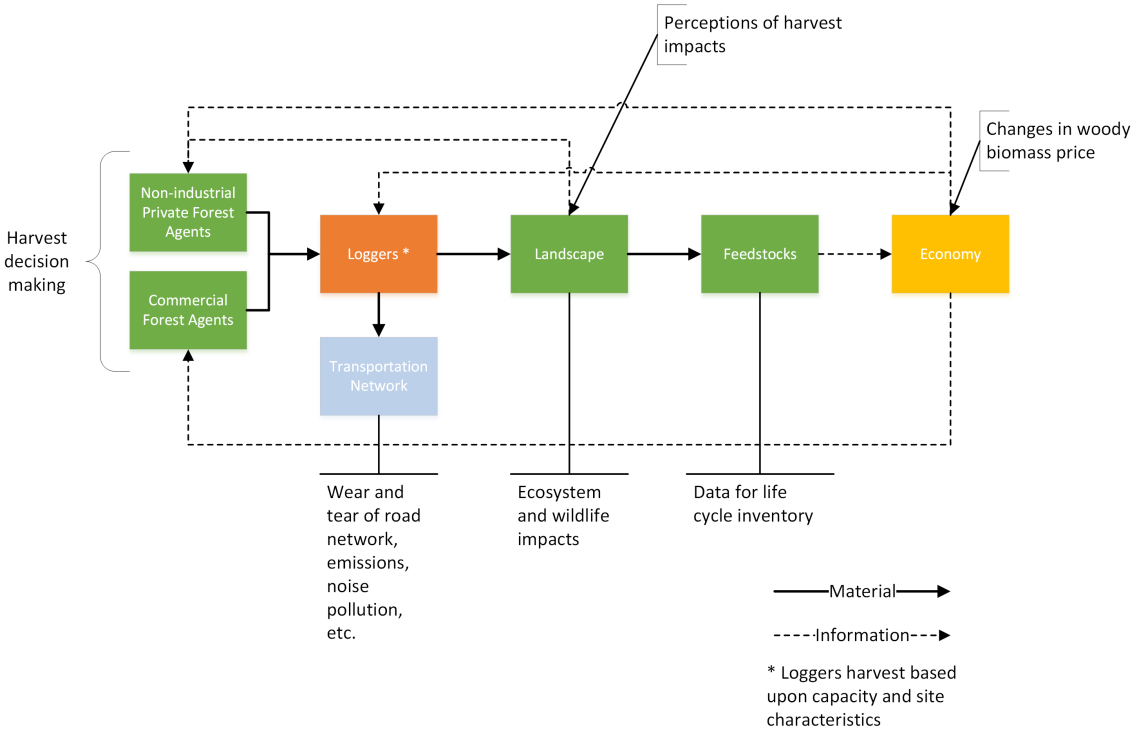

Figure 4.2: Summary of interactions between forest owners, loggers, and the landscape

being assessed. An evaluation of the actors and landscapes in the system boundary helps to delimit the boundaries of the ABM to be developed vice versa in the produce life cycle. This allows the practitioner to assess the relevance of possible impacts of the product (e.g., greenhouse gas, or GHG, emissions) and assess modeling goals to to ensure proper alignment with the assessment. Next, inventory analysis determines the flows from nature to the product and vice versa. The planned ABM may be evaluated to determine if the model contains appropriate sources or sinks for flows, or if they may be abstract entities (e.g., biomass harvested from a simulated forest or pollution emitted to waterway). Furthermore, recalling the coupling of the ABM to the LCSA, considerations for agent decision making may be developed throughout the process. For example, the role that agents have in generating inputs (e.g., timber harvests), or responding to landscape impacts, highlights the need for the LCI and agent decision making to be considered in tandem. Likewise, impact assessment may proceed from the material and energy flows associated with the LCA, but also from agent decision making and variables being considered by the agents (e.g., a count of agents declining to supply feedstocks as an economic indicator). Aggregation of these variables from the ABM may then ultimately result in an indicator for critical evaluation. Finally, per ISO 14040, an interpretive process throughout the LCA would also apply to the ABM during model development and execution.

4.4 Case Study

4.4.1 Introduction

The purpose of this case study is to evaluate the potential impacts that an integrated hydropyrolysis and hydroconversion (IH^2) biorefinery would have on Ontonagon, Michigan and the surrounding region. Ontonagon was selected due to existing commercial interest in constructing a biorefinery in the village [120, 122]. In the process of conducting this case study, the application of agent-based LCSA is also

demonstrated. One complication in presenting this case study is that while descriptions of both ABM and LCA have been formalized [184, 185], the combination of the two has not. Since the Overview, Design concepts, and Details (ODD) protocol [185] doesn't appropriately capture the full scope of an LCSA, the case study is presented using the LCA structure [184] with relevant aspects of the ABM highlighted. The complete description of the ABM is included in Appendix 4.A.

4.4.2 Goal and Scope

The goal of this agent-based LCSA is to conduct a cradle-to-grave assessment a proposed IH^2 biorefinery located in Ontonagon, Michigan. This study builds upon the LCA conducted by [186] and incorporates the same system boundary of feedstock collection and transportation; manufacturing, transport, and use of IH^2 fuels; and disposal of any waste products (see Figure 4.3). As with the predecessor study, ammonia/ammonia sulfate is accounted for as a co-product, but credits were not assigned for it. Life cycle assumptions outlined in the Renewable Fuel Standard (RFS) regarding biomass regrowth and sequestration of carbon released during the use of IH^2 fuels are also incorporated [147]. Unlike the precursor study [186], issues related to market rebounding effects or soil carbon were excluded from the study scope.

The functional unit is one megajoule (MJ) of gasoline or diesel produced through the IH^2 process. An ABM is used to produce data for woody biomass production and transportation data. The environment of the ABM is the forested landscape which consists of 30 m^2 forest stands contained within parcel boundaries registered as commercial forests with the State of Michigan under Michigan law [160, 187]. Two primary types of agents are present in the ABM: forest owners who are responsible for deciding to harvest the forest stands, and loggers who decide if woody biomass should be collected, transported, and sold to the biorefinery. One run of the ABM consists of fifty years with each time step representing one year. To minimize model variance, the

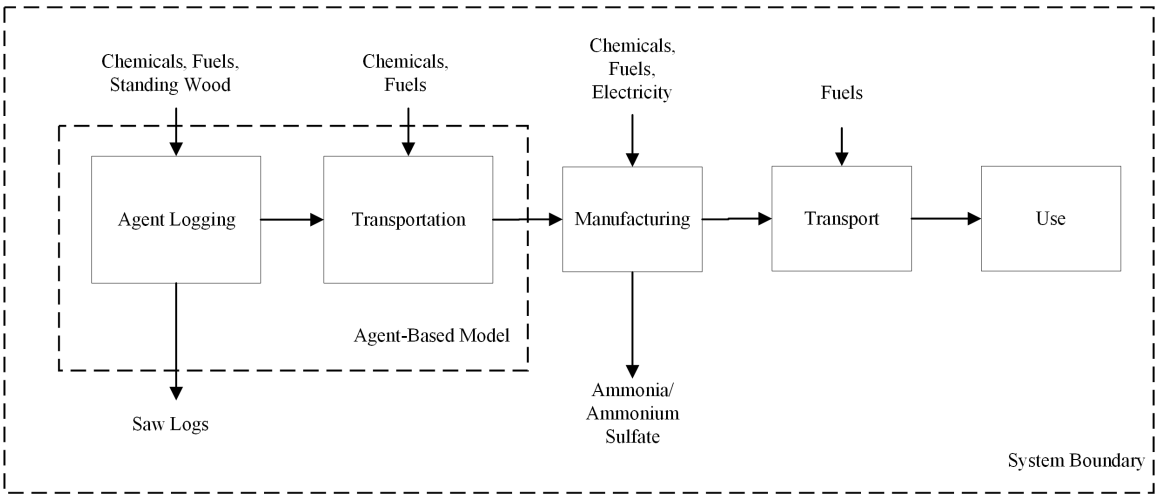

Figure 4.3: Boundary of the agent-based LCSA case study

mean results from fifty model runs were used for the LCI. Data from the ABM as well as inventory items were entered into SimaPro 8.5 [123], and the DATASMART Life Cycle Inventory Package [124] and U.S. Life-Cycle Inventory [125] databases provided additional inventory data. In addition to indicators from the ABM, the Cumulative Energy Demand 1.10 and Greenhouse Gas Protocol 1.02 packages in SimaPro were used to conduct the assessment [126].

4.4.3 IH^2 Description

The IH^2 process utilizes organic feedstocks, such as woody biomass, to produce hydrocarbon fuels (i.e., gasoline and diesel) [114]. These fuels are a direct substitute for petroleum counterparts and are compatible with existing blending and distribution systems. The IH^2 process is briefly summarized as follows: following feedstock aggregation, drying, and resizing, they are introduced to a hydropyrolysis reactor. The reactor produces hydropyrolysis vapors that are directed to a hydroconversion reactor where hydrodeoxygenation and hydrogenation take place in the presence of a catalyst. Hydropyrolysis by-products are either discharged (e.g., H_2O and COx) or redirected for other uses by the biorefinery (e.g., biochar and C1-C3 gases). Previous LCAs of the process found the processes results in approximately 86% to 95%

fewer greenhouse gas (GHG) emissions compared to petroleum counter parts, with a significant degree of variability accounted for by location conditions and facility configurations [114–116, 186]. An LCA conducted for the Ontonagon facility supported these findings. However, it was unclear if sufficient feedstocks to support the facility would be generated by harvesting activity within an acceptable distance [186]. This is a significant concern since the positive environmental value of using biomass decreases the farther feedstocks must travel to a biorefinery to bioenergy facility.

4.4.4 Regional Description

Ontonagon is a rural community located in the Western Upper Peninsula (WUP) region of Michigan which consists of Gogebic, Ontonagon, Houghton, Keweenaw, Baraga, and Iron County. The region contains 13,343 km^2 of forested land. Tourism is a major part of the depressed economy [186, 188], but the forested landscape also makes the region an attractive target for a biorefinery. However, it is unknown if a facility can be sufficiently supplied with local feedstocks. The likely source for feedstocks is commercial forests registered with the State of Michigan, which accounts for about 34% of forests in the region. Owners of registered commercial forests agree follow a formal forest management plan, which includes harvesting, in exchange for a tax incentive [187]. Analysis of the registry indicates that twenty-four commercial entities own approximately 4,031 km^2 of the 4,898 km^2 (about 82%) of registered commercial forests in the region [160]. The remainder of registered commercial forests are held by 816 NIPF owners that consist of family forests as well as other entities (e.g., non-profit organizations, trusts, etc.). Public access to registered commercial forests is a condition of the program, resulting in a number of trails crossing them (see Figure 4.4). As a result, improperly managed timber harvests could negatively affect public perceptions of the biorefinery, the industry, or adversely impact tourism in the region.

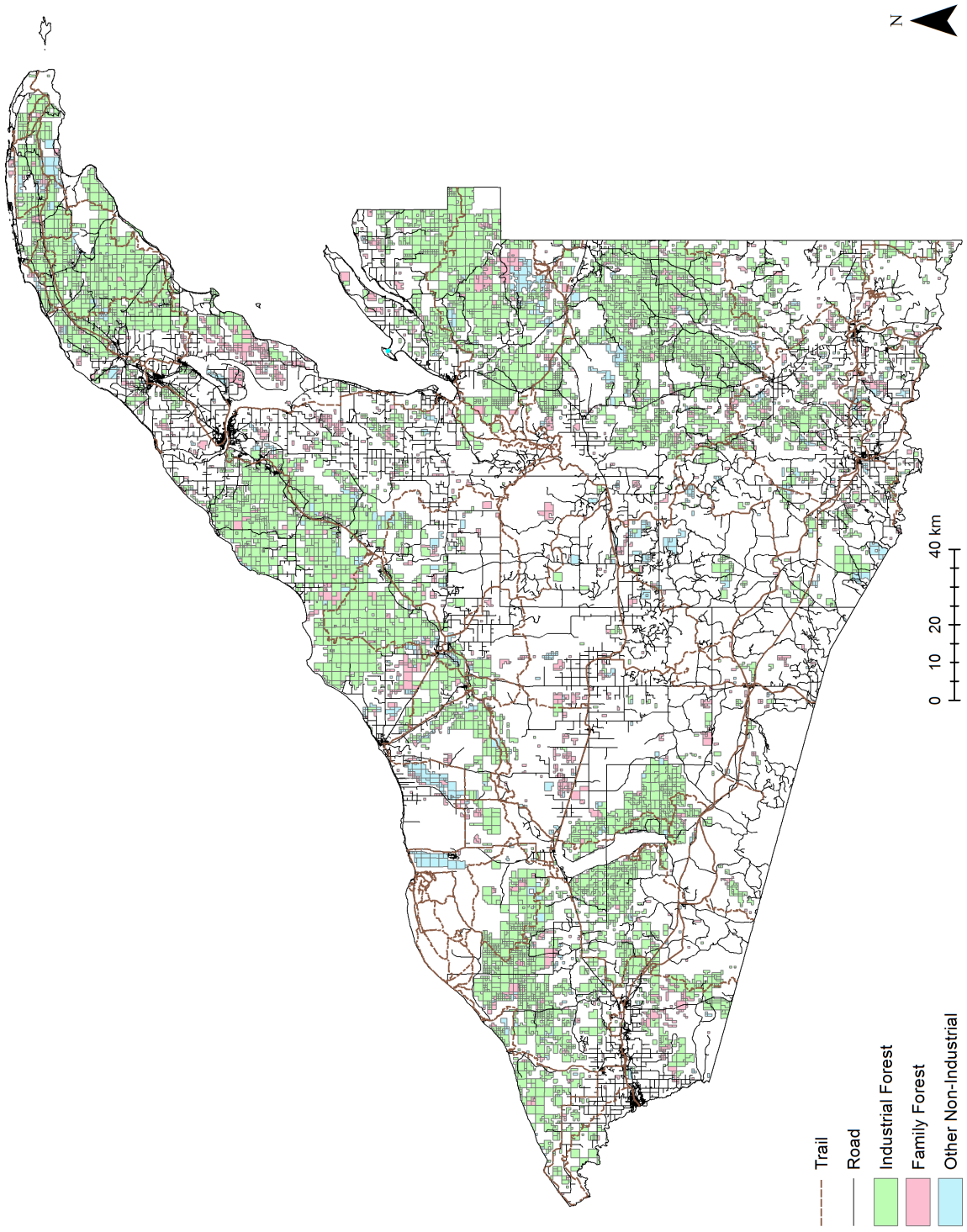

Figure 4.4: Study region with trails, roads, and registered commercial forests

4.4.5 Life Cycle Inventory

The inventory for this case study is based upon previous studies of IH^2 process fuels (see [114–116, 186]) as well as the results of the ABM. The ABM is used to generate LCI data based upon woody biomass collected (see Section 4.4.5.1) and transported to the biorefinery (see Section 4.4.5.2). A summary of key aspects of the model follows in the context of the life cycle stages, while a complete description using the ODD protocol [185], can be found in Appendix 4.A.

4.4.5.1 Feedstock Production

The Ontonagon facility plans to use chipped woody biomass from timber harvests as the primary feedstock for the IH^2 process. Woody biomass is produced during logging operations and consists of the non-merchantable potion of the stem and branches. To be used as a biomass feedstock, it must be collected and chipped to reduce its bulk before transport. Since woody biomass may be used during harvest operations to prevent soil compaction, or used as a soil abatement, the ABM assumes that 30% of it is retained on site, consistent with the previous study [186]. Furthermore, the quantity of woody biomass produced during a harvest is dependent upon the species and maturity of the tree. When a forest owner (i.e., agent) elects to harvest, the merchantable timber and woody biomass is calculated on a per stand basis by the ABM using equations developed by [105] (see Appendix 4.A). Since woody biomass is a co-product of logging operations for saw logs, impacts associated with harvesting are allocated to both the merchantable biomass (i.e., the stem of the tree) as well as the woody biomass. The allocation is calculated based upon the percentage of the above-ground biomass for the tree of the merchantable biomass and woody biomass. Since the biorefinery only generates a new market for woody biomass, no changes to harvest decision making is anticipated. This is a reasonable assumption since the market value of merchantable biomass as pulpwood or saw logs greatly exceeds its

value as woody mass, thus it is unlikely forest owners will harvest exclusively for woody biomass.

The decision to harvest for timber is made by commercial forest agents who manage parcels that are owned by commercial entities, while NIFP agents are assigned all other parcels. These agents may manage multiple parcels of land, which is consistent with ownership patterns. Harvest decision making was based literature data for forest owners in the WUP and similar regions (see [71, 91, 189, 190]). As registrants in Michigan's Commercial Forest Program, it is assumed that agents are economically motivated and seek to produce a profit from their forested land. Since the commercial forest program requires harvesting, social barriers to harvesting such as psychological distance [191], or family legacies and community networks [91] are not considered by the ABM.

Harvest decision making both commercial forest and NIPF agents seek to harvest a minimum of softwood saw logs (i.e., minimum DBH of 22.86 cm). Commercial forest agents also target a consistent area (i.e., patch size) for each year of the model as well. The patch is determined by the total area of forests they control, less a reserve percentage, divided by the number of years they are planning for. When the agents are activated they proceed to harvest the largest contiguous area of forest, with the highest value harvest. During this process wetlands are discounted (i.e., assigned value of zero) due to the complications associated with harvesting them. In the event that no saw timber is available to be harvested, they will decline to harvest that year. Woody biomass is then made available for the logger to sell. If the target patch is greater than a single parcel, they will continue this process until the target patch size is met, or no more saw timber remains. In contrast, NIPF agents randomly select one of their parcels to be bid on. The bid is evaluated to determine if it exceeds their target profit, which is set at model initialization from the range of $\mathcal{N}(\$1292.38, \$304.11)$ per hectare [71]. If the bid is acceptable, the agent will request the harvest takes place and offers woody biomass to the logger at price set at model

initiation from the range $\mathcal{N}(\$73.80, \$55.28)$ per hectare [71, 189]. More complete details can be found in Appendix 4.A.

Agents representing loggers are responsible for conducting requested timber harvests, as well as determining if woody biomass will be collected and sold. The delivered price for chipped woody biomass is fixed at the start of the model. Five price points were examined: \$5.00, \$6.25, \$7.50, \$8.75, and \$10.00 per chipped green ton. The minimum price point was selected based the rate currently expected by managers of commercial forestland [189]. Loggers are presumed to be willing to collect and sell the woody biomass if the payment exceeds their costs by a given margin. Five scenarios were considered for the margin: fixed rates of 5%, 10%, 15%, and 20%, along with variable rates drawn from $\mathcal{U}(5\%, 20\%)$ each activation. These margins were selected due to being within the range of profits by loggers [192] while also allowing for concerns such as fluctuating fuel prices to be absorbed by the model. The costs to the logger for the woody biomass are the sum of the labor and fuel associated with the collection, chipping, and transportation of woody biomass from the job site to the biorefinery, as well as any payment to the landowner.

Table 4.1
Aggregated inventory item for annual woody biomass production

	Item	**Quantity**
Nature	Standing wood	From ABM, green tons
Logging	Diesel	36.63 L/hr * [hours logging]
	Gasoline	0.11 L/hr * [hours logging]
	Grease	0.1 kg/hr * [hours logging]
	Lubricants	2.69 L/hr * [hours logging]
Chipping	Diesel	25.5 L/hr * [hours chipping]
	Steel blades	0.06175 kg/hr * [hours chipping]
Outputs	Chipped woody biomass	From ABM, green tons
	Saw logs, cut-to-length	From ABM, green tons

At the end of each ABM time step, the results of agent harvesting are aggregated to generate the inventory data (see Table 4.1). Since the ABM does not distinguish between different harvesting systems, the inventory is based upon proportional usage using data from regional studies [58] (see Table S1, Electronic Supplementary Material).[2] The hourly consumption rates are then multiplied by the total system hours recorded by the ABM for logging and chipping operations, ensuring that impacts are appropriately attributed to collection of the woody biomass.

4.4.5.2 Feedstock Transport

Chipped woody biomass is loaded on chip vans that then deliver the material to the IH^2 facility. As with feedstock production, transportation is aggregated on an annual basis for the inventory data. Inventory data for transportation are calculated assuming a round trip basis (i.e., from worksite to biorefinery and back) with both the total distance traveled and hours worked being tracked. The inventory is based upon the chip van used in [186] with the consumption of diesel (1.78 km/L), grease (1,257.14 km/kg), and lubricants (3,771.43 km/kg) being accounted for.

4.4.5.3 IH^2 Production, Product Transportation, and Use

Following delivery of chipped woody biomass to the IH^2 facility, the inventory follows the same assumptions as [186]. Briefly this entails the following. First, the regional energy grid is used which deviates from national averages by having a greater reliance on fossil fuels. Second, manufactured IH^2 fuels may be transported to the nearest blending terminal in Superior or Green Bay, Wisconsin by either Great Lakes Barge or railroad. Finally, following delivery to the blending terminal, product use will follow the same usage pattern as the GREET model for the United States [139].

4.4.6 Life Cycle Impact Assessment

The assessment indicators selected for this case study were drawn from the predecessor LCA [186] as well as regional concerns identified by the local community [141, 142].

[2] see Appendix B

Six assessment indicators were selected (see Table 4.2) and were verified against the results of the expert survey by [143] to ensure that global concerns where not overlooked. The assessment indicators incorporate results drawn directly from the ABM (e.g., wetland disturbance, aesthetics, etc.), as well as supplementary analysis using LCI data (e.g., GHG emissions).

The environmental impacts of the biorefinery are assessed through the GHG emissions and wetland disturbance. GHG emissions were selected due to their use in RFS assessments [147], and to allow the IH^2 fuels to be compared to their petroleum counterparts. As there are approximately 2,722 km^2 of wetlands in the WUP region, and 829 km^2 within the area designated as commercial forests, disturbances to them are a concern due to ecosystem impacts. This concern is shared by local residents [141]. To monitor the impacts to wetlands, the total area of harvests impacting wetlands, as indicated by NCLD data (see Appendix 4.B), is tracked by the ABM.

Table 4.2
Indicators selected for impact assessment

Principle	**Criteria**	**Indicator**	**Method**
Environment	Air and GHGs	GHG Emissions	Greenhouse Gas Protocol
	Ecosystems and wildlife habitat	Wetland Disturbance	Regional analysis and monitoring in ABM
Economic	Economic viability	EROI	Extended EROI
	Competition for resources	Availability of woody biomass	Results from ABM
Social	Cultural value	Aesthetics, forest cover	Regional analysis and monitoring in ABM
	Contributions to local economy	Employment	Labor required to produce woody biomass

Two economic indicators were selected: the energy return on energy invested (EROI) was selected along with availability of woody biomass. The EROI is calculated using the extended EROI approach by [133]. This approach evaluates the total energy returned to society ($Energy_{out}$), by the total energy required to produce that energy ($Energy_{in}$), or,

$$EROI = \frac{Energy_{out}}{Energy_{in}} \tag{4.1}$$

The cumulative energy demand to produce the IH^2 fuel, as calculated by SimaPro, is used for $Energy_{in}$ while conventional gasoline is assumed to produce 46.536 MJ/kg when consumed and 45.575 MJ/kg for low-sulfur diesel [134]. While residents of the region have a number of economic concerns [142], sufficient supply as woody biomass was selected for this case study due to its criticality in facility operations. The developers of the IH^2 biorefinery, SynSel, have indicated that they intend to use "...1,900 tons of wood waste per day and [produce] 90,000 gallons of synthetic fuel ..."[3] [121]. This equates to an annual consumption of approximately 574,550 green tons per 8,000 hours of operation, where 8,000 is a typical target up-time for planning purposes. The quantity of woody biomass produced during logging and delivered to the biorefinery is tracked by the ABM, the basis for assessing the availability of woody biomass.

Assessment of social concerns is a challenge for this case study, since some key concerns identified by WUP residents are either unlikely to be affected by the biorefinery (e.g., access to recreation areas), or cannot be assessed *a priori* (e.g., work conditions). Community concerns within the parameters of the study are employment and aesthetics [141]. While employment may be considered an economic concern, it effectively acts as a hybrid indicator due to the significant role it plays in society and sustainable development [193, 194]. Employment was therefore treated as a social

[3] 1,723.651 metric tons of green woody biomass to produce 340,687.06 liters of fuels

indicator for this study and is assessed based upon the increased demand for labor directly attributable to woody biomass collection, processing, and transport.

Local residents also indicate that they value forest aesthetics [141, 142], but qualifications of the subjective impacts of clear-cutting can be quite variable (see [195–197]). However, the spatial coupling of the ABM does allow the identification of harvesting that may take place within possible view of the public. Given the public tendency to view the results of recent logging as having a "negative" aesthetic value, [195] accounting for harvesting visual by the public is a reasonable means of assessing the aesthetic impacts. As a result, this study designated a buffer zone along roads and trails as "visually sensitive" (see Appendix 4.B) to account for the impacts of harvesting. The total area of the buffer zone is approximately 2,313 km^2 for the WUP region and 356 km^2 is within registered commercial forests. The aggregate harvest that takes place within this buffer is tracked by the ABM and reported as having a likely negative impact upon forest aesthetics.

Table 4.3
Comparison of production of chipped woody biomass and potential biorefinery operations under various woody biomass pricing scenarios

	Price per Green Ton				
	\$5.00	\$6.25	\$7.50	\$8.75	\$10.00
Logger, hr	$5,156.27 \pm 807.35$	$6,924.70 \pm 905.05$	$9,750.01 \pm 592.20$	$11,805.92 \pm 651.64$	$12,311.39 \pm 661.40$
Driver, hr	$8,015.55 \pm 725.86$	$13,058.21 \pm 1,218.28$	$23,443.31 \pm 1,541.65$	$32,016.47 \pm 2,099.59$	$34,316.08 \pm 2,591.96$
Biomass, green tons	$229,917.90 \pm 35,999.54$	$308,772.39 \pm 40,356.15$	$434,752.87 \pm 26,406.34$	$526,425.94 \pm 29,056.46$	$548,964.73 \pm 29,491.90$
Biomass, % of potential	$41.87\% \pm 5.96\%$	$56.33\% \pm 4.84\%$	$79.43\% \pm 1.73\%$	$95.66\% \pm 1.47\%$	$99.09\% \pm 0.42\%$
Ops, hr	$3,201 \pm 501$	$4,299 \pm 562$	$6,053 \pm 368$	$7,330 \pm 405$	$7,644 \pm 411$

4.4.7 Results

Following execution and analysis of the ABM for all price points (see Section 4.4.8), the results of the $8.75 per green ton with variable logger margins scenario was used for the assessment. This price point is reasonable considering it is the lowest rate at which 80% operational hours per year is met. The life cycle GHG emissions for the IH^2 fuels was calculated at 10.76 $\pm$ 0.03 g CO_2 equiv/MJ for diesel and 10.43 $\pm$ 0.02 g CO_2 equiv/MJ for gasoline. The results are tightly bound with diesel having a range of 10.72 to 10.8 g CO_2 equiv/MJ and gasoline has a range of 10.39 to 10.46 g CO_2 equiv/MJ over the 50 year time frame of the ABM (Figure 4.5). When evaluated under RFS guidelines, there is an 88.06% reduction in GHG emissions for diesel and an 88.56% reduction for gasoline. These figures are quite similar to the previous study using an aggregation approach which found 11.08 g CO_2 equiv/MJ for diesel and 10.73 g CO_2 equiv/MJ for gasoline [186].

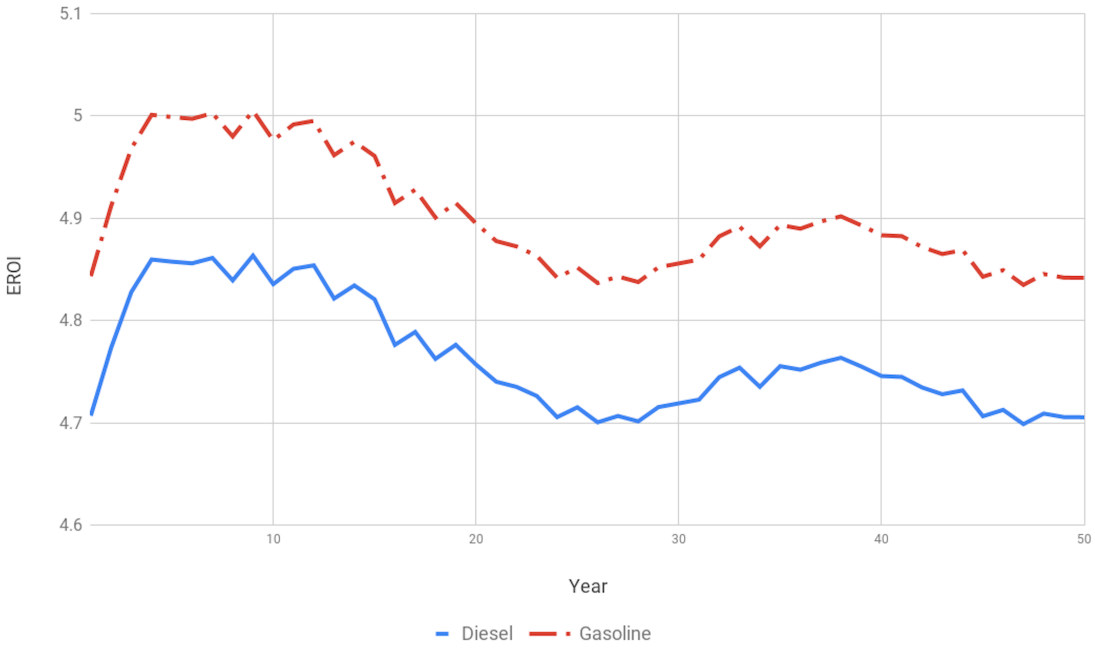

Figure 4.5: Fluctuations in EROI over the course of the model for diesel and gasoline

Production of 1 kg of diesel was found to have a cumulative energy demand (CED) of 9.57 ± 0.2 MJ for an EROI of 4.76 ± 0.05. Similarly 1 kg of gasoline required 9.5 ± 0.18 MJ of energy resulting in an EROI of 4.9 ± 0.06. Similar to the GHG emissions, the cumulative energy demands have a fairly tight range of 9.37 to 9.7 MJ for diesel and 9.3 to 9.63 MJ per kg of diesel and gasoline produced, respectively (see Figure 4.6). The EROI represents a fairly significant increase of 13.6% for diesel and 13.69% for gasoline over the previous study. As the manufacturing assumptions remain unchanged, this is attributable to the improvements in calculating the woody biomass collection and transportation due to the ABM accounting for variance between years (as opposed to an allocation model).

Availability of woody biomass is a concern for the biorefinery as there is significant variance in the quantity delivered under the various price points (see Table 4.3). Over the 50 year period of the ABM an average of 118,556 system hours of logging

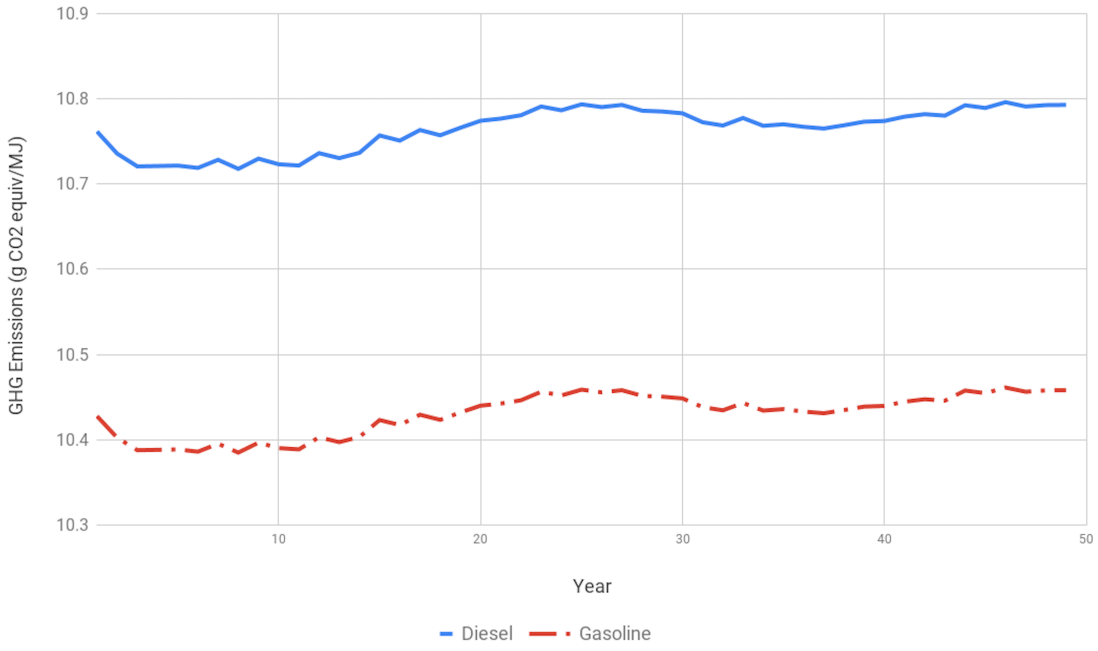

Figure 4.6: Fluctuations in GHG emissions of the course of the model for diesel and gasoline

operations resulted in 1,971,688.28 ± 93,846.77 green tons of removals yielding in 550,285 ± 28,278 harvestable green tons of woody biomass with 526,425 ± 29,056 green tons delivered (95.66% of total possible). This would result in sufficient supply for 7,330 ± 405 hours of production by the biorefinery, or about 83.68% uptime. While this is short of the 8,000 hours commonly used for planning, it may be acceptable given the first-generation nature of the facility and the need to work with solid materials as a feedstock. Furthermore, the fact that the ABM failed to meet the target of 139,318 system hours of logging within the bounds of the registered commercial forests allows for the possibility of additional feedstocks from logging on other forested lands. Under the $8.75 per green ton scenario, 11,805.92 additional hours of work for loggers would be generated and 32,016.47 hours for drivers of chip vans. In total this would result in $927,564.20 in additional wages being paid, assuming national averages for hourly pay (see Appendix 4.A). While this represents a positive contribution to the local economy, quantifying the results in terms of the number of jobs created is difficult because the totals are low enough to potentially be absorbed by existing employed persons (e.g., part-time employees moving to full-time employment).

Given a typical total annual harvest of 5,147.85 ± 563.67 hectare, the ABM projects that 517.08 ± 134.69 hectare of wetlands (about 10% of the land harvested) and 128.35 ± 17.61 hectare of visually sensitive forest (about 2.5% of the land harvested) would be impacted each year (see Figure 4.7). In aggregate over 50 years, the ABM projected that 31.21% of wetlands within registered commercial forests and 9.5% of wetlands in the WUP are impacted by logging operations. Additionally, 18.02% trails within registered commercial forests and 2.77% of trails in the WUP are impacted. As these impacts are coupled to the underlying timber operations, they are consistent throughout all of the scenarios evaluated (see Section 4.4.8). While the aesthetic impacts to the landscape can be mitigated through the use of visual buffers during the time of harvest, the wetland impacts are more concerning. These wetland impacts occurs despite a model basis against harvesting them (e.g., no value

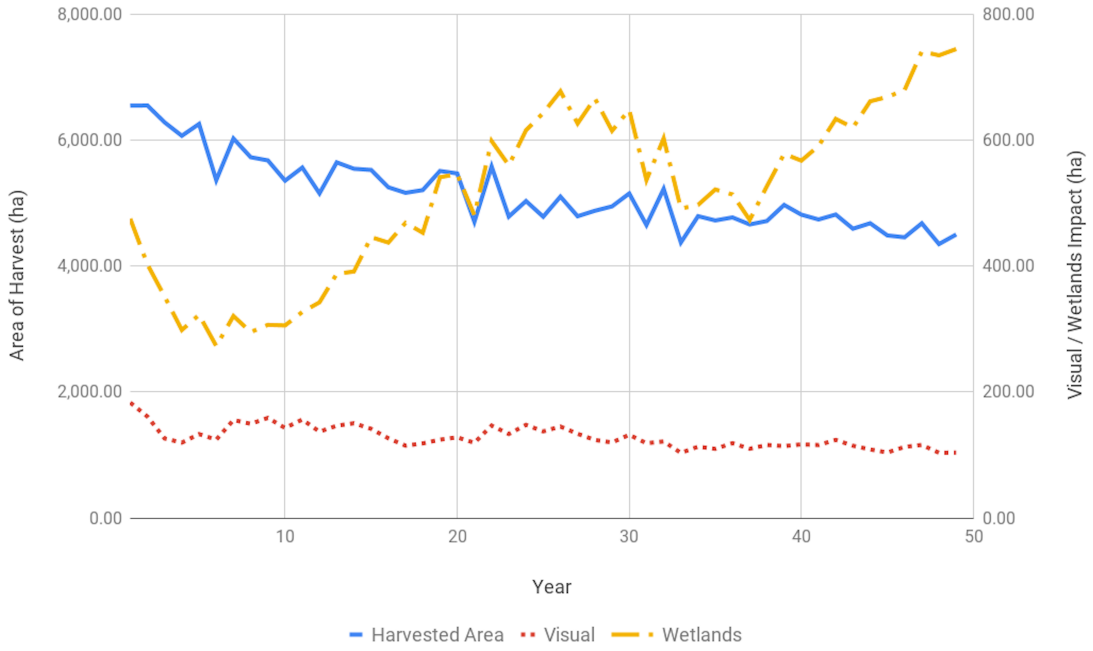

Figure 4.7: Annual harvesting, wetlands, and visual impact in hectares at $8.75 per green ton, other prices exhibit a similar pattern

for timber in wetlands) (see Section 4.A.7.3), implying that timber harvests inevitably impacts wetlands in the region.

4.4.8 Sensitivity Analysis

Sensitivity analysis of the model began with adjustments to the economic parameters (i.e., price per green ton and logger margins). This informed not only the conditions for the assessment (see Section 4.4.7), but also how the model responds to changes in prices or logger margins. As shown in Table 4.4, the EROI, CED, and GHG emissions are fairly consistent across all of the price points. Some trends are apparent in the results and a negative linear relationship exists for CED and GHG emissions, while EROI has a positive one. These relationships are likely due to the allocation of impacts used in the LCA, since the percentage is unchanged by lower delivery rates of woody biomass. While the allocation could be adjusted so that only woody biomass

consumed is used, this is inappropriate since the intent of the biorefinery is to use the woody biomass that is a co-product of harvesting activities.

While it is expected that loggers will have variable margins, the model uses a uniform distribution to produce sufficient stochasticity, while a normal distribution is more likely (i.e., loggers are likely to be targeting a common profit margin for their business). Since $\mathcal{U}(5\%, 20\%)$ results in a mean of 12.5% and a variance of 0.19%, the variable margins used the model approximate a fixed margin of 12.5%. This is demonstrated by the results in Table 4.5 where \$7.50 per green ton was offered for woody biomass. To evaluate the behavior of the model different margins, fixed margins of 5%, 10%, 15% and 20% were evaluated when \$7.50 per green ton was offered. The results of this evaluation show that the model behaves in an intuitive manner with higher margins leading to lower deliveries (and *vice versa*). When \$7.50 per green ton is offered, the model projects a negative linear relationship that is well described by a linear regression ($R^2 = 0.998$). This is consistent with the positive linear relationship in the model between prices and operations at \$8.75 per green ton, with variable margins ($R^2 = 0.993$). This implies that the ABM may be used to construct economic models that would be useful to developers of biorefineries or bioenergy facilities, although care is required to ensure that the model's assumptions were in line with the region.

Table 4.4
Calculated EROI, CED, and GHG emissions for diesel and gasoline at various price points

	Diesel			**Gasoline**		
	EROI	CED	GHG Emissions	EROI	CED	GHG Emissions
\$ 5.00	4.52	10.09	10.91	4.65	10.01	10.58
\$ 6.25	4.49	10.16	10.93	4.62	10.08	10.59
\$ 7.50	4.69	9.71	10.81	4.83	9.64	10.47
\$ 8.75	4.77	9.56	10.76	4.90	9.49	10.43
\$10.00	4.77	9.55	10.76	4.91	9.48	10.43

Table 4.5
Comparison of production of chipped woody biomass and potential biorefinery operations under various logger margins at $7.50 per green ton

	Targeted Margin				
	5%	10%	15%	20%	Variable
Logger, hr	$11,025.15 \pm 561.15$	$10,209.27 \pm 542.93$	$9,239.25 \pm 577.39$	$8,282.45 \pm 643.31$	$9,750.01 \pm 592.20$
Driver, hr	$28,593.80 \pm 1,769.90$	$25,197.88 \pm 1,848.91$	$21,293.71 \pm 1,675.69$	$17,665.33 \pm 1,550.88$	$23,443.31 \pm 1,541.65$
Biomass, green tons	$491,611.51 \pm 25,021.67$	$455,231.34 \pm 24,209.34$	$411,978.33 \pm 25,745.70$	$369,314.33 \pm 28,685.39$	$434,752.87 \pm 26,406.34$
Biomass, % of potential	$89.81\% \pm 1.77\%$	$83.03\% \pm 1.75\%$	$74.98\% \pm 2.10\%$	$67.21\% \pm 2.82\%$	$79.43\% \pm 1.73\%$
Ops, hr	$6,845 \pm 348$	$6,339 \pm 337$	$5,736 \pm 358$	$5,142 \pm 399$	$6,053 \pm 368$

Next, the sensitivity of the model to the site of the biorefinery was evaluated using five alternative sites in the WUP region: Bruce Crossing, Copper Harbor, Greenland, L'Anse, and Toivola (see Figure 4.8). Copper Harbor was selected since it is one of the farthest points away from Ontonagon, while L'Anse has previously been identified as an ideal location [198]. The remaining sites were selected due to their proximity to major roads and forests in the region. Following calculation of the transportation distances for the alternative sites (see Appendix 4.B), the model was run using variable margins and $8.75 per green ton of feedstock delivered. Across all scenarios the timber harvest was consistent, and Copper Harbor had the least woody biomass delivered (see Table 4.6) while the results for Greenland are similar to Ontonagon. Interestingly, while L'Anse is not as central to the study region as Ontonagon or Greenland, woody biomass deliveries are only nominally lower. Furthermore, despite Bruce Crossing's proximity to Ottawa National Forest, biomass delivery rates were unexpectedly low. This is likely attributed to Bruce Crossing lacking immediate proximity to registered commercial forests.

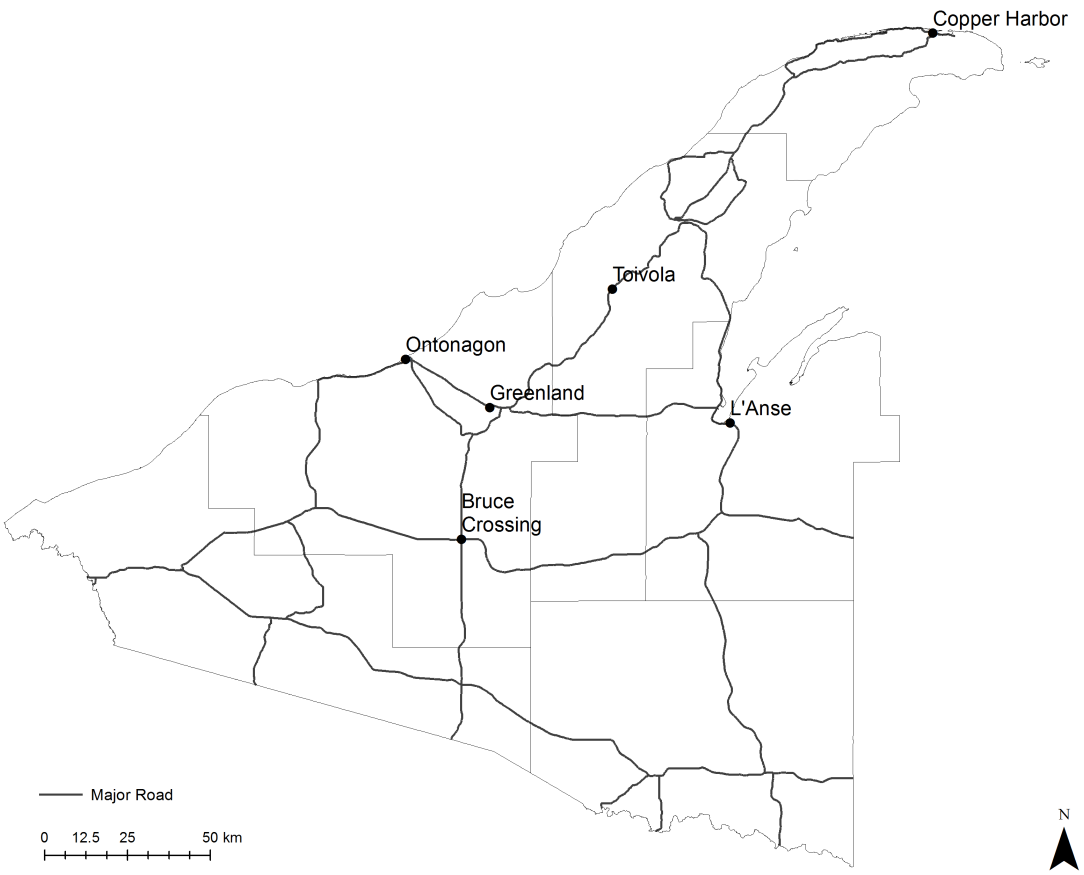

Figure 4.8: Alternative sites for a biorefinery used for sensitivity analysis

Finally, the sensitivity of the model to the area of the commercial forests was evaluated by using state and federal lands as a proxy for additional industrial forests. Parcels were included where owned by the State of Michigan, the Michigan Department of National Resources, or the federal government (e.g., "U.S. Government"), regardless of whether harvesting is permitted or not in practice. The parcels were then aggregated based upon the owner (see Figure 4.9) and the model was then run using variable margins and \$8.75 per green ton of feedstock delivered. The model projected a total of 134,283.76 ± 3,661.06 system hours of logging with 1,342,837.57 ± 36,610.56 green tons of timber harvested per year. In contrast to the other scenarios, the annual harvest limit was met or exceeded for some years. Additionally,

Table 4.6
Sensitivity of the model to alternative sites for a biorefinery, at $8.75 per green ton with variable margins.

	Possible Alternative Sites				
	Bruce Crossing	Copper Harbor	Greenland	L'Anse	Toivola
Logger, hr	10,430.70 ± 409.82	10,086.02 ± 437.12	11,813.45 ± 507.18	11,538.85 ± 559.35	10,739.54 ± 401.36
Driver, hr	25,792.05 ± 798.17	24,988.17 ± 874.25	27,006.25 ± 1,158.28	25,475.21 ± 1,289.09	26,316.00 ± 692.31
Timber, green tons	1,185,492.13 ± 71,761.99	1,184,308.59 ± 71,180.01	1,183,899.17 ± 74,444.85	1,185,499.24 ± 77,493.27	1,185,803.92 ± 70,368.81
Biomass, green tons	465,104.93 ± 18,273.87	449,735.66 ± 19,491.38	526,761.74 ± 22,614.94	514,517.48 ± 24,941.42	478,875.89 ± 17,896.81
Biomass, % of potential	84.59% ± 1.52%	81.88% ± 1.88%	95.95% ± 0.95%	93.61% ± 1.51%	87.06% ± 1.39%
Ops, hr	6,476 ± 254	6,262 ± 271	7,335 ± 315	7,164 ± 347	6,668 ± 249

579,359.50 ± 26,382.11 green tons of woody biomass (96.93% ± 1.13% of total possible) were projected to be delivered to the biorefinery resulting in 8,067 ± 367 hours of operation. This shows that the model is sensitive to the total area of the registered commercial forests and supports the conclusion that supply is a concern if facility managers are solely dependent upon harvest in commercial forests.

4.4.9 Validation

Model validation is a typical aspect of ABM development [56], but in the case of this agent-based LCSA, the lack of similar operating IH^2 biorefinaries prevents validation against a known standard. However, one possibility for validation is to use proxy data from sites such as the cellulosic ethanol biorefinery that was planned for Kinross, Michigan [199]. As part of the facility planning, an assessment of timber harvests in the region supplying the facility was conducted and annual removals where found to be approximately 3.6 million green tons [200]. While this figure is significantly higher

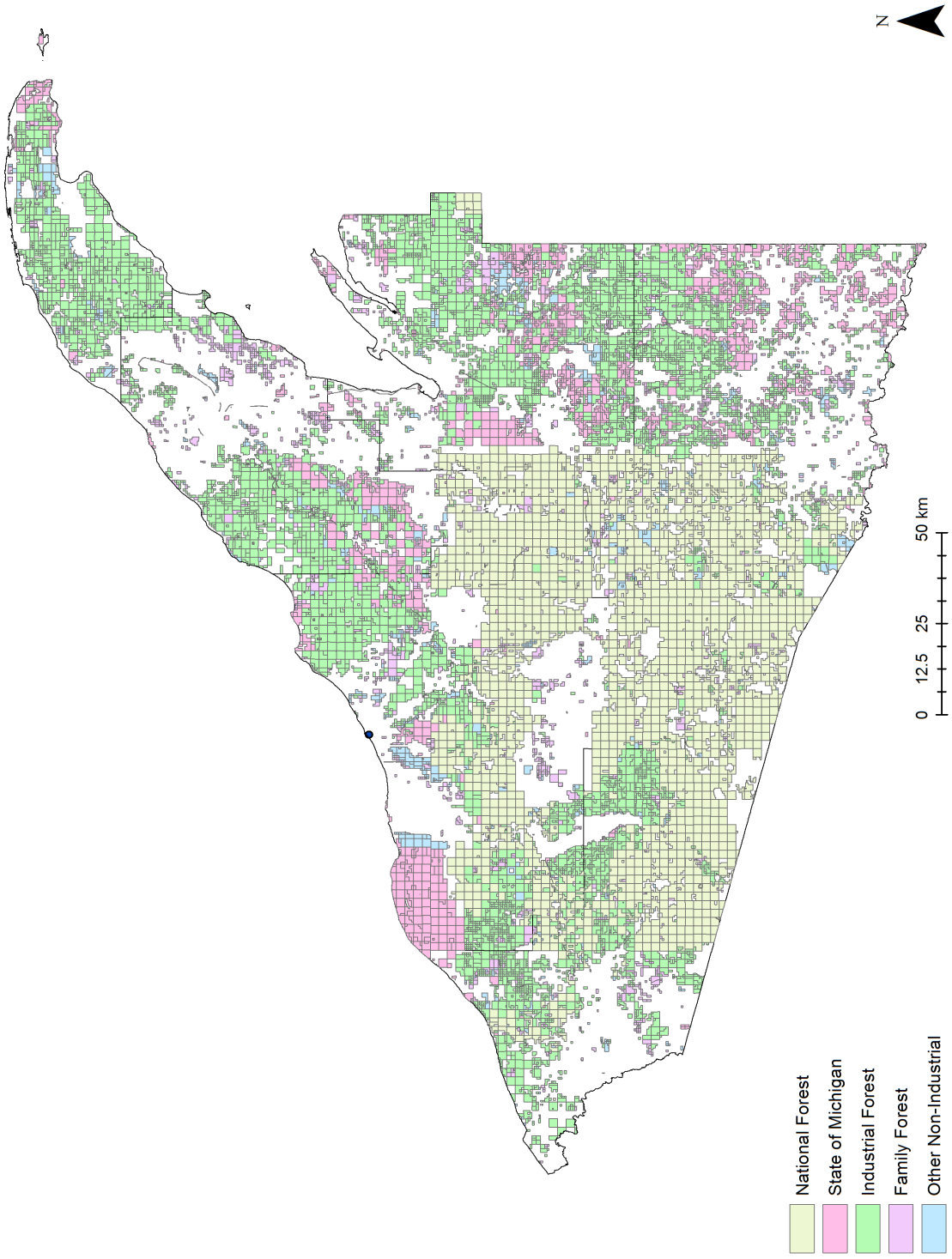

Figure 4.9: Parcels used when evaluating the sensitivity of the model to the total area of the commercial forests

than the approximately 2.0 million green tons projected by the model, the assessment includes both the Eastern Upper Peninsula and northern portions of the lower peninsula of Michigan. As such, the results for the Kinross study are questionable given the Mackinac Bridge acting as a "choke point" for deliveries from the Upper Lower Peninsula to Kinross, Michigan.

Another possibility for model verification is comparison against forest loss as revealed by Landsat imagery, which informs the Global Forest Change (GFC) data set [201]. To conduct the assessment, the GFC data was clipped to the WUP region and the latitude of Ontonagon, Michigan (46.8711°N) was used to convert the GFC pixels, in arc-seconds, to meters. The GFC data showed a measured losses for the years 2001 to 2018 of 4,302.24 ± 1,310.35 hectares per year, with harvesting increasing closer to the year 2018 (see Figure 4.10). While the mean of the GFC losses is below the 5,147.85 ± 563.67 hectares per year projected by the model, it is within

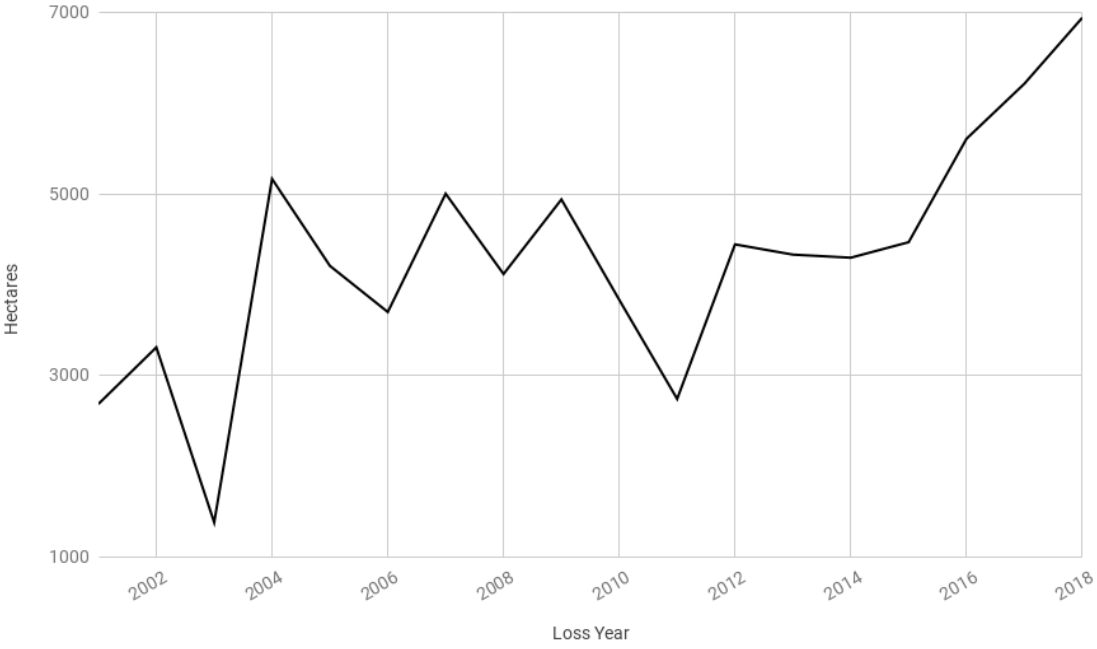

Figure 4.10: Annual forest loss, in hectares, in the Western Upper Peninsula region, as determined using Global Forest Change data [201]

the range of permissible values and doesn't exceed the maximum single year loss of 6,943.14 hectares in the GFC data. This supports the overall validity of the model, although the mean harvesting projected may be considered to be optimistic with a percent error of approximately 20% against the GFC data. However, if the trend of increased harvests from 2014 to 2018 continues or represents a new baseline average of 5,508.40 ± 1,129.78, the model results would in fact be slightly low compared to the GFC data with a percent error of about -6.5%.

4.5 Discussion

4.5.1 Case Study

The results of the case study offers indicate that an IH^2 biorefinery may be successful if sited in Ontonagon, Michigan. The GHG emissions are consistent with previous studies [114–116, 186] and continue to support the conclusion that IH^2 fuels will meet RFS requirements. Additionally, an improvement in the EROI is projected due to a better understanding of the feedstock sources allowed by the ABM. Economically the major concern for the facility would be ensuring a constant and consistent supply of feedstocks that meet the facility's uptime targets. Since the model projects that registered commercial forests are unlikely to supply sufficient feedstocks for 8,000 hours of annual operation, planners need to explore how the gap may be closed. Additionally, since the model uses a time step of a full year, the actual supply may be inconsistent throughout the year and significant on-site storage may be needed. Finally, while the model projects an increase in work for loggers and truck drivers, it may not be significant enough to generate many new, full-time, jobs within those fields.

In the context of the landscape as a whole, the projected impacts to wetlands within registered commercial forests are significant over the fifty year time span examined. While these may not be as a result of woody biomass harvests specifically,

impacts to them are attributed to the IH^2 fuels as a result of the feedstocks used. This attribution is consistent with life cycle thinking and is something that facility operators would need to be mindful of if they wish to use feedstocks with minimal environmental impacts. Furthermore, changes in policy that prevent logging in wetlands or avoidance of them by loggers would reduce the quality of feedstocks that are supplied under this model. As with the projections for the quantity of feedstocks, this supports the recommendation that facility operators develop additional sources of feedstocks. While the impacts on aesthetics due to harvesting in visually sensitive areas is fairly low in the context of total area, the impact that these harvests have may be quite high if they are in heavily traveled areas. While not an aspect of this study, travel information could be incorporated into future models to determine the high travel areas. However, aesthetic impacts may also be mitigated completely if visual buffers are mandated since harvesting could shift to other available forested land.

Interpretation of the results of the agent-based LCSA must be done with a note of caution. While extremely precise figures are being generated as a result of the model, these are fundamentally projections that are the result of multiple iterations of the model due to the underlying stochasticity. As such, the results need to be interpreted with an awareness of the sensitivity of the model. However, this is typical with any LCA [184].

Another limitation of this study is that rebound effects were not evaluated, a significant concern when evaluating biofuels [148, 158, 202]. While a basic projection of the rebound effects can be conducted (see [186]), a more appropriate application of agent-based LCSA would be to incorporate a marketplace for the biofuels and allow agents to respond to these changes. This could be done at the level of just the loggers and biorefinery operations (i.e., increase or decrease price paid for woody biomass in response to market forces). However, a more appropriate application would be to include the consumers of the fuels, allowing rebounding effects to be studied. However,

such a model is beyond the scope of this case study since it would expand the scope of the agents involved.

4.5.2 Broader Implications

Recalling the objective of this manuscript to demonstrate how agent-based LCSA allows sustainablity projections to be made for biorefineries in development, the results of the case study demonstrate the effectiveness of the technique. While some of the conclusions from the case study may be intuitive (e.g., use of visual buffers will have minimal impact upon the overall supply of woody biomass), others such as the quantity of woody biomass projected to be supplied are quite significant to biorefinery and bioenergy siting. Furthermore, replication of the GHG emissions from the previous LCA in the region [186] acts as a form of cross-validation of the approach demonstrating its ability to yield useful results.

McKone et al. [203] noted several "grand challenges" for the LCA of biofuels. These grand challenges include our understanding of feedstock production, spatial heterogeneity, accounting for changes over time, and the uncertainty and variability associated with assessments of biofuels. The case study demonstrated that agent-based LCSA is capable of addressing some of these grand challenges. First, the model allows for a better understanding of the source and production of feedstocks, as noted by the price and margin scenarios performed. Second, the ABM is generating LCI data based upon projected harvesting in a virtual landscape, allowing spatial heterogeneity to be incorporated into the results. Likewise, the ABM allows time to be a factor in the assessment and trends over time to be assessed. Finally, the underlying stochasticity of the processes involved are accounted for in the model, allowing stakeholders and policy makers additional information when considering the role that biofuels may play within their communities.

4.6 Conclusion

Biofuels are commonly cited as one component of climate change mitigation strategies, but determining if they can meet projected needs without adverse impacts is a complicated endeavor. The development of biofuels takes place within in a complex system in which the interactions of multiple parties (e.g., landowners, feedstock harvesters, facility operators, etc.) along with the landscape play a role in their successful development. While techniques such as ABM and LCSA may be capable of evaluating the sustainability of components of this complex system, they are each limited. Their integration into agent-based LCSA overcomes these limitations. The case study of the proposed IH2 biorefinery in Ontonagon, Michigan demonstrates the applicability of the technique to project possible impacts. While the site is promising, there are concerns related to the feedstock supply and impacts to wetlands in the region.

Supplementary Material

4.A Agent-Based Model

This section provides a description of the agent-based model (ABM) used in the case study described in Section 4.4. This description follows the ODD (Overview, Design concepts, Details) protocol [185, 204] The model is built upon the ForestSim ABM platform [205] which drives the overall architecture of the model (see Figure 4.11). The source code for the model can be found at https://github.com/rjzupkoii/cabals/tree/master/model under the MIT License.

4.A.1 Purpose

The primary purpose of this model is to generate life cycle inventory (LCI) data and sustainability indicators for a life cycle sustainability assessment (LCSA) of an integrated hydropyrolysis and hydroconversion (IH^2) biorefinery in Ontonagon, Michigan. This is accomplished by modeling the decision making that plays a role in the collection, processing and transport of woody biomass to the biorefinery as well as the forested environment. Since the model is intended to evaluate the sustainability impacts of the refinery, a fifty year time span was selected since it slightly exceeds the forty years typically used for planning large capital projects. During model execution, data related to the location and quantity of woody biomass is produced for the LCI allowing for a more accurate understanding of the environmental impacts of the

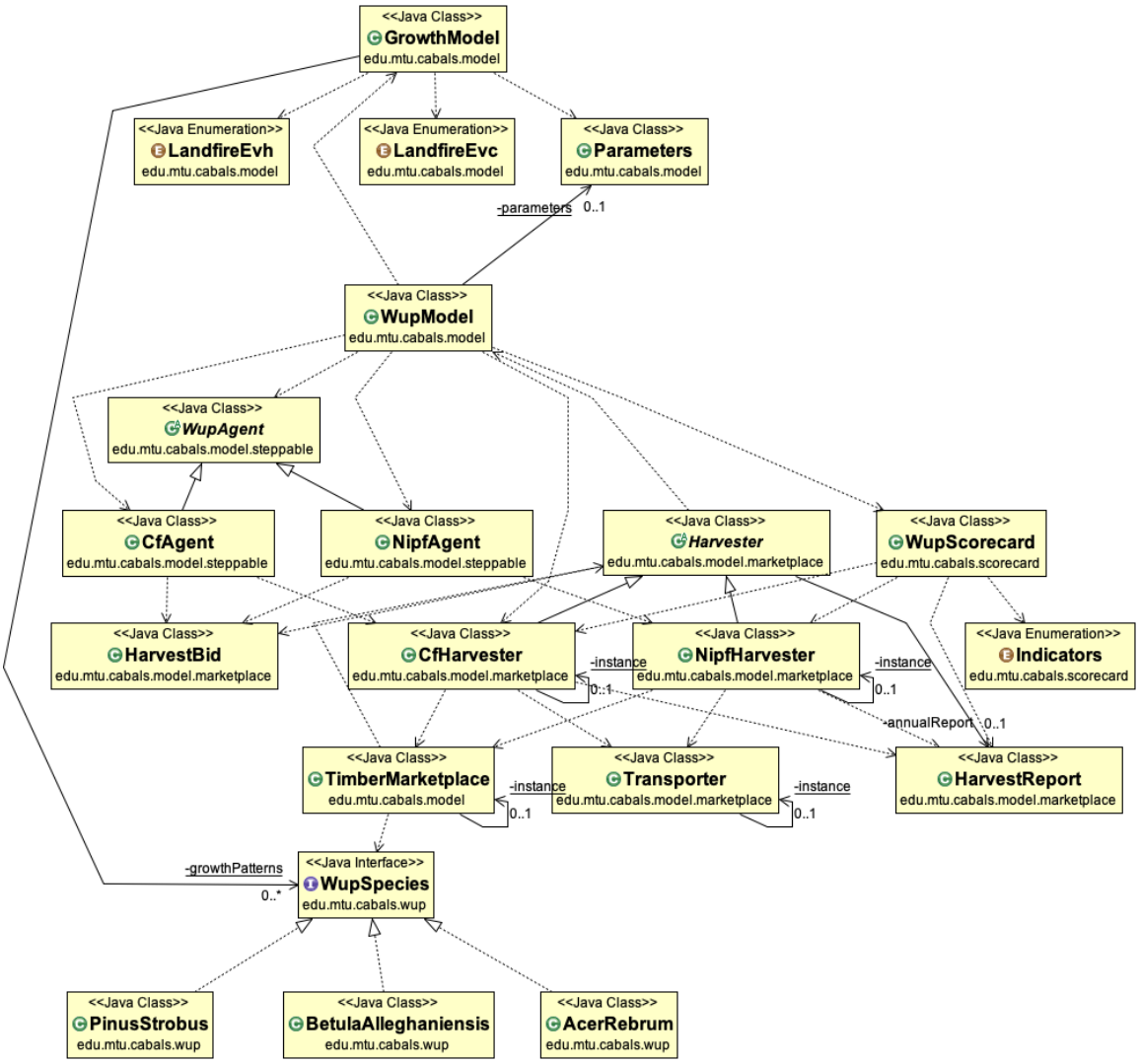

Figure 4.11: Summary UML diagram of the key classes in the ABM

IH^2 fuels. In addition to LCI data, the model also captures information related to the estimated labor involved with harvests, if selling woody biomass is profitable for agents, and so forth, allowing economic and social impacts to be determined.

4.A.2 Entities, state variables, and scales

4.A.2.1 Agents

The model contains two types of agents: forest owners who manage one or more forested parcels, and loggers who harvest parcels and determine if woody biomass

is to be collected and sold. Forest owners represent either commercial forest owners (i.e., commercial entities engaged in industrial forestry), or NIFP owners (i.e., smaller commercial entities, non-profits, or family forests), both of whom may own multiple forested parcels. These agents determine when trees are harvested, which in turn determines the quantity of woody biomass that is available for collection and sale to the biorefinery. Commercial forest agents have the state variable *target harvest* in hectares which is used to determine the size of a harvest. The target harvest size is determined by the number of *years* and percent *forest reserve*, which are given at initialization (see Section 4.A.5). NIPF owners have several state variables given at model initialization that influence harvest decision making. The *target harvest* in hectares determines how large of a harvest they commit to. The *minimum profit* per hectare determines if a bid will be rejected or not. Finally, the *woody biomass* bid per green ton determines the price at which they are willing to sell woody biomass.

The second type of agent in the model is loggers who harvest the forest when requested by forest owners, and then determine if the woody biomass produced during the harvest is to be collected and sold to the biorefinery. Two types of loggers are included in the model, a commercial logger that operates in forests managed by commercial forests agents, and a NIPF logger that operates in NIPF forests. Both types inherit from an abstract logger class that contains the primary logic for bidding and harvesting (see Section 4.A.7.3). Both types of loggers share two state variables. The first is a markup which is set at initialization and determines the markup applied when determining if woody biomass sales are profitable (see Section 4.A.7.3). The second is an annual limit set at initiation that determines how many hours loggers may work each time step, which is tracked by the current hours.

4.A.2.2 Spatial Units

The model is mapped to the geographic coordinates of the WUP region and includes the counties of Gogebic, Ontonagon, Houghton, Keweenaw, Baraga, and Iron County. Within these coordinates are parcels, representing registered commercial forests with

the State of Michigan. These parcels, in turn, contain forest stands where each stand is a 30 m^2 pixel.

4.A.2.3 Environment

The forested landscape is the primary environment of the model, this is further divided into 30 m^2 pixels that represent forest stands. The forest stands are managed by ForestSim which provides such data as the species of trees, mean DBH and height of trees, and so forth. This data is provided to ForestSim during model initialization (see Section 4.A.5).

4.A.3 Process overview and scheduling

Each time step of the model represents one year and is managed by ForestSim which also controls the growth of the forested environment. During model execution, each time step proceeds in the following fashion:

1. Forest owners are activated and decide if they will harvest or not.
2. If the agent harvests then,
    2.1. The appropriate logger is activated.
    2.2. The harvest is performed.
    2.3. The logger determines if they can collect and sell the woody biomass at a profit.
    2.4. If the woody biomass is sold, this is noted for later data collection
3. Once all forest owners have been activated, data collection takes place.
    3.1. Harvesting done by the loggers is recorded, and totals reset.
    3.2. The quantity of woody biomass sold is recorded, and totals reset.

4.A.4 Design concepts

4.A.4.1 Basic principles

The overall design of the model, in terms of the agents, their decision making, and the environment, was informed both by the literature describing forest owners in

the WUP (see [88, 91, 190]) and sustainability indicators selected for the LCSA (see Section 4.4.6). The technical design of the model is informed by object-oriented programming principles as well as the architecture of ForestSim. The decision making for both commercial forests owners and NIPFs is similar, so an abstract class contains the core logic while the concrete class is invoked by agents during model execution. As a simplification, when agents did not need to be spatially embedded, a singleton pattern was used to minimize model overhead.

The model only contains parcels that have been registered as commercial forests with the State of Michigan [160]. As a result, two simplifications can be made with regards to agent decision making. First, agents will attempt harvest some, if not all, all of their forested land over the course of model execution. This is justified by the requirement that registered commercial forests have a forest management plan that includes harvesting [127]. Second, agents act as economic optimizers that are seeking to either maximize their profits at time of harvest, or ensure a continuous income from harvesting. This is justified by studies that indicate that NIPFs have minimum acceptable bid ranges that influence their decision making (see [71, 189]) and is intuitive in the case of registered commercial forests managed as industrial forests. However, the limited harvest rates in the region, with growth exceeding harvesting [206], justify a conservative approach in the model to harvest decision making since harvesting should not exceed these growth rates. Finally, materials published by developers of the IH^2 biorefinery indicate they believe that existing harvesting activities will be sufficient to supply the facility (see [121]). As such, the introduction of the facility is assumed to create a market for woody biomass, but will not impact harvest decision making otherwise. This is justified by the low value of woody biomass, so maintaining existing patterns of harvesting pulpwood and saw logs will be unchanged.

Forests in the WUP are predominantly even-aged, medium-to-fully stocked, and of sufficient DBH to be harvested as saw logs [206]. However, individual parcels

and stands may have been previously harvested, have different conditions affecting growth, and so forth, which influence the decision to harvest. As a result, the model is initialized with a forest that closely resembles the current state of forests in the region as determined by land cover data [103, 207] and U.S. Forest Service reports [206]. Following initialization of the environment, it is assumed that stands will grow in a matter consistent with the average rate of growth for the species. The use of species averages for regrowth introduces some error into the model over time due to the variance in real ground conditions affecting growth. However, this is not a significant concern since the comparatively short period of assessment (i.e., fifty years) limits most agents to one and at most two harvests per stand due to tree growth rates.

4.A.4.2 Emergence

The model is concerned with two forms of emergence. First, sufficient supply of feedstocks for the biorefinery are an emergent property of logging, along with the collection and transport of woody biomass. Second, the model assumes that sustainability is an emergent property of interactions between forest owners, loggers, and the landscape. This arises on the basis of the environmental, economic, and social impacts on the region, as assessed using the criteria outlined in Section 4.4.6.

4.A.4.3 Objectives

Agents representing forest owners seek to maximize economic returns when harvesting the parcels under their control. Commercial forest owners seek the highest value harvest across all their parcels. NIPF owners are somewhat naïve in that they randomly select a parcel to be bid upon each time step. The naïvety of NIPF owners allows for a degree of stochasticity that acts as a proxy for influences on harvest decision making, such as peer influence [190]. Finally, the loggers of commercial and NIPF forests seek to maximize profits when determining if woody biomass is to be sold.

4.A.4.4 Sensing

Forest owners are able to access the parcels that they control and use the area of these parcels to determine the size of harvests. When requesting a bid for a timber harvest, the logger agents are able to access a "timber marketplace" (see Section 4.A.7.5) that contains the current rates for timber products. Loggers are also aware of the total logging (i.e., total system hours) that has taken place each time step, which allows them to limit their operations to the configured maximum system hours per time step.

4.A.4.5 Interaction

Three forms of interaction take place in the model. First, forest owners interact with the parcels they control to collect descriptive information such as area, which is used to determine harvest sizes. Second, forest owners may interact with loggers who determine the bid for a harvest. Finally, loggers interact with parcels and forest stands when a harvest is requested by a forest owners to conduct the timber harvest and determine if woody biomass is to be collected.

4.A.4.6 Stochasticity

Initiation and growth of the forest, while based upon forestry models for species in the region, contain a degree of variation upon initialization to account for natural variation in tree growth. Prices within the marketplace are also initialized with some variation based upon the standard deviations of data from the State of Michigan [208]. This allows for some degree of variance in pricing which in turn influences if NIPF owners will harvest, or not. Finally, NIPF owners who control multiple parcels randomly select the parcel that receives a bid each time step.

4.A.4.7 Observation

In order to supply LCI data, as well as capturing sustainability indicators, a number of observations are made of the model each time step which is shown in Table 4.7.

These observations are used for one of two purposes: one, to generate LCI data for the LCSA; and two, as an impact assessment indicator.

4.A.5 Initialization

The order of operations for model initialization is controlled by ForestSim, which starts by first requesting the model initialize the forested landscape (see Listing 4.1). This is done by loading the NLCD raster data, and the pixel data for deciduous and mixed forests are mapped to Red Maple (*acer rubrum*), evergreen forest to Eastern

Table 4.7
Observations made during model execution

Source	Observation	Purpose
Harvesters	Woody Biomass Produced, green tons	Total woody biomass produced during harvesting
	Woody Biomass Recovered, green tons	Total woody biomass sold, LCI item
	Woody Biomass Recovery Labor, hours	Impact assessment indicator, total additional labor to recover woody biomass
	Aboveground Biomass, green tons	Indicates total aboveground biomass impacted, used to determine LCI allocations
	Merchantable Timber, green tons	Indicates total timber production in the region, used to determine LCI allocations
	Visual Impact, hectares	Impact assessment indicator, total area of visually sensitive areas harvested each year
	Wetlands Impact, hectares	Impact assessment indicator, total area of wetlands harvested each year
Transporter	Distance Traveled, km	Total distance traveled transporting chipped woody biomass, LCI item
	Woody Biomass Transported, green tons	Total chipped woody biomass transported, LCI item

Listing 4.1: Pseudo-code for initialization of the forested environment

```
1. Load GIS data
2. Load stocking guides
3. FOR ndx = 0 to map width
  3.1 FOR ndy = 0 to map height
    3.1.1 SET code to nlcd[ndx, ndy]
    3.1.2 IF code is not forest THEN CONTINUE
    3.1.3 SET species to CALL nlcdMapping(code)
    3.1.4 SET dbh to CALL calculateDbh(ndx, ndy)
    3.1.5 SET treeCount to CALL calculateTrees(ndx, ndy)
    3.1.6 Update forest with species, dbh, and treeCount
```

White Pine (*pinus strobus*), and woody wetlands to Yellow Birch (*betula alleghaniensis*). This mapping was selected based upon Michigan Forest Canopy data in the study region [209], with the most common species selected for each pixel type. Following species mapping, the LANDFIRE height data is loaded and the height (HT) is noted at each pixel. Chapman-Richards equations [210, 211] are then solved for the DBH, using the stand height, where DBH is in cm, and HT is in meters.

$$DBH = -\frac{ln\left(1 - \frac{ht-1.37}{a}^{\frac{1}{c}}\right)}{b} \tag{4.2}$$

Since this equation loses predictive value as HT approaches the maximum height for the species, the DBH is capped at the predicted value for the maximum height of the species. Once the DBH is calculated, the number of trees is extrapolated based upon the stocking tables for the species. The values for fully stocked stands is used as the baseline since the region is predominantly fully-stocked [206]. This figure is then skewed by plus or minus twenty percent as a proxy for natural stand stochasticity.

Following the generation of the forested landscape, agents are embedded in the landscape which required overriding the default method that ForestSim uses. The model embedded agents in the landscape as seen in Listing 4.2. First, the parcel map is loaded into memory and a hash table structure is used to track the owners. The

Listing 4.2: Pseudo-code for assignment of agents to parcels

```
1. Load parcels
2. SET owners as Map<Id, Agent>
3. FOR parcel in parcels
  3.1 IF parcel boundaries are invalid THEN CONTINUE
  3.2 SET id to parcel.ownerId
  3.3 IF NOT owners.contains(id) THEN
    3.3.1 SET agent to CALL createAgent(parcel.type)
    3.3.2 Add id and agent to owners
  3.4 SET agent to owners.get(id)
  3.5 CALL agent.addParcel(plat)
4. SET ids to owners.keys()
5. SET ids to shuffle(ids)
6. FOR id in ids
  6.1 SET agent to owners.get(id)
  6.2 CALL schedule(agent)
```

parcels in the parcel map are then iterated through and the owner id is extracted.[4] The boundaries of the parcel are checked to ensure that they align with NLCD data, and if they are not the parcel is discarded. If the owner id exists in the hash table, then the parcel is assigned to the existing agent. Otherwise, a new agent is generated based upon the plat type (see Section 4.B). Once all parcels have been assigned, agents are shuffled using a Fisher-Yates shuffle [93] and scheduled as repeating entities. This ensures that they will be called by ForestSim once per time step. Upon completion of forest generating and agent assignments, the marketplace is initialized by loading the relevant data and randomly selecting a normally distributed value based upon the range indicated.

4.A.6 Input Data

Table 4.8 contains all of the input values that are used during model execution; however, a couple additional notes are warranted. First, the markup variable used in the ABM improves accuracy by ensuring that marginally profitable actions (ex.,

[4] This occurs when the polygon for a parcel doesn't completely surround any pixels of the raster data. This affects 18 of the 8,390 parcels in the model and the parcels are under 8093.71 m^2 (2 ac) in area implying a minimum impact on the model overall.

Table 4.8
Initialization values and data sources used as inputs to the model

Entity	Attribute	Initialization
Logger	Chipper Fuel	25.5 L/h [138]
	Chipping Rate	44.59 green t per h [138]
	Diesel Cost	National average of \$0.84/L (\$3.178/gal) [212]
	Limit	Annual limit of 139,318 system h, regardless of requesting agent type, may be exceeded for harvests in progress (Table S3, Electronic Supplementary Material; [206])
	Logger Pay	\$19.15/h based upon national average [213]
	Markup	5%, 10%, 15%, 20%, and variable $\mathcal{U}(5\%, 20\%)$
	Productivity	10 t system h (Table S1, Electronic Supplementary Material)
Transporter	Capacity	24 green tons (12 dry tons) [186]
	Driver Pay	\$21.91/h based upon national average [214]
	Truck Fuel	1.78 km/L [59]
	Truck Speed	88.5 km/h (55 mph speed limit)
Commercial Forest Agent	Minimum DBH	Softwood saw timber, 22.86 cm or larger
	Planning Period	50 years
	Timber Reserve	30% of the forest (70% is harvested)
NIPF Agent	Harvest Patch	$\mathcal{N}(19, 15)$ hectare [58], or entire parcel, whichever is smaller
	Minimum DBH	Softwood saw timber, 22.86 cm or larger
	Timber Profit	Minimum of $\mathcal{N}(\$1292.38, \$304.11)$ hectare [215]
	Timber Residues Profit	Minimum of $\mathcal{N}(\$73.80, \$55.28)$ hectare [215]

loggers will not provide woody biomass if they only expect $1.00 as a profit) are not done. Markups are commonly used by contractors to avoid cost overburdens [216], and these may also impact logging operations (e.g., equipment repairs, fuel fluctuations, insurance, etc.). Second, annual harvest limits are based upon total timber harvests in the WUP region; less harvests that took place in Ottawa National Forest (see Table S3, Electronic Supplementary Material; [206, 217]). Data from 2014 sales was used to ensure conformance with the aggregated data on Michigan forest removals. The rates of production for chipping along with fuel use are based upon the data in [138], using the assumption that 1 m^3 has a dry weight of 380 kg (see Table S2, Electronic Supplementary Material).[5] Finally, marketplace data is based upon bids published by the State of Michigan for timber harvests on state lands [208]. Model inputs were generated by selecting sales data of relevant species that took place in the WUP region, as well as Upper Peninsula and statewide averages. The values were then weighted using the total volume and the median and standard deviation was calculated based upon the weighted volume and variance (see Table S4, Electronic Supplementary Material).[6]

4.A.7 Submodels

4.A.7.1 Forest Growth

At the end of each time step ForestSim grows each forested stand by calling a method implemented in the model. For each stand an even-aged whole stand growth approach is used [72], in which the DBH for the stand is increased by a normally distributed value centered on typical annual growth for the species. Growth is capped when the maximum DBH for the species is reached. In the event that the stand is over-stocked, up to 10% of the trees may be thinned in accordance with natural processes. When a harvest takes place, stands are replanted by ForestSim to ensure that model assumption remain consistent.

[5] see Appendix B
[6] ibid.

Table 4.9
Summary of species and equations used in model

Species	Equation	Source
Red Maple (*acer rebrum*)	Above ground biomass	[105]
	Stem wood to biomass ratio	[105]
	DBH to height, Wykoff functional form	[218]
	Height to DBH	[219]
White Pine (*pinus strobus*)	Above ground biomass	[105]
	Stem wood to biomass ratio	[105]
	DBH to height, Curtis-Arney equation	[218]
	Height to DBH	[219]
Yellow Birch (*betula alleghaniensis*)	Above ground biomass	[105]
	Stem wood to biomass ratio	[105]
	DBH to height, Wykoff functional form	[218]
	Height to DBH	[220]

Table 4.9 outlines the equations that are used in the model along with the relevant sources. The equation for above ground biomass is used during logging to determine how much woody biomass is produced. The remainder of the equations are used for initialization of the forest or as part of forest growth. Descriptive data for the species such as maximum heights or typical annual growth were based upon North American sources [66, 221, 222]. As these equations are in bone dry tons, green tons are approximated by doubling the weight which is consistent with biomass bids [189].

4.A.7.2 Harvest Decision Making

While both commercial forest agents and NIPF owners seek to harvest each time step, their decision making is slightly different. In the case of commercial forest agents, the first time they are called in the first time step, they determine how much forested land they control. This sum is used to calculate the annual harvest target, less the quantity of their land being held in reserve. This reserve value is used as a proxy circumstances that would prevent all their forested land from being harvested (e.g.,

for marginal lands that may be prohibitive to harvest). During model execution, the agent will then harvest their parcels until the annual target is met, the logging limit is met, or all eligible timber has been harvested, as determined by the commercial forest logger (see Section 4.A.7.3).

In contrast to commercial forest agents, NIPFs randomly select one of their parcels and request a bid based upon the patch size assigned at initialization. The bid is then checked against their desired profit. A harvest is requested if the bid exceeds the desired profit. In the case of both commercial forest agents and NIPF owners, the bid they receive on a harvest is based upon the total price paid for pulpwood, sawtimber, and cull wood in the harvested patch, with values derived from State of Michigan timber sales. For sawtimber, the total board footage is based upon Scribner Decimal C log rule with a 10.0 inch (25.4 cm) top diameter in bark due to State of Michigan bids for the Upper Peninsula [208].

4.A.7.3 Harvest Operations

Both the commercial forest and NIPF logger are derived from the same abstract logger class. The abstract logger class contains two key methods: a means of finding the highest value contiguous patch when a bid is requested, and means of harvesting in the patch. When a forest owner requests a bid for a patch, the best patch on the parcel is first found using the greedy algorithm in Listing 4.3. Briefly the algorithm works as follows. First a grid is overlaid on the parcel where each square is one hectare. While the size of the squares may be larger, or smaller, one hectare is used since target NIPF profits are quoted in hectares (see [71]). The average DBH of forest stands in the square is calculated from for all values greater than the minimum DBH the agent wishes to harvest. By only adding stands with a DBH greater than the agents target DBH for harvesting, a penalty is introduced for the square when most stands are smaller than the target size. Likewise, since points containing wetlands are not included, and the agent avoids harvesting them as a proxy for legal complications in their harvest. Since lower value products may be taken during a harvest, or wetlands

Listing 4.3: Algorithm for finding the highest value patch to be bid on

```
1. IF patchSize >= parcelSize THEN RETURN parcel
2. Divide the parcel into an evenly sized grid
3. FOR stand in parcel
  3.1 Increment point count for section in grid
  3.2 IF stand.type = wetland THEN CONTINUE
  3.3 IF stand.dbh >= minimumDBH THEN
    3.3.1 Add stand.dbh to total for section in grid
4. FOR point in grid
  4.1 Calculate mean DBH at point and store in grid
  4.2 IF mean DBH at point is less than target THEN
    4.2.1 SET point value to zero and CONTINUE
  4.3 IF mean is largest seen THEN SET point to location
5. SET patch to List<Point>
6. Add location to patch
7. WHILE sum(patch) < target size
  7.1 IF no more selections THEN RETURN patch
  7.2 WITH largest adjacent square
    7.2.1 Add square to patch
    7.2.2 SET location to square
```

may be impacted, allowing for a section of the harvest to potentially contain low value stands improves the overall realism of the harvest selection. Following examination of the stands, the average DBH of the squares is calculated. During this step the largest square noted which acts as the starting point for the patch. The largest adjacent square is then selected until the total area is equal to the target patch size, or no more selections are possible. The squares selected are then returned as the best patch to be bid on.

When a harvest is requested, a check is first made to see if the annual logging limit has been met or exceeded. If so, the harvest does not take place. Otherwise, all of the stands in the patch are clear-cut and replanted with 300 seedlings per acre by the underlying ForestSim harvest method. The results of this harvest are then reported back to the logger, and these results are used to determine if woody biomass will be collected and sold to the biorefinery. This is done by determining if profits exceed costs and margins:

$$profit = (biomass * rate) - (collection + transport) * (1 + margin) \tag{4.3}$$

Where *collection* is the cost of collecting and chipping the woody biomass, and *transport* is the cost of transportation to the refinery and back to the job site. The markup *margin* is a percentage; *biomass* is the total woody biomass in green tons; and *rate* is the bid offered per green ton. Collection cost is determined as follows:

$$collection = \frac{biomass}{rate} * fuel * fuelCost \tag{4.4}$$

Where *rate* is the rate of chipping in green tons per hour, *fuel* is the rate of fuel consumption in liters per hour, and *fuelCost* is in liters. Finally, the transport cost is determined:

$$totalDistance = \left\lceil \frac{biomass}{capacity} \right\rceil * distance * 2 \tag{4.5}$$

$$cost = \frac{totalDistiance}{kmph} * hourlyPay + \frac{totalDistance}{fuelConsumption} * fuelCost \tag{4.6}$$

Where the chip van *capacity* is measured in green tons; *distance* is from the job site to the biorefinery in kilometers; and the remaining variables are self-explanatory.

4.A.7.4 Transportation

To account for the transportation of woody biomass, a conceptually abstract transporter manages the process. While actual transportation logistics is managed by multiple chip vans, drivers, and so forth, for the purposes of sustainability assessment the model only needs to produce aggregate results for each time step. To manage this, a *transporter* singleton tracks the quantity of chipped woody biomass that is transported to the biorefinery each time step using the state variables, *distance* and

total weight. Upon the decision to sell woody biomass to the biorefinery, the logger provides the location of the parcel being harvested along with the weight of the woody biomass, which is used to update the running total. At the end of each time step, the running total is reset.

4.A.7.5 Timber Marketplace

As a proxy for a real marketplace, a "timber marketplace" concept is incorporated in the model as central location for the price offered for pulpwood and saw logs. The key method in the timber marketplace calculates a bid for a forested stand. The bid returned is based upon the species of tree in the stand, DBH, height of trees, and price as determined at model initialization. In the event that the stand is wetlands, a value of zero is returned to reinforce the model bias against harvesting woody wetlands.

4.B Data Processing and Preparation

This section provides an overview of the preparation and processing of geographic information systems (GIS) data that was used in the case study. First, parcel data from the State of Michigan depicting the registered commercial forests [160] was prepared so agents could be spatially coupled to the natural landscape. The polygon data was first clipped to the Western Upper Peninsula (WUP) region based upon the county boundaries [159]. Next, the parcels were annotated as commercial forests (CF), family forests (FF), and all others (NIPF) based upon inspection of parcel ownership data, as well as cross-referencing parcels with previous annotation work (see Appendix A). This was done in order to calculate described data for the region as well as ensuring that agents would be assigned parcels based upon their actual ownership patterns. The near geodesic distance was calculated from the centroid of each parcel to the biorefinery in Ontonagon, Michigan and stored as a polygon attribute for use during model execution.

Following preparation of parcel data, land cover raster files were then prepared to inform the generation of the forested landscape. First, parcel data was dissolved into a mask which could be used to extract land cover raster data for the study region. This mask was used to prepare the LANDFIRE vegetation height data [207] and National Landcover Database (NLCD) data [103].

In order to account for forest aesthetics as an assessment indicator (see Section 4.4.6), a raster file was generated for the model that would designate visually sensitive areas. This was done by first merging all of the relevant Michigan Department of Natural Resources (DNR) trails (e.g., ATV, bicycle, equestrian, hiking, motorcyce, ski, and snowmobile trails; ORV routes; and railtrails) from the State of Michigan's GIS Open Data website [223–231] into a single polygon file. The polygon data was then merged with road network data [232] and clipped to the WUP region. A 50 m buffer was then created around all trails and roads, and was selected since it is within the bounds of a 200 ft. buffer that is typically recommended. This buffer was dissolved into a single entity and used to create a raster file that could be checked by the model to determine if a harvested pixel was in the zone (see Figure 4.12).

The last step in preparing GIS data for the ABM was to ensure that that the extents were uniform, raster pixels were consistently sized, and geographic coordinates were consistent. This was done by ensuring that raster files (i.e., NLCD data, LANDFIRE data, and visual buffer data) were aligned to the extents of the parcel map. To do so the raster files were projected to the same NAD 1983 UTM Zone 16N projection as the parcel data. Raster files were then clipped to the same extent and undersized files were increased to match the target size. A second projection was then performed to ensure that raster pixels were 30 by 30 meters.

Finally, since harvesting is limited by the number of hours loggers can work per year, the total system hours per year was calculated based upon the harvesting reported by the U.S. Forest Service [206]. The Western Upper Peninsula Forest Inventory and Analysis (FIA) region includes the counties of Marquette and Dickinson and

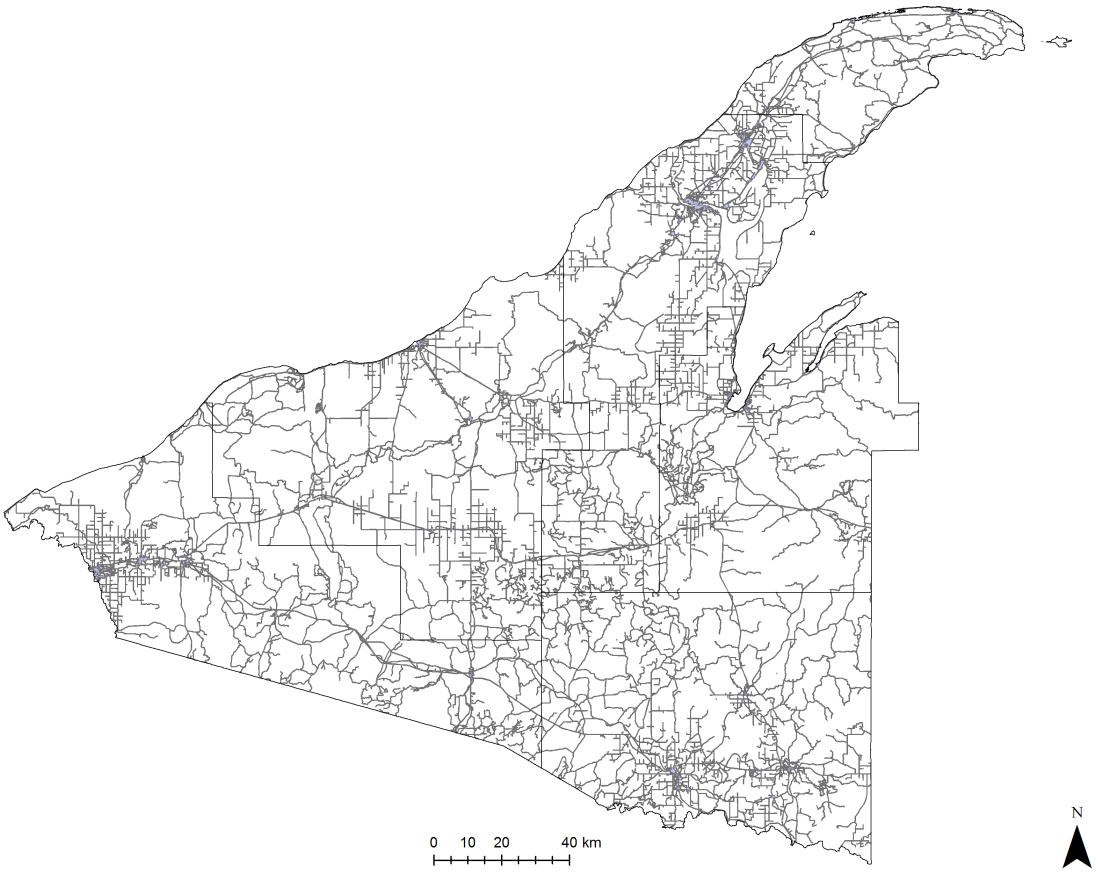

Figure 4.12: Map of the visual buffer created for the model

the total logging was adjusted to exclude them. This was done by calculating the total forested land per county by summing the count of woody wetlands, deciduous, evergreen, and mixed forest NLCD pixels and multiplying by 30 m^2. Then, assuming that logging patterns would follow geographic patterns defined by the forested land, county boundaries [159] used to define the relevant region and NLCD data was clipped to the counties. The total area of NLCD pixels was then tabulated and the forest allocation was then calculated (see Table S2, Electronic Supplementary Material). Harvest removals [206] were then adjusted to exclude known harvesting that took place in Ottawa National Forest [217].

Chapter 5

Development of an Agent-Based Model to Predict the Fate of Organic Contaminants Degradation in Aqueous-Phase Advanced Oxidation Process

Robert Zupko, Divya Kamath, Mark Rouleau, and Daisuke Minakata[1]

[1] The material in this chapter is intended for submission to *Environmental Modeling & Software*

Abstract

Advanced oxidation processes (AOPs) can treat organic contaminants in wastewater; however, care is needed since intermediate by-products of the process can be more toxic than the parent contaminant. Transformation by-products can be studied in laboratory settings, but the number of chemical species make this approach impractical. Typically concentration profiles of a target contaminant and transformation byproducts are predicted by solving ordinary differential equations (ODEs), which are very stiff and challenging to numerically solve. In this study we develop a novel agent-based model (ABM) to study intermediate radicals and stable by-products involved in peroxyl radical biomolecular decay in AOPs. The model is discussed along with the results of two *in silico* studies. Using a comprehensive list of elementary reaction pathways, the model replicates concentration profiles for major chemical species observed by the experiment. As a novel application of ABM to AOPs, we conclude that the technique shows considerable promise.

Keywords: agent-based modeling - advanced oxidation processes - water treatment

5.1 Introduction

The presence of trace organic contaminants in both natural waterways and in treated water and wastewater is alarmingly high [233]. These contaminants can also have serious but uncertain toxicological risks to both human health and natural ecosystems [234]. While there are efforts by researchers and policy makers to develop a better understanding of these contaminants [235, 236]; treatment of contaminants is also needed due to de facto [237] and planned water-reuse projects [238].

One means of remediating contaminants in water and wastewater treatment processes is the use of advanced oxidation processes (AOPs). AOPs have the ability

to destroy known and emerging organic contaminants through the creation of hydroxyl radicals in aqueous phase solutions at ambient temperature and atmospheric pressure [45, 46]. Hydroxyl radicals produced react rapidly with electron rich sites of organic contaminants resulting in degradation through a series of chain-reactions. When AOPs are appropriately designed, a target organic contaminant is mineralized into water and carbon dioxide. The complexity of AOPs reaction pathways makes it difficult to predict the formation of intermediate radicals and by-products, which may be more toxic than the parent compounds. While it is possible to study the reactions and by-products of AOPs in a laboratory setting, the hundreds of thousands of chemicals in commercial use and production make laboratory studies untenable as a means of producing reaction pathways for all contaminants. As a result, there has been significant research into the development of a predictive model that can determine intermediate radicals and by-products (see Section 5.2.1). Such a model would greatly aid in the development of AOPs and help guide assessment of potentially toxic chemicals in manufacturing processes.

The purpose of this manuscript is to address the limitations in existing approaches to studying AOPs (i.e., ordinary differential equations) through the development of an agent-based model (ABM) of the chemical entities and their reactions involved in an AOP. The use of an ABM allows us to reduce the complexity in conducting *in silico* studies by overcoming the issues that lead to ODEs that are stiff to solve, and have a tendency to produce unstable numerical solutions. Our ABM demonstrates that it?s possible to comprehensively model the reactions involved an AOP as a complex system, allowing for approximation of the expected results. Furthermore, these solutions can be reached in approximately half an hour on desktop computing environments. This paper proceeds as follows, in Section 5.2 we provide a review of previous approaches to AOPs *in silico* and discuss the benefits of using an ABM to study AOPs. Section 5.3 discusses the design of the ABM for AOPs in several parts. This section includes a molecular simulation that was developed, followed by

highlighting key aspects of the model?s implementation. The section concludes with a discussion of the model validation. Then, in Section 5.4, we examine the application of the ABM to study acetone degradation induced by hydroxyl radicals followed by discussion and concluding remarks in Sections 5.5 and 5.6 respectively.

5.2 Background

5.2.1 Previous approaches to in slico AOP models

Generally the literature reflects two approaches to modeling AOPs: conventional steady-state/non-steady-state models, and kinetic descriptions of the system without steady state approximations. Studies involving conventional steady-state/non-steady-state models are typically constructed with the intent of addressing a specific problem. In the case of [239] the authors used a kinetic model of UV/H_2O_2 processes with a steady-state approximation to predict final concentrations of 1,2-dibromo-3-chloropropane (DBCP), ultimately finding that the degradation of DBCP follows pseudo-first-order kinetics irrespective of experimental conditions (e.g., variations in pH, concentrations of hydrogen peroxide, dissolved organic matter, or alkalinity). [240] also used steady-state approximation to estimate both time-based and fluence-based rate constants for N-nitrosodimethylamine (NDMA) degradation resulting from both photolysis and hydroxyl radical induced reactions respectively. Their calculated rate constants were found to be consistent with experimental observations. This work was followed by [5] who derived a similar model by including the photolysis of target compounds. They then calculated the estimated removal efficiency from both photolysis and the hydroxyl radical induced reactions for more than 100 emerging contaminants. Their study also included a cluster analysis and classification of those compounds based upon the hydroxyl radical reaction rate, quantum yields, and molar absorptivity. Finally, [48] developed UV/H_2O_2 process models with steady-state approximations for various flow type reactors (e.g., completely mixed batch reactors,

complexity mixed flow reactors, plug flow reactors, tank-in-series reactors, etc.) with a disperse flow model [241] using MathCAD. These models were able to calculate the steady-state concentrations of hydroxyl radicals, the removal efficiency, and energy efficiency per removal of order, given any specified target compound and other water quality parameters.

While there has been some success with the aforementioned steady-state/non-steady-state models, the most detailed level of modeling in the literature involves models with complete kinetic description of the systems without steady-state approximations [49]. In these models all reactions in the system are considered and rate equations are written for all chemical species. Additionally, reactions are modeled at the sub-microsecond timescale in contrast to typical UV/H_2O_2 processes which typically take place on the order of minutes. These models result in a set of stiff differential equations whose integration may require 10^8-10^{12} steps depending upon the number of ODEs assigned [49].

One of example of these complex models was developed by [242] who used ACUCHEM software [243] to develop a UV/H_2O_2 kinetic model. However, this model was limited since ACHUCHEM does not consider acid-base equilibrium, variable photolysis rates, or complex flow reactor kinetics. However it is critical to simulate pH changes in a solution since the pH of a solution can drop as organic compounds are oxidized into mineral acids, carbon dioxide, or acidic intermediates during the UV/H_2O_2 process. To address these concerns, [244] developed a dynamic kinetic model of the UV/H_2O_2 process in a completely mixed batch reactor with non-steady state approximation, which included known elementary chemical and photochemical reactions along with literature reported photochemical parameters with chemical reaction rate constants. In the model the target organic compound(s) would react with hydroxyl radicals, carbonate radicals, phosphorus radicals, superoxide, and hydroperoxyl radicals while including scavenging reactions of hydroxyl radicals with alkalinity, phosphorus buffers, and carbonate radicals. In order to account for changes in pH

over time, the model tracks the net charge balance of anions and cations. Ultimately the model solves a set of very stiff ODEs for all identified species using Gear's Method [245] by adapting a package designed by [246]. The resulting kinetic model was validated against experimental studies by [247] and [239]'s pseudo-steady-state model. One limitation was that the scavenging reaction by natural organic matter (NOM) was not included in [244] but was included in the resulting AdOx™ software [248] that was developed and enables users to select various reactor types, flow conditions, and UV lamps. The AdOx software also includes functionality for tracer studies making it possible to estimate removal efficiency of target compounds using a disperse flow model of a physical reactor. The AdOx software was used in a study by [249] to evaluate the efficiency of a UV/H_2O_2 process for the removal of methyl tert-butyl ether and tert-Butyl alcohol from a drinking water source, demonstrating the applicability of these complex models to water treatment objectives. [250] compared the pseudo-first-order rate constants of DBCP from the Sim-pSS model, pseudo-steady-state model, and AdOx kinetic model with those from [239] under various experimental conditions and found that the AdOx kinetic model was more accurate than the other two models. The authors concluded that this was due to AdOx more accurately modeling containment destruction due realistic changes in hydroxyl radical concentrations over time from the initial pH and hydrogen peroxide concentrations.

Finally, [251] also developed a kinetic model of UV and UV/H_2O_2 processes in a collimated beam system employing monochromatic low pressure UV lamp and later developed a similar kinetic model for polychromatic medium-pressure UV lamps [252]. These kinetic models were used to predict the water quality impacts of the UV and UV/H_2O_2 process on treated wastewater. Both models assigned rate constants for forward and backward reactions to account for equilibrium reactions and avoided the use of steady-state approximation to account for the changes in solution pH. The models were validated with their own experiments for the degradation of thirty-six pharmaceuticals in the presence of bicarbonate, nitrate, and NOM. However it

was found that the model consistently predicted the degradation for five compounds when compared to experiment observations due to pH effects during photolysis and the radical scavenging of the NOM. These two kinetic models were later combined with a computational fluid dynamics model to predict the degradation of a group of thirty-five pharmaceuticals in a pilot-scale UV/H_2O_2 reactor [50].

5.2.2 Advantages of agent-based modeling of AOPs

The key limitation of the AOP models reviewed is that they are dependent upon underlying ODEs that are stiff to solve and have a tendency to produce unstable numerical solutions. The stiffness of the solutions are attributable to the dramatic differences in reaction rates (i.e., the product of the reaction rate constant and the concentration) that often vary by more than 10 orders of magnitude in an AOP (i.e., 10 M^{-1} s^{-1} vs. 10^{10} M^{-1} s^{-1}). Whereas the unstable numerical solutions are a consequence of the lumped reactions that often occur in studies of AOPs. The unstable numerical solutions are of particular interest since these are a consequence of the feedback loops that are inherent in the underlying chemical reactions (i.e., products of reactions being reactants in previous or subsequent reactions). While lumped reactions may allow AOPs to be studied using ODEs, elimination of them from the model also results in solutions that do not reflect the actual reactions that are taking place.

One means of addressing the limitations of models of AOPs (e.g., lumped elementary reactions), is to model the AOP as a complex system. While chemistry is infrequently studied as a complex system [7, 44], the underlying processes involved in an AOP share the characteristics of a complex system; namely, nonlinearity, feedback loops, and emergence. If the concentration profiles of an AOP are viewed as the emergent property of the system, then the nonlinearity and feedback loops are intuitively correlated to the elementary reaction pathways in an AOP.

In order to examine AOPs from the perspective of a complex system, we develop an agent-based model (ABM) to simulate the complex reactions and resulting by-products. ABM is a computational modeling technique in which individual software "agents" are used to represent entities in the system (i.e., chemical species) that interact with other agents and the environment in which they are embedded [15]. Upon execution of the model it is possible to observe how agent interactions result in complex patterns at the system level, while avoiding complex systems of equations required to replicate system level behaviors. This can also be quite useful for "theory testing" in which the ABM is used to verify an understanding of a system by replicating the observed behavior of the system in the simulation [15, 28]. Since ABM is focused on modeling interactions at the entity level, iteratively incorporating reactions is possible and as a result the technique offers a promising solution to advance AOP modeling over other existing techniques. Effectively, the completeness of the reactions used in the ABM is only limited by the overall understanding of the elementary reaction pathways. While the use of ABM is fairly new to chemical modeling, there has been increasing interest in using ABM to explore biochemical systems such as intracellular signaling and reactions [51, 52], biomolecular modeling [53], and complex biochemistry [253].

5.3 Agent-Based Model of Advanced Oxidation Processes

5.3.1 Introduction

A more technical discussion of the model now follows and is organized in two parts. First, the details of the molecular simulation are discussed and the underlying mathematical models for the relevant chemical reactions are detailed. Then, in Section

5.3.3, relevant computational aspects of the model are highlighted which either deviate from typical ABM development, or were a necessary aspect of ensuring that the model runs on typical desktop computers.

5.3.2 Molecular Simulation

The molecular simulation encapsulates the relevant aspects of the underlying chemistry (i.e., movement and reactions) as well as model initialization. As components of an ABM, the chemical entities are the agents, while the environment is a simulated space within the reactor in which the AOP is taking place. This simulated space is a to-scale (i.e., nanometre) limited by the number of agents the model is configured to run with by the user. The model assumes that the reactor continues to be well mixed (i.e., circulation is present) and that UV can uniformly reach all parts of the reaction. These considerations allow the model to assume that any part of the reactor can be modeled as a representation of the processes involved.

5.3.2.1 Initialization

Prior to the start of chemical reactions, the model is initialized using the list of chemical entities and molar concentrations provided by the user. In order to convert these molar concentrations to a count of chemical entities, a statistical normalization is applied:

$$normalizer = \frac{1}{v_1 + v_2 + ... + v_n} \tag{5.1}$$

$$molecules_i = v_i * normalizer * target \tag{5.2}$$

$$scalar = normalizer * target \tag{5.3}$$

Where v_i is the number of moles for a given compound; $target$ is the maximum number of total molecules; and $molecules_i$ is the quantity of the given molecule. The

scalar value is also used when the count of chemical entities are converted back to molar concentrations on model termination. It is also during model initialization that the size of the simulated space is calculated:

$$d = \sqrt[3]{\frac{molecules}{8x10^{-5} * N_a}} \tag{5.4}$$

Where *molecules* is the number of molecules in the simulation; N_a is Avogadro's constant; and d is the length of the simulated space along one edge in meters. Equation 5.4 is in turn derived from the parameters of the reference implication of [254], which was used for model verification (see Section 5.3.6) and results in the constant 8x10^{-5}.

5.3.2.2 Reactions

The model simulates the relevant chemical reactions in AOPs, namely: photolysis, bimolecular reactions, unimolecular decay, and acid dissociation, which occur in that order. This order of operations ensures that low probability reactions (i.e., photolysis and bimolecular reactions) may occur before high probability reactions (i.e., unimolecular decay and acid dissociation) within the context of a serial computing environment. Acid dissociation is resolved at the end of each time step since the total number of molecules in needed before the relevant calculations can be performed. Likewise, the model assumes that unimolecular decay will occur within a given time step when the reaction is defined. This requires that bimolecular reactions and photolysis come first so the conditions can be checked to see if those reactions may occur. Bimolecular reactions and photolysis may occur in any order and here photolysis was selected to go first since it starts the UV/H_2O_2 reaction starts the processes being studied.

(1) Photolysis: Photolysis, specifically the UV/H_2O_2 reaction, is assumed to follow a zero-th order kinetic rate constant, which we obtained through the experiment

outlined in Section 5.4.1. This allows the probability of hydrogen peroxide undergoing a reaction to be calculated as follows:

$$m = \frac{rate * volume * scalar * \Delta t * 10^{-3}}{60} \tag{5.5}$$

$$Pr(molecule) = \frac{q_1 - (m * \Delta t + q_0)}{q_1} \tag{5.6}$$

Where *rate* is the experimentally determined decay rate in liters per minute; *volume* is the volume of the experimental reactor in liters; *scalar* is the value calculated in Equation 5.3; Δt is the simulation time step in seconds; and q_0 and q_1 are the quantity of molecules at time steps zero and one, respectively. This probability is then applied to each time step, to each hydrogen peroxide chemical entity in the model.

(2) Bimolecular Reaction: Bimolecular reactions are modeled according to an interaction radius r, as governed by the reaction rate k and diffusion rate k_{diff}:

$$k_{chem} = \frac{k * k_{diff}}{k + k_{diff}} \tag{5.7}$$

$$r = \sqrt[3]{\frac{3k_{chem}\Delta t}{4\pi 10^3 N_a}} \tag{5.8}$$

These equations are based upon prior work by [52] and the interaction radius the boundary of a sphere wherein the presence of the appropriate chemical entities implies the reaction occurs. As demonstrated by [52] the size of the sphere is determined by the total volume occupied by reactions that occur in the given time span Δt given the reaction rate k. We expand upon the work of [52] by incorporating the diffusion rate, yielding k_{chem} (Equation 5.7), prior to the calculation of r (Equation 5.8). This approach to the bimolecular reaction allows the simulation to occur with the designated Δt as opposed to requiring that the collusion of chemical entities be modeled

(i.e., sub-microsecond time spans for Δt) while still incorporating the underlying kinetics. Furthermore, while the radius may be seen as a crisp boundary, it is more appropriate to consider it probabilistically [254, p. 54] with the likelihood of a reaction occurring the closer the two reactants are. To account for this the complementary Gauss error function is incorporated as part of the bimolecular reaction algorithm (see Algorithm 5.1), and used to determine the probability by which a reaction occurs.

The algorithm for bimolecular reactions may be summarized as follows (see Algorithm 5.1). First, the provided chemical entity is checked to see if it is the center of the interaction radius sphere as determined by the reaction registry (see Section 5.3.3), if it is not then the function returns. This check is a result of the interaction radius describing the volume of the resulting reaction, so only one of the involved reactants needs to be checked. Next, each possible reactant for the given chemical entity is checked in a loop. First the interaction boundary *radius* is calculated using Equations 5.7 - 5.8. The simulated space around the chemical entity is checked for a reactant within the given radius. If no reactant is found, or the reactant returned (i.e., chemical entity) was already activated this time step, the loop proceeds to checking the next reaction. Checking to see if the reactant returned has already been active the time step is necessary since its continued presence in the model means that it could not find an appropriate reactant on its time step. Again recalling the equation describing the resulting volume, once a chemical entity has been checked in a given time step and a reaction does not occur, it cannot be in the volume of the reaction. The Euclidean Distance of the chemical entity and reactant is then calculated and the complementary Gauss error function is applied to determine the likelihood that the reaction will occur.

(3) Unimolecular Decay: In the event that neither photolysis nor bimolecular reactions occur, unimolecular decay takes place if defined for the chemical entity. Since the model assumes that unimolecular decay will always occurs within the given Δt,

Listing 5.1: Pseudo-code of bimolecular reaction function in ChemSim

```
function bimolecularReaction(entity)
1. IF [entity] is not center of sphere THEN RETURN
2. FOR EACH [reaction] involving [entity]
  2.1 [radius] = calculateBoundary([reaction].[k])
  2.2 [reactant] = space.find([reaction].[reactant], [radius])
  2.3 IF no [match] THEN CONTINUE
  2.4 IF [match] has been activated THEN CONTINUE
  2.5 [distance] = euclideanDistance([entity], [reactant])
  2.6 IF random.gaussian() < erfc([distance] / [radius]) THEN
    2.61. Do reaction
```

the products of the reaction are simply introduced into the model while the reactant is removed.

(4) Acid dissociation: Acid dissociation (i.e., pKa balancing) reactions which takes place at the end of each time step. These reactions occur at the end of each time step since, recalling the serial nature of the model, the quantity of chemical entities must be fixed before the quantities can be updated per Equations 5.10 - 5.13. Assuming reactions are defined as follows:

$$HA \Leftrightarrow A^- + H^+ \tag{5.9}$$

The quantity of agents in the model is calculated as follows:

$$quantity_{A^-} = count_{A^-} * \frac{10^{-pKa}}{10^{-pH}} \tag{5.10}$$

$$quantity_{A^-} = quantity_{A^-} > count_{A^-} \; then \; count_{A^-} \; else \; quantity_{A^-} \tag{5.11}$$

$$quantity_{H^+} = quantity_{A^-} \tag{5.12}$$

$$quantity_{HA} = count_{HA} - quantity_{A^-} \tag{5.13}$$

Where pKa is the acid dissociation quantity, pH is the overall acidity or basicity, and $count_{A^-}$ is the quantity of the molecule in the model. The calculated *quantity* then represents the number of chemical entities that need to be removed, or added, to the model. The number of chemical entities is then adjusted as needed by removing, or adding, entities at random locations to ensure a well-mixed solution.

5.3.2.3 Movement

As chemical entities are not static in space, Brownian motion is approximated through movement along a random vector for each entity, each time step. This is done by selecting a random direction of movement, along which entities then move. In the event an entity encounters the boundaries of the simulated space, the movement is clipped to the bounds of the space. As a baseline, a speed of approximately 590 nm/s with some random noise is used. While slow compared to the average speed of molecules in water at room temperature (i.e., 590 m/s), this value is consistent with the minimum speed found by [254] required to ensure proper mixing of the simulated space, which is the ultimate objective of the simulated movement.

5.3.3 Simulation Engine

The simulation engine consists of all parts of the model's architecture (see Figure 5.1) that are not directly associated with stimulating the chemical entities or reactions. While an ABM can be described in terms of the agents, their environment, and so forth (see [185]), the simulation engine contains significant computational approaches and implementation decisions that are a necessary part of the molecular simulation and performant execution of the model. Specifically, the following are deviations from a typical ABM implementation: the scheduler which is responsible for the order of execution of the chemical entities, the sparse lattice containing the simulated space, and a "reaction registry" that contains all of the reactions possible in the model. In addition to these deviations, the model also performs a rudimentary form of garbage collection by allowing stale references to chemical entities to persist after they are

consumed in a reaction. While this increases the memory requirements of the model during execution, the trade-off is that compute overhead related to searching for the destroyed chemical entities across all data structures is eliminated.

5.3.3.1 Scheduler

A scheduler was written for the model to ensure that the chemical entities were activated each time step, allowing the molecular simulation to take place. Since the model runs in a serial manner (i.e., each chemical entity is activated once, in order, per time step) it is necessary to ensure that the scheduler is computationally efficient and incorporates randomization of the order to prevent modeling bias due to activation order. The schedule is a deque array backed by a list array to receive entities for the next time step, which allows for constant time insertion and retrieval as well as a variable number of chemical entities per time step. Each time step chemical entities are popped from the deque array, checked to see if they have not already been used in a reaction, and checked for movement and reaction operations, and then flagged to indicate its time step is complete until the next round. This last step is required to ensure proper execution of bimolecular reactions (see Algorithm 5.1). Upon exhaustion of the deque array (i.e., the end of a time step), the list array is shuffled using a Fisher-Yates shuffle [93] copied to the deque array (i.e., the new time step).

5.3.3.2 Sparse Lattice

The sparse lattice tracks the location of all chemical entities in the simulated space and offers a means of locating them to determine if a bimolecular reaction should occur. During model execution chemical entities either undergo a reaction, which results in the creation of inserting and deletion of chemical entities, or move to a new location. As a result of these constant updates, the tree-based data structured typical of spatial datasets (e.g., kd-tree, R-tree, etc.) incur performance penalties due

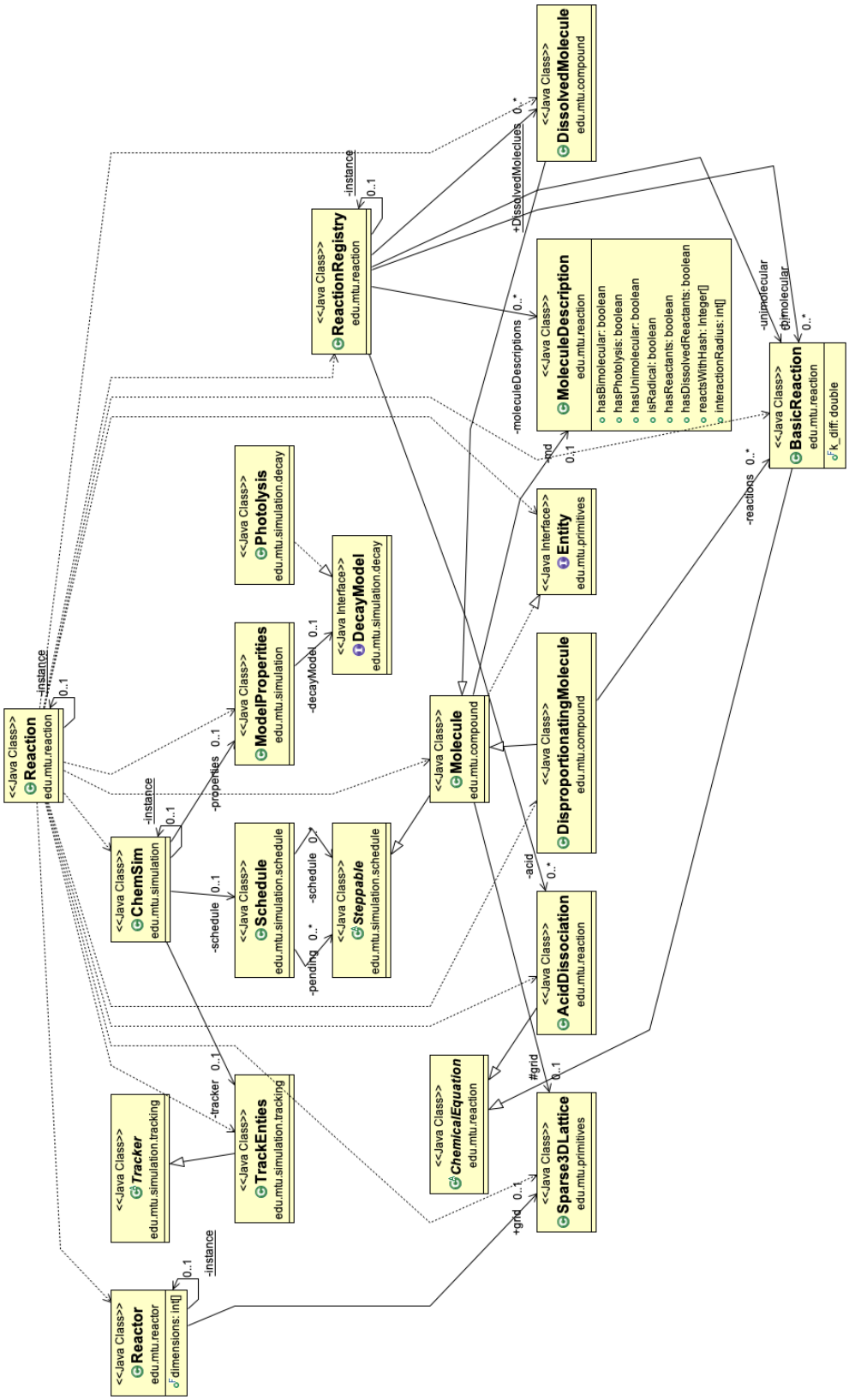

Figure 5.1: UML diagram of the core ChemSim classes.

to the mutability involved [255]. To address these problems, the simulated space is represented as a sparse lattice, reducing the memory footprint of the model.

The sparse lattice is divided into two parts: the agent's location in space, and the agent's relationship with other agents of the same type. These are stored using array-based hashmaps as three structures: 1) a spatial integer lattice, 2) an entity (i.e., agent) map, and 3) a tag map containing queues of like types of agents. This is similar to neighbor lists and Verlet neighbor lists [256]. However, as implemented, the structure lacks distance information as part of the data structure and represents a distinct implementation. Since queues are inefficient to scan each time a chemical entity is destroyed to a reaction, the maps may contain references to chemical entities that no longer exist. When these destroyed chemical entities are encountered, the objects are disposed of.

During initialization the structures are constructed in memory, with arrays pre-allocated for twice the number of agents the model has at initialization. During model execution, entities are stored based upon a hashing scheme by [257],

$$hash(x, y, z) = ((x * p1) \oplus (y * p2) \oplus (z * p3)) \mod n \tag{5.14}$$

Where $x, y, z \in \mathbb{Z}$, $p_1, p_2, p_3 \in PRIME$, and n is the size of the allocated array for the values. This ensures a uniform distribution of the entities across the memory allocated, and that probing can be used to determine if agents are nearby (i.e. within the known bounds of a radius r). The drawback to probing is that it is efficient only total points in the sphere is less than the entities to be searched. In these situations the simulation scans the appropriate tab map for agents within the correct Euclidean distance of a target chemical entity.

5.3.3.3 Reaction Registry

The reaction registry contains all of the chemical reactions that can take place in the model and provides the function of agent decision making in the ABM. In addition to providing a single point for checking what reactions can occur in the model, the reaction registry also ensures the consistent selection of the chemical entities that act as the center of the bimolecular reactions. Consistent selection is needed since the same reactant may appear in multiple reactions (e.g., A + B $\rightarrow$ C and A + D $\rightarrow$ E) thus, by limiting chemical entities that are used a the center (e.g., A in the previous example) once the chemical entity has been checked for all possible reactions, it can safely be excluded from reactions for the rest of the time step. Conversely, by not being used as the center of the interaction radius the chemical entity can be excluded, upon checking for any other reactions.

5.3.4 Simulation Execution Overview

Execution of ChemSim requires that two input files are first prepared by the user. First, the starting conditions (i.e., reactor size, UV/H_2O_2 photolysis rate, starting chemical species, concentrations, and reactions) for the simulated reactor needs to described. Second, the complete list of reaction pathways to be modeled needs to be prepared and reactions in the model are evaluated in the order they appear in the input file. Execution of the model then proceeds in the following manner:

1. Model initialization takes place
    1.1. Starting chemical entities and concentrations are read from input files
    1.2. Reactions lists are read from input files
    1.3. The reaction registry is generated
    1.4. The number of starting chemical entities is calculated and added to the model
2. Simulation runs for the designated number of time steps
    2.1. Each chemical entity is activated in the scheduled order

2.1.1. The chemical entity attempts to perform a reaction and is removed from the simulation if one occurs

2.1.2. Otherwise the chemical entity moves to a new location

2.2. Any pKa reactions are calculated and the molecule counts balanced[2]

2.3. The schedule for the next time step is generated

5.3.5 Implementation Details

The ABM was developed in Java 8 and contains some source code from the MASON Multiagent Simulation Toolkit [54]. The Xoroshiro128+ pseudo-random number generator [258] in the DSI Utilities library [259] is used for high performance random numbers. Additionally, fastutil [260] is used for preallocated, high performance hash maps. The simulations described in the case studies were conducted on a Late 2013 iMac (2.9 GHz Intel Core i5, 8 GB 1600 MHz DDR3). The source code for the simulation is available on GitHub under an MIT license at https://github.com/forestsim-mtu/chemsim

5.3.6 Model Verification

The basic correctness of the model was checked by using the results the two-particle interactions tests described by [254] as a known standard. While the intent of Pogson is ultimately a model of intracellular chemical interactions, their work begins with a verification of the ABM against general reaction kinetics and includes a reference implementation of the model in Matlab [254, p. 120-127]. This reference implementation is in turn verified by ODE solutions for the specific chemical systems. The general approach of Pogson's ABM is based upon matrix operations to determine which agents may undergo a reaction as well as bulk movement operations. This deviates significantly from ChemSim which uses a strictly serial approach to agent operations. As a result, replication of general reaction kinetics tests performed by

[2] Recall that pKa reactions occur at the end of the time step

[254] ensures that the model has correctly implemented the general reaction kinetics and that constants selected for the model are also appropriate.

Verification of the model began with the digitization of graphical results [254, p.60] using WebPlotDigitizer [261] since tabular data was not available. The two-particle interaction parameters were modeled using the simple abstract reaction A + B $\rightarrow$ C with the reaction rate of 10^6 M^{-1} S^{-1}. A reactor size of 1 L containing a starting concentration of 50 nM of A, B starting at 30 nM, with 1600 agents (i.e., chemical entities), and a time step of 1 second was used for the simulation. The mean absolute percentage error (MAPE) of the results was then calculated based upon the digitized data from [254]:

$$MAPE_i = \frac{\left(\sum_{j=1}^{N_i} \frac{\left|C_{exp,j} - C_{cal,j}\right|}{C_{exp,j}}\right)}{N_i} \tag{5.15}$$

Where i indicates the species (i.e., A, B, or C); N is the number of data points for the species; and $C_{exp,j}$ and $C_{cal,j}$ indicate the experimental, and calculated concentrations for the species i, respectively. As shown in Figure 5.2, the results of the model are consistent with [254], and the overall MAPE of 5.27% $\pm$ 6.93% is within the bounds of error due to digitization. Additionally, much of the error is due to the B molecule which had a MAPE of 10.05% $\pm$ 9.71% (largely due to differences in the count towards the end of the simulation, also known as the "curse of small numbers"). In contrast, the A molecule MAPE was 2.07% $\pm$ 1.19% and C was 3.47% $\pm$ 2.61%.

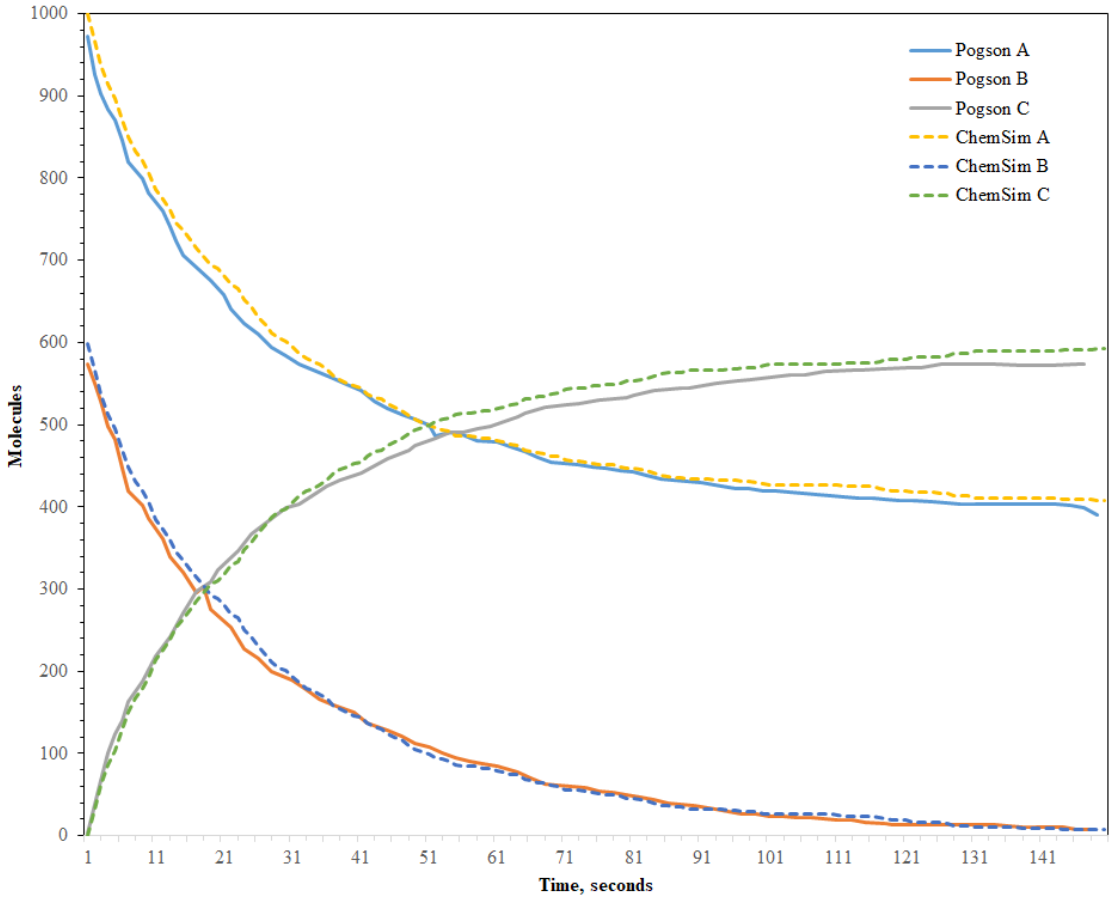

Figure 5.2: Comparison of results between [254] and ChemSim.

5.4 Case Study of Acetone Degradation Induced by Hydroxyl Radicals in UV/H_2O_2 AOP

5.4.1 Experiments

A benchtop photoreactor was used to perform UV/H_2O_2 AOP for a test target compound, acetone. The photoreactor was comprised of four Wheaton Roller Bottles with a volume of 1.8 L surrounding a low pressure Atlantic UV lamp with a wavelength of 254 nm, based upon the spectral distribution provided for the lamp by Ace Glass Inc. A quartz immersion well was used to circulate water around the lamp to prevent overheating and reactor vessels were surrounded by circulating water to maintain a

Table 5.1
Experimentally measured acetone by-products

Conc. (mM) **Min**	**Acetone**	**Acetic Acid**	**Hydrogen Peroxide**	**Formic Acid**	**Oxalic Acid**
0	1.2850	-	10.8726	0.0008	-
30	0.9536	0.1874	9.5794	0.0869	0.0001
60	-	0.2980	-	0.1053	0.0018
90	0.7963	0.4083	-	0.1034	0.0067
150	0.3676	0.5186	-	0.0846	0.0289
180	0.4300	0.5489	5.5621	0.0744	0.0472
210	0.3029	0.5733	-	0.0630	0.0745
263	0.1895	0.5774	4.0723	0.0502	0.1147
300	0.1287	0.5634	-	0.0424	0.1452
323	0.0452	0.5479	3.1997	0.0381	0.1628
370	0.0433	0.4802	-	0.0280	0.1802
420	0.0083	0.4561	1.8475	0.0237	0.2177
480	-	0.3736	-	0.0159	0.2289

constant temperature. The entire photoreactor was contained in a glass box covered by aluminum foil to prevent the escape of UV light. Each reactor vessel was equipped with a magnetic stir plate and stir rod to ensure that completely mixed conditions were maintained and a dye study was conducted to verify the conditions. During experiments the desired organic compound and hydrogen peroxide were added to the reactor vessels and sampled at desired time steps. Samples were placed in amber vials when drawn and stored at 4°C until they could be analyzed using gas chromatography, high performance liquid chromatography, and ion chromatography.

ACS grade chemicals were obtained from Sigma-Aldrich for both the experimental solutions (acetone and hydrogen peroxide) and stock solutions (oxalic acid, formic acid, acetic acid, glyoxylic acid, pyruvaldehyde 40% weight in solution, and pyruvic acid); along with formaldehyde from Fisher Scientific. Experimental solutions were prepared using MilliQ water (resistance $>$ 18.2 MΩ.cm) obtained from a Millipore purification system and 10 mM hydrogen peroxide to 1 mM of acetone along with

parachloro benzoic acid (pCBA) solution, 0.25 μM, was also added as a probe compound for hydroxyl radicals. Stock solutions were made for desired concentrations and diluted to create standard solutions in the anticipated concentration range for calibration curves.

During actual UV photolysis experiments only one photoreactor was used. Light intensity in the reactor was measured to be 5.16x10^{-7} Einstein/L-s using ferrioxalate actinometry and temperature controls kept the photoreactor within 1°C of the initial temperature. As a result, kinetics were observed to be those occurring at room temperature. Acetone, formaldehyde, and pyruvic aldehyde were measured via derivatization with 2,4-dinitrophenyl hydrazine followed by analyses using a UHPLC 2000 series Dionex equipped with a reverse phase C-18 column (4.5 mm x 250 mm) using acetonitrile and water in a gradient flow condition at 0.8 mL/min as the mobile phase. Retention times for formaldehyde, acetone, and pyruvate were 10.1 min, 21.1 min, and 14 min, respectively using this method. Concentrations of pCBA were also determined using this system and reverse phase HPLC with a C-18 column although a different eluent with 45% of acetonitrile and 55% of 10 mM H 3 PO 4 was used to find a retention time of 7.8 min at a 254 nm wavelength for pCBA. To determine the concentration of hydrogen peroxide, 2,9-dimethyl-1,10-phenanthroline (DMP) method was used for a diluted sample to ensure that concentrations were within the valid μM range. Ion chromatography with a Dionex ICS 2100 series equipped with an ion-exchange column was used to determine concentration of organic anions, acetate, formate, pyruvate and oxalate. Finally, total organic carbon (TOC) was determined using a TOC analyzer, GE sievers. The results of this study are presented in Table 1 and are the basis of the assessment of the *in silico* studies.

5.4.2 Lumped reactions *in silico* study

To study the intermediate radicals and stable by-products generated during AOPs we developed an ABM that we colloquially call ChemSim, for UV/H_2O_2. Using Figure

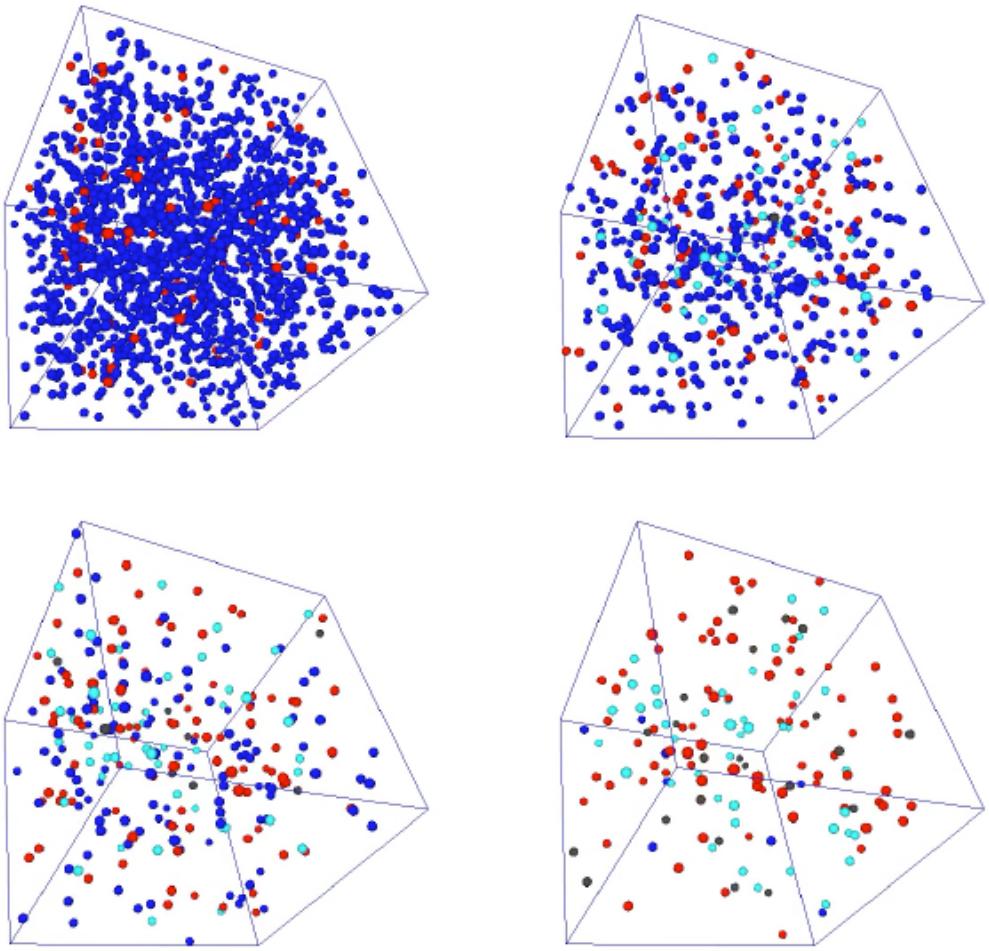

Figure 5.3: Visualizations showing ChemSim during model execution.

5.3 as a guide, the simulation may summarized as follows. First, starting from the upper left and proceeding left-to-right, top-to-bottom, the model is initialized with hydrogen peroxide (blue) and the initial contaminant (teal) as a well-mixed solution. Also shown are the hydroxyl radicals that form shortly after the model starts (red) due to the UV/H_2O_2 photolysis reaction. As model execution proceeds, the hydroxyl radicals which rapidly react to form byproducts (gray) with the contaimate being gradually eliminated. Following the exhaustion of hydrogen peroxide, the final steady-state may still contain the initial contaminate and byproducts, although chemical reactions typically cease once hydroxyl radicals are no longer created.

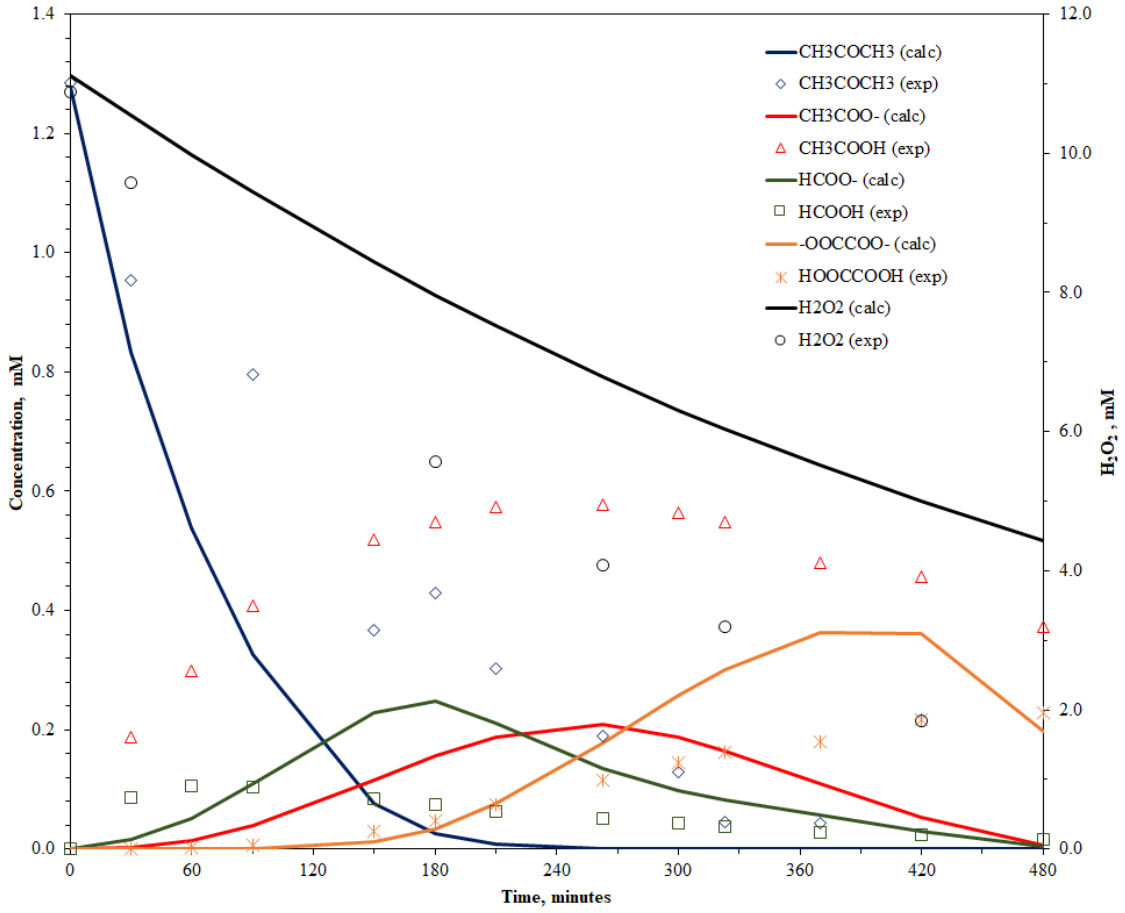

Figure 5.4: Predicted concentration profiles following acetone degradation induced by hydroxyl radicals using lumped reaction pathways, note that significant deviation from experimental concentrations is present.

Following basic validation of the ABM, the ability of the model to assess concentration profiles using lumped reactions was assessed. Acetone was selected due to its toxicity as well as being a simple compound. This allows it to be a "stepping stone" to studies involving more complex contaminants. Despite the simple structure, acetone has a complex reaction pathway when treated using UV/H_2O_2 processes with at least 88 reactions predicted before mineralization [262].

One of approaches to studying acetone degradation induced by hydroxyl radicals is through the use of lumped reactions that incorporate multiple steps as part of a single reaction. To explore the use of lumped reactions (see Table 5.2 for reactions),

Table 5.2
Lumped UV/H_2O_2 reactions for AOP treatment of acetone.

Reactant	**Reaction Rate (Ratios)**	**Source**
$H_2O_2 + h\nu \rightarrow HO^{\bullet}$	-2.38x10^{-2} M s	
$CH_3COCH_3 + HO^{\bullet} \rightarrow {}^{\bullet}CH_2COCH_3$	1.0x10^8 $M^{-1}s^{-1}$	[263]
${}^{\bullet}CH_2COCH_3 + O_2 \rightarrow {}^{\bullet}O-CH_2COCH_3$	5.0x10^9 $M^{-1}s^{-1}$	[262]
${}^{\bullet}OO-CH_2COCH_3 + {}^{\bullet}OO-CH_2COCH_3 \rightarrow 2\,{}^{\bullet}O-CH_2COCH_3 + O_2$	1.0x10^9 $M^{-1}s^{-1}$ (15%)	[262]
${}^{\bullet}OO-CH_2COCH_3 + {}^{\bullet}OO-CH_2COCH_3 \rightarrow H_2O_2 + 2\,CH_3COCHO$	1.0x10^9 $M^{-1}s^{-1}$ (25%)	[262]
${}^{\bullet}OO-CH_2COCH_3 + {}^{\bullet}OO-CH_2COCH_3 \rightarrow CH_3COCHO + CH_3COCH_2OH + O_2$	1.0x10^9 $M^{-1}s^{-1}$ (60%)	[262]
${}^{\bullet}O-CH_2COCH_3 \rightarrow {}^{\bullet}COCH_3 + HCHO$	1.4x10^6 s^{-1}	[262]
$CH_3COCHO + HO^{\bullet} \rightarrow CH_3COCOOH$	5.0x10^8 $M^{-1}s^{-1}$	[264]
$CH_3COCOOH + HO^{\bullet} \rightarrow CH_3COOH$	1.0x10^7 $M^{-1}s^{-1}$	[262]
$CH_3COCH_2OH + HO^{\bullet} \rightarrow HCHO$	1.0x10^8 $M^{-1}s^{-1}$	[262]
$HCHO + HO^{\bullet} \rightarrow HCOOH$	1.0x10^8 $M^{-1}s^{-1}$	[262]
$CH_3COOH + HO^{\bullet} \rightarrow HOCCOOH + HCOOH$	1.6x10^7 $M^{-1}s^{-1}$	[265]
$HOCCOOH + HO^{\bullet} \rightarrow HOOCCOOH$	1.9x10^8 $M^{-1}s^{-1}$	[266]
$HOOCCOOH + HO^{\bullet} \rightarrow CO_2$	1.4x10^6 $M^{-1}s^{-1}$	[267]
$HCOOH + HO^{\bullet} \rightarrow CO_2$	4.5x10^7 $M^{-1}s^{-1}$	[265]

the model was configured for their use with a photolysis rate of -0.0238 M^{-1} S^{-1} that was calculated using the results from the laboratory study (see Section 5.4.1). The remaining parameters were then set to k_{diff} of 1.1x10^{10}, 1.8 L for the reactor volume, and a 0.02 mol concentration of hydrogen peroxide and 0.0023 mol for acetone. The starting limit for chemical entities in the model was 100,000 resulting in 89,686 hydrogen peroxide entities and 10,313 acetone entities being generated in a 12,757 nm^3 simulated space. Following execution of the mode five species were evaluated against their experimental measurements (i.e., acetone/CH_3COCH_3, acetic acid/CH_3COOH, hydrogen peroxide/H_2O_2, formic acid/HCOOH, and oxalic acid/HOOCCOOH) and

two assessments of the results were made using the experimental results from the laboratory study. Along with the MAPE, the sample deviation (SD) was calculated:

$$SD_i = \sqrt{\frac{1}{N_i - 1} \sum_{j=1}^{N_i} \left[\frac{C_{exp,j} - C_{cal,j}}{C_{exp,j}} \right]^2} \tag{5.16}$$

Where the variables are the same as the MAPE calculation.

This case study resulted in an overall MAPE of 82.06% for the system (acetone = 74.31%, acetic acid = 80.44%, hydrogen peroxide = 63.45%, formic acid = 115.18%, oxalic acid= 63.57%) as well as high SD for most species (acetone = 2.48, acetic acid = 2.91, hydrogen peroxide = 1.70, formic acid = 2.55, oxalic acid= 0.04). Significantly, the concentration profiles calculated did not match the experimental results (see Figure 5.4). However, this outcome was not unexpected: indeed it is consistent with the behavior of an ABM. Recall that one of the applications of ABM is to conduct theory testing. These results show that the use of lumped reaction pathways in the model are problematic and that more complete reaction pathways are required.

5.4.3 Comprehensive pathways *in silico* study

The next study conducted using the model was performed using recently developed elementary reaction pathways [262]. For this study the objectives were two-fold: first, to replicate the experimentally observed second order reaction kinetics for acetone using complete reaction pathways; second, to evaluate the predicted by-products against the experimental measures. Additionally, the running time of the ABM was logged to evaluate the running time of the model.

The first step in the study was to prepare the reaction list for the model. To do so the elementary reaction pathways [262] were adjusted to assume a neutral pH and the authors calculated the branching ratios not present in [262]. Table 5.3

Table 5.3
Elementary reaction pathways for acetone degradation induced by hydroxyl radicals

no.	**Reaction**	**Rate M^{-1} s^{-1} (Ratio)**
0	$H_2O_2 + h\nu \rightarrow 2\,HO^{\bullet}$	-2.38x10^{-2}
1	$CH_3COCH_3 + HO^{\bullet} \rightarrow {}^{\bullet}CH_2COCH_3 + H_2O$	1.10x10^{8}
2	${}^{\bullet}CH_2COCH_3 + O_2 \rightarrow {}^{\bullet}OOCH_2COCH_3$	2.00x10^{9}
3	${}^{\bullet}OOCH_2COCH_3 + {}^{\bullet}OOCH_2COCH_3 \rightarrow$ $CH_3COCH_2OOOOCH_2COCH_3$	1.40x10^{9} (1%)
4	${}^{\bullet}OOCH_2COCH_3 + {}^{\bullet}OOCH_2COCH_3 \rightarrow$ $2\,{}^{\bullet}OCH_2COCH_3 + (3)\,O_2$	1.40x10^{9} (37.6%)
5	${}^{\bullet}OOCH_2COCH_3 + {}^{\bullet}OOCH_2COCH_3 \rightarrow$ $2\,CH_3COCHO + H_2O_2$	1.40x10^{9} (53.6%)
6	${}^{\bullet}OOCH_2COCH_3 + {}^{\bullet}OOCH_2COCH_3 \rightarrow$ $CH_3COCHO + CH_3COCH_2OH + (3)\,O_2$	1.40x10^{9} (1%)
7	${}^{\bullet}OOCH_2COCH_3 + {}^{\bullet}OOCH_2COCH_3 \rightarrow$ $CH_3COCHO + CH_3COCH_2OOOH$	1.40x10^{9} (1%)
8	${}^{\bullet}OOCH_2COCH_3 + {}^{\bullet}OOCH_2COCH_3 \rightarrow$ ${}^{\bullet}OCH_2COCH_3 + HO_2{}^{\bullet} + CH_3COCHO$	1.40x10^{9} (5.8%)
9	${}^{\bullet}OOCH_2COCH_3 + HO_2{}^{\bullet} \rightarrow$ $CH_3COCH_2OH + (3)\,O + (3)\,O_2$	1.20x10^{7}
10	${}^{\bullet}OCH_2COCH_3 + HO_2{}^{\bullet} \rightarrow CH_3COCH_2OH +$ $(3)\,O_2$	1.00x10^{6}
12	${}^{\bullet}OCH_2COCH_3 + {}^{\bullet}OCH_2COCH_3 \rightarrow$ $CH_3COCHO + CH_3COCH_2OH$	2.20x10^{3}
13	${}^{\bullet}OCH_2COCH_3 \rightarrow {}^{\bullet}CH(OH)COCH_3$	9.75x10^{5} (28%)
14	${}^{\bullet}OCH_2COCH_3 \rightarrow {}^{\bullet}COCH_3 + HCHO$	9.75x10^{5} (72%)

Table 5.3 continued from previous page

no.	Reaction	Rate M^{-1} s^{-1} (Ratio)
15	$^{\bullet}COCH_3 + O_2 \rightarrow {}^{\bullet}OOCOCH_3$	2.50x10^{9}
16	$CH_3COCH(OH)_2 + HO^{\bullet} \rightarrow {}^{\bullet}CH_2COCH(OH)_2 + H_2O$	1.20x10^{8}
17	$CH_3COCH(OH)_2 + HO^{\bullet} \rightarrow {}^{\bullet}C(OH)_2COCH_3 + H_2O$	1.50x10^{8}
18	$^{\bullet}C(OH)_2COCH_3 + O_2 \rightarrow {}^{\bullet}OOC(OH)_2COCH_3$	7.40x10^{8}
19	$^{\bullet}OOC(OH)_2COCH_3 \rightarrow HO_2^{\bullet} + CH_3COCOO^-$	8.00x10^{3}
20	$CH_3COCOO^- + HO^{\bullet} \rightarrow {}^{\bullet}CH_2COCOO^- + H_2O$	3.90x10^{7}
21	$CH_3COCOO^- + HO^{\bullet} \rightarrow {}^{\bullet}OC(OH)(CH_3)COO^-$	1.00x10^{7}
22	$CH_3COCOO^- + H_2O_2 \rightarrow CH_3COO^- + CO_2 + H_2O$	1.10x10^{-1}
23	$CH_3COCHO + HO^{\bullet} \rightarrow {}^{\bullet}OC(OH)(CH_3)CHO$	7.43x10^{7}
24	$CH_3COCHO + HO^{\bullet} \rightarrow {}^{\bullet}CH_2COCHO + H_2O$	5.00x10^{8}
25	$CH_3COCHO + H_2O_2 \rightarrow CH_3COO^- + HCOO^- + H2O$	2.00e-01
26	$CH_3COCH_2OH + HO^{\bullet} \rightarrow {}^{\bullet}CH_2COCH_2OH + H_2O$	1.00x10^{8}
27	$CH_3COCH_2OH + HO^{\bullet} \rightarrow {}^{\bullet}CH(OH)COCH_3 + H_2O$	5.00x10^{8}
28	$^{\bullet}OOCOCH_3 + {}^{\bullet}OOCOCH_3 \rightarrow 2\,{}^{\bullet}OCOCH_3 + (3)\,O_2$	8.30x10^{9}

Table 5.3 continued from previous page

no.	Reaction	Rate M^{-1} s^{-1} (Ratio)
29	$^{\bullet}OOCOCH_3 + HO_2^{\bullet} \rightarrow CH_3COO^- + (3)\,O + (3)\,O_2$	2.00x10^6
30	$^{\bullet}OOCOCH_3 \rightarrow HO_2^{\bullet} + CH_2CO$	1.82 s
31	$CH_2CO + H_2O \rightarrow CH_3COO^-$	4.40x10^1
32	$^{\bullet}OCOCH_3 \rightarrow {}^{\bullet}CH_3 + CO_2$	1.00x10^6
33	$^{\bullet}CH_3 + O_2 \rightarrow {}^{\bullet}OOCH_3$	2.80x10^9
34	$^{\bullet}OOCH_3 + {}^{\bullet}OOCH_3 \rightarrow 2\,{}^{\bullet}OCH_3 + (3)\,O_2$	3.40x10^8 (50%)
35	$^{\bullet}OOCH_3 + {}^{\bullet}OOCH_3 \rightarrow 2\,HCHO + H_2O_2$	3.40x10^8 (50%)
36	$^{\bullet}OOCH_3 + {}^{\bullet}OOCH_3 \rightarrow HCHO + CH_3OH + (3)\,O_2$	1
37	$^{\bullet}OOCH_3 + HO_2^{\bullet} \rightarrow CH_3OH + (3)\,O + (3)\,O_2$	1.00x10^7
38	$^{\bullet}OOCH_3 + {}^{\bullet}OOCH_2COCH_3 \rightarrow {}^{\bullet}OCH_3 + {}^{\bullet}OCH_2COCH_3 + (3)\,O_2$	4.00x10^8
39	$^{\bullet}OOCH_3 + {}^{\bullet}OOCH_2COCH_3 \rightarrow CH_3COCHO + CH_3OH + (3)\,O_2$	1
40	$^{\bullet}OOCH_3 + {}^{\bullet}OOCH_2COCH_3 \rightarrow H_2O_2 + HCHO + CH_3COCHO$	1.00x10^7
41	$^{\bullet}OCH_3 \rightarrow {}^{\bullet}CH_2OH$	5.00x10^5
42	$CH_3OH + HO^{\bullet} \rightarrow {}^{\bullet}CH_2OH + H_2O$	9.60x10^8
43	$^{\bullet}CH_2OH + O_2 \rightarrow {}^{\bullet}OOCH_2OH$	1.20x10^9
44	$CH_2(OH)_2 + HO^{\bullet} \rightarrow {}^{\bullet}CH(OH)_2 + H_2O$	1.00x10^9
45	$^{\bullet}CH(OH)_2 + O_2 \rightarrow {}^{\bullet}OOCH(OH)_2$	4.50x10^9
46	$^{\bullet}OOCH_2OH + {}^{\bullet}OOCH_2OH \rightarrow 2\,{}^{\bullet}OCH_2OH + (3)\,O_2$	8.90x10^8
47	$^{\bullet}OOCH_2OH + {}^{\bullet}OOCH_2OH \rightarrow 2\,HCOO^-$	1.60x10^9

Table 5.3 continued from previous page

no.	Reaction	Rate M^{-1} s^{-1} (Ratio)
48	$^{\bullet}OOCH_2OH + {}^{\bullet}OOCH_2OH \rightarrow CH_2(OH)_2 + HCOO^-$	1
49	$^{\bullet}OOCH_2OH + HO_2^{\bullet} \rightarrow CH_2(OH)_2 + (3)\,O + (3)\,O_2$	2.00x10^6
50	$^{\bullet}OOCH_2OH \rightarrow HO_2^{\bullet} + HCHO$	48.1 s
51	$^{\bullet}OCH_2OH + {}^{\bullet}OCH_2OH \rightarrow HCOO^- + CH_3(OH)_2$	1.60x10^9
52	$^{\bullet}OCH_2OH \rightarrow HCHO + HO^{\bullet}$	1.00x10^6
53-54	$HCOO^- + HO^{\bullet} \rightarrow {}^{\bullet}COO^- + H_2O$	2.40x10^9
55	$^{\bullet}COO^- + O_2 \rightarrow {}^{\bullet}OOCOO^-$	1.00x10^10
56	$^{\bullet}OOCOO^- + {}^{\bullet}OOCOO^- \rightarrow {}^{\bullet}OCOO^- +$ (3)O2	8.70x10^9
57	$^{\bullet}OCOO^- + {}^{\bullet}OCOO^- \rightarrow CO_2 + (3)\,O_2$	7.80x10^9
58-59	$CH_3COO^- + HO^{\bullet} \rightarrow {}^{\bullet}CH_2COO^- + H_2O$	1.00x10^8
60	$^{\bullet}CH_2COO^- + O_2 \rightarrow {}^{\bullet}OOCH_2COO^-$	2.00x10^9
61	$^{\bullet}OOCH_2COO^- + {}^{\bullet}OOCH_2COO^- \rightarrow 2\,{}^{\bullet}OCH_2COO^- + (3)\,O$	5.80x10^8 (50%)
62	$^{\bullet}OOCH_2COO^- + {}^{\bullet}OOCH_2COO^- \rightarrow 2\,HOCCOO^- + H_2O_2$	5.80x10^8 (50%)
63	$^{\bullet}OOCH_2COO^- + {}^{\bullet}OOCH_2COO^- \rightarrow HOCCOO^- + HOCH_2COO^-$	1
64	$^{\bullet}OOCH_2COO^- + HO_2^{\bullet} \rightarrow HOCH_2COO^- + (3)\,O + (3)\,O_2$	1.00x10^5
65	$^{\bullet}OCH_2COO^- + {}^{\bullet}OCH_2COO^- \rightarrow HOCCOO^- + HOCH_2COO^-$	7.30x10^9

Table 5.3 continued from previous page

no.	Reaction	Rate M^{-1} s^{-1} (Ratio)
66	$^{\bullet}OCH_2COO^- \rightarrow {}^{\bullet}COO^- + HCHO$	1.00x10^6
67-68	$HOCCOO^- + HO^{\bullet} \rightarrow {}^{\bullet}COCOO^- + H_2O$	2.60x10^9
69	$^{\bullet}COCOO^- + O_2 \rightarrow {}^{\bullet}OOCOCOO^-$	3.30x10^9
70	$^{\bullet}OOCOCOO^- + {}^{\bullet}OOCOCOO^- \rightarrow (3)\,O_2 +$ $-OOCCOO-$	5.00x10^8
71	$^{\bullet}OOCOCOO^- + HO_2^{\bullet} \rightarrow -OOCCOO- +$ $(3)\,O + (3)\,O_2$	2.00x10^6
72-74	$-OOCCOO- + HO^{\bullet} \rightarrow {}^{\bullet}OOCCOO^- + H_2O$	1.60x10^8
75	$^{\bullet}CH(OH)COCH_3 + O_2 \rightarrow$ $^{\bullet}OOCH(OH)COCH_3$	9.50x10^8
76	$^{\bullet}OOCH(OH)COCH_3 + {}^{\bullet}OOCH(OH)COCH_3$ $\rightarrow CH_3COCOO^- + CH_3COCH(OH)_2$	5.80x10^6
77	$^{\bullet}OOCH(OH)COCH_3 + {}^{\bullet}OOCH(OH)COCH_3$ $\rightarrow 2\,{}^{\bullet}OCH(OH)COCH_3 + (3)\,O_2$	1.70x10^9
78	$^{\bullet}OOCH(OH)COCH_3 + {}^{\bullet}OOCH(OH)COCH_3$ $\rightarrow H_2O_2 + CH_3COCOO^-$	3.00x10^8
79	$^{\bullet}OOCH(OH)COCH_3 + HO_2^{\bullet} \rightarrow$ $CH(OH)_2COCH_3 + (3)\,O + (3)\,O_2$	2.00x10^6
80	$^{\bullet}OOCH(OH)COCH_3 \rightarrow CH_3COCHO +$ $HO_2^{\bullet}$	2.2
81	$^{\bullet}OCH(OH)COCH_3 + {}^{\bullet}OCH(OH)COCH_3 \rightarrow$ $CH_3COCOO^- + CH_3COCH(OH)_2$	1.00x10^3
82	$^{\bullet}OCH(OH)COCH_3 \rightarrow HCOO^- + {}^{\bullet}COCH$	1.00x10^6
83	$^{\bullet}OOCH(OH)_2 + {}^{\bullet}OOCH(OH)_2 \rightarrow$ $2\,{}^{\bullet}OCH(OH)_2 + (3)\,O_2$	7.90x10^7 (50%)

Table 5.3 continued from previous page

no.	Reaction	Rate M^{-1} s^{-1} (Ratio)
84	$^{\bullet}OOCH(OH)_2 + {}^{\bullet}OOCH(OH)_2 \rightarrow 2\,HOC(OH)_2 + H_2O_2$	7.90x10^7 (50%)
85	$^{\bullet}OOCH(OH)_2 + {}^{\bullet}OOCH(OH)_2 \rightarrow CH(OH)_3 + HOC(OH)_2$	1
86	$^{\bullet}OOCH(OH)_2 \rightarrow {}^{\bullet}HO_2 + HCOO^-$	8.70x10^3
87	$^{\bullet}OOCH(OH)_2 + HO_2^{\bullet} \rightarrow CH(OH)_3 + (3)\,O + (3)\,O_2$	2.00x10^6
88	$^{\bullet}OCH_2OH \rightarrow HCOO^- + HO^{\bullet}$	6.30x10^5
89	$^{\bullet}OOCCOO^- + {}^{\bullet}OOCCOO^- \rightarrow 4\,CO_2$	8.26x10^9
90	$H_2O_2 + HO^{\bullet} \rightarrow HO_2^{\bullet} + H_2O$	2.70x10^7
91	$H_2O_2 + HO_2^{\bullet} \rightarrow HO^{\bullet} + H_2O + O_2$	5.00x10^{-1}
92	$H_2O_2 + O_2^{\bullet -} \rightarrow HO^{\bullet} + OH^- + O_2$	1.30x10^{-1}
93	$HO^{\bullet} + HO_2^- \rightarrow HO_2^{\bullet} + OH^-$	7.50x10^9
94	$HO^{\bullet} + HO_2^{\bullet} \rightarrow H_2O + O_2$	6.60x10^9
95	$HO^{\bullet} + HO^{\bullet} \rightarrow H_2O_2$	5.50x10^9
96	$HO_2^{\bullet} + O_2^{\bullet -} \rightarrow H_2O_2 + O_2$	8.86x10^7
97	$HO_2^{\bullet} + HO_2^{\bullet} \rightarrow H_2O_2 + O_2$	7.61x10^5
98	$H_2O_2 \Leftrightarrow HO_2^- + H^+$	pKa = 11.6
99	$HO_2^{\bullet} \Leftrightarrow O_2^{\bullet -} + H^+$	pka = 4.8

lists the reactions used for the study and follows the same numbering convention as [262]. Reaction 11 was excluded due to the slow reaction rate and the rest of the CH_2=C+OCH_3 reactions were not included in the study. A range indicates the use of a single reaction assuming a constant pH of seven. Reaction 89 is based upon calculations by the authors, while reactions 90 through 99 are from [268]. Finally, since the model attempts reactions in the order they are read, we sorted the reaction

list to have the faster reactions first. To account for the hydroxyl cage effect, hydroxyl radicals produced as result of photolysis (i.e., Reaction 0) each have a 70% chance of entering the model. The model was then run using the same parameters outlined in Section 5.4.2 and the MAPE and SD calculated.

In contrast to the lumped reactions, the concentration profiles calculated using the elementary reaction pathways are consistent with the experimental data (see Figure 5.5). The numerical results of the study also show promise as well, despite showing a fairly high error rate for the MAPE (overall = 80.39%, acetone = 84.04%, acetic acid = 19.55%, hydrogen peroxide = 11.15%, formic acid = 61.17%, oxalic acid = 193.63%) and SD (acetone = 2.64, acetic acid = 0.60, hydrogen peroxide = 0.03, formic acid = 2.30, oxalic acid = 4.89). The predicted concentration profile for hydrogen peroxide had the best fit to experimental data overall. The next is acetone until about 300 minutes into the model where it deviates from the experimental data. Acetic acid starts with a close fit to experimental data, but deviates at about 120 minutes with lower predicted concentrations than were observed. Formic acid is consistently under predicted by the model, but the behavior of the curve is consistent with the experimental results (i.e., rapid peak followed by long decay). Similarly, oxalic acid follows the observed behavior of the experimental data, but is generally under predicted throughout the model starting at 180 minutes. Prior to that, the model over predicts which may lead to the MAPE and SD being high given an experimental measurement of $9.58\text{x}10^{-5}$ mM at 30 minutes. When that value is excluded, the numerical results for oxalic acid drop considerably (MAPE = 102.71%, SD = 1.35). Execution of the model took on average 27 minutes 41 seconds, over 10 runs with a standard deviation of 2 minutes 38 seconds on a Late 2013 iMac (2.9 GHz Intel Core i5, 8 GB 1600 MHz DDR3).

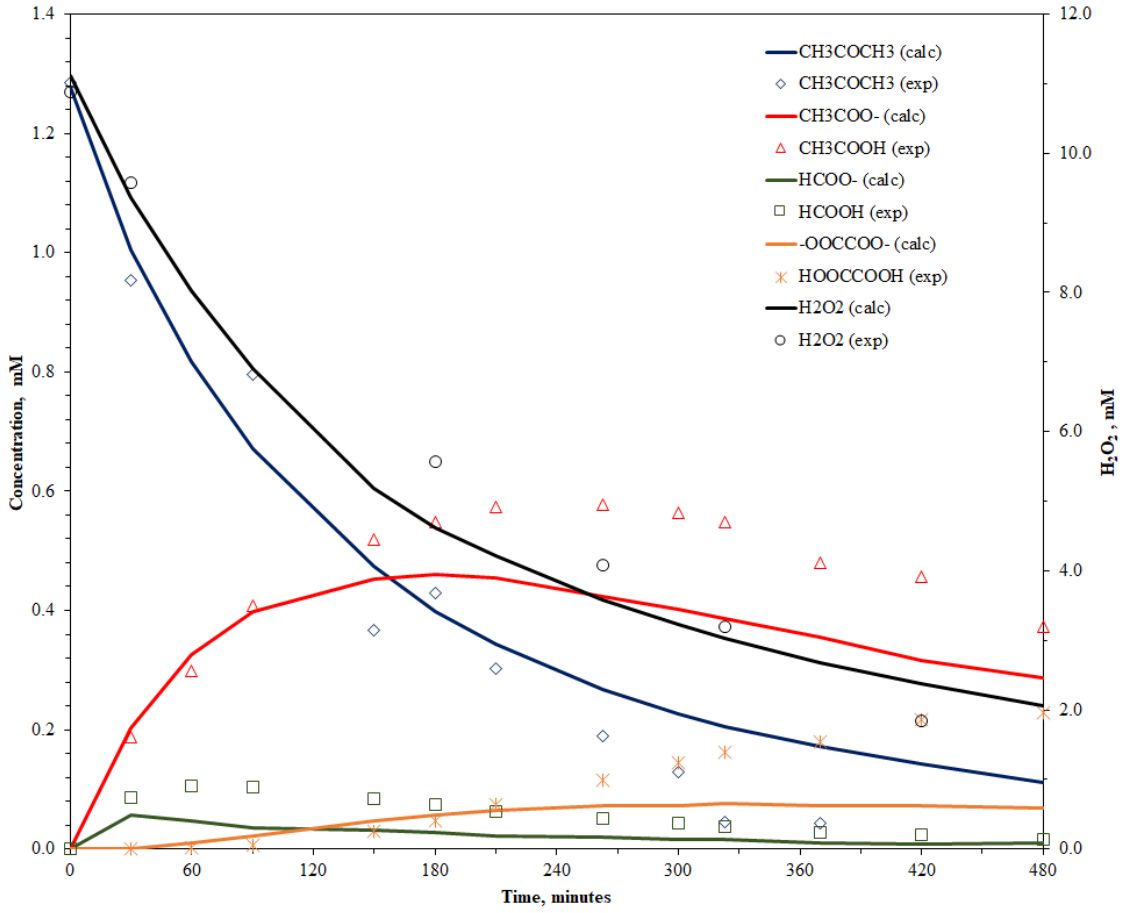

Figure 5.5: Predicted concentration profiles following acetone degradation induced by hydroxyl radicals using elementary reaction pathways, note that while there are deviations in the calculated concentrations, the concentration profiles are consistent with experimental data.

5.4.4 Sensitivity Analysis

Sensitivity analysis for the model was conducted in two phases and complete details can be found in the Supplementary Material. For the first phase the reaction rates were adjusted between 2x and 0.5x for select reactions (see Table 5.4) and the model was run using the same parameters outlined in Section 5.4.3. During this analysis it was observed that the concentrations for formic acid and acetic acid were both found to be significantly dependent upon the rate constants for hydroxyl radicals. Additionally, the formation of $HOCCOO^{-}$ was found exhibit significant fluctuations which is

likely attributable to the number of agents in the model since $HOCCOO^-$ fluctuated between 50 and 200 agents. This implies that the model has some sensitivity to the number of agents for chemical species with very low concentrations.

Since reductions in the reaction rate for reactions no. 58-59, no. 53-54, and no. 72-74 resulted in the sample deviation for oxalic acid being significantly reduced, a second phase of sensitivity analysis was conducted. For this evaluation, the reaction rates for reactions no.53-54, no.58-59, and no.72-74 were set to 6.0×10^8 M^{-1} s^{-1}, 5.0×10^7 M^{-1} s^{-1}, and 8.0×10^7 M^{-1} s^{-1}, respectively. Reaction rates were then adjusted between 2x and 0.5x for select reactions (see Table 5.6). Under these scenarios the SD was found to improve significantly against the baseline scenario (see Table 5.7) supporting the conclusion the formation of by-products are significantly dependent upon the rate constants for hydroxyl radicals.

5.5 Discussion

One significant observation from the model is that while the concentration profile for acetone tends to align with the experimental data until about 300 minutes into the model. This holds for both the baseline results (see Section 5.4.3) as well as during sensitivity analysis. The exact cause of this remains somewhat elusive. While the sensitivity analysis revealed that the by-products are very sensitive to hydroxyl radical rate constants, in the case of the acetone reaction, variations in the reaction rate resulted in the concentration profile deviating significantly from the experimental values. However, in the case of scenario 19b (i.e., reactions no. 3 through 8 having k reduced by 0.5x) acetone had a SD at 1.16 (SD of 0.31 for 0 through 300 minutes) with good agreement with experimental measurements. This implies that acetone degradation is at least influenced by subsequent reactions and that some of the error be a result of measurement error during the experiment.

While the results of the model are promising, more work can be done to improve the overall fidelity. First, while the elementary reaction pathways were adjusted to assume a neutral pH, during an AOP the pH is expected to fluctuate and accounting for this will likely improve the results. Second, we used a probabilistic approximation of the photolysis reaction based upon experimental results. The significant deviation in concentration profiles for lumped pathways and elementary reaction pathways indicates that incorporation of scavenging reactions is necessary in order to predict the hydrogen peroxide concentrations. While this indicates that the results are more than just the model fitting the experimental results, it is also quite limited since it requires experimental data to calculate the photolysis rate. As such, further research is needed to model photolysis based upon the underlying photo-physical and photochemical behavior in the context of the ABM.

5.6 Conclusion

The use of ABM to study AOPs is a novel application and even in the context of chemical modeling the application of ABM has remained quite limited. However, as we have demonstrated, ABM has the potential to address the limitations in existing approaches to studying AOPs by modeling the chemical entities and relevant reactions. While the numeric errors for the elementary reaction pathways where high, the predicted concentration profiles were consistent with the behavior of the experimental concentrations. This shows considerable promise for ABM in the context of AOPs and warrants further investigation of the technique.

Acknowledgements

This research was supported by National Science Foundation grant CBET-1435926 and a student research grant from the Great Lakes Research Center. The authors would like to thank Erica Coscarelli for their assistance in the studies.

Supplementary Material

5.A Sensitivity Analysis

5.A.1 Part I

The first part of the sensitivity analysis evaluated the response of the model to adjustments in the reaction rate for key reactions as outlined in scenarios number 1a though 11b (see Table 5.4). Since it was observed that formic acid and acetic acid were significantly dependent upon the rate constants for hydroxyl radicals (see Table 5.5), additional scenarios were conducted to verify this. The results of these scenarios are included as Figures 5.16 through 5.21.

5.A.2 Part II

For the second part of the sensitivity analysis, the sensitivity of formic acid and acetic acid were significantly dependent upon the rate constants for hydroxyl radicals was further evaluated. This was done by adjusting the reaction rate for reactions no. 53-54, no. 58-59, and no. 72-74 (see Table 5.3) to 6.0×10^8 M^{-1} s^{-1}, 5.0×10^7 M^{-1} s^{-1}, and 8.0×10^7 M^{-1} s^{-1}, respectively. These settings were then used to generate the baseline calculated concentration profiles for figures 5.22 - 5.32. The scenarios outlined in Table 5.6 were then run to generate the sample deviation (See Table 5.7) and the plots.

Table 5.4
Adjustments to reaction rates for the first part of the sensitivity analysis

Scenario No.	Description
1a	Reaction No. 1: 2 times k
1b	Reaction No. 1: 1/2 times k
2a	Reaction No. 2: 2 times k
2b	Reaction No. 2: 1/2 times k
3a	Reactions No. 3-8: 2 times k
3b	Reactions No. 3-8: 1/2 times k
4a	Reaction No. 9: 2 times k
4b	Reaction No. 9: 1/2 times k
5a	Reactions No. 13-14: 2 times k
5b	Reactions No. 13-14: 1/2 times k
6a	Reaction No. 29: 2 times k
6b	Reaction No. 29: 1/2 times k
7a	Reactions No. 58-59: 2 times k
7b	Reactions No. 58-59: 1/2 times k
8a	Reactions No. 53-54: 2 times k
8b	Reactions No. 53-54: 1/2 times k
9a	Reactions No. 71: 2 times k
9b	Reactions No. 71: 1/2 times k
10a	Reactions No. 72-74: 2 times k
10b	Reactions No. 72-74: 1/2 times k
11a	Reactions No. 67-68: 2 times k
11b	Reactions No. 67-68: 1/2 times k
12	Reactions No. 58-59, 53-54, and 72-74: 2 times k
13	Reactions No. 58-59, 53-54, and 72-74: 0.5 times k
14	Reactions No. 58-59: 0.5 times k, No. 53-54 and 72-74: 0.25 times k
15	Reactions No. 58-59: 0.5 times k, No. 53-54: 0.4 times k, and 72-74: 0.1 times k
16	Reactions No. 58-59: 0.5 times k, No. 53-54: 0.4 times k, and 72-74: 0.05 times k

Table 5.5
Calculated sample deviation for first sensitivity analysis versus experimental results

	Compound				
Scenario No.	Acetone	Acetic Acid	Hydrogen Peroxide	Formic Acid	Oxalic Acid
1a	1.01	0.04	0.01	2.44	9.68
1b	7.62	1.39	0.07	2.40	6.12
2a	2.42	0.58	0.03	2.34	6.86
2b	2.34	0.57	0.02	2.34	7.20
3a	2.62	0.60	0.00	2.31	6.73
3b	2.44	0.63	0.03	2.36	5.69
4a	1.61	0.68	0.11	2.41	7.79
4b	1.41	0.74	0.13	2.46	7.66
5a	2.44	0.61	0.03	2.37	8.21
5b	2.58	0.61	0.03	2.36	10.47
6a	2.31	0.61	0.05	2.36	10.28
6b	2.43	0.60	0.03	2.34	8.26
7a	2.75	1.66	0.01	2.32	22.92
7b	2.00	0.50	0.06	2.37	1.82
8a	2.36	0.58	0.02	2.85	9.67
8b	2.25	0.55	0.03	1.20	8.07
9a	2.50	0.64	0.03	2.32	7.34
9b	2.57	0.62	0.03	2.33	6.49
10a	2.55	0.63	0.03	2.35	7.09
10b	2.50	0.64	0.04	2.33	8.50
11a	2.62	0.57	0.04	2.23	9.00
11b	2.33	0.55	0.05	2.39	4.01
12	2.93	1.67	0.00	2.87	12.37
13	2.18	0.50	0.06	1.29	3.94
14	2.15	0.45	0.06	0.78	2.80
15	1.85	0.49	0.05	0.94	2.48
16	1.96	0.53	0.08	0.85	1.96

Table 5.6
Adjustments to reaction rates for the second part of the sensitivity analysis

Scenario No.	**Description**
17a	Reaction No. 1: 2 times k
17b	Reaction No. 1: 1/2 times k
18a	Reaction No. 2: 2 times k
18b	Reaction No. 2: 1/2 times k
19a	Reactions No. 3-8: 2 times k
19b	Reactions No. 3-8: 1/2 times k
20a	Reaction No. 9: 2 times k
20b	Reaction No. 9: 1/2 times k
21a	Reactions No. 13-14: 2 times k
21b	Reactions No. 13-14: 1/2 times k
22a	Reaction No. 29: 2 times k
23b	Reaction No. 29: 1/2 times k
23a	Reactions No. 58-59: 2 times k
23b	Reactions No. 58-59: 1/2 times k
24a	Reactions No. 53-54: 2 times k
24b	Reactions No. 53-54: 1/2 times k
25a	Reactions No. 71: 2 times k
25b	Reactions No. 71: 1/2 times k
26a	Reactions No. 72-74: 2 times k
26b	Reactions No. 72-74: 1/2 times k
27a	Reactions No. 67-68: 2 times k
27b	Reactions No. 67-68: 1/2 times k

Table 5.7
Calculated sample deviation for second sensitivity analysis versus experimental results

	Compound				
Scenario No.	Acetone	Acetic Acid	Hydrogen Peroxide	Formic Acid	Oxalic Acid
17a	1.32	1.27	0.02	0.37	3.01
17b	7.31	0.53	0.09	0.36	0.28
18a	2.06	0.45	0.08	0.85	0.04
18b	1.26	0.38	0.16	0.25	4.33
19a	2.07	0.51	0.06	0.70	1.39
19b	1.16	0.45	0.16	0.30	3.14
20a	1.80	0.37	0.07	0.72	0.82
20b	1.92	0.33	0.07	0.72	0.07
21a	2.02	0.38	0.07	0.78	0.17
21b	1.89	0.36	0.06	0.92	0.66
22a	1.97	0.41	0.05	0.91	0.38
22b	2.02	0.30	0.06	0.85	0.07
23a	2.35	0.69	0.05	0.92	4.07
23b	1.66	1.21	0.10	0.60	1.88
24a	2.02	0.35	0.07	1.39	1.46
24b	1.75	0.36	0.08	5.38	1.22
25a	1.96	0.33	0.07	0.87	0.25
25b	2.00	0.33	0.06	0.66	0.06
26a	2.13	0.36	0.06	0.83	1.30
26b	1.96	0.33	0.07	0.80	1.55
27a	2.06	0.31	0.06	0.84	0.33
27b	1.94	0.35	0.07	0.74	0.50

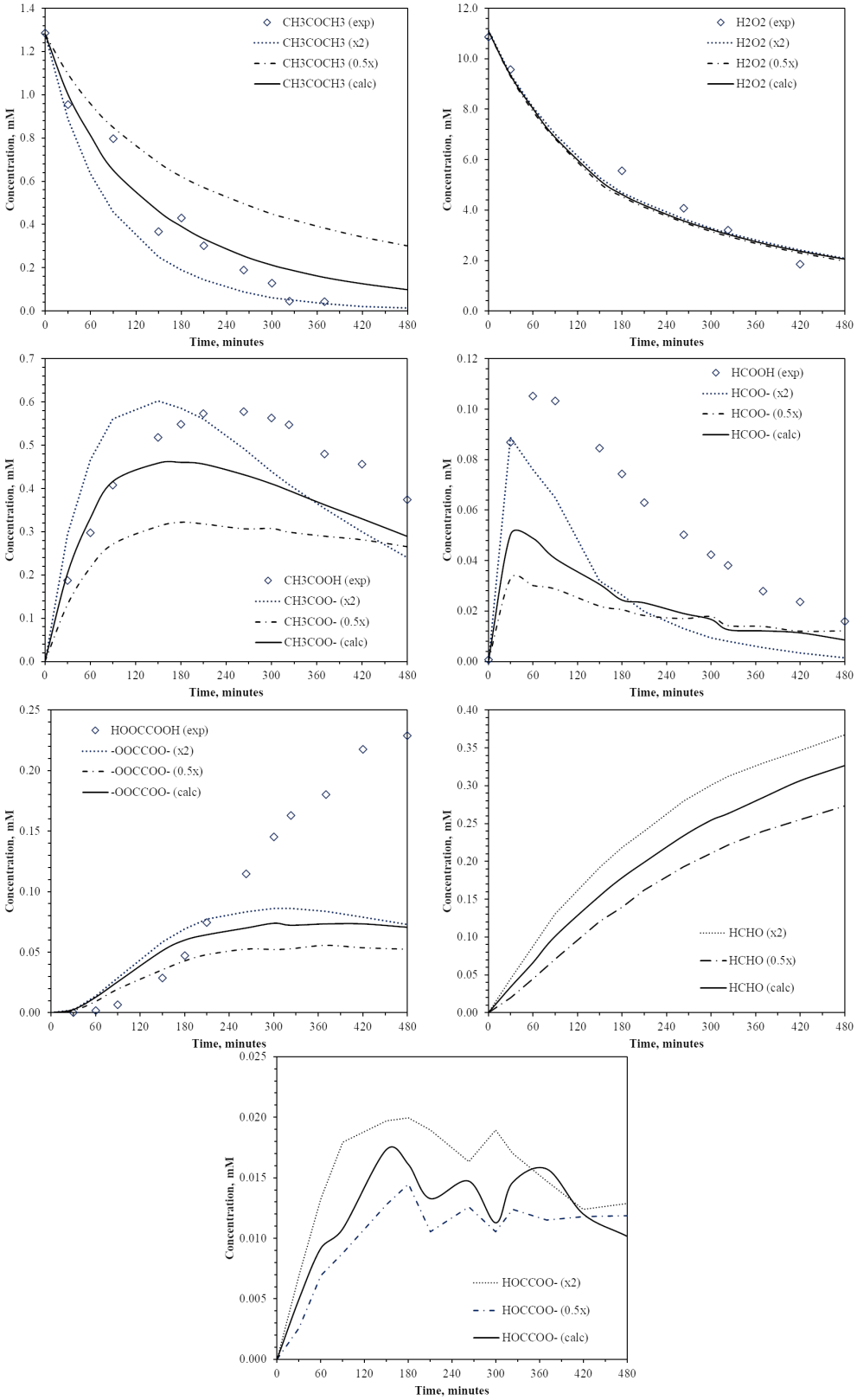

Figure 5.6: Scenario Number 1a and 1b

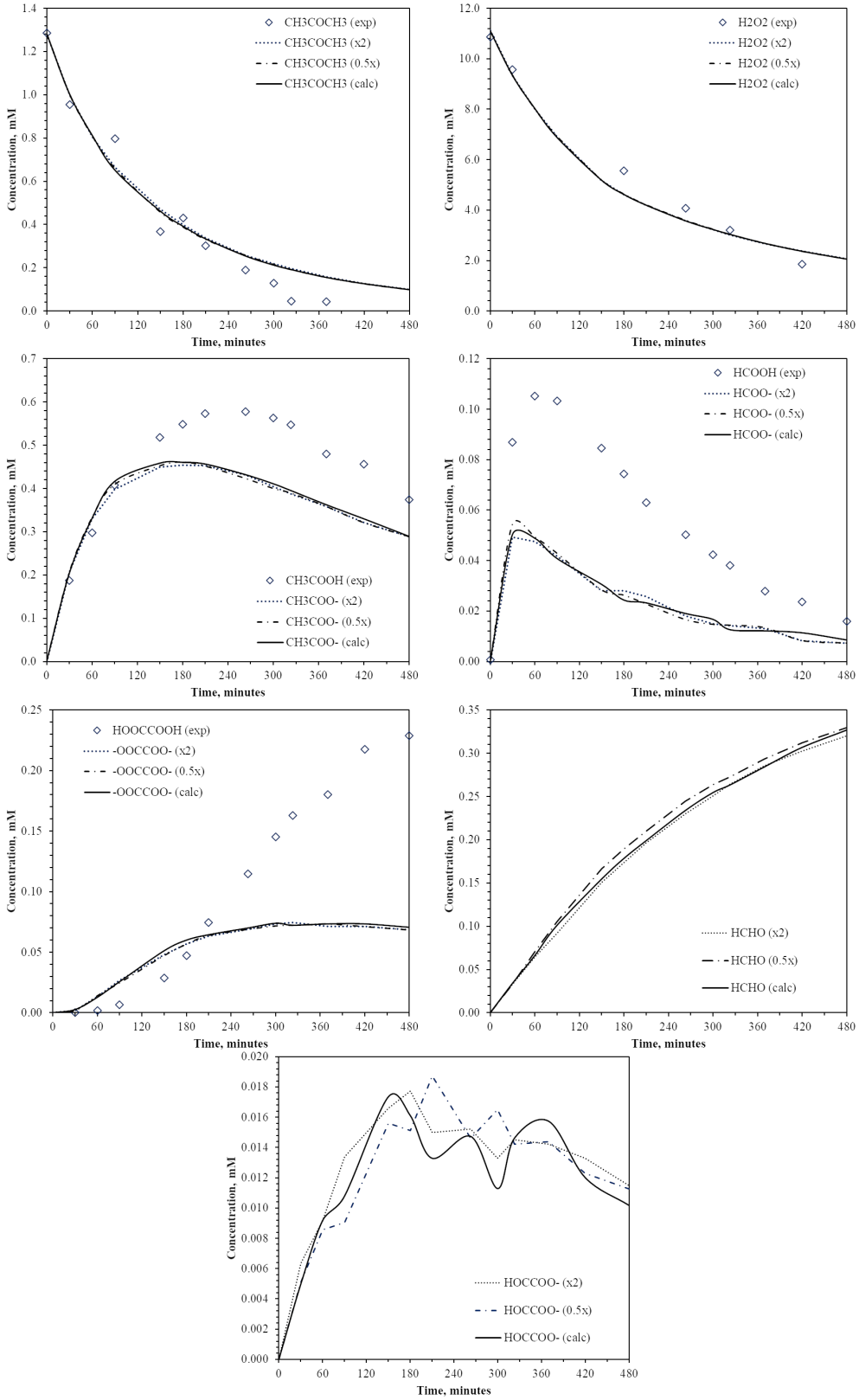

Figure 5.7: Scenario Number 2a and 2b

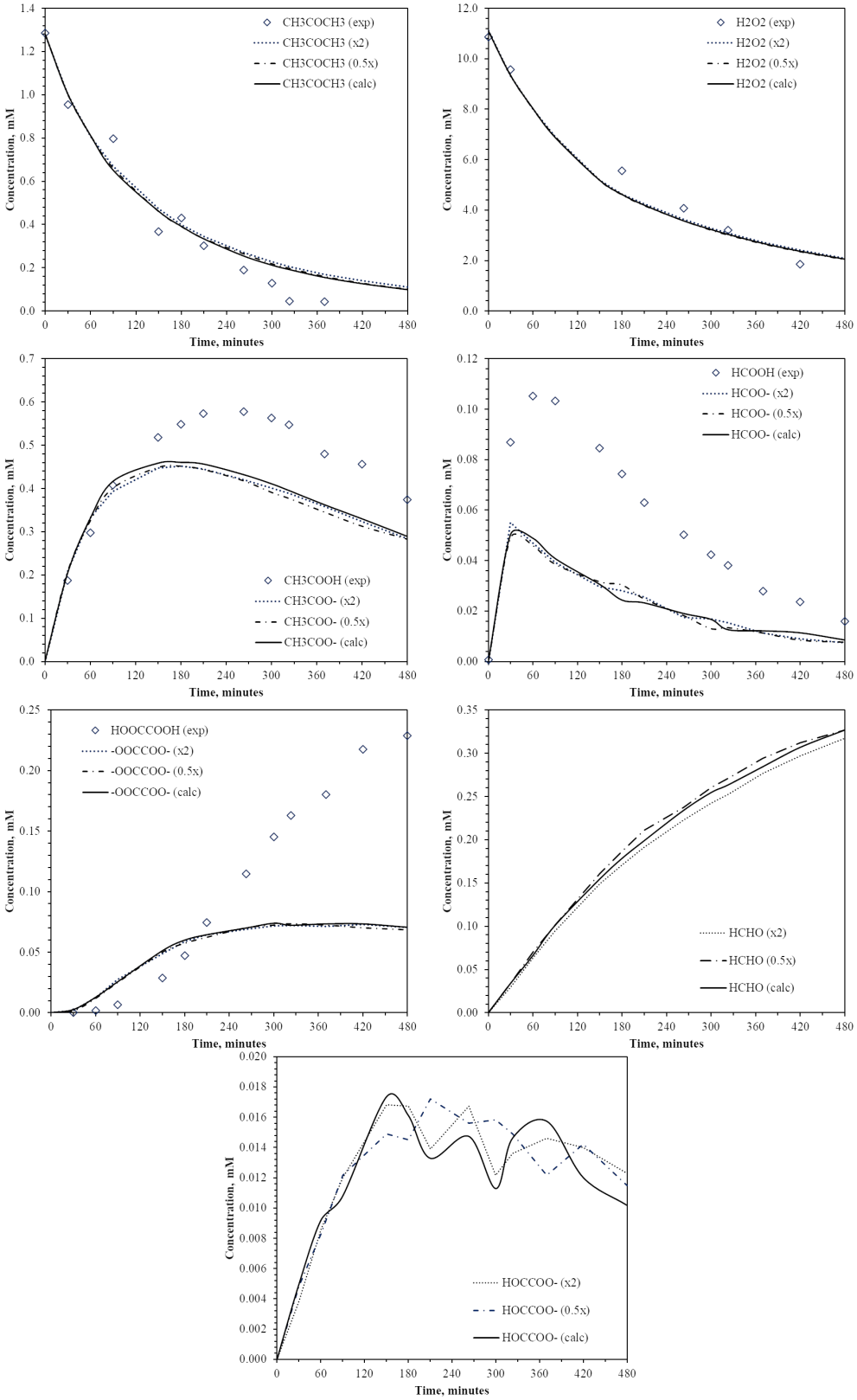

Figure 5.8: Scenario Number 3a and 3b

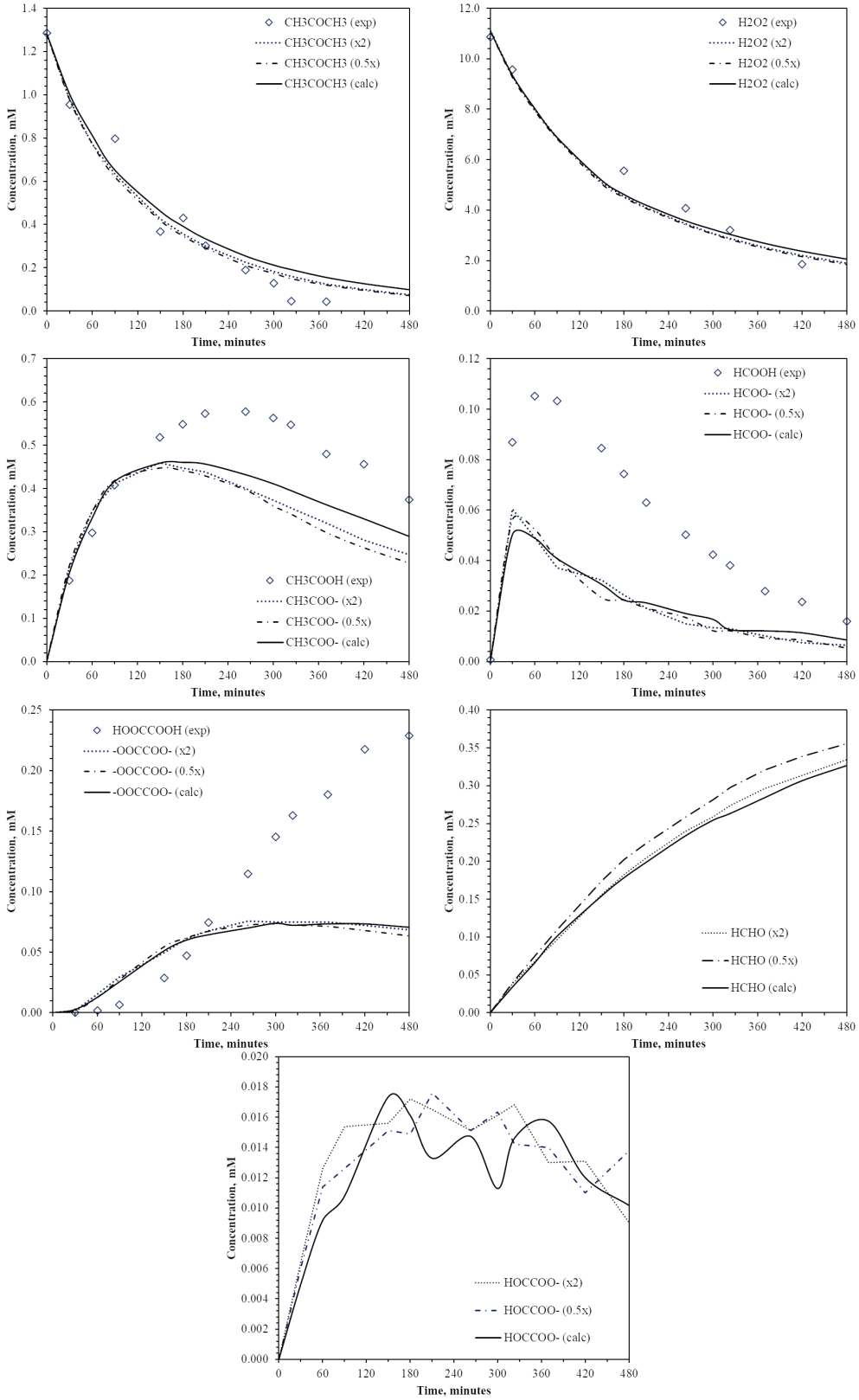

Figure 5.9: Scenario Number 4a and 4b

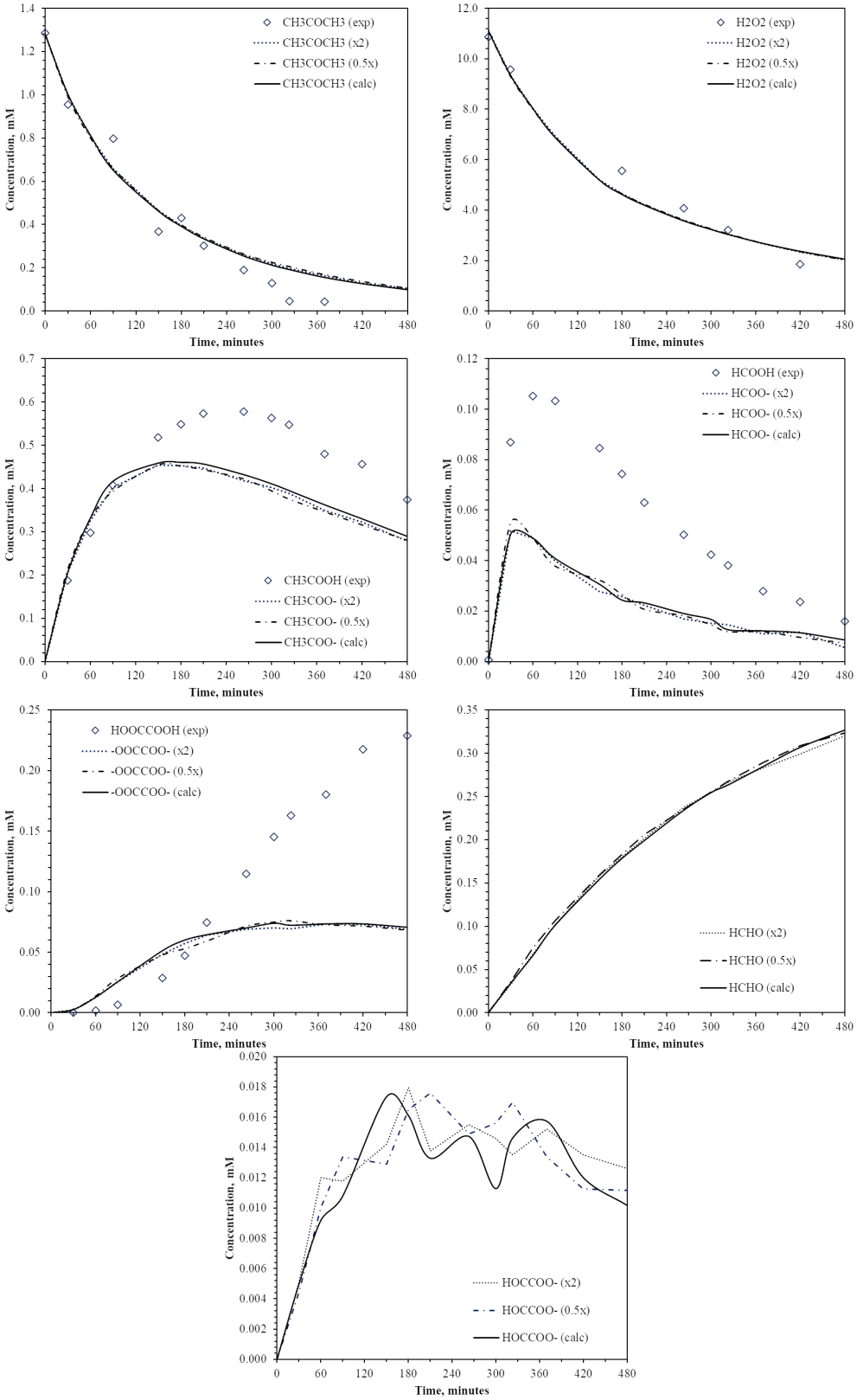

Figure 5.10: Scenario Number 5a and 5b

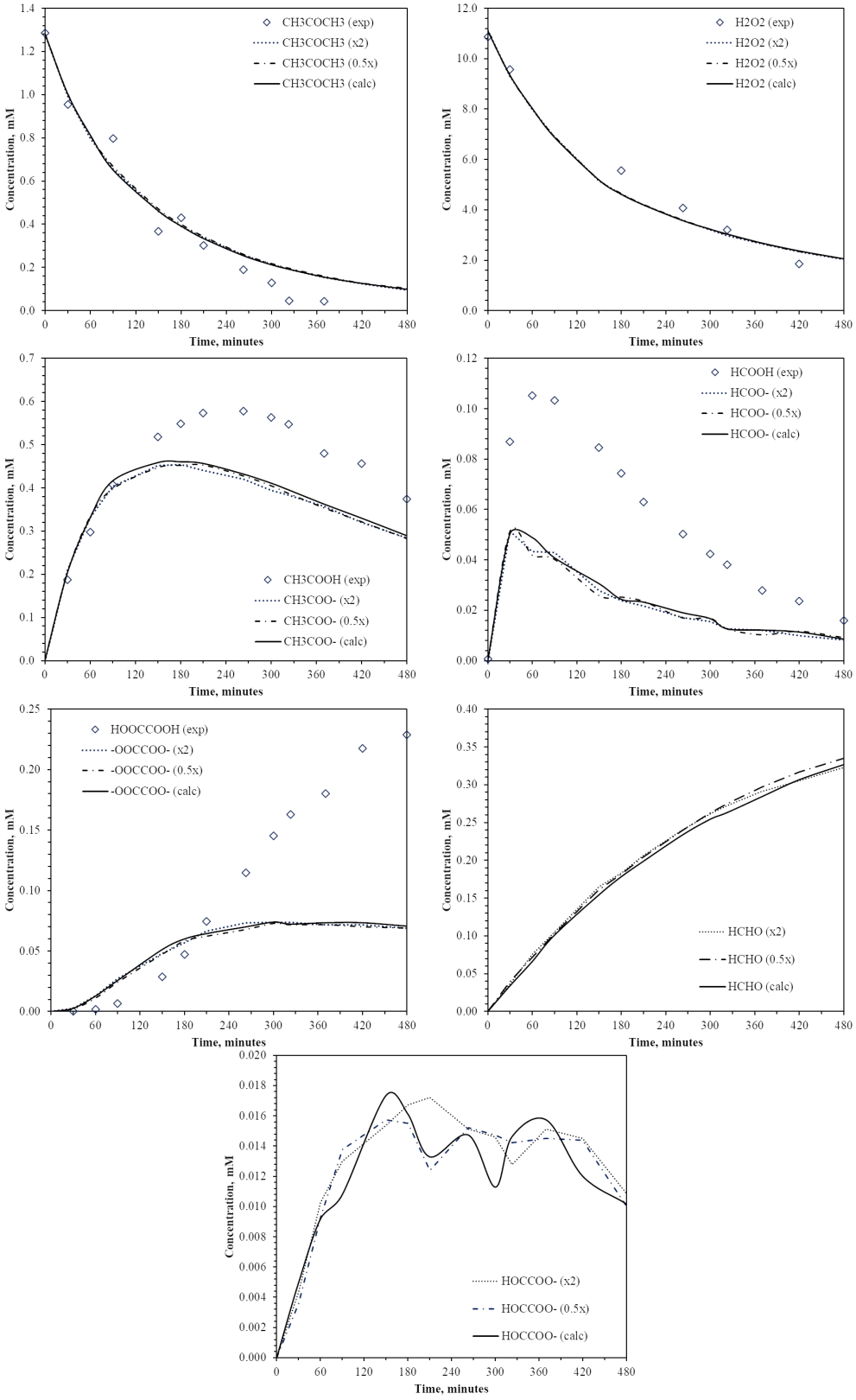

Figure 5.11: Scenario Number 6a and 6b

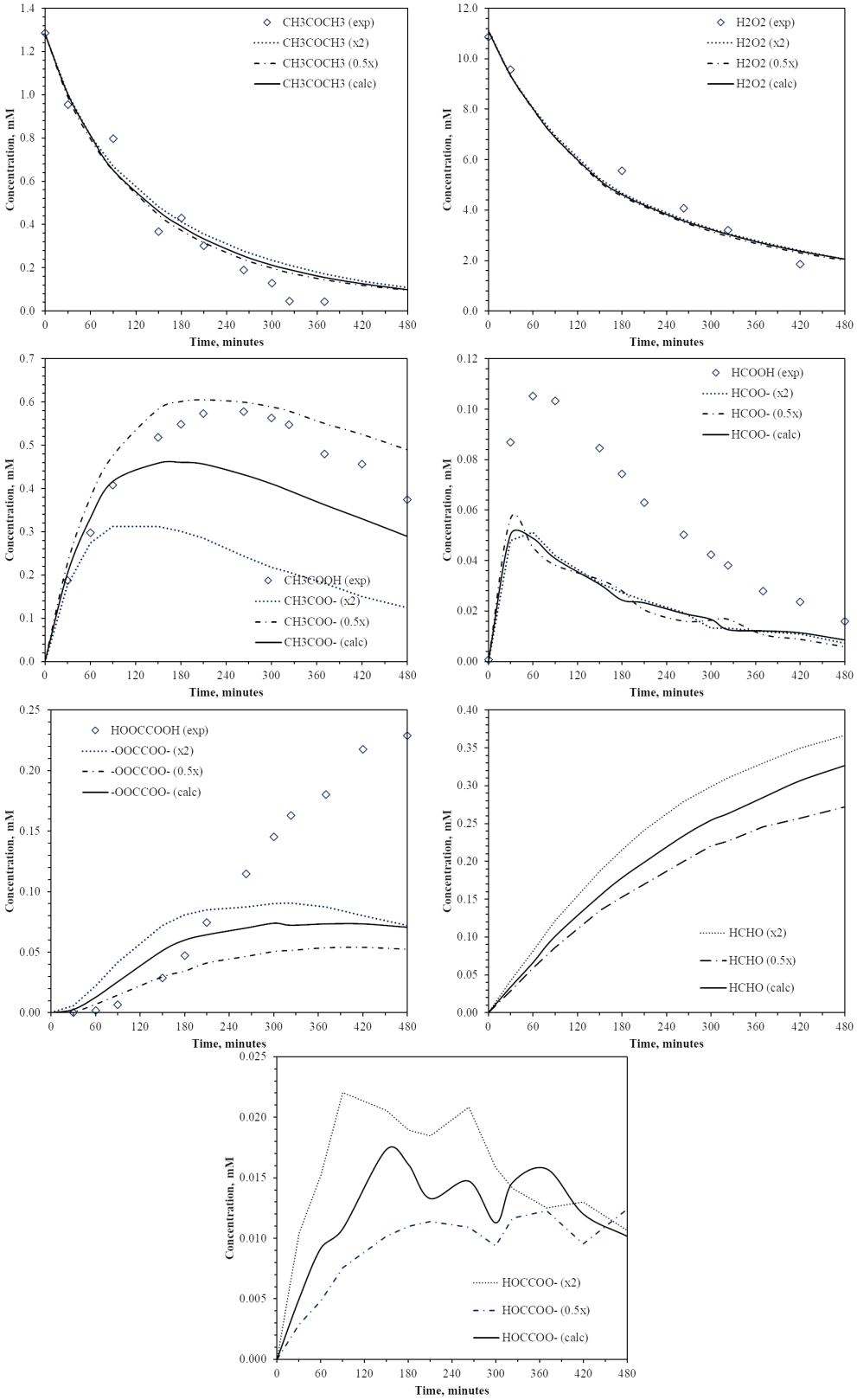

Figure 5.12: Scenario Number 7a and 7b

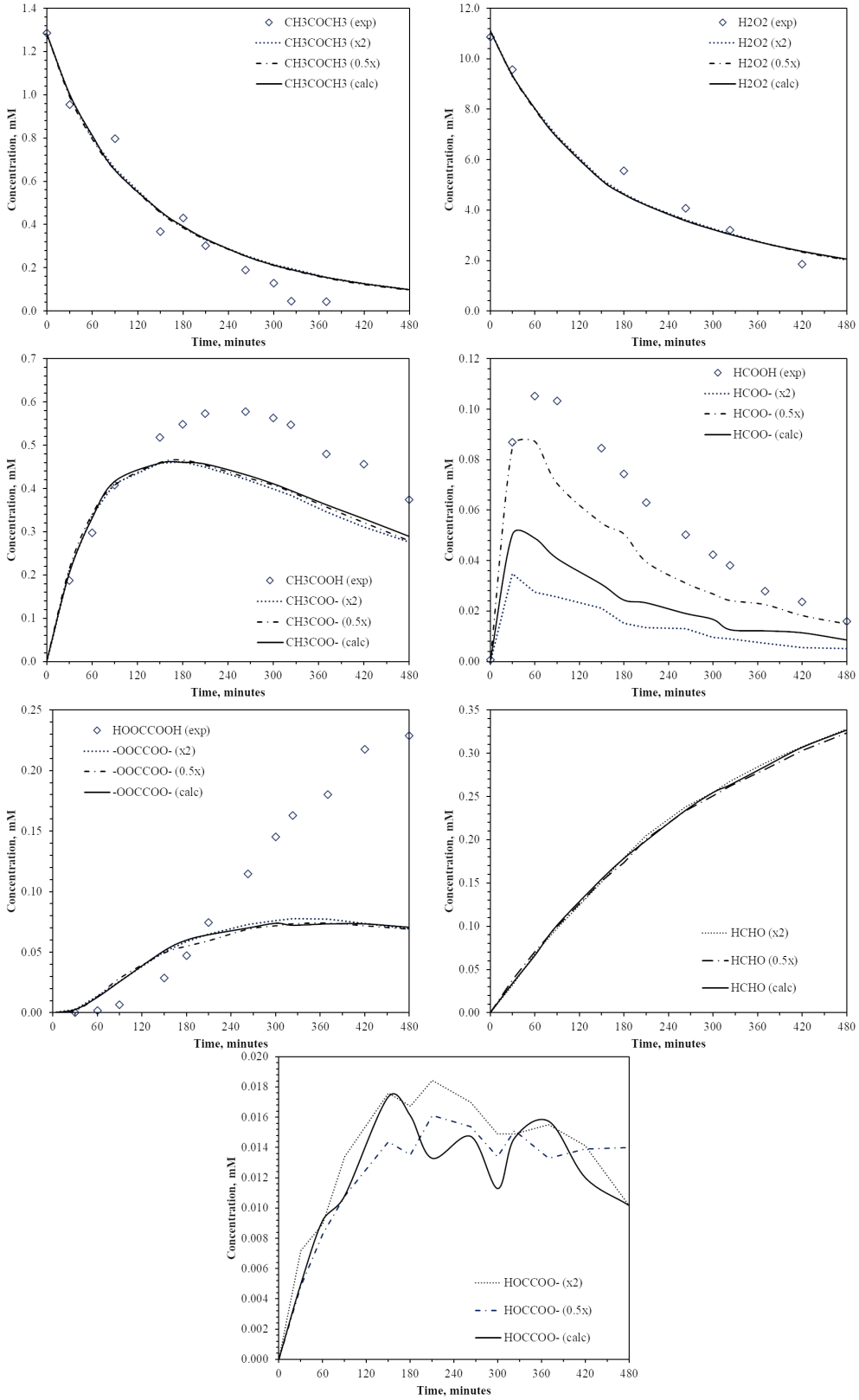

Figure 5.13: Scenario Number 8a and 8b

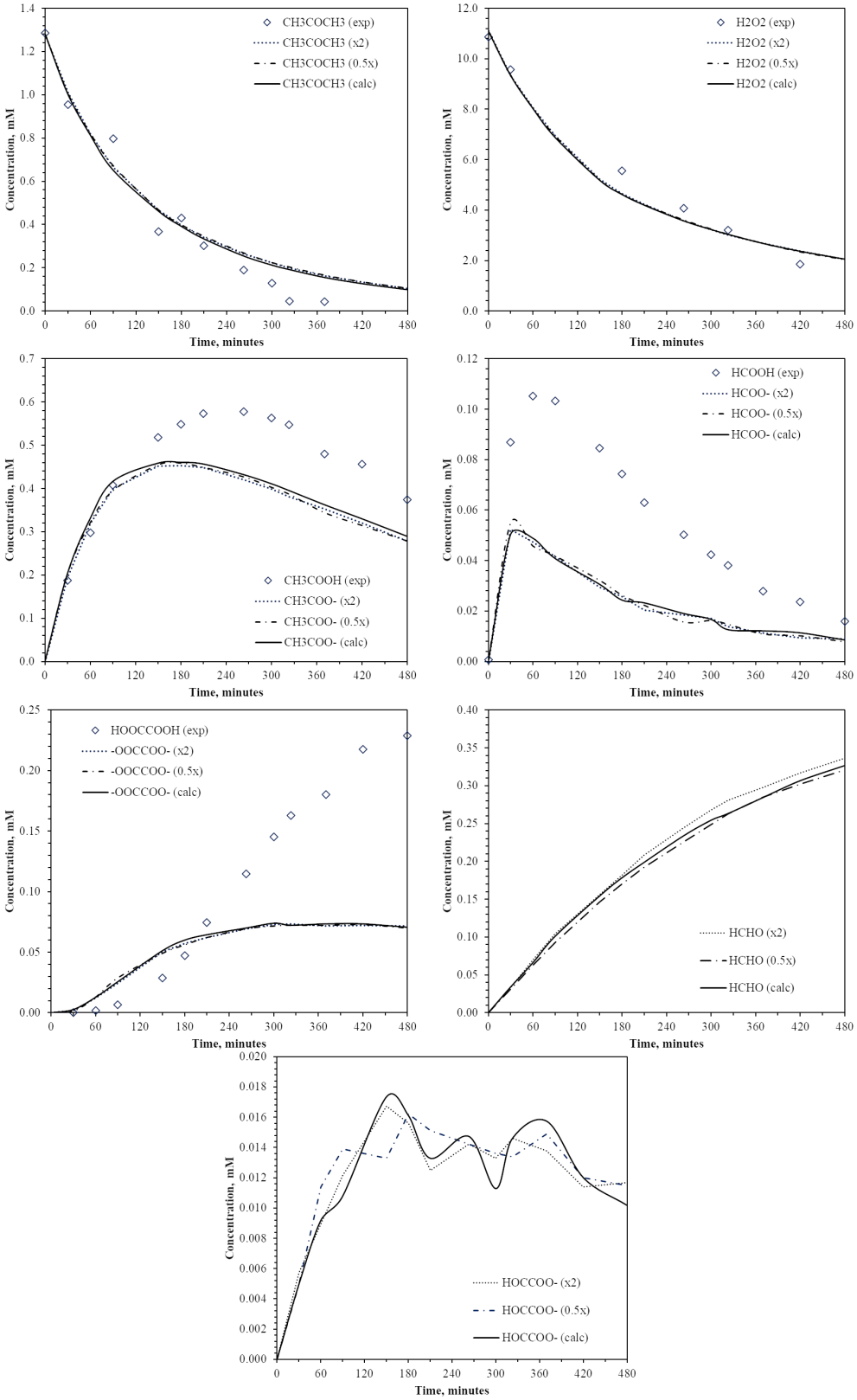

Figure 5.14: Scenario Number 9a and 9b

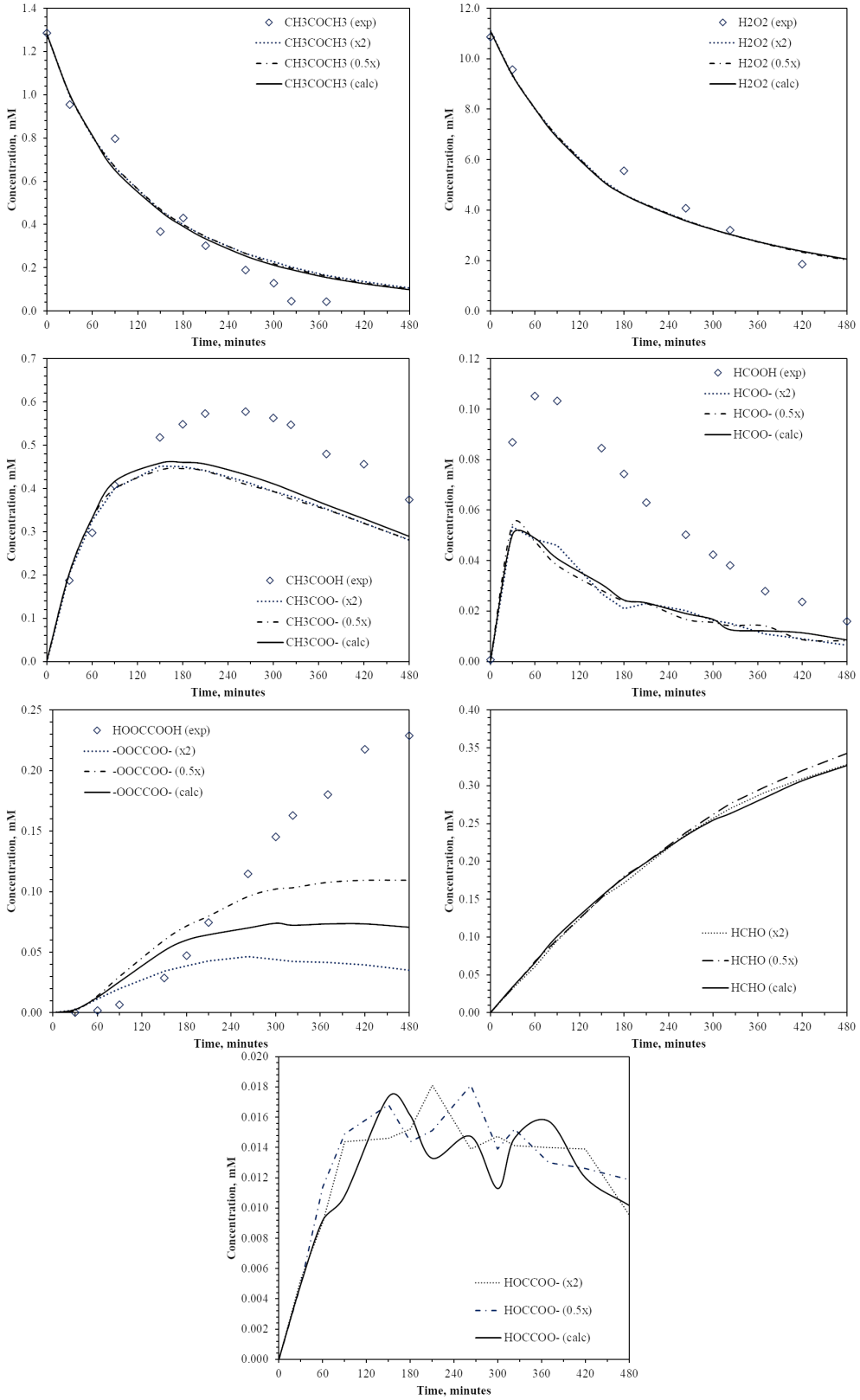

Figure 5.15: Scenario Number 10a and 10b

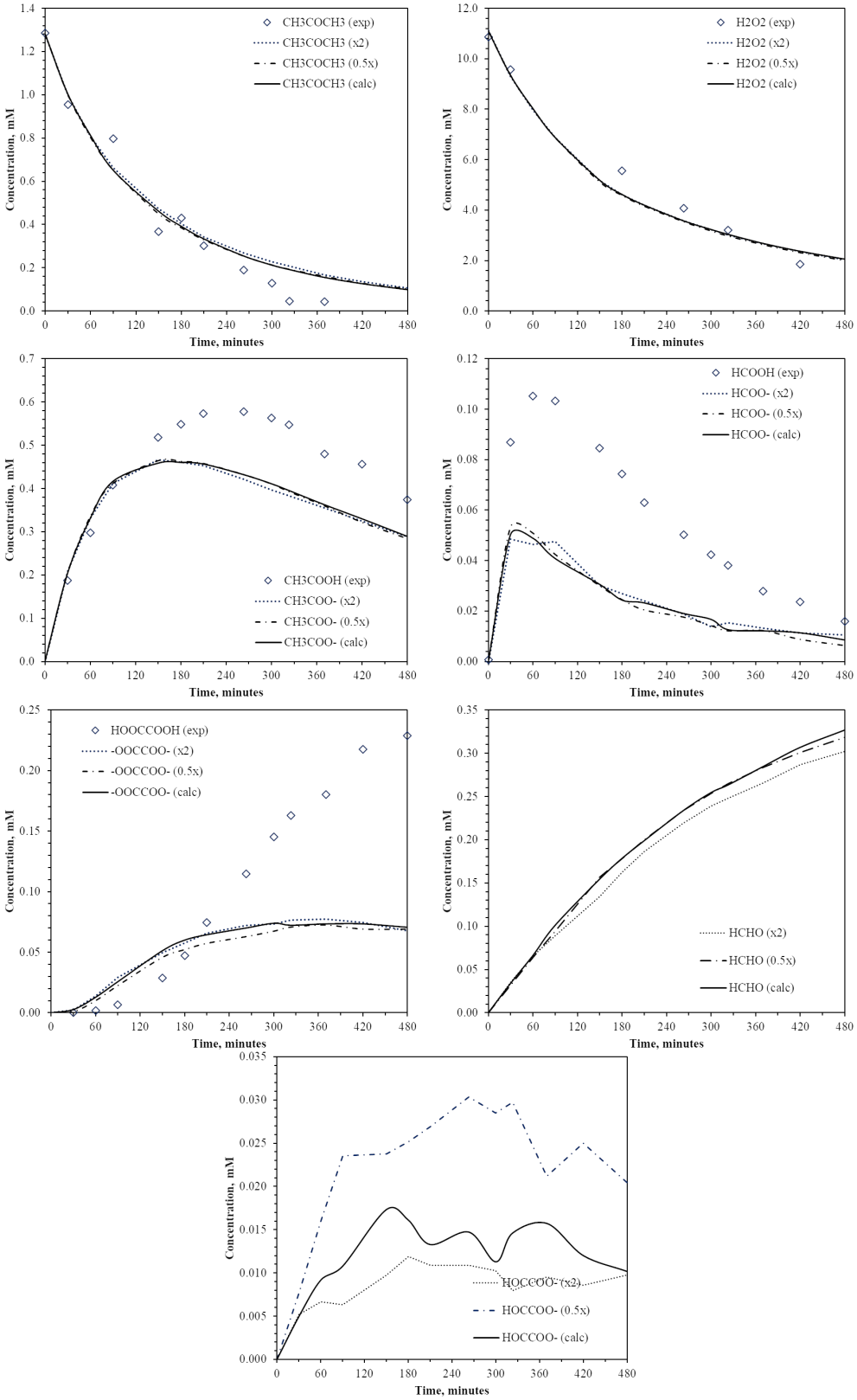

Figure 5.16: Scenario Number 11a and 11b

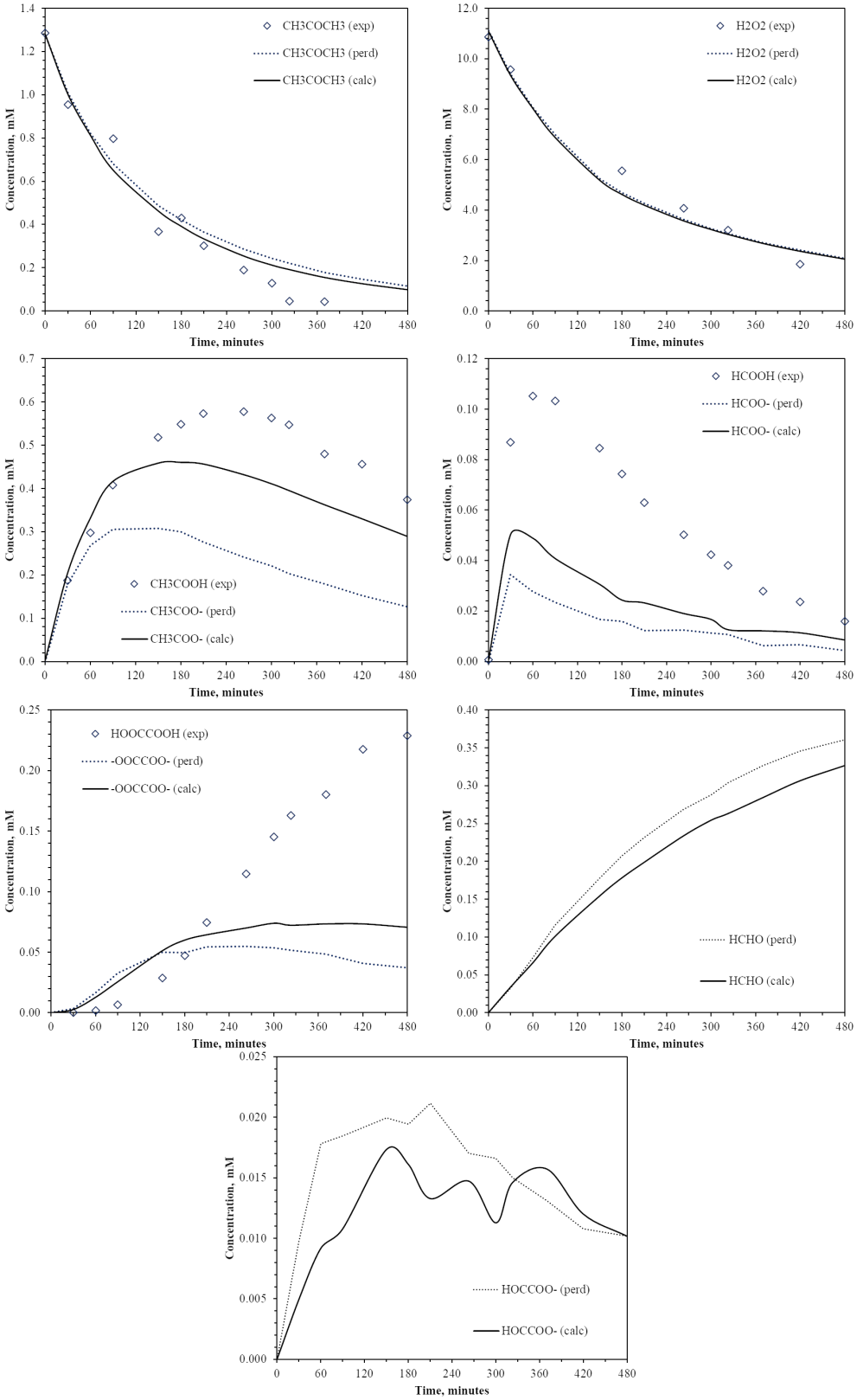

Figure 5.17: Scenario Number 12

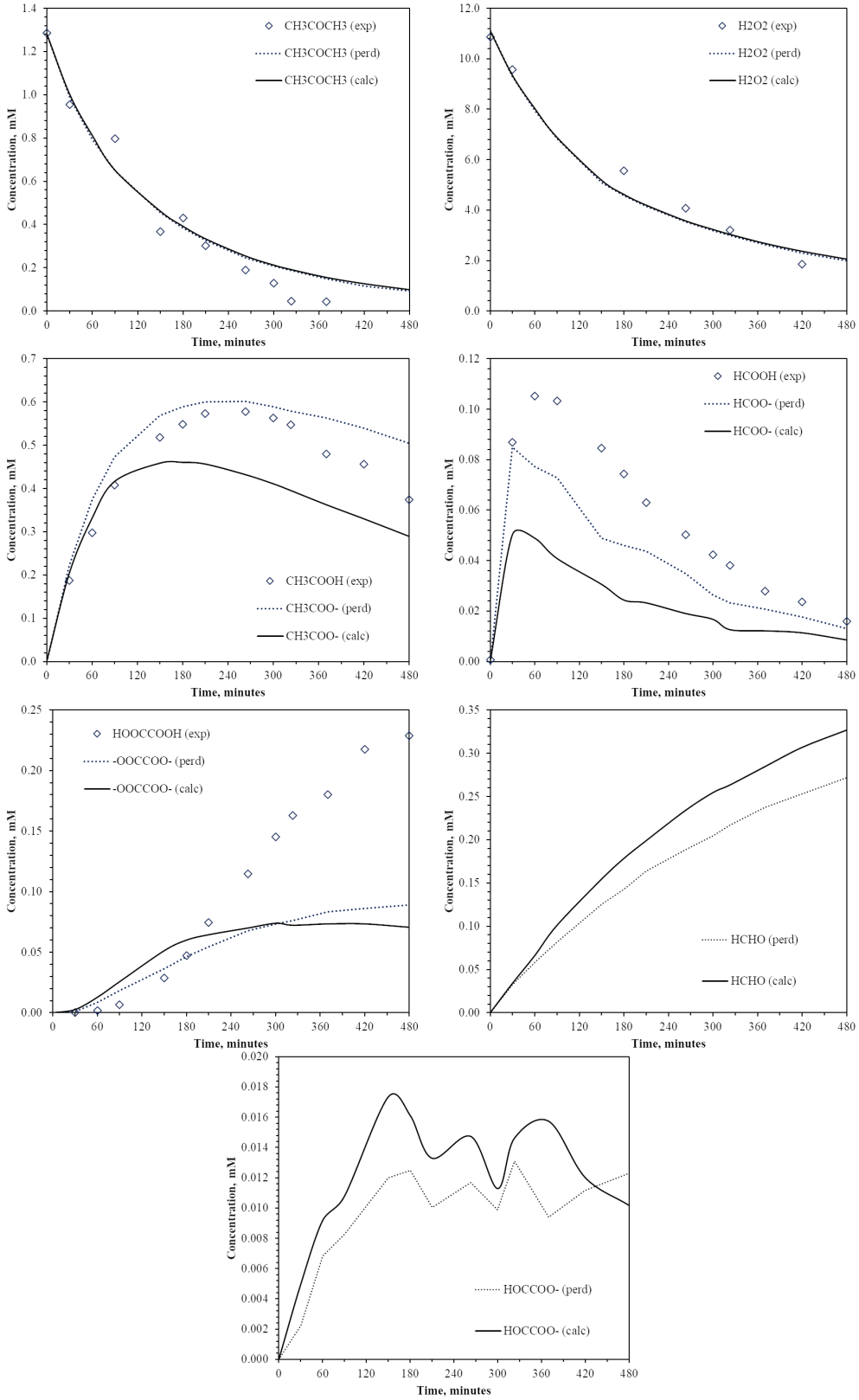

Figure 5.18: Scenario Number 13

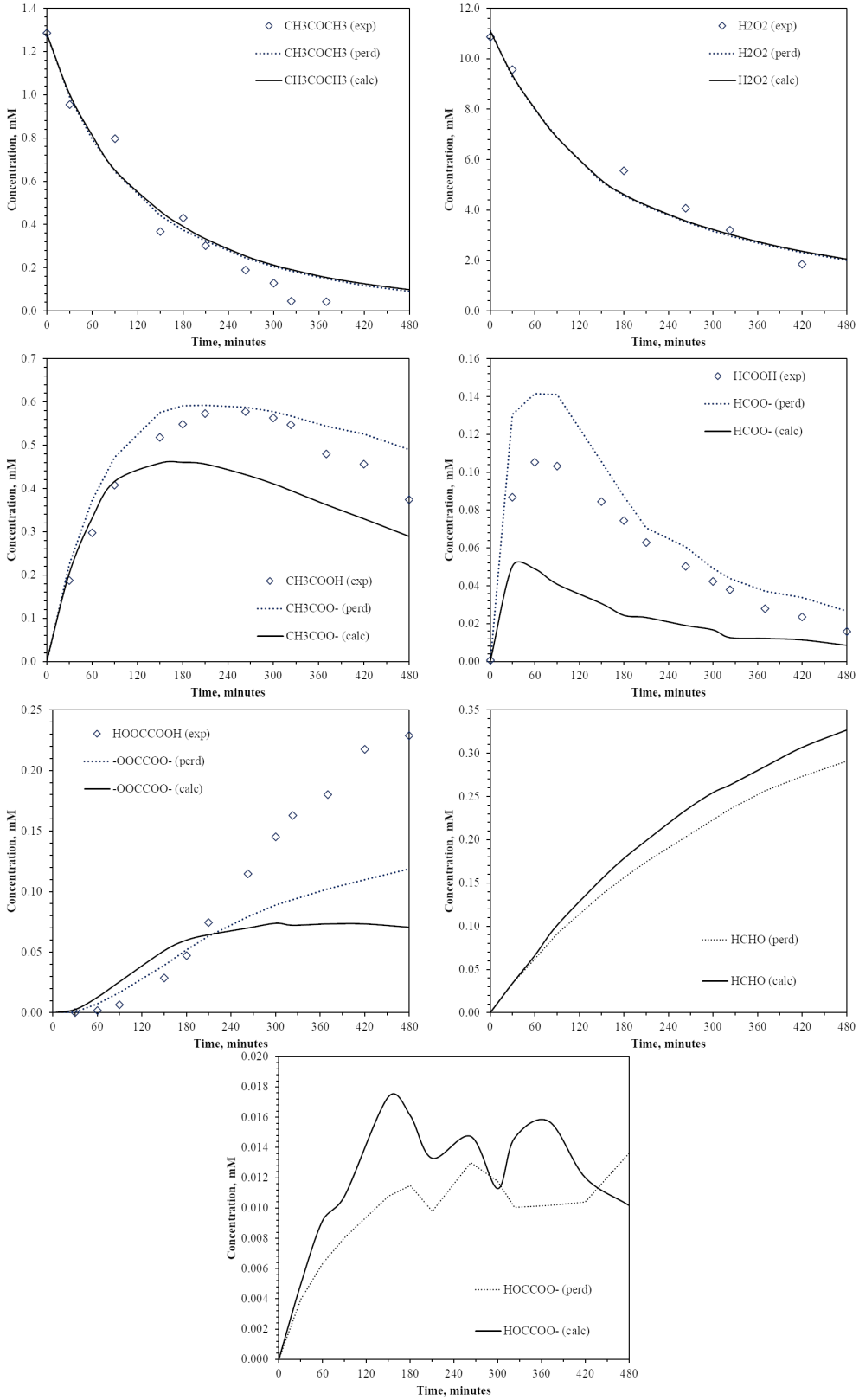

Figure 5.19: Scenario Number 14

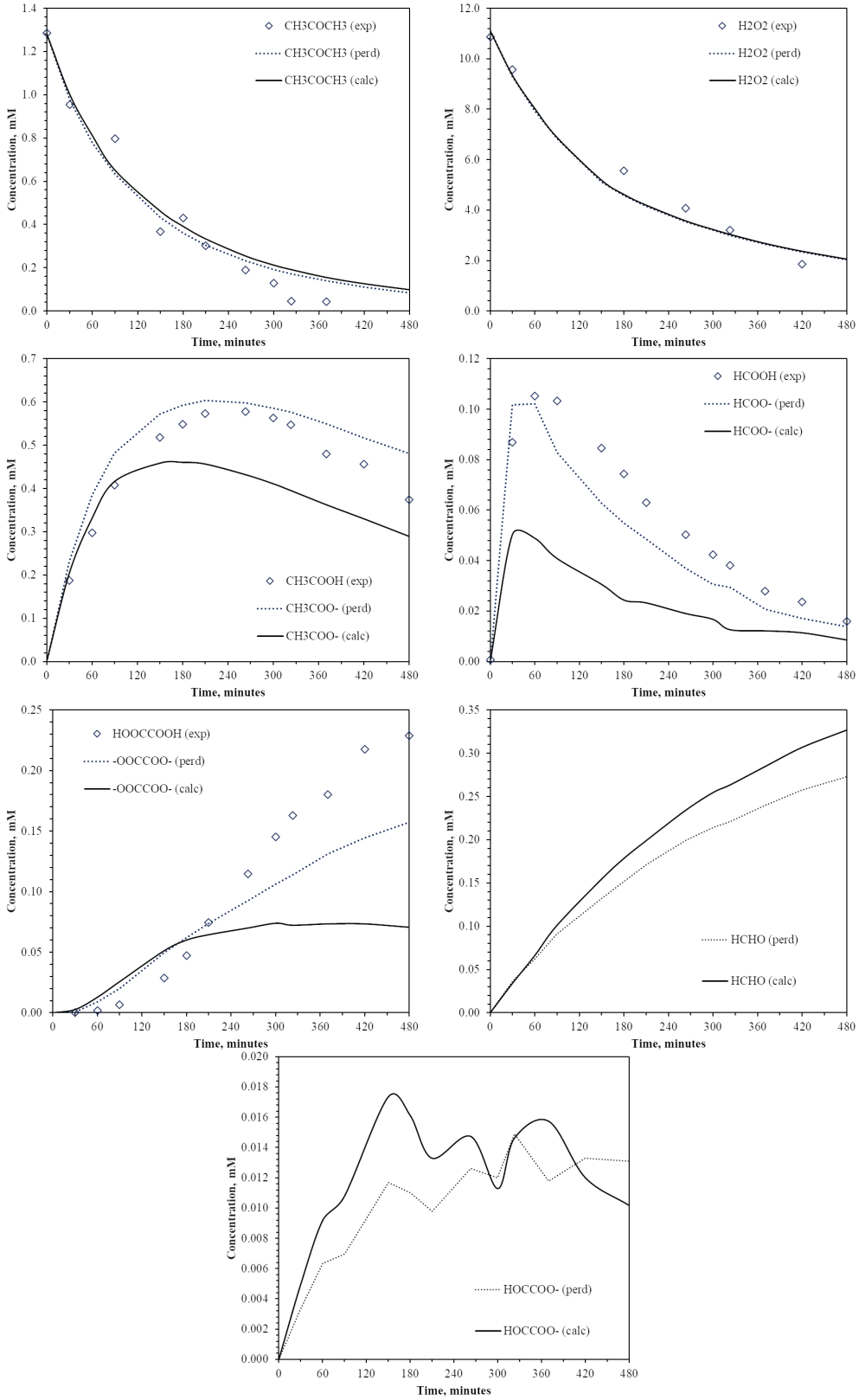

Figure 5.20: Scenario Number 15

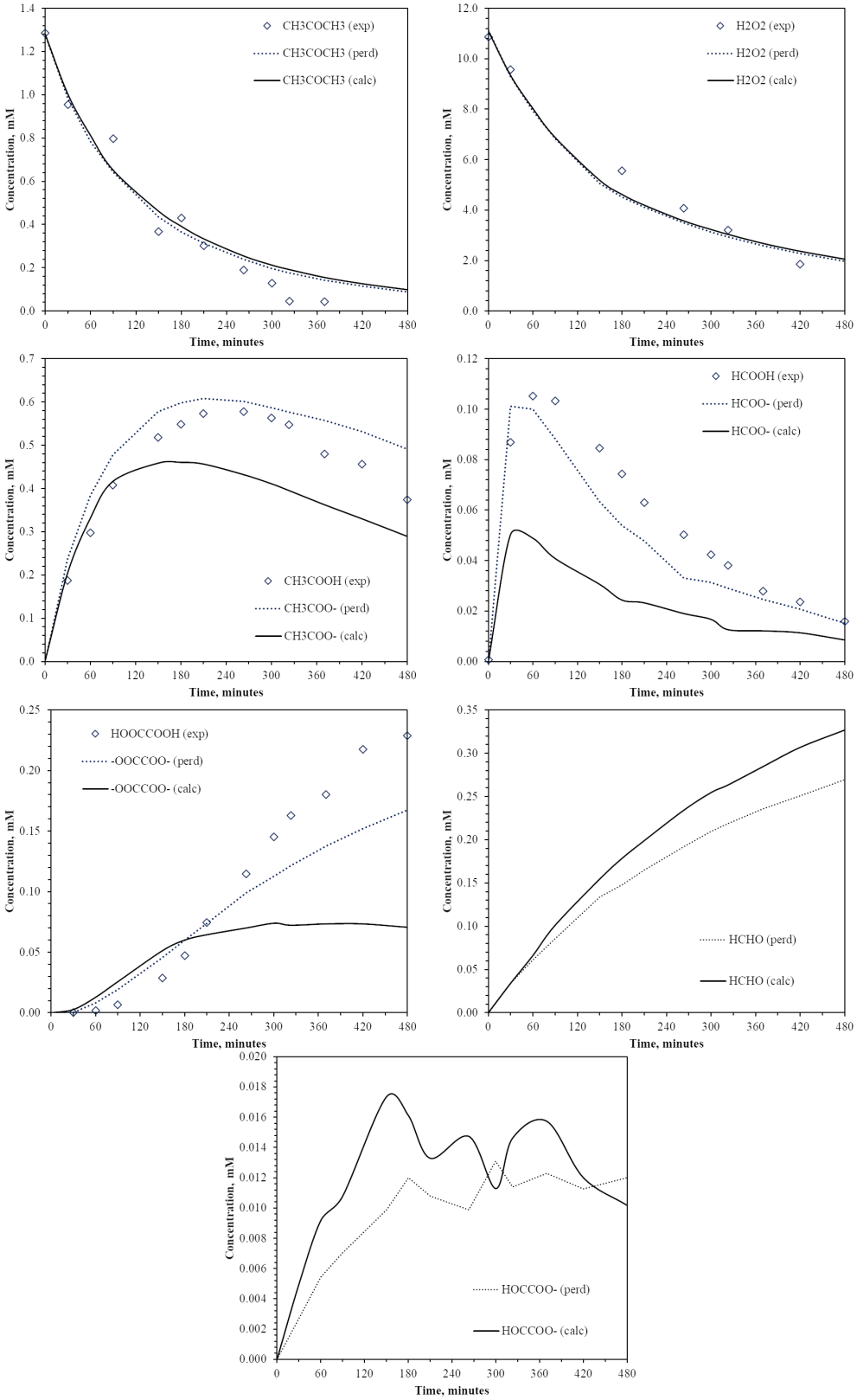

Figure 5.21: Scenario Number 16

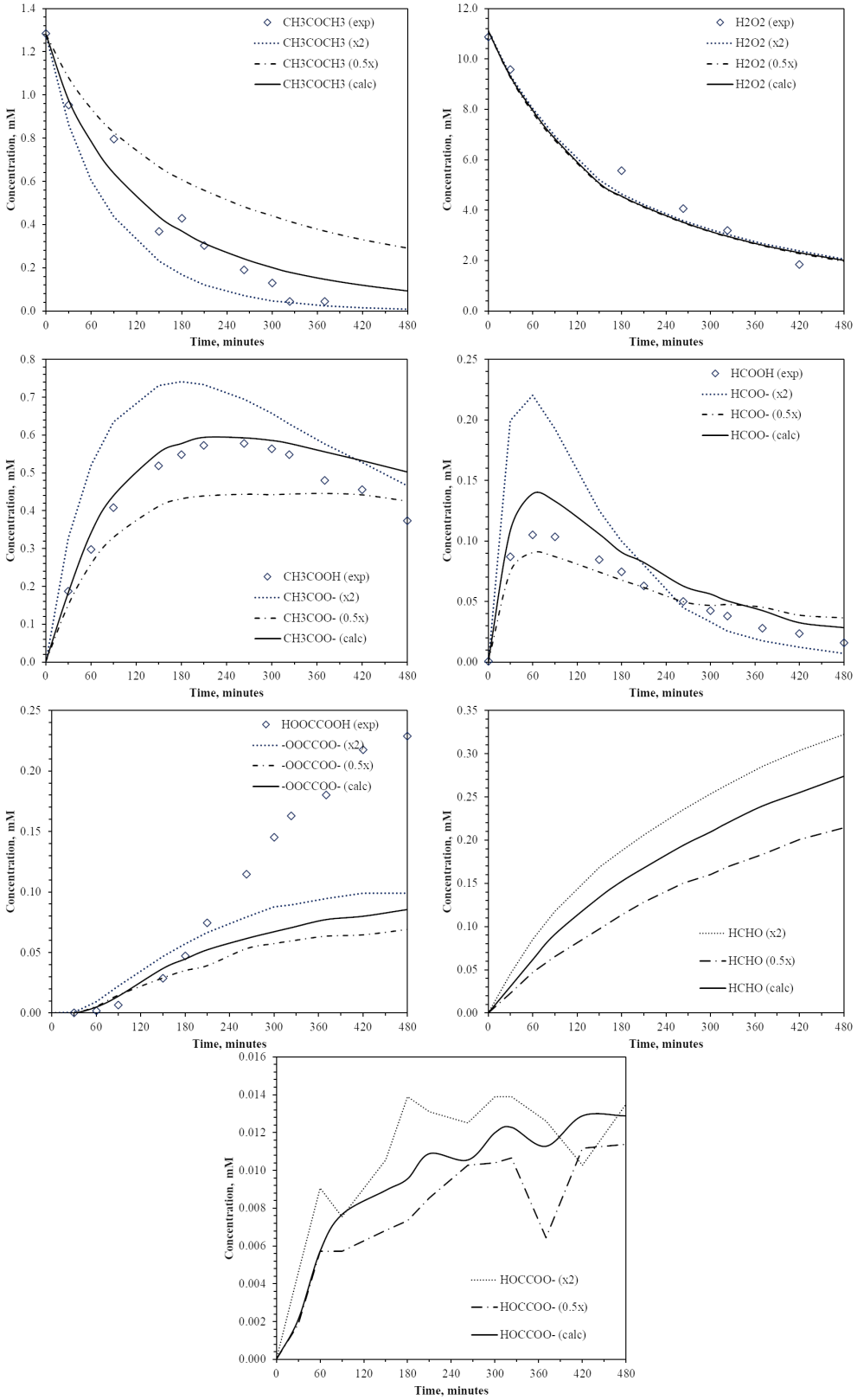

Figure 5.22: Scenario Number 17a and 17b

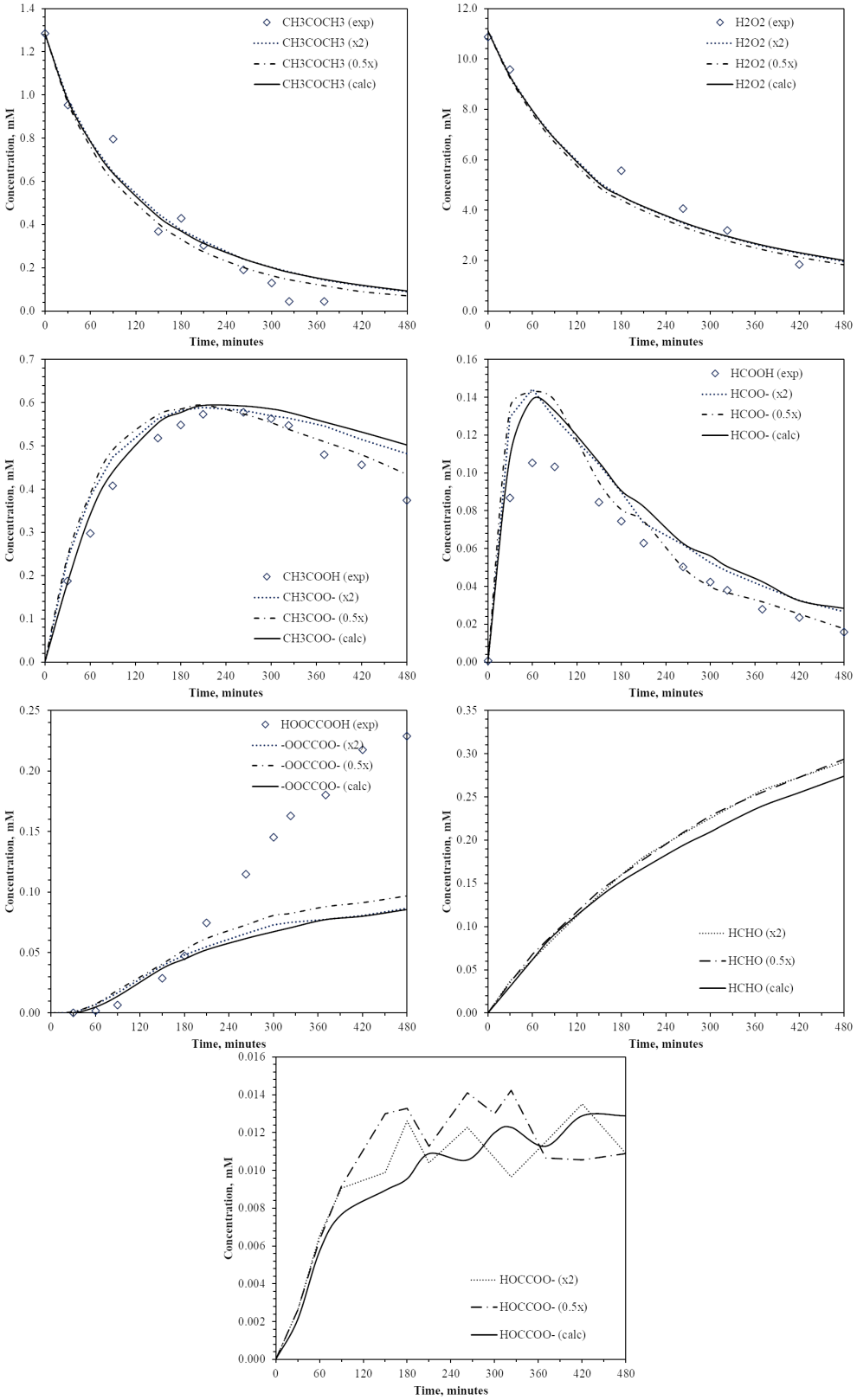

Figure 5.23: Scenario Number 18a and 18b

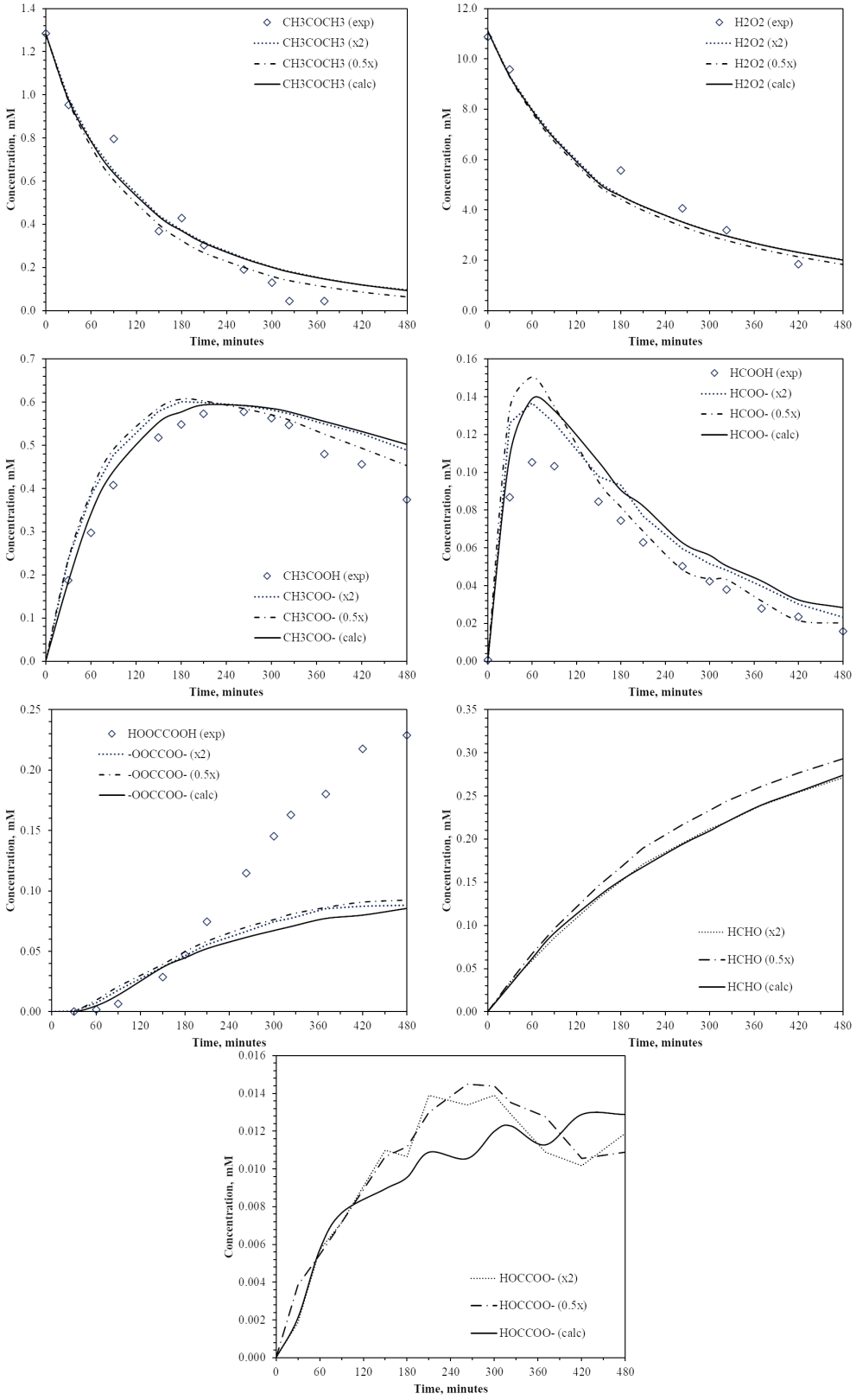

Figure 5.24: Scenario Number 19a and 19b

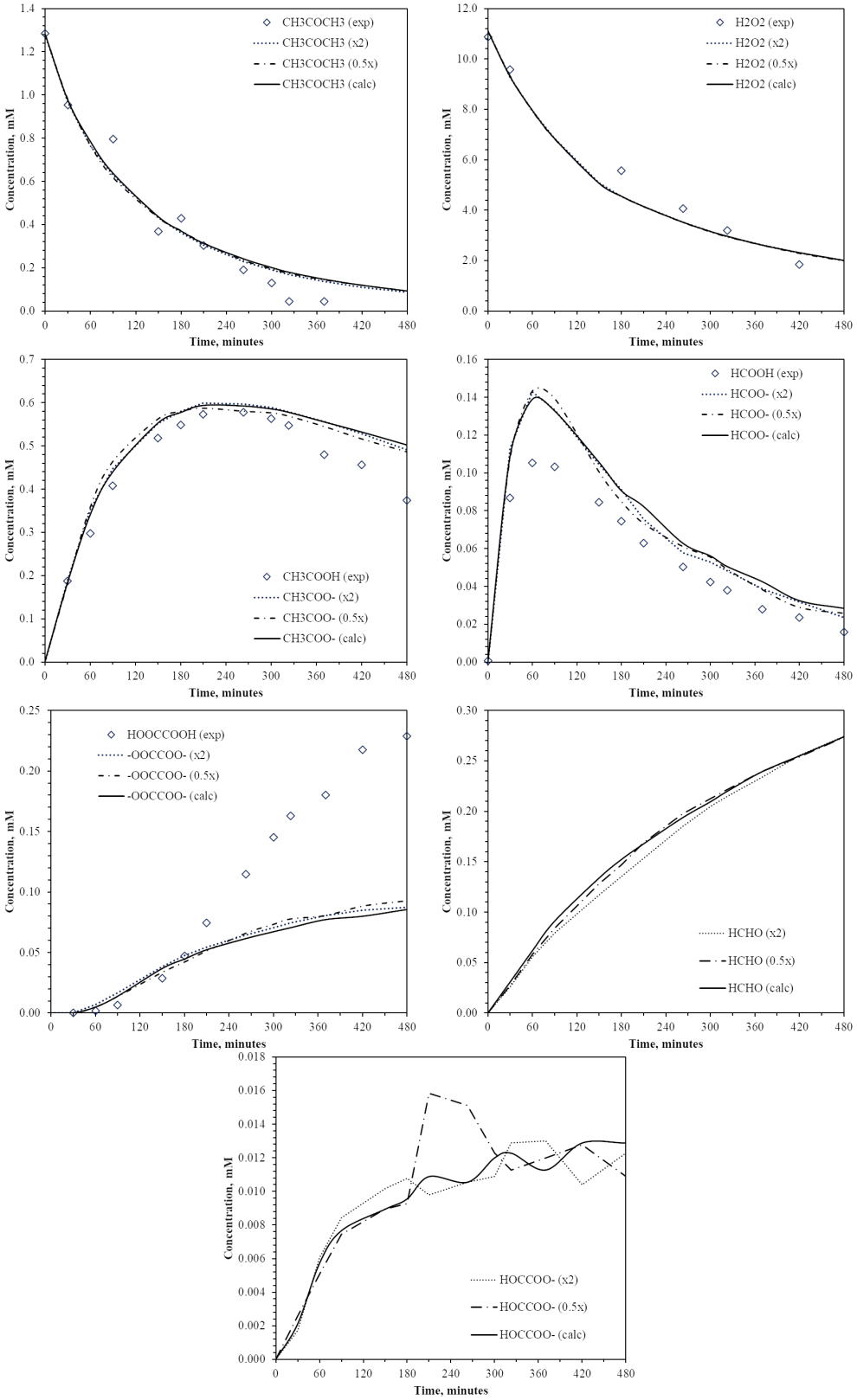

Figure 5.25: Scenario Number 20a and 20b

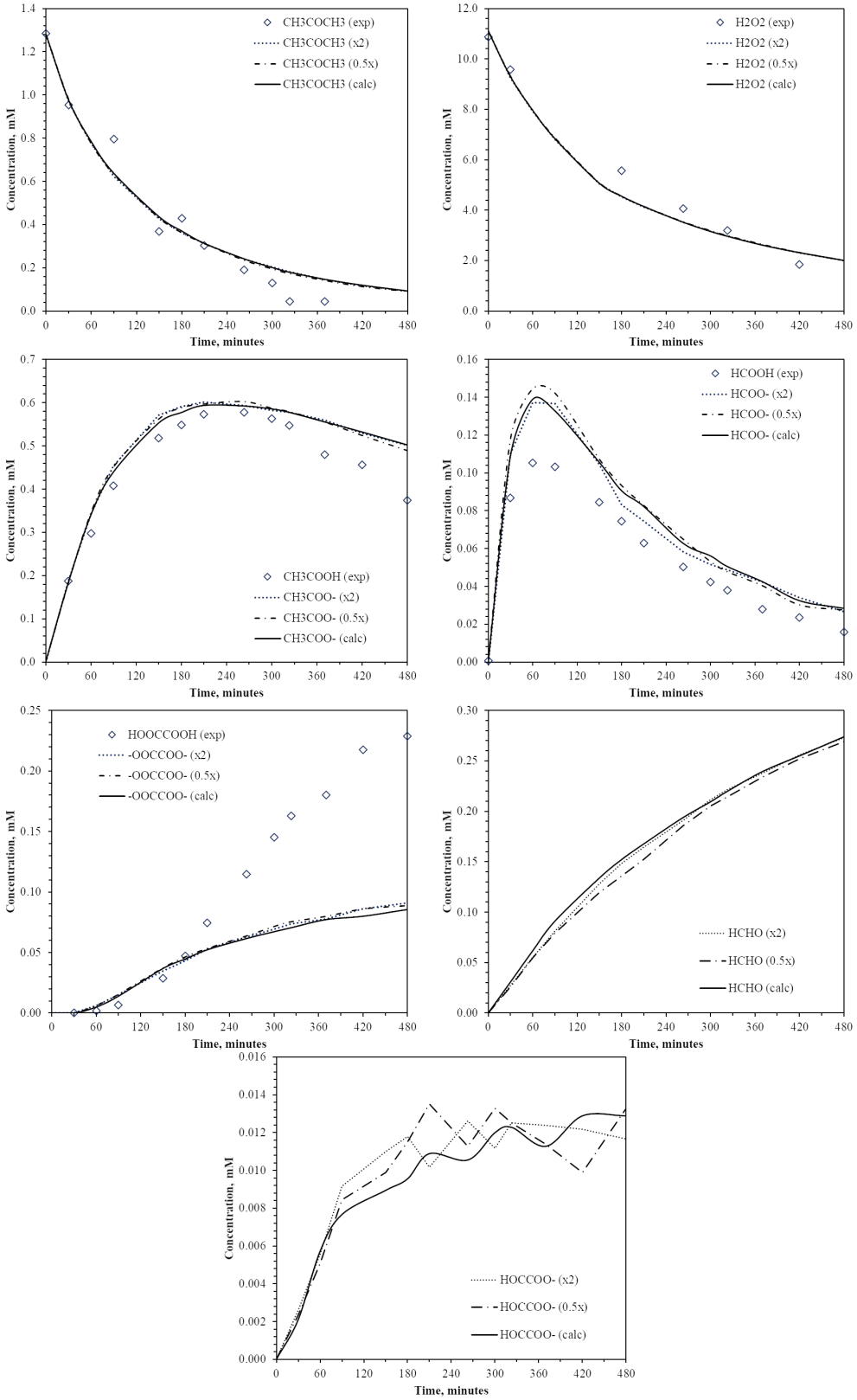

Figure 5.26: Scenario Number 21a and 21b

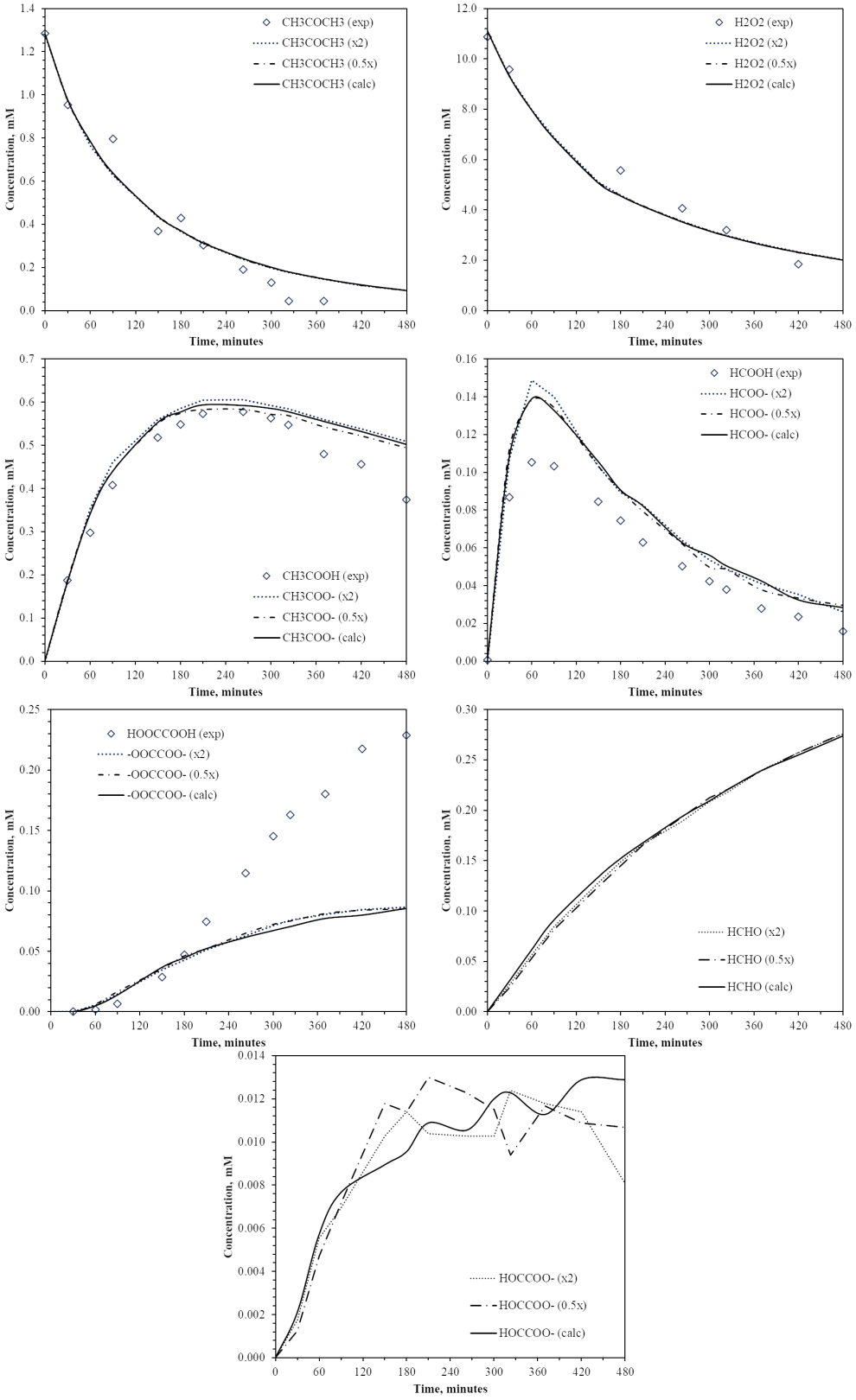

Figure 5.27: Scenario Number 22a and 22b

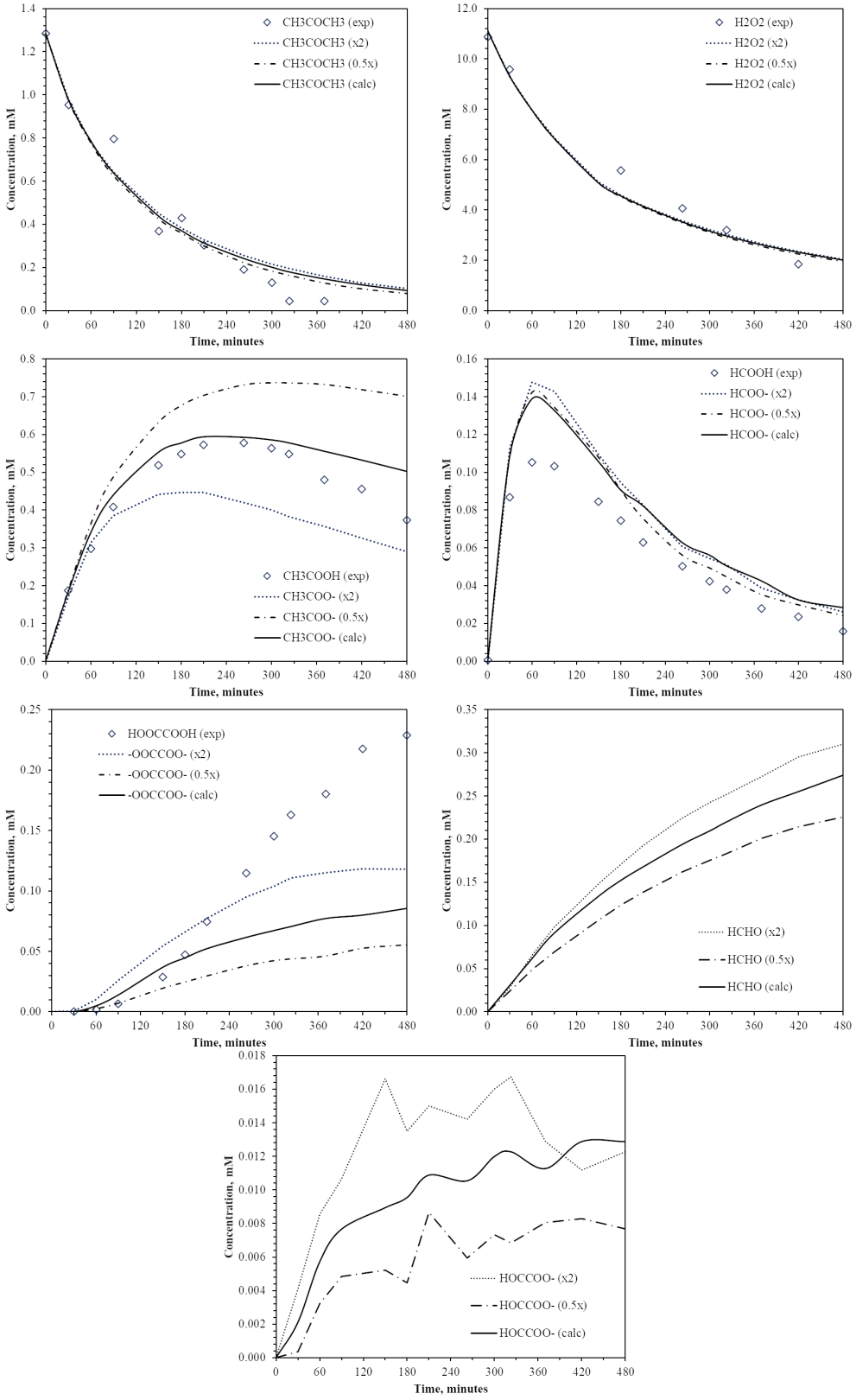

Figure 5.28: Scenario Number 23a and 23b

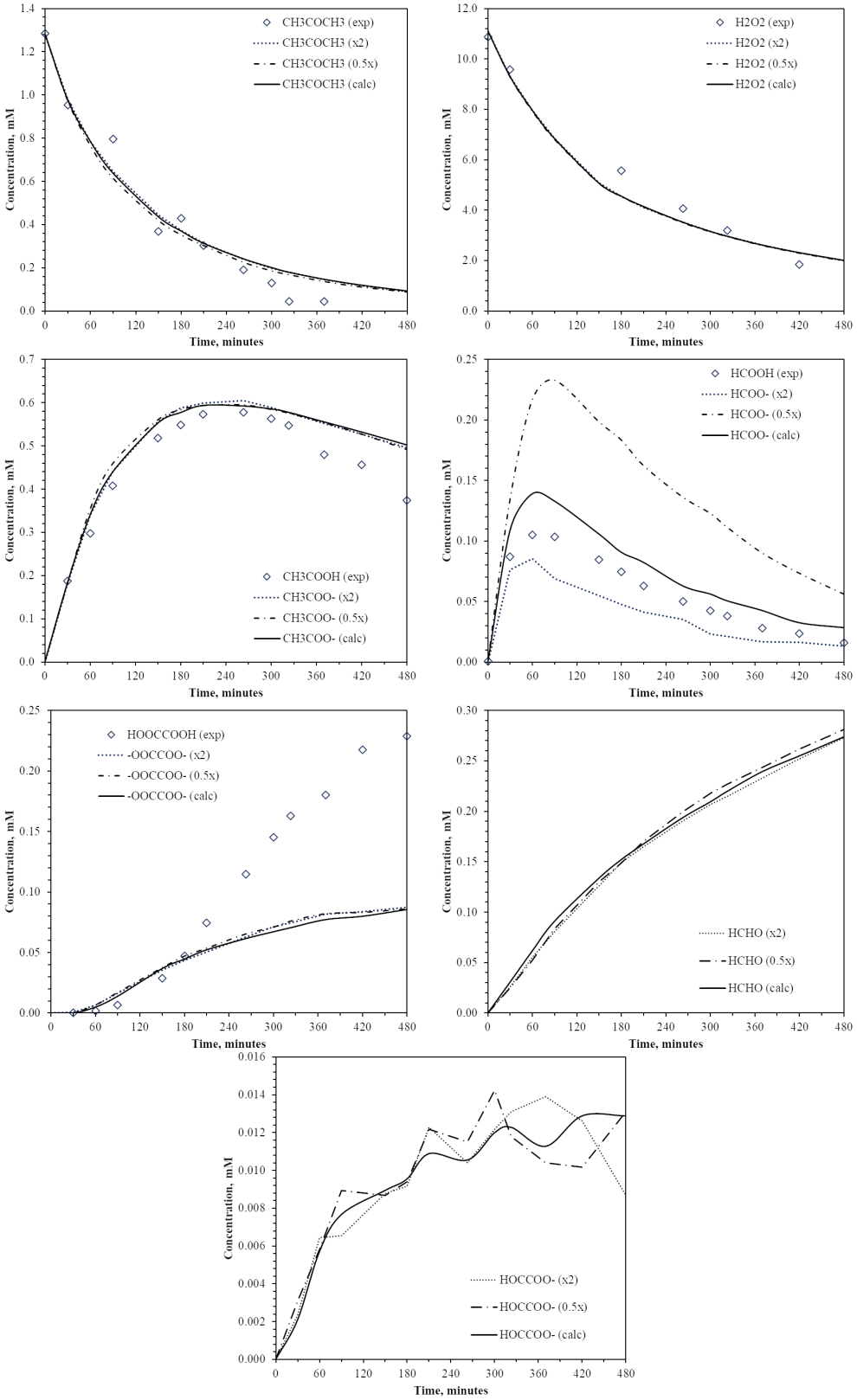

Figure 5.29: Scenario Number 24a and 24b

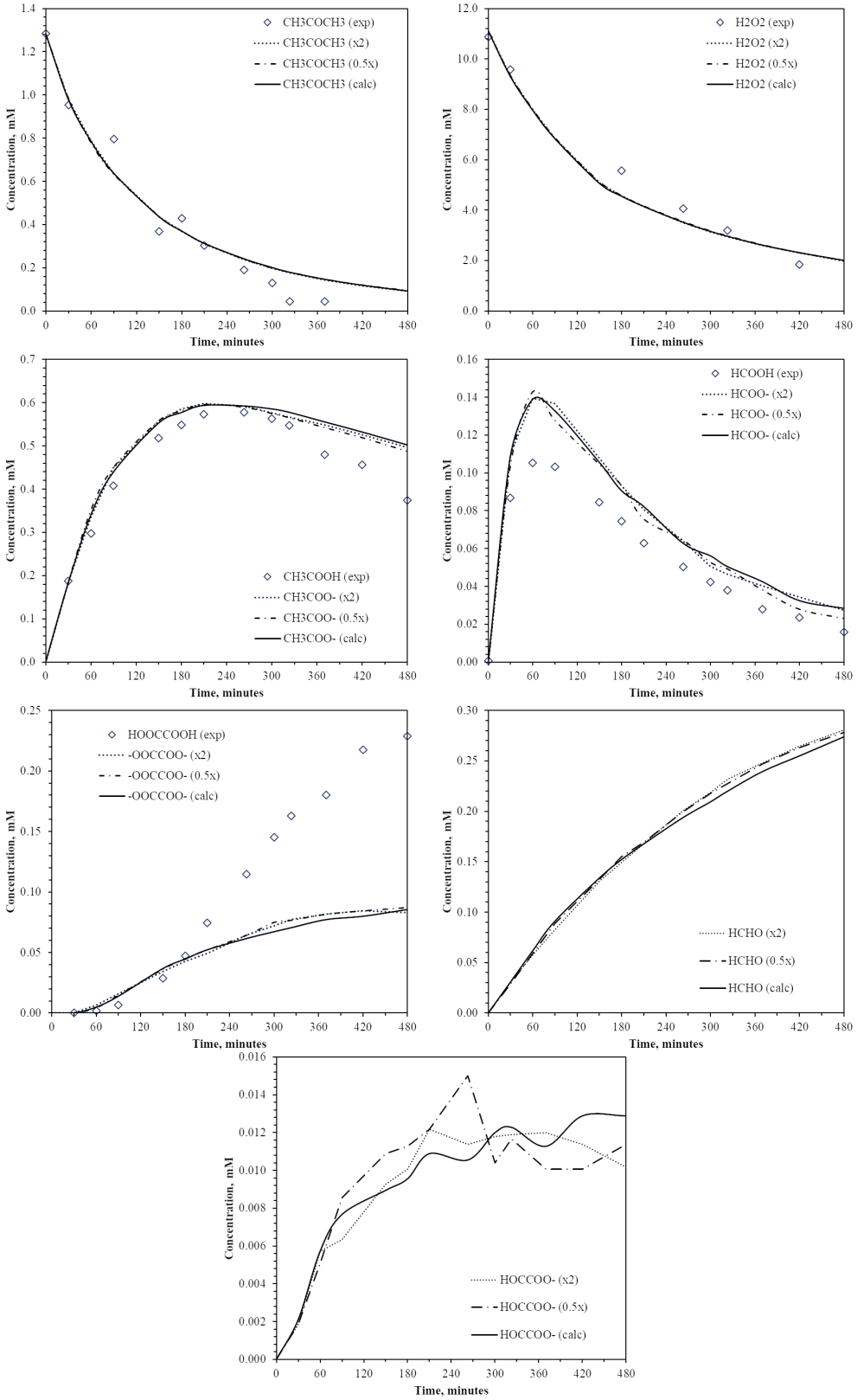

Figure 5.30: Scenario Number 25a and 25b

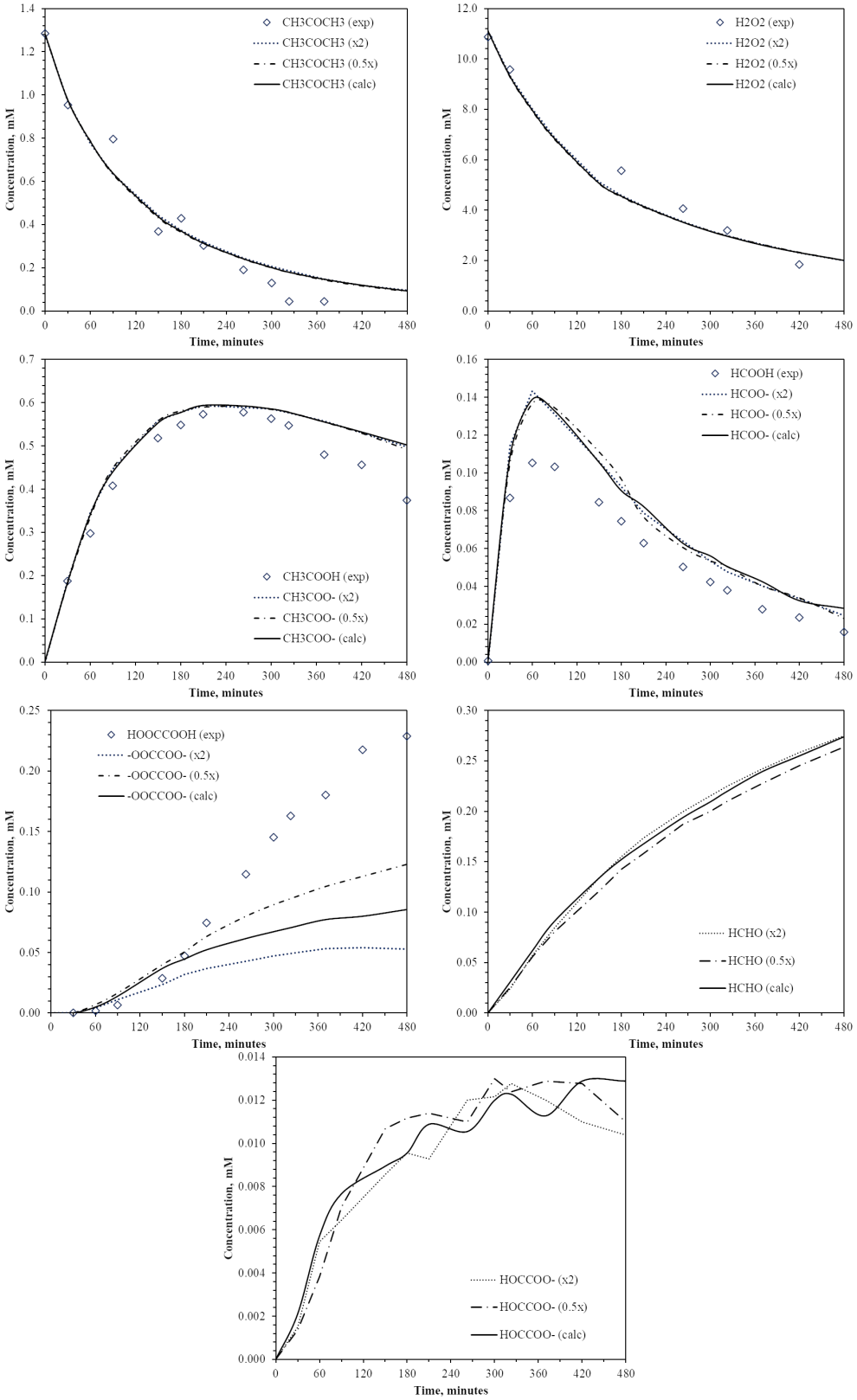

Figure 5.31: Scenario Number 26a and 26b

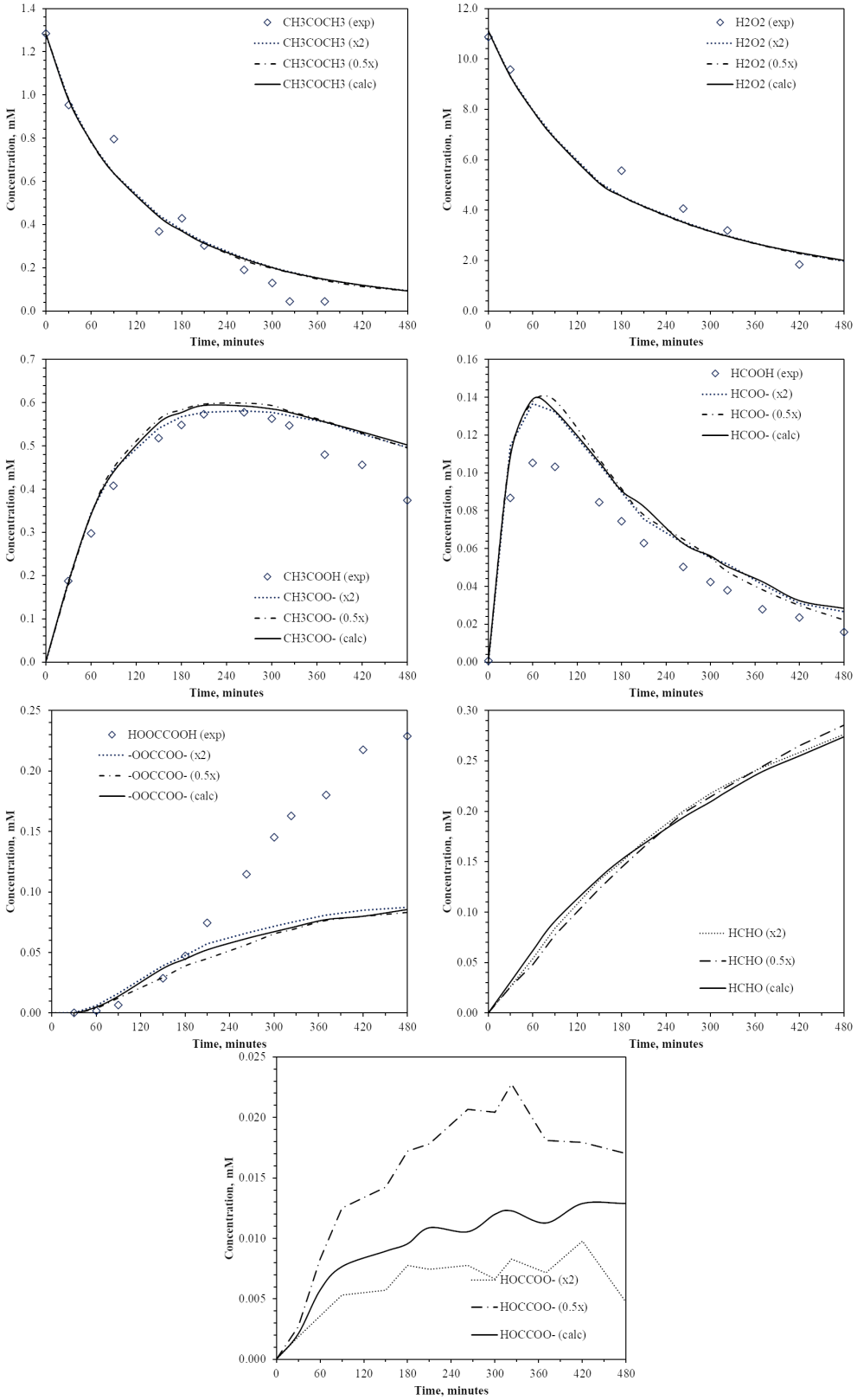

Figure 5.32: Scenario Number 27a and 27b

Chapter 6

Conclusion

6.1 Introduction

THIS dissertation is ambitious, with a broad goal to show how agent-based modeling (ABM) can be applied to two different complex systems to overcome the limitations of existing tools seeking to project future states in the systems, which is framed as the question: "How can ABM be used to address the limitations in existing tools used to study complex systems?" As a result of this goal, the works in Chapters 2 - 5 touch upon the fields of sustainability science, chemistry, and the practice of ABM and contributes to each area as a result. First, Chapter 2 addresses a need for an ABM platform that can conduct simulated policy experiments in which various policy instruments may be tested and impacts projected and evaluated. Next, in Chapter 3, the LCA provides a standard against which the results of an agent-based life cycle sustainability assessment (agent-based LCSA) can be evaluated against. The aforementioned agent-based LCSA is the culminating contribution in Chapter 4, and leverages ABM to addresses the limitations of existing sustainability assessment tools when projecting the environmental, economic, and social impacts of woody biomass based biofuels. Finally, in Chapter 5, the development of an ABM to study advanced

oxidation processes (AOPs) addresses the limitations of existing techniques by projecting concentration profiles based upon a comprehensive list of elementary reaction pathways. Ultimately, his dissertation also points to several possibilities for future work with broad impacts upon scientific discourse and discovery.

6.2 Contributions

6.2.1 Contributions to sustainability science

Chapter 2 describes the agent-based model (ABM) platform, ForestSim, and is a necessary component of the case study application of agent-based LCSA described in Chapter 4. While the immediate application of ForestSim is the aforementioned agent-based LCSA, it was also designed for forest management policy experimentation as well as broader bioenergy sustainability assessment studies. Sustainable production of bioenergy from forest resources requires policies that can anticipate complex social, environmental, and economic impacts. Since these impacts may require years to manifest, the use of computer modeling to project possible policy impacts may help to avoid future policy failures. ForestSim supports this goal by offering a means to conduct simulated policy experiments in which various policy instruments may be tested and impacts projected and evaluated.

Chapter 3 presents the results of a life cycle assessment (LCA) conducted for the proposed integrated hydropyrolysis and hydroconversion (IH^2) biorefinery in Ontonagon, Michigan. The complete life cycle impacts of IH^2 fuels is still incomplete and the manuscript advances out understanding of the impacts. The calculation of the energy return on investment (EROI) also contributes to the broader discussion concerning the replacement of petroleum derived fuels with fuels from renewable sources. This LCA also assists in the development of the agent-based LCSA and is a component of the case study described in Chapter 4.

In Chapter 4, ABM and life cycle sustainability assessment (LCSA) are integrated to form a new methodological approach: agent-based LCSA. The argument presented draws upon the current discourse regarding the limitations of existing tools, and advances it by arguing that the integration of ABM and LCSA (i.e., agent-based LCSA) addresses these limitations. As the literature reflects the preliminary development of the approach, an operationalization is outlined using ISO 14040 [60] as the basis. While contextualized against a backdrop of biofuels to provide examples for the reader, the intent is that methodology is generic in its application. The second half of the chapter develops a case study application of agent-based LCSA. This contributes to the literature by reinforcing the results of Chapter 3 through their replication using a different methodological approach and cross-validation of agent-based LCSA. The results of the case study further contribute to the literature. While the immediate application of the results case study may be limited to Ontonagon, Michigan and the Western Upper Peninsula region, the means by which the feedstock projections are made are applicable to site selection for projects requiring large capital expenditure that are dependent upon resources from the local community for their process inputs. Finally, the implications of the aesthetic impacts of logging (i.e., the visual buffers assessed), and the annual impacts upon wetlands due to logging, present an area of concern for policy makers in the region. Ultimately this chapter contributes to the broader purpose of this dissertation through the development of agent-based LCSA to project future states of the system being studied.

6.2.2 Contributions to chemistry

The application of ABM to study UV/H_2O_2 processes in Chapter 5 represents a novel contribution to the study of AOPs and advances the possibilities of projecting future states of chemical reactions. Furthermore, as a novel application of ABM, there is a possibility for advancements to other applications of models of chemical interactions and molecular dynamics, although that work is beyond the scope of this dissertation. While the ABM presented in this dissertation builds upon prior

work through the bimolecular reaction model used (see [52, 254]), other applications are primarily limited to biological models and intracellular signaling pathways (see [51, 269]). This may be partially attributed to the seminal article examining the NF-κB signaling pathway [52]. As such, the ABM has considerable flexibility in terms of the reactions incorporated. So, while the focus of Chapter 5 was UV/H_2O_2 processes, the ABM is not limited to just this application.

6.2.3 Contributions to the practice of agent-based modeling

While not the intent of this dissertation, the development of the ABMs contributes to the common body of knowledge that ABM practitioners draw upon when implementing (i.e., deciding the software implementation and programming) their models. This is due to the decision to apply an ABM to a research problem being fairly simple compared to designing the model (i.e., identifying the agents, environment, variables, decision making, and so forth) and implication of the ABM. For example, the justification to use an ABM to study a complex system can be generalized in three steps:

1. Identify the aspects of the research question that share the characteristics of a complex system.
2. Identify how those characteristics manifest as limitations in existing tools, or prevent existing tools from fully modeling the problem.
3. Discuss the ways that ABM addresses those limitations by allowing the complex system to be modeled.

This approach is used in Chapter 4 and 5 when explaining why an ABM is better suited for assessing the impacts of woody biomass based biofuels and AOPs, respectively. However, once the decision to use an ABM has been made and justified, and the model is designed, the practitioner is still faced with the issue of implementation. With tools such as NetLogo [55] the practitioner is limited to the capabilities

of the tools selected for use. While practitioners may not commonly encounter such problems, this dissertation offers practitioners insight beyond the ability to see how ABMs were implemented in this dissertation.

First, ForestSim, as presented in Chapter 2 offers contributions to the border community of ABM practitioners. While tools such as MASON [54] and GeoMason [89] offers the means of developing ABMs that incorporate geographic data, their integration and use requires a degree of technical expertise. ForestSim provides a modeling platform that integrates ABM along with spatial coupling of agents (e.g., forest owners) with parcel boundaries and landscape data (e.g., National Land Cover Database [103] and LANDFIRE [207]). As a result, ForestSim alleviates some underlying technical concerns (e.g., parallel processing of landscape data) allowing researchers to focus more on the development of an agent's environment and decision making.

Further contributions are a result of the ABM developed for AOPs in Chapter 5, specifically, the treatment of space (i.e., the sparse lattice structure) and some commentary on problems addressed during model construction. The sparse lattice structure is quite significant within the context of the model as the simulation of 100,000 chemical entities requires that approximately 13 μm^3 of space for the environment.[1] The size of the environment is relevant since the use of the interaction radius in the model requires an efficient means of storing the location of agents and finding other agents. To address these requirements, the sparse lattice data structure was developed and is time and space efficient at approximately $O(n)$ and $O(mn)$, respectively. This minimizes the amount of time spent searching for possible reactants and allows the model to increase the number of agents simulated, a requirement for model accuracy.

[1] To put this in context, assuming 13,000 nm^3 is implemented using a multi-dimensional matrix data structure, and only 32 bits of data is needed per point, about 8.8 TB of memory would be needed for storage.

The reaction registry in the AOP ABM also overcomes a critical issue in development that is hinted at in the source code included in [254]: namely, an increasing number of chemical entities and possible reactions results in a combinatorial explosion. As a result, while agent actions may be summarized as "move" and "react," it is not possible to program all of the relevant reactions into the agents themselves. This is overcome in Chapter 5 by using a method for agent decision making and for arbitrary lists of reactions to be loaded into the model. This is counterintuitive to how agent decision making is typically presented (i.e., programmed as part of the agent) and that optimizations can take place in code by hashing compound names that are friendly to chemists (e.g., C_3H_6O or acetone) into values that can be efficiently compared by the computer. This approach also allows the model to take advantage of pathway awareness to prevent, or eliminate, products that have no subsequent reaction (i.e., they can be counted, but it is not necessary to add them to the simulation).

6.3 Future Work

As an ABM platform, there are limited directions that ForestSim can be taken as a discrete entity, although continued work to add new features is always an option. However, as demonstrated by its use in Chapter 4, ForestSim has a strong possibility of being a productive entity as part of other research projects. In contrast, the LCA conducted in Chapter 3 offers several possible directions for future work. First, the extent of soil organic carbon loss due to timber harvests is presently unknown and is difficult to quantify as part of an LCA. While there is literature to support the assumption that soil organic carbon will be replenished during the regrowth cycle, it may be inappropriate to assume complete restoration. LCAs evaluating the impacts of woody biomass based biofuels would benefit from work done to fully quantify the loss and restoration of forest carbon sinks. As a result of these concerns, Chapter 3 raises some questions about the Renewable Fuel Standard (RFS). While a critique of

the RFS was beyond the scope of the chapter, and indeed this dissertation, examining the RFS in the context of rebounding effects and carbon sequestration is necessary if it is to remain the standard by which biofuels are measured.

The agent-based LCSA developed in Chapter 4 presents considerable opportunities for future work as a methodological advancement. First, while intuitive, this approach has applications beyond just the woody biomass based biofuels used in the case study. Effectively, any LCA or LCSA conducted that is projecting impacts and there are heterogenetic actors and spatial decision making plays a significant role. One of the more interesting applications of the approach, although not explored in this dissertation, is to generate geographic information systems (GIS) data so that land-use/land-use change (LU/LUC) can be fully explored. While the techniques used in Chapter 4 (i.e., GIS data for visual buffers and wetlands) are appropriate to projecting the impacts quantitatively, GIS data may allow for qualitative assessments to be made by members of the community though data visualizations. There have been some explorations of this in the context of local knowledge and LU/LUC (see [270]). Also worth highlighting are the values of the projections of woody biomass feedstocks that the model produced. While possible using other approaches, if a biofuel or biorefinery operator does not have a secure source of feedstocks (e.g., contracts with industrial forests or short rotation crops) then these projections have value when informed by local data (e.g., parcel ownership, survey data, etc.).

The ABM of AOPs, as presented in Chapter 5, offers a considerable opportunity for future work by effectively opening up a new line of enquiry in the study of AOPs. As discussed in Chapter 5 ordinary differential equations are the primary means of studying AOPs; however, the technique is limited due to compute times and the stiff nature of the equations. By overcoming several key barriers in developing an ABM-based approach, there is increased flexibility in AOP studies. For example, the ABM allows for reaction pathways to iteratively adjusted and results to be evaluated in a reasonable amount of time. While not used to full effect in the UV/H_2O_2 case

study, it is possible to use Monte Carlo techniques to adjust values until predicted concentration profiles are within an acceptable margin of experimental data. When combined with the prediction of reaction pathways based upon molecular graph and network analysis techniques [271], it may be possible to solely use computational techniques to study AOP treatments. This likely represents a broad research agenda as more immediate questions arose from the development of the model. However, the implications of such a research agenda are considerable since effective integration of reaction pathway prediction with ABM to calculate concentration profiles may allow for AOP treatments for emergent organic contaminants to be generated without the need for extensive laboratory experimentation.

The ABM in Chapter 5 owes a great deal of its performance to the underlying sparse lattice data structure and there exists room for improvement in the implementation. Currently the data structure represents a trade-off between mutability (i.e., update and insert operations) and searching with a preference for minimizing operations needed to mutate the data structure. While some tree-based spatial data structures were examined during the development of the model, the expected performance penalties due to tree mutations were found [255]. Likewise, the space complexity of the data structure is largely driven by very conservative estimates about the amount of space needed. Currently the model over-allocates memory on the conservative assumption that the number of molecules during module execution may exceed the initial amount by a considerable margin. However, this was not extensively tested and careful study of the behavior of the ABM under various reaction pathways may allow for a more efficient use of space. Ultimately, improvements in the time and space complexity of the data structure allows for more agents to be used in models, or parameters to be tested in the same amount of time.

Appendix A

Forest Ownership Patterns in the Western Upper Peninsula of Michigan, USA

A.1 Introduction

THERE is increasing scholarship focused on the Western Upper Peninsula (WUP) region of Michigan, USA to gain insight into how the forests are managed (see [88, 91, 190]). Such studies are joined by research into the potential for biofuel development in the state of Michigan (see [90, 198, 272]) which highlight the suitability of the region for biofuels. The WUP is approximately 16,000 sq.km. and consists of the counties of Baraga, Gogebic, Houghton, Iron, Keweenaw, and Ontonagon. While the WUP is heavily forested, the economy is depressed with tourism being the primary sector [188]. This has led to some speculation that woody biomass-based biofuels could be an economic driver for the region [273]. One potential barrier to this development is the prevalence of family forests (i.e., forest ownership by individuals and families) and more broadly non-industrial private forests (NIPF) (i.e., private forests lacking woody processing facilities) in the region, cited as controlling approximately one-third of the forested land [91, 274]). While studies show that family forests in the region are typically against harvesting [91] it may be required to meet the feedstock

requirements if biofuels are developed. Tax incentivization programs such as Michigan's Commercial Forest Lands [127] can encourage harvesting, but the requirement for 40 acres (161,874 sq.m) of forested land might eliminate a significant number of landowners. However, family forests are by no means the only actor in the regional landscape as commercial concerns, government agencies, and trusts own significant quantities of forested land.

This appendix summarizes the work done to prepare parcel data for use in the studies described in this dissertation. This work contributes to the current scholarship by conducting an improved accounting of the forest ownership patterns that will be of interest to scholars studying family forests, biofuels, and land-use, land-use change patterns in the region or similar regions in the United States. Land-use characteristics are based upon the National Land Cover Database (NLCD) 2011 dataset [103]. The results of this study are compared to previous national surveys of forest owners and possible directions for future scholarship are noted.

A.2 Methods

Parcel data was collected from WUP counties and aggregated into a single map in ArcGIS 10.6.1 [275] containing a total of 65,461 parcels representing 15,724 sq.km of land as bounded by the counties (see Figure A.1). Valid ownership records were extracted and parcel references to towns and physical features were discarded. Duplicated records resulting from ownership of multiple parcels were eliminated and a unique id was assigned to each owner. An ArcPy script was then used to look for additional duplication based upon differences in county entries (e.g., "John and Jane Doe" versus "John Doe et ux"). The Levenshtein Distance [276] - or similarity score - between the names was calculated when matching addresses were found. Scores above 0.548356696 were assumed to be matches based upon the statistical threshold *min*, determined by,

$$min = avg(score) + \alpha * \sigma(score) \tag{A.1}$$

Once the matches were identified, the records were updated with the relevant parent record and source of match (e.g., name or address records). Upon consolidation of ownership records, labels were assigned based upon the scheme outlined in Table A.1. Family forests where commonly verified with visual inspection of the ownership record and specific labels were not assigned if classification could not be made.

The second phase of the study focused on assessing the parcel characteristics using the NLCD 2011 dataset and the Commercial Forest Land registry [160]. First parcels smaller than one acre were removed since they cannot meet the minimum area to qualify as forest [274]. Next, the Commercial Forest Land registry was used to identify commercial forests based upon centroid intersection. The Tabulate Areas

Table A.1
Ownership Labels and Scheme for Assignment

Label	**Description**
Native American	Parcel owner is local Native American community (ex., "Keweenaw Bay Indian Community"), or records indicated land held in trust by government for Native Americans.
Federal	Parcel ownership is associated with the "US Government" or a federal agency.
State	Parcel ownership is associated with the "State of Michigan" or a state agency.
Municipal	Parcel ownership is associated with the county (e.g. "Houghton County"), local community (e.g., "Houghton Township"), or local community services (e.g., "Houghton-Portage Twp Schools").
Commercial	Parcel appears in Commercial Forest Lands [127] .
Family Forest	Parcel has at least one acre (4046.86 sq.m) of forest and owner appears to an individual or family.
Trust	Parcel ownership record clearly indicates association with a trust (ex., "Doe Family Trust"), the owner is listed as a trustee, or the organization is a 501(c)(3) registered non-profit.

tool was then used to calculate the area in each parcel by NLCD code and the results were aggregated into forest (NLCD codes 41, 42, and 43 for deciduous, evergreen, and mixed forest respectively) and woody wetlands (NLCD code 90) for evaluation. Following aggregation, parcels with less than one acre of forest were removed and unlabeled parcels with at least one acre of forested land were manually reviewed to determine if they fit into any of the categories. Finally, parcels were clipped to ensure they were bound to the counties lines [159].

A.3 Results and Discussion

Following analysis, a total of 39,119 parcels remained, accounting for control of about 10,910 sq.km of forests and 2,680 sq.km of wetlands (see Table A.2, Figure A.2). The parcels account for 15,367 sq.km of land or about 98% of the total area. Land ownership is approximately 30% federal, 23% family forests, and 28% registered as commercial forest independent of any other attributes. Across all ownership patterns, 6,231 parcels and 3,712 sq.km of forests were found to be registered in the Commercial Forest program with an additional 3,745 parcels and 1,369 sq.km of forests eligible for registration (see Table A.3).

Table A.2
Summary of labels applied in sq.km; commercial forests represent properties that are solely registered as such.

	Count	**Forest**	**Wetlands**	**Total**
Native American	120	18	3	23
Federal	2,546	3,418	857	4,620
State	1,911	868	256	1,249
Municipal	790	203	79	325
Commercial Forest	4,776	3,332	706	4,336
Family Forest	24,498	2,280	563	3,553
Trust	1,796	242	69	369
Mixed / Corporate	2,682	549	147	892
Total	**39,119**	**10,910**	**2,680**	**15,367**

Table A.3
Breakdown of Commercial Forest registration and eligible parcels in sq.km

	Commercial Forests				Eligible Parcels			
	Count	Forest	Wetlands	Total	Count	Forest	Wetlands	Total
Commercial	4,749	3,326	704	4,328				
Family	1,199	304	90	432	2,654	810	117	1,085
Trust	154	51	9	64	298	109	20	147
Others	129	32	16	52	40	13	2	16
Mixed/ Corporate					793	437	93	665
Total	**6,231**	**3,712**	**819**	**4,876**	**3,785**	**1,369**	**232**	**1,913**

Forest ownership is generally dominated by a minority of entities (e.g., governments, timber companies, etc.) who control a minimum of one sq.km of forest and collectively control approximately 77% and 12,047 sq.km of the total land. Excluding federal, state, and local governments, 624 entities (e.g., corporations, trusts, and private individuals) control more than one sq.km of forest with a mean of 2,340 sq.km. As shown in Table A.4, the majority of family forest owners (about 53%) own between 80,937.1 to 404,686 sq.m (20 and 100 acres) with the average family forest being approximately 121,406 sq.m (30 acres). NIPFs were estimated using the Commercial Forest Land registry by excluding properties listed as "Forest Industry" (see Figure A.3) resulting in a total of 31,080 parcels in the region, with 3,712 sq.km of forest and 5,695 sq.km of total land. It is important to note that quantity of NIPFs may be off by as much as 15% due to parcels potentially owned by the forest industry not being labeled as such (i.e., appearing as "Mixed/Corporate"). However, given the prevalence of the industry's participation with the Commercial Forest Land program in the region, failure to register a parcel may also imply that logging may not be possible on the land.

The extent of federal holdings in the WUP is not surprising due to presence of Isle Royale and Ottawa National Forest. Likewise, state and municipal holdings are also consistent with parks such as Porcupine Mountains Wilderness State Park.

Table A.4
Family Forest holdings, in acres with breaks based upon total forest owned using patterns established by [277] and [274].

	Count	Forest	Wetlands	Total	Percent Total
1 to <10	7,388	33,095	23,986	88,350	5.87%
10 to <20	3,292	48,151	19,534	91,733	8.55%
20 to <50	5,150	166,171	36,221	251,088	29.49%
50 to <100	1,882	130,847	23,417	189,173	23.22%
100 to <200	710	95,893	16,651	133,860	17.02%
200 to <500	184	51,996	10,415	71,938	9.23%
500 to <1,000	34	22,404	4,296	30,498	3.98%
1,000 to <5,000	10	14,900	4,643	21,226	2.64%

Interestingly, family forest ownership patterns break with the national averages found in Family Forest Owners of the United States, 2006 [277] and National Woodland Owner Survey (NWOS) [274], which found that the majority would have one and nine acres of forest. Rates are similar to those found in the NWOS breakout for the state of Michigan [278]; although, ownership is more concentrated in the 20 to 49 acres range at 31.33% than the state rate of 26.2%. Since family forests control approximately 21% of the total forests in the region, they have the potential to be regionally significant actors in forest conservation or timber production. Likewise, since family forests are part of the broader NIPF classification [277], collective management of 34% of the region's forests by NIPFs also underscores their importance in the region.

A.4 Conclusions

The data that is presented here represents an improved understanding of the forest ownership patterns in the WUP region. While ownership is largely dominated by a minority of entities such as the federal government and industrial forests; family forests and NIPFs are also extremely common highlighting the need for scholars to understand their motivations. Also noteworthy is a significant number of parcels

that eluded easy classification (i.e., "Mixed/Corporate" parcels) that, when combined with trusts, account for about 7% of forests in the region and almost one-third of the parcels and 40% of the forest eligible for registration as Commercial Forest Land. Understanding why the forests are not registered may be useful to policy makers seeking to increase enrollment in the program or understand the possible limits of timber-based economy in the region.

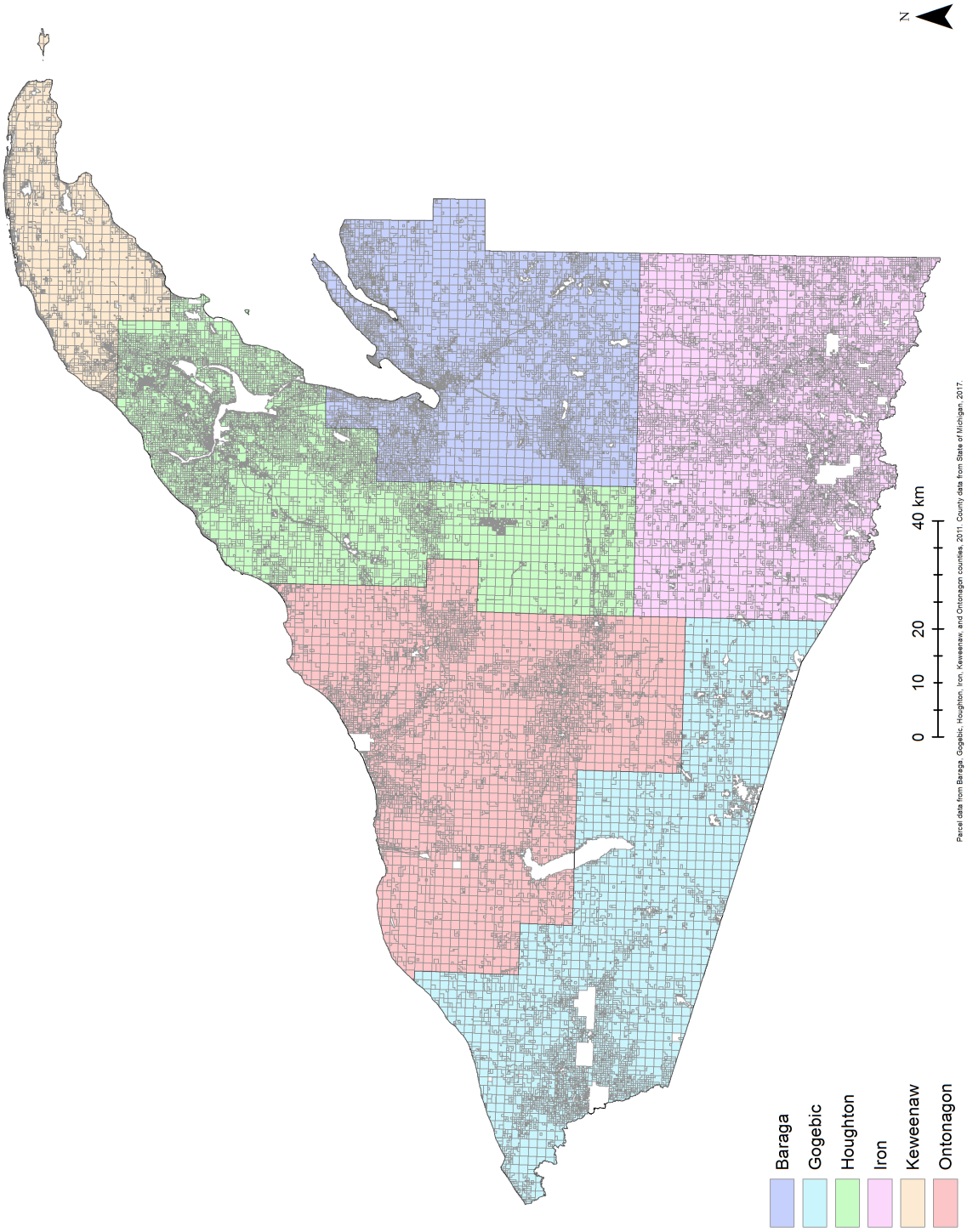

Figure A.1: Parcels in the WUP labeled by county, note that Isle Royale is not shown.

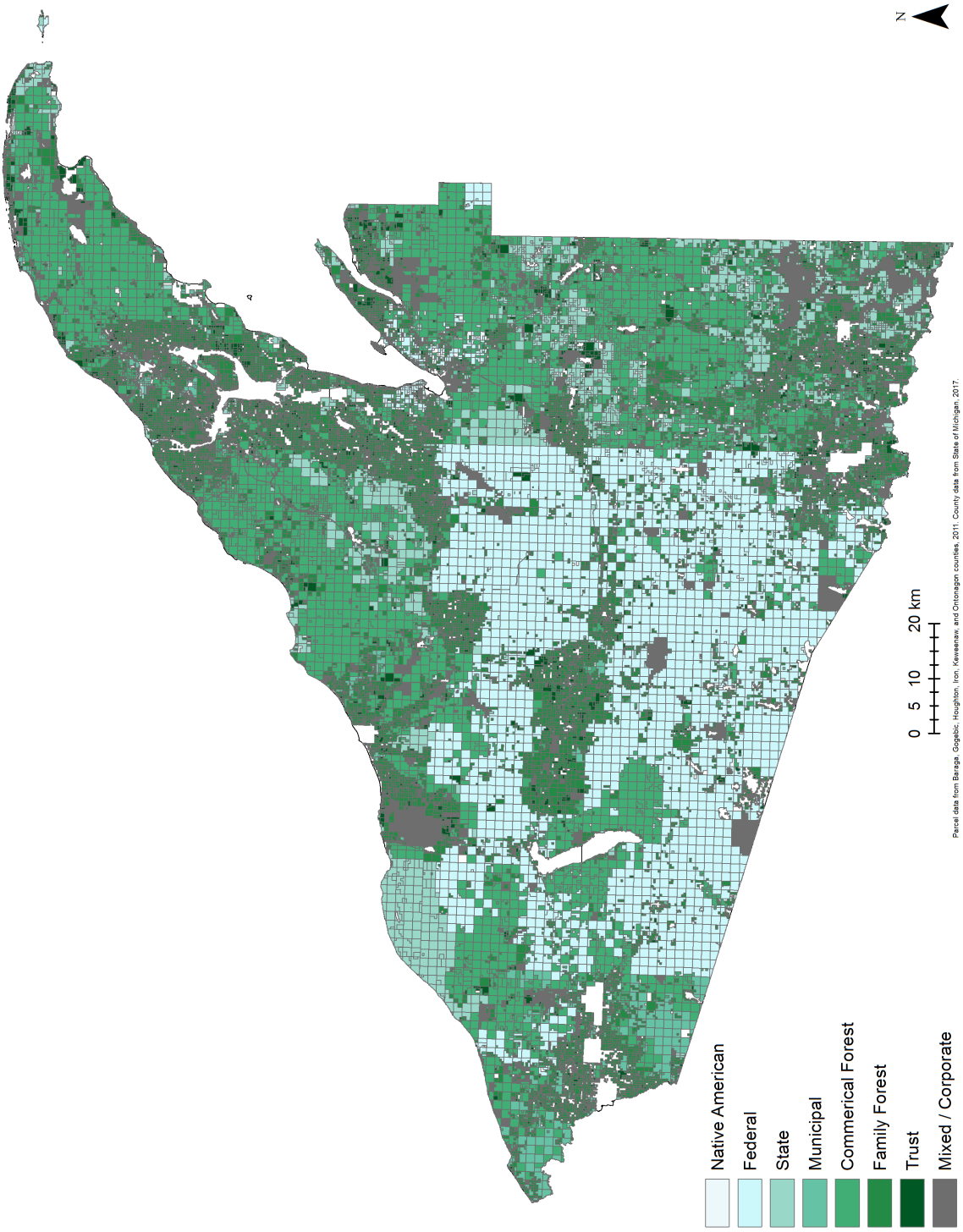

Figure A.2: Parcels in the WUP labeled with ownership type, note that Isle Royale is not shown.

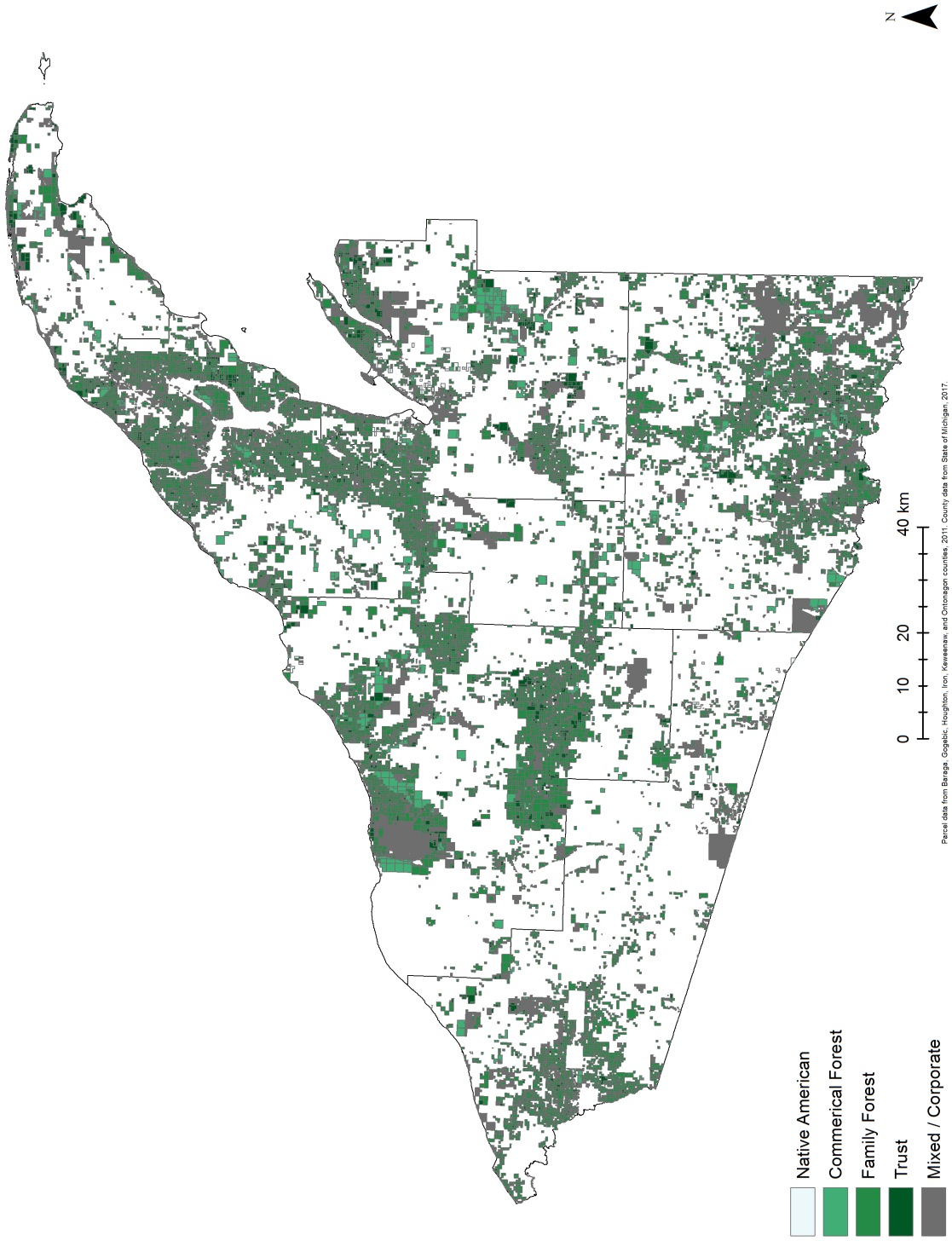

Figure A.3: Likely NIPF parcels in the WUP, note that "Commercial Forests" indicates enrollment in the Commercial Forest Lands program.

Appendix B

Guide to Supplementary Information

B.1 Chapter 3

Two additional files were included with the manuscript that do not appear in this dissertation. The first is referred to as "Electronic Supplementary Material 2" in the manuscript and consists of the file `ESM2_Calculations_and_Analysis.xlsx`. The file consists of several spreadsheets that were used to prepare calculations for the life cycle assessment. The second file is referred to as "Electronic Supplementary Material 3" in the manuscript and consists of the file `ESM3_SimaPro_Inputs.xlsx`. The file consists of several spreadsheets that were exported by SimaPro as a backup. In order to replicate the work it would be necessary to export the spreadsheets to individual files for import into SimaPro, or re-enter the data.

B.2 Chapter 4

One additional file was included with the manuscript hat does not appear in this dissertation. In the chapter it is referred to as "Electronic Supplementary Material 2", and corresponds to the file `ESM2_Calculations_and_Analysis.xlsx`. The file

contains several spreadsheets that were used to prepare calculations for the agent-based model as well as illustrating some of the algorithms used to prepare the initial forested environment.

Appendix C

Sample ChemSim Output

The following is the abbreviated console output of ChemSim when running the *in silico* study described in Chapter 5, Section 5.4.3. Since most of the logging is redundant during model execution, only the first three steps and last step are included.

```
ChemSim 0.7 / 60b8f6c

Max Memory:       4294967296b
Molecule Size:    384b
Staring Molecule Limit: 1E5 (38400000b)

delta T (sec): 1.0
Inital pH: 7.0
Reactor Dimensions (nm): 12757, 12757, 12757

Reactions: experiment/ems.csv [2019-05-09 - 16:04:10]
*COO- + O2 -> *OOCOO-, r = 1276 (bimolecular)
*OOCOO- + *OOCOO- -> *OCOO- + (3)O2, r = 1244 (bimolecular)
*OOCOCH3 + *OOCOCH3 -> *OCOCH3 + *OCOCH3 + (3)O2, r = 1233 (bimolecular)
*OOCCOO- + *OOCCOO- -> CO2 + CO2 + CO2 + CO2, r = 1232 (bimolecular)
*OCOO- + *OCOO- -> CO2 + (3)O2, r = 1219 (bimolecular)
HO* + HO2- -> HO2* + OH-, r = 1209 (bimolecular)
*OCH2COO- + *OCH2COO- -> HOCCOO- + HOCH2COO-, r = 1203 (bimolecular)
HO* + HO2* -> H2O + O2, r = 1178 (bimolecular)
HO* + HO* -> H2O2, r = 1133 (bimolecular)
*CH(OH)2 + O2 -> *OOCH(OH)2, r = 1082 (bimolecular)
*COCOO- + O2 -> *OOCOCOO-, r = 1002 (bimolecular)
*CH3 + O2 -> *OOCH3, r = 960 (bimolecular)
```

HOCCOO- + HO* -> *COCOO- + H2O, r = 941 (bimolecular)
*COCH3 + O2 -> *OOCOCH3, r = 931 (bimolecular)
HCOO- + HO* -> *COO- + H2O, r = 921 (bimolecular)
*CH2COCH3 + O2 -> *OOCH2COCH3, r = 875 (bimolecular)
*CH2COO- + O2 -> *OOCH2COO-, r = 875 (bimolecular)
*OOCH(OH)COCH3 + *OOCH(OH)COCH3 -> *OCH(OH)COCH3 + *OCH(OH)COCH3 + (3)O2,
r = 836 (bimolecular)
*OOCH2OH + *OOCH2OH -> HCOO- + HCOO-, r = 821 (bimolecular)
*OCH2OH + *OCH2OH -> HCOO- + CH3(OH)2, r = 821 (bimolecular)
*OOCH2COCH3 + *OOCH2COCH3 -> CH3COCH2OOOOCH2COCH3, r = 790 (bimolecular,
0.01)
*OOCH2COCH3 + *OOCH2COCH3 -> *OCH2COCH3 + *OCH2COCH3 + (3)O2, r = 790
(bimolecular, 0.376)
*OOCH2COCH3 + *OOCH2COCH3 -> CH3COCHO + CH3COCHO + H2O2, r = 790
(bimolecular, 0.536)
*OOCH2COCH3 + *OOCH2COCH3 -> CH3COCHO + CH3COCH2OH + (3)O2, r = 790
(bimolecular, 0.01)
*OOCH2COCH3 + *OOCH2COCH3 -> CH3COCHO + CH3COCH2OOOH, r = 790
(bimolecular, 0.01)
*OOCH2COCH3 + *OOCH2COCH3 -> *OCH2COCH3 + HO2* + CH3COCHO, r = 790
(bimolecular, 0.058)
*CH2OH + O2 -> *OOCH2OH, r = 754 (bimolecular)
CH2(OH)2 + HO* -> *CH(OH)2 + H2O, r = 714 (bimolecular)
CH3OH + HO* -> *CH2OH + H2O, r = 705 (bimolecular)
*CH(OH)COCH3 + O2 -> *OOCH(OH)COCH3, r = 702 (bimolecular)
*OOCH2OH + *OOCH2OH -> *OCH2OH + *OCH2OH + (3)O2, r = 689 (bimolecular)
*C(OH)2COCH3 + O2 -> *OOC(OH)2COCH3, r = 650 (bimolecular)
*OOCH2COO- + *OOCH2COO- -> *OCH2COO- + *OCH2COO- + (3)O, r = 602
(bimolecular, 0.5)
*OOCH2COO- + *OOCH2COO- -> HOCCOO- + HOCCOO- + H2O2, r = 602 (bimolecular,
0.5)
CH3COCHO + HO* -> *CH2COCHO + H2O, r = 574 (bimolecular)
CH3COCH2OH + HO* -> *CH(OH)COCH3 + H2O, r = 574 (bimolecular)
*OOCOCOO- + *OOCOCOO- -> (3)O2 + -OOCCOO-, r = 574 (bimolecular)
*OOCH3 + *OOCH2COCH3 -> *OCH3 + *OCH2COCH3 + (3)O2, r = 535 (bimolecular)
*OOCH3 + *OOCH3 -> *OCH3 + *OCH3 + (3)O2, r = 508 (bimolecular, 0.5)
*OOCH3 + *OOCH3 -> HCHO + HCHO + H2O2, r = 508 (bimolecular, 0.5)
*OOCH(OH)COCH3 + *OOCH(OH)COCH3 -> H2O2 + CH3COCOO-, r = 487 (bimolecular)
-OOCCOO- + HO* -> *OOCCOO- + H2O, r = 397 (bimolecular)
CH3COCH(OH)2 + HO* -> *C(OH)2COCH3 + H2O, r = 389 (bimolecular)
CH3COCH(OH)2 + HO* -> *CH2COCH(OH)2 + H2O, r = 361 (bimolecular)
CH3COCH3 + HO* -> *CH2COCH3 + H2O, r = 351 (bimolecular)
CH3COCH2OH + HO* -> *CH2COCH2OH + H2O, r = 340 (bimolecular)
CH3COO- + HO* -> *CH2COO- + H2O, r = 340 (bimolecular)
HO2* + O2*- -> H2O2 + O2, r = 327 (bimolecular)

*OOCH(OH)2 + *OOCH(OH)2 -> *OCH(OH)2 + *OCH(OH)2 + (3)O2, r = 314
(bimolecular, 0.5)
*OOCH(OH)2 + *OOCH(OH)2 -> HOC(OH)2 + HOC(OH)2 + H2O2, r = 314
(bimolecular, 0.5)
CH3COCHO + HO* -> *OC(OH)(CH3)CHO, r = 308 (bimolecular)
CH3COCOO- + HO* -> *CH2COCOO- + H2O, r = 249 (bimolecular)
H2O2 + HO* -> HO2* + H2O, r = 220 (bimolecular)
OOCH2COCH3 + HO2 -> CH3COCH2OH + (3)O + (3)O2, r = 168 (bimolecular)
CH3COCOO- + HO* -> *OC(OH)(CH3)COO-, r = 158 (bimolecular)
OOCH3 + HO2 -> CH3OH + (3)O + (3)O2, r = 158 (bimolecular)
*OOCH3 + *OOCH2COCH3 -> H2O2 + HCHO + CH3COCHO, r = 158 (bimolecular)
*OOCH(OH)COCH3 + *OOCH(OH)COCH3 -> CH3COCOO- + CH3COCH(OH)2, r = 132
(bimolecular)
OOCOCH3 + HO2 -> CH3COO- + (3)O + (3)O2, r = 93 (bimolecular)
OOCH2OH + HO2 -> CH2(OH)2 + (3)O + (3)O2, r = 93 (bimolecular)
OOCOCOO- + HO2 -> -OOCCOO- + (3)O + (3)O2, r = 93 (bimolecular)
OOCH(OH)COCH3 + HO2 -> CH(OH)2COCH3 + (3)O + (3)O2, r = 93 (bimolecular)
OOCH(OH)2 + HO2 -> CH(OH)3 + (3)O + (3)O2, r = 93 (bimolecular)
OCH2COCH3 + HO2 -> CH3COCH2OH + (3)O2, r = 73 (bimolecular)
*OCOCH3 -> *CH3 + CO2, r = 73 (unimolecular)
OCH2OH -> HCHO + HO, r = 73 (unimolecular)
*OCH2COO- -> *COO- + HCHO, r = 73 (unimolecular)
*OCH(OH)COCH3 -> HCOO- + *COCH, r = 73 (unimolecular)
*OCH2COCH3 -> *CH(OH)COCH3, r = 73 (unimolecular, 0.28)
*OCH2COCH3 -> *COCH3 + HCHO, r = 73 (unimolecular, 0.72)
HO2* + HO2* -> H2O2 + O2, r = 67 (bimolecular)
OCH2OH -> HCOO- + HO, r = 63 (unimolecular)
*OCH3 -> *CH2OH, r = 58 (unimolecular)
OOCH2COO- + HO2 -> HOCH2COO- + (3)O + (3)O2, r = 34 (bimolecular)
*OOCH(OH)2 -> *HO2 + HCOO-, r = 15 (unimolecular)
OOC(OH)2COCH3 -> HO2 + CH3COCOO-, r = 15 (unimolecular)
*OCH2COCH3 + *OCH2COCH3 -> CH3COCHO + CH3COCH2OH, r = 10 (bimolecular)
*OCH(OH)COCH3 + *OCH(OH)COCH3 -> CH3COCOO- + CH3COCH(OH)2, r = 7
(bimolecular)
OOCH2OH -> HO2 + HCHO, r = 3 (unimolecular)
CH2CO + H2O -> CH3COO-, r = 3 (bimolecular)
OOCH(OH)COCH3 -> CH3COCHO + HO2, r = 1 (unimolecular)
OOCOCH3 -> HO2 + CH2CO, r = 1 (unimolecular)
*OOCH3 + *OOCH3 -> HCHO + CH3OH + (3)O2, r = 1 (bimolecular)
*OOCH3 + *OOCH2COCH3 -> CH3COCHO + CH3OH + (3)O2, r = 1 (bimolecular)
*OOCH2OH + *OOCH2OH -> CH2(OH)2 + HCOO-, r = 1 (bimolecular)
*OOCH2COO- + *OOCH2COO- -> HOCCOO- + HOCH2COO-, r = 1 (bimolecular)
*OOCH(OH)2 + *OOCH(OH)2 -> CH(OH)3 + HOC(OH)2, r = 1 (bimolecular)
H2O2 + HO2* -> HO* + H2O + O2, r = 1 (bimolecular)
CH3COCHO + H2O2 -> CH3COO- + HCOO- + H2O, r = 0 (bimolecular)

```
H2O2 + O2*- -> HO* + OH- + O2, r = 0 (bimolecular)
CH3COCOO- + H2O2 -> CH3COO- + CO2 + H2O, r = 0 (bimolecular)
H2O2 + UV -> HO* + HO*, r = 0 (photolysis)
H2O2 <=> HO2- + H+, pKa = 11.6 (acid dissociation)
HO2* <=> O2*- + H+, pKa = 4.8 (acid dissociation)

Molecule to mol scalar: 4484304.932735425

Generating 89686 molecules of H2O2
Generating 10313 molecules of CH3COCH3
Adding molecules to the schedule...
H2O2 photolysis decay rate: -2.91 molecules/timestep
Estimated running time of 30819 time steps, padded to 31719

2019-05-09T20:26:16.123: Starting simulation...
2019-05-09T20:26:16.125: 0.0 / 0 of 31719
2019-05-09T20:26:24.055: 60.0 / 60 of 31719
...
2019-05-09T20:52:28.200: 31680.0 / 31680 of 31719

Molecule counts written to: data/results-1.csv
Molar counts written to: data/molar-1.csv

2019-05-09T20:52:29.355
```

Appendix D

Copyright Information

CHAPTER 2 was adapted for publication in the Open Access journal *SoftwareX* where it appears as Zupko, R., & Rouleau, M. (2019). ForestSim: Spatially explicit agent-based modeling of non-industrial forest owner policies. *SoftwareX*, 9, 117-125. `https://doi.org/10.1016/j.softx.2019.01.008` under the Creative Commons Attribution License (CC BY) license, the standard license for which is included first in this appendix.

Chapter 3 was published in *The International Journal of Life Cycle Assessment* and reappears with the permission of Springer Nature. The permission letter has been included in this appendix.

Chapter 5 includes data from a figure that appears in [52, 254] and is reproduced with permission from Elsevier. The permission letter appears last in this appendix.

SPRINGER NATURE LICENSE
TERMS AND CONDITIONS

Mar 29, 2019

This Agreement between Robert Zupko ("You") and Springer Nature ("Springer Nature") consists of your license details and the terms and conditions provided by Springer Nature and Copyright Clearance Center.

License Number	4558310075182
License date	Mar 29, 2019
Licensed Content Publisher	Springer Nature
Licensed Content Publication	The International Journal of Life Cycle Assessment
Licensed Content Title	Life cycle assessment of the production of gasoline and diesel from forest residues using integrated hydropyrolysis and hydroconversion
Licensed Content Author	Robert Zupko
Licensed Content Date	Jan 1, 2019
Type of Use	Thesis/Dissertation
Requestor type	academic/university or research institute
Format	print and electronic
Portion	full article/chapter
Will you be translating?	no
Circulation/distribution	<501
Author of this Springer Nature content	yes
Title	Application of Agent-Based Modeling to Complex Systems
Institution name	Michigan Technological University
Expected presentation date	May 2019
Requestor Location	Robert Zupko 1105 Datolite St Apt A HOUGHTON, MI 49931 United States Attn: Robert Zupko
Total	0.00 USD
Terms and Conditions	

Springer Nature Terms and Conditions for RightsLink Permissions

Springer Nature Customer Service Centre GmbH (the Licensor) hereby grants you a non-exclusive, world-wide licence to reproduce the material and for the purpose and requirements specified in the attached copy of your order form, and for no other use, subject to the conditions below:

1. The Licensor warrants that it has, to the best of its knowledge, the rights to license reuse of this material. However, you should ensure that the material you are requesting is original to the Licensor and does not carry the copyright of another entity (as credited in the published version).

   If the credit line on any part of the material you have requested indicates that it was reprinted or adapted with permission from another source, then you should also seek permission from that source to reuse the material.

2. Where **print only** permission has been granted for a fee, separate permission must be obtained for any additional electronic re-use.

3. Permission granted **free of charge** for material in print is also usually granted for any electronic version of that work, provided that the material is incidental to your work as a whole and that the electronic version is essentially equivalent to, or substitutes for, the print version.

4. A licence for 'post on a website' is valid for 12 months from the licence date. This licence does not cover use of full text articles on websites.

5. Where **'reuse in a dissertation/thesis'** has been selected the following terms apply: Print rights of the final author's accepted manuscript (for clarity, NOT the published version) for up to 100 copies, electronic rights for use only on a personal website or institutional repository as defined by the Sherpa guideline (www.sherpa.ac.uk/romeo/).

6. Permission granted for books and journals is granted for the lifetime of the first edition and does not apply to second and subsequent editions (except where the first edition permission was granted free of charge or for signatories to the STM Permissions Guidelines http://www.stm-assoc.org/copyright-legal-affairs/permissions/permissions-guidelines/), and does not apply for editions in other languages unless additional translation rights have been granted separately in the licence.

7. Rights for additional components such as custom editions and derivatives require additional permission and may be subject to an additional fee. Please apply to Journalpermissions@springernature.com/bookpermissions@springernature.com for these rights.

8. The Licensor's permission must be acknowledged next to the licensed material in print. In electronic form, this acknowledgement must be visible at the same time as the figures/tables/illustrations or abstract, and must be hyperlinked to the journal/book's homepage. Our required acknowledgement format is in the Appendix below.

9. Use of the material for incidental promotional use, minor editing privileges (this does not include cropping, adapting, omitting material or any other changes that affect the meaning, intention or moral rights of the author) and copies for the disabled are permitted under this licence.

10. Minor adaptations of single figures (changes of format, colour and style) do not require the Licensor's approval. However, the adaptation should be credited as shown in Appendix below.

Appendix — Acknowledgements:

For Journal Content:
Reprinted by permission from [**the Licensor**]: [**Journal Publisher** (e.g.

Nature/Springer/Palgrave)] [**JOURNAL NAME**] [**REFERENCE CITATION** (Article name, Author(s) Name), [**COPYRIGHT**] (year of publication)

For **Advance Online Publication papers:**
Reprinted by permission from [**the Licensor**]: [**Journal Publisher** (e.g. Nature/Springer/Palgrave)] [**JOURNAL NAME**] [**REFERENCE CITATION** (Article name, Author(s) Name), [**COPYRIGHT**] (year of publication), advance online publication, day month year (doi: 10.1038/sj.[JOURNAL ACRONYM].)

For Adaptations/Translations:
Adapted/Translated by permission from [**the Licensor**]: [**Journal Publisher** (e.g. Nature/Springer/Palgrave)] [**JOURNAL NAME**] [**REFERENCE CITATION** (Article name, Author(s) Name), [**COPYRIGHT**] (year of publication)

Note: For any republication from the British Journal of Cancer, the following credit line style applies:

Reprinted/adapted/translated by permission from [**the Licensor**]: on behalf of Cancer Research UK: : [**Journal Publisher** (e.g. Nature/Springer/Palgrave)] [**JOURNAL NAME**] [**REFERENCE CITATION** (Article name, Author(s) Name), [**COPYRIGHT]** (year of publication)

For **Advance Online Publication** papers:
Reprinted by permission from The [**the Licensor**]: on behalf of Cancer Research UK: [**Journal Publisher** (e.g. Nature/Springer/Palgrave)] [**JOURNAL NAME**] [**REFERENCE CITATION** (Article name, Author(s) Name), [**COPYRIGHT**] (year of publication), advance online publication, day month year (doi: 10.1038/sj.[JOURNAL ACRONYM])

For Book content:
Reprinted/adapted by permission from [**the Licensor**]: [**Book Publisher** (e.g. Palgrave Macmillan, Springer etc) [**Book Title**] by [**Book author**(s)] [**COPYRIGHT**] (year of publication)

Other Conditions:

Version 1.1

Questions? customercare@copyright.com or +1-855-239-3415 (toll free in the US) or +1-978-646-2777.

ELSEVIER LICENSE
TERMS AND CONDITIONS

May 13, 2019

This Agreement between Robert Zupko ("You") and Elsevier ("Elsevier") consists of your license details and the terms and conditions provided by Elsevier and Copyright Clearance Center.

License Number	4587310922255
License date	May 13, 2019
Licensed Content Publisher	Elsevier
Licensed Content Publication	Biosystems
Licensed Content Title	Formal agent-based modelling of intracellular chemical interactions
Licensed Content Author	Mark Pogson,Rod Smallwood,Eva Qwarnstrom,Mike Holcombe
Licensed Content Date	Jul 1, 2006
Licensed Content Volume	85
Licensed Content Issue	1
Licensed Content Pages	9
Start Page	37
End Page	45
Type of Use	reuse in a thesis/dissertation
Portion	figures/tables/illustrations
Number of figures/tables /illustrations	1
Format	both print and electronic
Are you the author of this Elsevier article?	No
Will you be translating?	No
Original figure numbers	Figure 5
Title of your thesis/dissertation	Application of Agent-Based Modeling to Complex Systems
Publisher of new work	Michigan Technological University
Expected completion date	May 2019
Estimated size (number of pages)	1
Requestor Location	Robert Zupko 1105 Datolite St Apt A HOUGHTON, MI 49931 United States Attn: Robert Zupko
Publisher Tax ID	98-0397604
Total	0.00 USD

10. Indemnity: You hereby indemnify and agree to hold harmless publisher and CCC, and their respective officers, directors, employees and agents, from and against any and all claims arising out of your use of the licensed material other than as specifically authorized pursuant to this license.
11. No Transfer of License: This license is personal to you and may not be sublicensed, assigned, or transferred by you to any other person without publisher's written permission.
12. No Amendment Except in Writing: This license may not be amended except in a writing signed by both parties (or, in the case of publisher, by CCC on publisher's behalf).
13. Objection to Contrary Terms: Publisher hereby objects to any terms contained in any purchase order, acknowledgment, check endorsement or other writing prepared by you, which terms are inconsistent with these terms and conditions or CCC's Billing and Payment terms and conditions. These terms and conditions, together with CCC's Billing and Payment terms and conditions (which are incorporated herein), comprise the entire agreement between you and publisher (and CCC) concerning this licensing transaction. In the event of any conflict between your obligations established by these terms and conditions and those established by CCC's Billing and Payment terms and conditions, these terms and conditions shall control.
14. Revocation: Elsevier or Copyright Clearance Center may deny the permissions described in this License at their sole discretion, for any reason or no reason, with a full refund payable to you. Notice of such denial will be made using the contact information provided by you. Failure to receive such notice will not alter or invalidate the denial. In no event will Elsevier or Copyright Clearance Center be responsible or liable for any costs, expenses or damage incurred by you as a result of a denial of your permission request, other than a refund of the amount(s) paid by you to Elsevier and/or Copyright Clearance Center for denied permissions.

LIMITED LICENSE

The following terms and conditions apply only to specific license types:
15. **Translation**: This permission is granted for non-exclusive world **English** rights only unless your license was granted for translation rights. If you licensed translation rights you may only translate this content into the languages you requested. A professional translator must perform all translations and reproduce the content word for word preserving the integrity of the article.
16. **Posting licensed content on any Website**: The following terms and conditions apply as follows: Licensing material from an Elsevier journal: All content posted to the web site must maintain the copyright information line on the bottom of each image; A hyper-text must be included to the Homepage of the journal from which you are licensing at http://www.sciencedirect.com/science/journal/xxxxx or the Elsevier homepage for books at http://www.elsevier.com; Central Storage: This license does not include permission for a scanned version of the material to be stored in a central repository such as that provided by Heron/XanEdu.
Licensing material from an Elsevier book: A hyper-text link must be included to the Elsevier homepage at http://www.elsevier.com . All content posted to the web site must maintain the copyright information line on the bottom of each image.

Posting licensed content on Electronic reserve: In addition to the above the following clauses are applicable: The web site must be password-protected and made available only to bona fide students registered on a relevant course. This permission is granted for 1 year only. You may obtain a new license for future website posting.
17. **For journal authors:** the following clauses are applicable in addition to the above:
Preprints:

A preprint is an author's own write-up of research results and analysis, it has not been peer-reviewed, nor has it had any other value added to it by a publisher (such as formatting, copyright, technical enhancement etc.).
Authors can share their preprints anywhere at any time. Preprints should not be added to or enhanced in any way in order to appear more like, or to substitute for, the final versions of articles however authors can update their preprints on arXiv or RePEc with their Accepted Author Manuscript (see below).
If accepted for publication, we encourage authors to link from the preprint to their formal publication via its DOI. Millions of researchers have access to the formal publications on ScienceDirect, and so links will help users to find, access, cite and use the best available version. Please note that Cell Press, The Lancet and some society-owned have different preprint policies. Information on these policies is available on the journal homepage.
Accepted Author Manuscripts: An accepted author manuscript is the manuscript of an article that has been accepted for publication and which typically includes author-incorporated changes suggested during submission, peer review and editor-author communications.
Authors can share their accepted author manuscript:

- immediately
    - via their non-commercial person homepage or blog
    - by updating a preprint in arXiv or RePEc with the accepted manuscript
    - via their research institute or institutional repository for internal institutional uses or as part of an invitation-only research collaboration work-group
    - directly by providing copies to their students or to research collaborators for their personal use
    - for private scholarly sharing as part of an invitation-only work group on commercial sites with which Elsevier has an agreement
- After the embargo period
    - via non-commercial hosting platforms such as their institutional repository
    - via commercial sites with which Elsevier has an agreement

In all cases accepted manuscripts should:

- link to the formal publication via its DOI
- bear a CC-BY-NC-ND license - this is easy to do
- if aggregated with other manuscripts, for example in a repository or other site, be shared in alignment with our hosting policy not be added to or enhanced in any way to appear more like, or to substitute for, the published journal article.

Published journal article (JPA): A published journal article (PJA) is the definitive final record of published research that appears or will appear in the journal and embodies all value-adding publishing activities including peer review co-ordination, copy-editing, formatting, (if relevant) pagination and online enrichment.
Policies for sharing publishing journal articles differ for subscription and gold open access articles:
Subscription Articles: If you are an author, please share a link to your article rather than the full-text. Millions of researchers have access to the formal publications on ScienceDirect, and so links will help your users to find, access, cite, and use the best available version.
Theses and dissertations which contain embedded PJAs as part of the formal submission can be posted publicly by the awarding institution with DOI links back to the formal publications on ScienceDirect.

References

[1] E. Coscarelli, *Predicting the Organic Compound Degradation in Aqueous-phase Ultraviolet (UV) and UV-based Advanced Oxidation Processes*. Open Access Master's Thesis, Michigan Technological University, Houghton, Michigan, 2018.

[2] P. Lauri, P. Havlík, G. Kindermann, N. Forsell, H. Böttcher, and M. Obersteiner, "Woody biomass energy potential in 2050," *Energy Policy*, vol. 66, pp. 19–31, Mar. 2014.

[3] M. J. Groom, E. M. Gray, and P. A. Townsend, "Biofuels and Biodiversity: Principles for Creating Better Policies for Biofuel Production," *Conservation Biology*, vol. 22, pp. 602–609, June 2008.

[4] B. Lattimore, C. T. Smith, B. Titus, I. Stupak, and G. Egnell, "Woodfuel Harvesting: A Review of Environmental Risks, Criteria and Indicators, and Certification Standards for Environmental Sustainability," *Journal of Sustainable Forestry*, vol. 32, pp. 58–88, Jan. 2013.

[5] B. Wols and C. Hofman-Caris, "Review of photochemical reaction constants of organic micropollutants required for UV advanced oxidation processes in water," *Water Research*, vol. 46, pp. 2815–2827, June 2012.

[6] P. Anderson, "Perspective: Complexity Theory and Organization Science," *Organization Science*, vol. 10, pp. 216–232, June 1999.

[7] S. Thurner, R. Hanel, and P. Klimek, *Introduction to the Theory of Complex Systems*. Oxford, United Kingdom: Oxford University Press, 2018.

[8] Y. Bar-Yam, *Dynamics of Complex Systems*. Studies in Nonlinearity, Reading, Massachusetts: Addison-Wesley, 1997.

[9] M. Gardener, "MATHEMATICAL GAMES: The fantastic combinations of John Conway's new solitaire game" life,"," *Scientific American*, vol. 223, pp. 120–123, 1970.

[10] P. Rendell, "Turing Universality of the Game of Life," in *Collision-Based Computing* (A. Adamatzky, ed.), pp. 513–539, London: Springer London, 2002.

[11] J. H. Miller and S. E. Page, *Complex Adaptive Systems: An Introduction to Computational Models of Social Life*. Princeton, New Jersey: Princeton University Press, 2007.

[12] S. A. Kauffman, *The Origins of Order: Self-Organization and Selection in Evolution*. New York: Oxford University Press, 1993.

[13] M. Scheffer, *Critical Transitiions in Nature and Society*. Princeton Studies in Complexity, Princeton, New Jersey: Princeton University Press, 2009.

[14] J. Wells, *Complexity and Sustainablity*, vol. 26 of *Routledge Studies in Ecological Economics*. London and New York: Routledge, 2013.

[15] J. M. Epstein and R. Axtell, *Growing Artificial Societies: Social Science from the Bottom Up*. Washington, D.C.: Brookings Institution Press, 1996.

[16] A. Borshchev and A. Filippov, "From system dynamics and discrete event to practical agent based modeling: reasons, techniques, tools," in *The 22nd International Conference of the System Dynamics Society*, (Oxford, England), p. 23, July 2004.

[17] H. Van Dyke Parunak, R. Savit, and R. L. Riolo, "Agent-Based Modeling vs. Equation-Based Modeling: A Case Study and Users' Guide," in *Multi-Agent Systems and Agent-Based Simulation: First International Workshop, MABS '98, Paris, France, July 4-6, 1998. Proceedings* (J. S. Sichman, R. Conte, and N. Gilbert, eds.), pp. 10–25, Berlin, Heidelberg: Springer Berlin Heidelberg, 1998. DOI: 10.1007/10692956_2.

[18] C. W. Reynolds, "Flocks, herds and schools: A distributed behavioral model," *SIGGRAPH Comput. Graph.*, vol. 21, no. 4, pp. 25–34, 1987.

[19] R. Axtell, "Why Agents? On the Varied Motivations for Agent Computing in the Social Sciences," Working Paper 17, The Brookings Institution, Center on Social and Economic Dynamics, Nov. 2000.

[20] J. M. Epstein, *Generative Social Science: Studies in Agent-Based Computational Modeling*. Princeton Studies in Complexity, Princeton, New Jersey: Princeton University Press, 2006.

[21] N. Gilbert, "Agent-based social simulation: dealing with complexity," tech. rep., University of Surrey, Centre for Research on Social Simulation, Dec. 2004.

[22] L. An, M. Linderman, J. Qi, A. Shortridge, and J. Liu, "Exploring Complexity in a Human–Environment System: An Agent-Based Spatial Model for Multidisciplinary and Multiscale Integration," *Annals of the Association of American Geographers*, vol. 95, pp. 54–79, Mar. 2005.

[23] L. An, "Modeling human decisions in coupled human and natural systems: Review of agent-based models," *Ecological Modelling*, vol. 229, pp. 25–36, Mar. 2012.

[24] C. Bone and S. Dragićević, "Evaluating Spatio-temporal Complexities of Forest Management: An Integrated Agent-based Modeling and GIS Approach," *Environmental Modeling & Assessment*, vol. 14, no. 4, pp. 481–496, 2009.

[25] F. Bousquet and C. Le Page, "Multi-agent simulations and ecosystem management: a review," *Ecological Modelling*, vol. 176, pp. 313–332, Sept. 2004.

[26] T. P. Evans and H. Kelley, "Multi-scale analysis of a household level agent-based model of landcover change," *Modelling land use change and environmental impact*, vol. 72, pp. 57–72, Aug. 2004.

[27] M. M. Bakker, S. J. Alam, J. van Dijk, and M. D. A. Rounsevell, "Land-use change arising from rural land exchange: an agent-based simulation model," *Landscape Ecology*, vol. 30, no. 2, pp. 273–286, 2015.

[28] A. Heppenstall, N. Malleson, and A. Crooks, ""Space, the Final Frontier": How Good are Agent-Based Models at Simulating Individuals and Space in Cities?," *Systems*, vol. 4, no. 1, 2016.

[29] A. L. Mayer, "Strengths and weaknesses of common sustainability indices for multidimensional systems," *Environment International*, vol. 34, pp. 277–291, Feb. 2008.

[30] J. Guinée, "Life Cycle Sustainability Assessment: What Is It and What Are Its Challenges?," in *Taking Stock of Industrial Ecology* (R. Clift and A. Druckman, eds.), pp. 45–68, Cham: Springer International Publishing, 2016.

[31] A. Levasseur, P. Lesage, M. Margni, L. Deschênes, and R. Samson, "Considering Time in LCA: Dynamic LCA and Its Application to Global Warming Impact Assessments," *Environmental Science & Technology*, vol. 44, pp. 3169–3174, Apr. 2010.

[32] B. Ness, E. Urbel-Piirsalu, S. Anderberg, and L. Olsson, "Categorising tools for sustainability assessment," *Ecological Economics*, vol. 60, pp. 498–508, Jan. 2007.

[33] R. Chaplin-Kramer, S. Sim, P. Hamel, B. Bryant, R. Noe, C. Mueller, G. Rigarlsford, M. Kulak, V. Kowal, R. Sharp, J. Clavreul, E. Price, S. Polasky, M. Ruckelshaus, and G. Daily, "Life cycle assessment needs predictive spatial modelling for biodiversity and ecosystem services," *Nature Communications*, vol. 8, p. 15065, Apr. 2017.

[34] G. Garver and M. S. Goldberg, "Boundaries and Indicators: Conceptualizing and Measuring Progress Toward an Economy of Right Relationship Constrained by Global Ecological Limits," in *Ecological Economics for the Anthropocene*, pp. 149–189, New York: Columbia University Press, 2015.

[35] R. W. Kates, W. C. Clark, R. Corell, J. M. Hall, C. C. Jaeger, I. Lowe, J. J. McCarthy, H. J. Schellnhuber, B. Bolin, N. M. Dickson, S. Faucheux, G. C. Gallopin, A. Grübler, B. Huntley, J. Jäger, N. S. Jodha, R. E. Kasperson, A. Mabogunje, P. Matson, H. Mooney, B. Moore, T. O'Riordan, and U. Svedin, "Sustainability Science," *Science*, vol. 292, p. 641, Apr. 2001.

[36] P. Baustert and E. Benetto, "Uncertainty analysis in agent-based modelling and consequential life cycle assessment coupled models: A critical review," *Journal of Cleaner Production*, vol. 156, pp. 378–394, July 2017.

[37] A. Marvuglia, T. N. Gutiérrez, P. Baustert, and E. Benetto, "Implementation of Agent-Based Models to support Life Cycle Assessment: A review focusing on agriculture and land use," *AIMS Agriculture and Food*, vol. 3, pp. 535–560, Dec. 2018.

[38] C. Davis, I. Nikolić, and G. P. J. Dijkema, "Integration of Life Cycle Assessment Into Agent-Based Modeling," *Journal of Industrial Ecology*, vol. 13, pp. 306–325, Apr. 2009.

[39] A. Heairet, S. Choudhary, S. Miller, and M. Xu, "Beyond life cycle analysis: Using an agent-based approach to model the emerging bio-energy industry," in *Proceedings of 2012 IEEE International Symposium on Sustainable Systems and Technology (ISSST)*, (Boston, MA), pp. 1–5, May 2012.

[40] S. R. Wu, X. Li, D. Apul, V. Breeze, Y. Tang, Y. Fan, and J. Chen, "Agent-Based Modeling of Temporal and Spatial Dynamics in Life Cycle Sustainability Assessment," *Journal of Industrial Ecology*, pp. 1507–1521, Sept. 2017.

[41] N. Bichraoui-Draper, M. Xu, S. A. Miller, and B. Guillaume, "Agent-based life cycle assessment for switchgrass-based bioenergy systems," *Resources, Conservation and Recycling*, vol. 103, pp. 171–178, Oct. 2015.

[42] Q. Florent and B. Enrico, "Combining Agent-Based Modeling and Life Cycle Assessment for the Evaluation of Mobility Policies," *Environmental Science & Technology*, vol. 49, pp. 1744–1751, Feb. 2015.

[43] T. N. Gutiérrez, S. Rege, A. Marvuglia, and E. Benetto, "Introducing LCA Results to ABM for Assessing the Influence of Sustainable Behaviours," in *Trends in Practical Applications of Agents, Multi-Agent Systems and Sustainability* (J. Bajo, J. Z. Hernández, P. Mathieu, A. Campbell, A. Fernández-Caballero, M. N. Moreno, V. Julián, A. Alonso-Betanzos, M. D. Jiménez-López, and V. Botti, eds.), pp. 185–196, Springer International Publishing, 2015.

[44] G. M. Whitesides and R. F. Ismagilov, "Complexity in Chemistry," *Science*, vol. 284, p. 89, Apr. 1999.

[45] W. H. Glaze and J. W. Kang, "Advanced oxidation processes. Test of a kinetic model for the oxidation of organic compounds with ozone and hydrogen peroxide in a semibatch reactor," *Industrial & Engineering Chemistry Research*, vol. 28, pp. 1580–1587, Nov. 1989.

[46] W. H. Glaze, J.-W. Kang, and D. H. Chapin, "The Chemistry of Water Treatment Processes Involving Ozone, Hydrogen Peroxide and Ultraviolet Radiation," *Ozone: Science & Engineering*, vol. 9, pp. 335–352, Sept. 1987.

[47] D. Minakata, S. P. Mezyk, J. W. Jones, B. R. Daws, and J. C. Crittenden, "Development of Linear Free Energy Relationships for Aqueous Phase Radical-Involved Chemical Reactions," *Environmental Science & Technology*, vol. 48, pp. 13925–13932, Dec. 2014.

[48] X. Guo, D. Minakata, J. Niu, and J. Crittenden, "Computer-Based First-Principles Kinetic Modeling of Degradation Pathways and Byproduct Fates in Aqueous-Phase Advanced Oxidation Processes," *Environmental Science & Technology*, vol. 48, pp. 5718–5725, May 2014.

[49] G. R. Peyton, "Guidelines for the Selection of a Chemical Model for Advanced Oxidation Processes," *Water Quality Research Journal*, vol. 27, pp. 43–56, Feb. 1992.

[50] B. Wols, D. Harmsen, J. Wanders-Dijk, E. Beerendonk, and C. Hofman-Caris, "Degradation of pharmaceuticals in UV (LP)/H2o2 reactors simulated by means of kinetic modeling and computational fluid dynamics (CFD)," *Water Research*, vol. 75, pp. 11–24, May 2015.

[51] M. T. Klann, A. Lapin, and M. Reuss, "Agent-based simulation of reactions in the crowded and structured intracellular environment: Influence of mobility and location of the reactants," *BMC Systems Biology*, vol. 5, p. 71, May 2011.

[52] M. Pogson, R. Smallwood, E. Qwarnstrom, and M. Holcombe, "Formal agent-based modelling of intracellular chemical interactions," *Biosystems*, vol. 85, pp. 37–45, July 2006.

[53] G. Pérez-Rodríguez, M. Pérez-Pérez, F. Fdez-Riverola, and A. Lourenço, "High performance computing for three-dimensional agent-based molecular models," *Journal of Molecular Graphics and Modelling*, vol. 68, pp. Pages 68–77, July 2016.

[54] S. Luke, C. Cioffi-Revilla, L. Panait, K. Sullivan, and G. Balan, "MASON: A Multiagent Simulation Environment," *Simulation*, vol. 81, pp. 517–527, July 2005.

[55] U. Wilensky, "NetLogo," 1999.

[56] S. M. N. Arifin and G. R. Madey, "Verification, Validation, and Replication Methods for Agent-Based Modeling and Simulation: Lessons Learned the Hard Way!," in *Concepts and Methodologies for Modeling and Simulation: A Tribute to Tuncer Ören* (L. Yilmaz, ed.), pp. 217–242, Springer International Publishing, 2015.

[57] B. G. Fitzpatrick, "Issues in Reproducible Simulation Research," *Bulletin of Mathematical Biology*, Sept. 2018.

[58] D. Abbas, R. Handler, B. Hartsough, D. Dykstra, P. Lautala, and L. Hembroff, "A survey analysis of forest harvesting and transportation operations in Michigan," *Croatian Journal of Forest Engineering: Journal for Theory and Application of Forestry Engineering*, vol. 35, no. 2, pp. 179–192, 2014.

[59] R. M. Handler, D. R. Shonnard, P. Lautala, D. Abbas, and A. Srivastava, "Environmental impacts of roundwood supply chain options in Michigan: life-cycle assessment of harvest and transport stages," *Journal of Cleaner Production*, vol. 76, pp. 64–73, Aug. 2014.

[60] ISO, "Environmental management – Life cycle assessment – Principles and framework," International Standard ISO 14040, ISO, Geneva, 2006.

[61] E.-D. Schulze, C. Körner, B. E. Law, H. Haberl, and S. Luyssaert, "Large-scale bioenergy from additional harvest of forest biomass is neither sustainable nor greenhouse gas neutral," *GCB Bioenergy*, vol. 4, pp. 611–616, Nov. 2012.

[62] K. A. Schaaf and S. R. Broussard, "Private forest policy tools: A national survey exploring the American public's perceptions and support," *Forest Policy and Economics*, vol. 9, pp. 316–334, Dec. 2006.

[63] A. M. York, M. A. Janssen, and L. A. Carlson, "Diversity of incentives for private forest landowners: An assessment of programs in Indiana, USA," *Land Use Policy*, vol. 23, pp. 542–550, Oct. 2006.

[64] H. Viana, W. B. Cohen, D. Lopes, and J. Aranha, "Assessment of forest biomass for use as energy. GIS-based analysis of geographical availability and locations of wood-fired power plants in Portugal," *Applied Energy*, vol. 87, pp. 2551–2560, Aug. 2010.

[65] P. Zambelli, C. Lora, R. Spinelli, C. Tattoni, A. Vitti, P. Zatelli, and M. Ciolli, "A GIS decision support system for regional forest management to assess biomass availability for renewable energy production," *Environmental Modelling & Software*, vol. 38, pp. 203–213, Dec. 2012.

[66] K. F. Wenger, ed., *Forestry Handbook*. John Wiley & Sons, Inc., second edition ed., 1984.

[67] B. M. Alam, R. Pulkki, C. Shahi, and T. Upadhyay, "Modeling Woody Biomass Procurement for Bioenergy Production at the Atikokan Generating Station in Northwestern Ontario, Canada," *Energies*, vol. 5, no. 12, 2012.

[68] C. E. Noon and M. J. Daly, "GIS-based biomass resource assessment with BRAVO," *Strategic Benefits of Biomass and Wasteful fuels*, vol. 10, no. 2–3, pp. 101–109, 1996.

[69] T. Kinoshita, K. Inoue, K. Iwao, H. Kagemoto, and Y. Yamagata, "A spatial evaluation of forest biomass usage using GIS," *Applied Energy*, vol. 86, pp. 1–8, Jan. 2009.

[70] S. Sánchez-García, E. Canga, E. Tolosana, and J. Majada, "A spatial analysis of woodfuel based on WISDOM GIS methodology: Multiscale approach in Northern Spain," *Applied Energy*, vol. 144, pp. 193–203, Apr. 2015.

[71] F. X. Aguilar, Z. Cai, and A. W. D'Amato, "Non-industrial private forest owner's willingness-to-harvest: How higher timber prices influence woody biomass supply," *Biomass and Bioenergy*, vol. 71, pp. 202–215, Dec. 2014.

[72] H. E. Burkhart and M. Tomé, *Modeling Forest Trees and Stands*. Dordrecht: Springer, 2012.

[73] A. R. Weiskittel, D. W. Hann, J. A. Kershaw Jr, and J. K. Vanclay, *Forest growth and yield modeling*. John Wiley & Sons, 2011.

[74] S. Kukrety, D. C. Wilson, A. W. D'Amato, and D. R. Becker, "Assessing sustainable forest biomass potential and bioenergy implications for the northern Lake States region, USA," *Biomass and Bioenergy*, vol. 81, pp. 167–176, Oct. 2015.

[75] A. N. Gray, T. J. Brandeis, J. D. Shaw, W. H. McWilliams, and P. D. Miles, "Forest Inventory and Analysis Database of the United States of America (FIA)," *Biodiversity & Ecology*, vol. 4, pp. 225–231, Sept. 2012.

[76] N. L. Crookston and G. E. Dixon, "The forest vegetation simulator: A review of its structure, content, and applications," *Decision Support Systems for Forest Management Decision Support in Multiple purpose Forestry*, vol. 49, pp. 60–80, Oct. 2005.

[77] W. F. Laurance, A. K. M. Albernaz, G. Schroth, P. M. Fearnside, S. Bergen, E. M. Venticinque, and C. D. Costa, "Predictors of deforestation in the Brazilian Amazon," *Journal of Biogeography*, vol. 29, pp. 737–748, 2002.

[78] P. Milling and N. Schieritz, "Modeling the Forest or Modeling the Trees - A Comparison of System Dynamics and Agent-Based Simulation," in *Proceedings of the 21st international conference of the System Dynamics Society*, (New York City, USA), pp. 1–15, System Dynamics Soc., July 2003.

[79] S. M. Manson and T. Evans, "Agent-based modeling of deforestation in southern YucatÃąn, Mexico, and reforestation in the Midwest United States," *Proceedings of the National Academy of Sciences*, vol. 104, pp. 20678–20683, Dec. 2007.

[80] M. R. Guzy, C. L. Smith, J. P. Bolte, D. W. Hulse, and S. V. Gregory, "Policy Research Using Agent-Based Modeling to Assess Future Impacts of Urban Expansion into Farmlands and Forests," *Ecology and Society*, vol. 13, no. 1, 2008.

[81] J. E. Leahy, E. G. Reeves, K. P. Bell, C. L. Straub, and J. S. Wilson, "Agent-Based Modeling of Harvest Decisions by Small Scale Forest Landowners in Maine, USA," *International Journal of Forestry Research*, vol. 2013, p. 12, 2013.

[82] F. J. Morgan and A. J. Daigneault, "Estimating Impacts of Climate Change Policy on Land Use: An Agent-Based Modelling Approach," *PLoS ONE*, vol. 10, May 2015.

[83] F. E. Bert, G. P. Podestá, S. L. Rovere, A. N. Menéndez, M. North, E. Tatara, C. E. Laciana, E. Weber, and F. R. Toranzo, "An agent based model to simulate structural and land use changes in agricultural systems of the argentine pampas," *Ecological Modelling*, vol. 222, pp. 3486–3499, Oct. 2011.

[84] H. Kelley and T. Evans, "The relative influences of land-owner and landscape heterogeneity in an agent-based model of land-use," *Ecological Economics*, vol. 70, pp. 1075–1087, Apr. 2011.

[85] R. B. Matthews, N. G. Gilbert, A. Roach, J. G. Polhill, and N. M. Gotts, "Agent-based land-use models: a review of applications," *Landscape Ecology*, vol. 22, no. 10, pp. 1447–1459, 2007.

[86] C. Brown, I. Bakam, P. Smith, and R. Matthews, "An agent-based modelling approach to evaluate factors influencing bioenergy crop adoption in north-east Scotland," *GCB Bioenergy*, vol. 8, pp. 226–244, Jan. 2016.

[87] J. Gan, J. W. A. Langeveld, and C. T. Smith, "An Agent-Based Modeling Approach for Determining Corn Stover Removal Rate and Transboundary Effects," *Environmental Management*, vol. 53, no. 2, pp. 333–342, 2014.

[88] D. M. Rouleau, F. J. Lind-Riehl, N. M. Smith, and L. A. Mayer, "Failure to Communicate: Inefficiencies in Voluntary Incentive Programs for Private Forest Owners in Michigan," *Forests*, vol. 7, no. 9, 2016.

[89] K. Sullivan, M. Coletti, and S. Luke, "GeoMason: GeoSpatial Support for MASON," Technical Report GMU-CS-TR-2010-16, George Mason University, Department of Computer Science, 2010.

[90] A. Brunner, W. S. Currie, and S. Miller, "Cellulosic ethanol production: Landscape scale net carbon strongly affected by forest decision making," *Biomass and Bioenergy*, vol. 83, pp. 32–41, Dec. 2015.

[91] J. Lind-Riehl, S. Jeltema, M. Morrison, G. Shirkey, A. L. Mayer, M. Rouleau, and R. Winkler, "Family legacies and community networks shape private forest management in the western Upper Peninsula of Michigan (USA)," *Land Use Policy*, vol. 45, pp. 95–102, May 2015.

[92] K. Perlin, "An image synthesizer," *SIGGRAPH Comput. Graph.*, vol. 19, no. 3, pp. 287–296, 1985.

[93] R. A. Fisher and F. Yates, *Statistical tables for biological, agricultural and medical research*. London: Oliver & Boyd, 3rd ed., 1948.

[94] A. L. Mayer and P. M. Tikka, "Biodiversity conservation incentive programs for privately owned forests," *Environmental Science & Policy*, vol. 9, pp. 614–625, Nov. 2006.

[95] M. G. Sorice, C.-O. Oh, T. Gartner, M. Snieckus, R. Johnson, and C. J. Donlan, "Increasing participation in incentive programs for biodiversity conservation," *Ecological Applications*, vol. 23, pp. 1146–1155, July 2013.

[96] M. Potoski and A. Prakash, "The Regulation Dilemma: Cooperation and Conflict in Environmental Governance," *Public Administration Review*, vol. 64, pp. 152–163, Apr. 2004.

[97] G. M. Parkhurst, J. F. Shogren, C. Bastian, P. Kivi, J. Donner, and R. B. Smith, "Agglomeration bonus: an incentive mechanism to reunite fragmented habitat for biodiversity conservation," *Ecological Economics*, vol. 41, pp. 305–328, May 2002.

[98] S. A. Pugh, L. D. Pedersen, D. C. Heym, R. J. Piva, C. W. Woodall, C. J. Barnett, C. M. Kurtz, and W. K. Moser, "Michigan's Forests 2009," Tech. Rep. NRS-66, U.S. Department of Agriculture, Forest Service, Northern Research Station, Newtown Square, PA, 2012.

[99] A. L. Mayer and M. D. Rouleau, "ForestSim Model of Impacts of Smallholder Dynamics: Forested Landscapes of the Upper Peninsula of Michigan," *International Journal of Forestry Research*, vol. 2013, p. 13, 2013.

[100] R. Bergman and J. Zerbe, "Primer on Wood Biomass for Energy," tech. rep., USDA Forest Service, State and Private Forestry Technology Marketing Unit, Forest Products Laboratory, Madison, Wisconsin, Jan. 2008.

[101] NuGen Engineering Ltd., "Feasibility Study for a 10 MW Biomass Fired Power Plant," feasibility Study, NuGen Engineering Ltd., Richmond, BC, Jan. 2010.

[102] TSS Consultants, "Feasibility Review for a Wood Waste to Energy Conversion Facility on the Northern Arizona University Campus," feasibility Study, TSS Consultants, Rancho Cordova, CA, Apr. 2014.

[103] C. G. Homer, J. A. Dewitz, L. Yang, S. Jin, P. Danielson, G. Xian, J. Coulston, N. D. Herold, J. D. Wickham, and K. Megown, "Completion of the 2011 National Land Cover Database for the conterminous United States-Representing a decade of land cover change information," *Photogrammetric Engineering and Remote Sensing*, vol. 81, no. 5, pp. 345–354, 2015.

[104] Michigan Department of Natural Resources Forest Resources Division, "Average Stumpage Price Report For 10/01/2016 to 12/31/2016," average Stumpage Price Report, Michigan Department of Natural Resources Forest Resources Division, Feb. 2017.

[105] J. Jenkins, D. Chojnacky, L. Heath, and R. Birdsey, "National-Scale Biomass Estimators for United States Tree Species," *Forest Science*, vol. 49, pp. 12–35, Feb. 2003.

[106] S. Magnussen and D. Reed, "Modeling for Estimation and Monitoring," in *Knowledge reference for national forest assessments*, pp. 111–136, Rome: Food and Agriculture Organization of the United Nations, 2015.

[107] A. Markevičius, V. Katinas, E. Perednis, and M. Tamašauskienė, "Trends and sustainability criteria of the production and use of liquid biofuels," *Renewable and Sustainable Energy Reviews*, vol. 14, pp. 3226–3231, Dec. 2010.

[108] B. D. Solomon, "Biofuels and sustainability," *Annals of the New York Academy of Sciences*, vol. 1185, pp. 119–134, Jan. 2010.

[109] K. Janda, L. Kristoufek, and D. Zilberman, "Biofuels: policies and impacts.," *Agricultural Economics/Zemedelska Ekonomika*, vol. 58, no. 8, 2012.

[110] F. L. Resende, "Recent advances on fast hydropyrolysis of biomass," *Transformations of Biomass and its derivatives to Fuels and Chemicals*, vol. 269, pp. 148–155, July 2016.

[111] T. L. Marker, L. G. Felix, M. B. Linck, and M. J. Roberts, "Integrated hydropyrolysis and hydroconversion (IH2) for the direct production of gasoline and diesel fuels or blending components from biomass, part 1: Proof of principle testing," *Environmental Progress & Sustainable Energy*, vol. 31, pp. 191–199, Dec. 2011.

[112] Q. Zhang, K. R. Goldstein, and J. R. Mihelcic, "A review of life cycle assessment studies on renewable energy derived from forest resources," in *Renewable Energy from Forest Resources in the United States*, vol. 12 of *Routledge Explorations in Environmental Economics*, pp. 163–195, London and New York: Routledge, 2009.

[113] T. Gomiero, "Are Biofuels an Effective and Viable Energy Strategy for Industrialized Societies? A Reasoned Overview of Potentials and Limits," *Sustainability*, vol. 7, no. 7, 2015.

[114] T. Marker, M. Roberts, M. Linck, L. Felix, P. Ortiz-Toral, J. Wangerow, L. Kraus, C. McLeod, A. DelPaggio, and E. Tan, "Biomass to gasoline and diesel using integrated hydropyrolysis and hydroconversion," technical Report, Gas Technology Inst., Des Plaines, IL (United States), 2012.

[115] E. Maleche, R. Glaser, T. Marker, and D. Shonnard, "A preliminary life cycle assessment of biofuels produced by the IH2 âĎć process," *Environmental Progress & Sustainable Energy*, vol. 33, pp. 322–329, Apr. 2013.

[116] J. Fan, J. Gephart, T. Marker, D. Stover, B. Updike, and D. R. Shonnard, "Carbon Footprint Analysis of Gasoline and Diesel from Forest Residues and Corn Stover using Integrated Hydropyrolysis and Hydroconversion," *ACS Sustainable Chemistry & Engineering*, vol. 4, pp. 284–290, Jan. 2016.

[117] A. Dutta, A. Sahir, E. Tan, D. Humbird, J. Snowden-Swan, P. Meyer, J. Ross, D. Sexton, R. Yap, and J. Lukas, "Process Design and Economics for the Conversion of Lignocellulosic Biomass to Hydrocarbon Fuels Thermochemical Research Pathways with In Situ and Ex Situ Upgrading of Fast Pyrolysis Vapors," Technical Report NREL/TP-5100-62455, PNNL -2382 3, National Renewable Energy Laboratory and Pacific Northwest National Laboratory, Mar. 2015.

[118] J. C. Meerman and E. D. Larson, "Negative-carbon drop-in transport fuels produced via catalytic hydropyrolysis of woody biomass with CO2 capture and storage," *Sustainable Energy & Fuels*, vol. 1, no. 4, pp. 866–881, 2017.

[119] C. A. Hall, B. E. Dale, and D. Pimentel, "Seeking to Understand the Reasons for Different Energy Return on Investment (EROI) Estimates for Biofuels," *Sustainability*, vol. 3, no. 12, 2011.

[120] SynSel, "Ontonagon SynSel: Site Qualification Guide," tech. rep., SynSel, n.d.

[121] SynSel, "Executive Summary," tech. rep., SynSel, Dec. 2017.

[122] TV6 & FOX UP, "SynSel Bio-refinery plant coming to Ontonagon," June 2018.

[123] PRé Consultants, "SimaPro," Feb. 2018.

[124] LTS, "DATASMART LCI Package (US-EI SimaPro Library)," 2016.

[125] National Renewable Energy Laboratory, "U.S. Life Cycle Inventory Database," 2012.

[126] PRé, "SimaPro Database Manual: Methods Library," Tech. Rep. Version 4.1, PRé, Feb. 2018.

[127] Michigan Department of Natural Resources, "Commerical Forests Summary," Tech. Rep. IC4171, Michigan Department of Natural Resources, Mar. 2018.

[128] D. E. Haugen, "Michigan timber industry, 2010," Resource Update FS-78, U.S. Department of Agriculture, Forest Service, Newtown Square, PA, 2016.

[129] ESRI, "ArcGIS 10.3.1 for Desktop," 2015.

[130] Center for Shared Solutions and Technology Partnerships, "All Roads (v17a)," June 2014.

[131] A. M. Evans, R. T. Perschel, and B. A. Kittler, "Overview of Forest Biomass Harvesting Guidelines," *Journal of Sustainable Forestry*, vol. 32, pp. 89–107, Jan. 2013.

[132] C. A. Hall, J. G. Lambert, and S. B. Balogh, "EROI of different fuels and the implications for society," *Energy Policy*, vol. 64, pp. 141–152, Jan. 2014.

[133] A. C. Hall, S. Balogh, and J. D. Murphy, "What is the Minimum EROI that a Sustainable Society Must Have?," *Energies*, vol. 2, no. 1, 2009.

[134] R. G. Boundy, S. W. Diegel, L. L. Wright, and S. C. Davis, "Biomass Energy Data Book: Edition 4," tech. rep., Oak Ridge National Lab, 2011.

[135] M. C. Guilford, C. A. Hall, P. O'Connor, and C. J. Cleveland, "A New Long Term Assessment of Energy Return on Investment (EROI) for U.S. Oil and Gas Discovery and Production," *Sustainability*, vol. 3, no. 10, 2011.

[136] E. G. Wilkerson and R. D. Perlack, "Resource assessment, economics and technology for collection and harvesting," in *Renewable Energy from Forest Resources in the United States*, vol. 12 of *Routledge Explorations in Environmental Economics*, pp. 69–91, Routledge, 2011.

[137] Michigan Department of Natural Resources, "Michigan Forestry Best Management Practices for Soil and Water Quality," Tech. Rep. IC4011, Michigan Department of Natural Resources, June 2018.

[138] R. Spinelli and N. Magagnotti, "Determining long-term chipper usage, productivity and fuel consumption," *Biomass and Bioenergy*, vol. 66, pp. 442–449, July 2014.

[139] M. Wang, A. Elgowainy, P. T. Benavides, A. Burnham, H. Cai, Q. Dai, T. R. Hawkins, J. C. Kelly, H. Kwon, and D.-Y. Lee, "Summary of Expansions and Updates in GREET 2018," tech. rep., Argonne National Lab (ANL), Argonne, IL (United States), 2018.

[140] T. J. Skone and K. Gerdes, "Development of baseline data and analysis of life cycle greenhouse gas emissions of petroleum-based fuels," Tech. Rep. DOE/NETL-2009/1346, National Energy Technology Laboratory, 2008.

[141] A. Vaidya and A. L. Mayer, "Criteria and indicators for a bioenergy production industry identified via stakeholder participation," *International Journal of Sustainable Development & World Ecology*, vol. 23, pp. 526–540, Nov. 2016.

[142] A. Vaidya and A. L. Mayer, "Use of a participatory approach to develop a regional assessment tool for bioenergy production," *Biomass and Bioenergy*, vol. 94, pp. 1–11, Nov. 2016.

[143] T. Buchholz, V. A. Luzadis, and T. A. Volk, "Sustainability criteria for bioenergy systems: results from an expert survey," *International Trade in Biofuels*, vol. 17, pp. S86–S98, Nov. 2009.

[144] Core Writing Team, "IPCC, 2014: climate change 2014: synthesis report. Contribution of Working Groups I," *II and III to the Fifth Assessment Report of the intergovernmental panel on Climate Change. IPCC, Geneva, Switzerland*, vol. 151, 2014.

[145] J. Bare, "TRACI 2.0: the tool for the reduction and assessment of chemical and other environmental impacts 2.0," *Clean Technologies and Environmental Policy*, vol. 13, pp. 687–696, Oct. 2011.

[146] J. Bare, "Tool for the Reduction and Assessment of Chemical and Other Environmental Impacts (TRACI) TRACI version 2.1," Tech. Rep. EPA/600/R-12/554, U.S. Environmental Protection Agency, Cincinnati, OH, Aug. 2012.

[147] Environmental Protection Agency, "Regulatory Impact Analysis: Renewable Fuel Standard Program," Regulatory Impact Analysis EPA420-R-07-004, Assessment and Standards Division Office of Transportation and Air Quality U.S. Environmental Protection Agency, Apr. 2007.

[148] J. Hill, L. Tajibaeva, and S. Polasky, "Climate consequences of low-carbon fuels: The United States Renewable Fuel Standard," *Energy Policy*, vol. 97, pp. 351–353, Oct. 2016.

[149] J. E. Smith, L. S. Heath, K. E. Skog, and R. A. Birdsey, "Methods for calculating forest ecosystem and harvested carbon with standard estimates for forest types of the United States," Gen. Tech. Rep. NE-343, U.S. Department of Agriculture, Forest Service, Northeastern Research Station, Newtown Square, PA, 2006.

[150] L. E. Nave, E. D. Vance, C. W. Swanston, and P. S. Curtis, "Harvest impacts on soil carbon storage in temperate forests," *Forest Ecology and Management*, vol. 259, pp. 857–866, Feb. 2010.

[151] D. J. Murphy, C. A. S. Hall, and B. Powers, "New perspectives on the energy return on (energy) investment (EROI) of corn ethanol," *Environment, Development and Sustainability*, vol. 13, pp. 179–202, Feb. 2011.

[152] W. H. Schlesinger, "Are wood pellets a green fuel?," *Science*, vol. 359, p. 1328, Mar. 2018.

[153] D. W. Johnson and P. S. Curtis, "Effects of forest management on soil C and N storage: meta analysis," *Forest Ecology and Management*, vol. 140, pp. 227–238, Jan. 2001.

[154] W. W. Covington, "Changes in Forest Floor Organic Matter and Nutrient Content Following Clear Cutting in Northern Hardwoods," *Ecology*, vol. 62, pp. 41–48, Feb. 1981.

[155] R. Lal, "Forest soils and carbon sequestration," *Forest Soils Research: Theory, Reality and its Role in TechnologY*, vol. 220, pp. 242–258, Dec. 2005.

[156] D. Johnson, J. Knoepp, W. Swank, J. Shan, L. Morris, D. Van Lear, and P. Kapeluck, "Effects of forest management on soil carbon: results of some long-term resampling studies," *Environmental Pollution*, vol. 116, pp. S201–S208, Mar. 2002.

[157] S. D. Peckham and S. T. Gower, "Simulated long-term effects of harvest and biomass residue removal on soil carbon and nitrogen content and productivity for two Upper Great Lakes forest ecosystems," *GCB Bioenergy*, vol. 3, pp. 135–147, Apr. 2011.

[158] Y. Yang, "Two sides of the same coin: consequential life cycle assessment based on the attributional framework," *Journal of Cleaner Production*, vol. 127, pp. 274–281, July 2016.

[159] Michigan Center for Geographic Information, "Michigan Counties V17," Sept. 2005.

[160] Michigan DNR Open Data, "Michigan Commercial Forest Land (Private Land Tax Incentive/Public Hunting and Fishing)," Nov. 2017.

[161] Internal Revenue Service, "Terminal Control Locations Directory," tech. rep., Internal Revenue Service, Nov. 2018.

[162] U.S. Oil, "Terminal Spec - Green Bay, WI," tech. rep., U.S. Oil, Feb. 2015.

[163] Esri Living Atlas, "US State Boundaries," June 2018.

[164] Esri, Federal Railroad Administration (FRA), and Bureau of Transportation Statistics (BTS), "USA Railroads," Feb. 2018.

[165] ESRI, "Commercial Waterway," Aug. 2017.

[166] US Army Corps of Engineers, "U.S. waterway data: National Waterway Network," 2018.

[167] P. R. Ehrlich, P. M. Kareiva, and G. C. Daily, "Securing natural capital and expanding equity to rescale civilization," *Nature*, vol. 486, pp. 68–73, June 2012.

[168] R. Costanza and B. C. Patten, "Defining and predicting sustainability," *Ecological Economics*, vol. 15, pp. 193–196, Dec. 1995.

[169] J. P. Bolte, D. W. Hulse, S. V. Gregory, and C. Smith, "Modeling biocomplexity âĂŞ actors, landscapes and alternative futures," *The Implications of Complexity for Integrated Resources*, vol. 22, pp. 570–579, May 2007.

[170] J. T. Rieb, R. Chaplin-Kramer, G. C. Daily, P. R. Armsworth, K. Böhning-Gaese, A. Bonn, G. S. Cumming, F. Eigenbrod, V. Grimm, B. M. Jackson, A. Marques, S. K. Pattanayak, H. M. Pereira, G. D. Peterson, T. H. Ricketts, B. E. Robinson, M. Schröter, L. A. Schulte, R. Seppelt, M. G. Turner, and E. M. Bennett, "When, where, and how nature matters for ecosystem services: challenges for the next generation of ecosystem service models," *BioScience*, vol. 67, no. 9, pp. 820–833, 2017.

[171] L. Vance, T. Eason, H. Cabezas, and M. E. Gorman, "Toward a leading indicator of catastrophic shifts in complex systems: Assessing changing conditions in nation states," *Heliyon*, vol. 3, p. e00465, Dec. 2017.

[172] W. Steffen, J. RockstrÃűm, K. Richardson, T. M. Lenton, C. Folke, D. Liverman, C. P. Summerhayes, A. D. Barnosky, S. E. Cornell, M. Crucifix, J. F. Donges, I. Fetzer, S. J. Lade, M. Scheffer, R. Winkelmann, and H. J. Schellnhuber, "Trajectories of the Earth System in the Anthropocene," *Proceedings of the National Academy of Sciences*, vol. 115, p. 8252, Aug. 2018.

[173] E. C. Ellis, N. R. Magliocca, C. J. Stevens, and D. Q. Fuller, "Evolving the Anthropocene: linking multi-level selection with long-term social–ecological change," *Sustainability Science*, vol. 13, pp. 119–128, Jan. 2018.

[174] M. Farsi, A. Hosseinian-Far, A. Daneshkhah, and T. Sedighi, "Mathematical and Computational Modelling Frameworks for Integrated Sustainability Assessment (ISA)," in *Strategic Engineering for Cloud Computing and Big Data Analytics* (A. Hosseinian-Far, M. Ramachandran, and D. Sarwar, eds.), pp. 3–27, Cham: Springer International Publishing, 2017.

[175] J. Wang, Y. Yang, Y. Bentley, X. Geng, and X. Liu, "Sustainability assessment of bioenergy from a global perspective: A review," *Sustainability*, vol. 10, no. 8, p. 2739, 2018.

[176] V. H. Dale, K. L. Kline, T. L. Richard, D. L. Karlen, and W. W. Belden, "Bridging biofuel sustainability indicators and ecosystem services through stakeholder engagement," *Using an Ecosystem Services perspective to assess biofuel sustainability*, vol. 114, pp. 143–156, July 2018.

[177] B. Phalan, "The social and environmental impacts of biofuels in Asia: An overview," *Bio-fuels in Asia*, vol. 86, Supplement 1, pp. S21–S29, Nov. 2009.

[178] L. J. Kulcsar, T. Selfa, and C. M. Bain, "Privileged access and rural vulnerabilities: Examining social and environmental exploitation in bioenergy development in the American Midwest," *Journal of Rural Studies*, vol. 47, pp. 291–299, Oct. 2016.

[179] L. Mancini, L. Benini, and S. Sala, "Characterization of raw materials based on supply risk indicators for Europe," *The International Journal of Life Cycle Assessment*, vol. 23, pp. 726–738, Mar. 2018.

[180] S. Sala, A. Anton, S. J. McLaren, B. Notarnicola, E. Saouter, and U. Sonesson, "In quest of reducing the environmental impacts of food production and consumption," *Towards eco-efficient agriculture and food systems: selected papers addressing the global challenges for food systems, including those presented at the Conference "LCA for Feeding the planet and energy for life" (6-8 October 2015, Stresa & Milan Expo, Italy)*, vol. 140, pp. 387–398, Jan. 2017.

[181] K. Koponen, S. Soimakallio, K. L. Kline, A. Cowie, and M. BrandÃčo, "Quantifying the climate effects of bioenergy âĂŞ Choice of reference system," *Renewable and Sustainable Energy Reviews*, vol. 81, pp. 2271–2280, Jan. 2018.

[182] M. A. Meyer and F. S. Leckert, "A systematic review of the conceptual differences of environmental assessment and ecosystem service studies of biofuel and bioenergy production," *Using an Ecosystem Services perspective to assess biofuel sustainability*, vol. 114, pp. 8–17, July 2018.

[183] J. Groeneveld, B. Müller, C. Buchmann, G. Dressler, C. Guo, N. Hase, F. Hoffmann, F. John, C. Klassert, T. Lauf, V. Liebelt, H. Nolzen, N. Pannicke, J. Schulze, H. Weise, and N. Schwarz, "Theoretical foundations of human decision-making in agent-based land use models – A review," *Environmental Modelling & Software*, vol. 87, pp. 39–48, Jan. 2017.

[184] M. Z. Hauschild, R. K. Rosenbaum, and S. I. Olsen, eds., *Life Cycle Assessment: Theory and Practice*. Cham, Switzerland: Springer International Publishing, 2018.

[185] V. Grimm, U. Berger, D. L. DeAngelis, J. G. Polhill, J. Giske, and S. F. Railsback, "The ODD protocol: A review and first update," *Ecological Modelling*, vol. 221, pp. 2760–2768, Nov. 2010.

[186] R. Zupko, "Life cycle assessment of the production of gasoline and diesel from forest residues using integrated hydropyrolysis and hydroconversion," *The International Journal of Life Cycle Assessment*, Mar. 2019.

[187] Michigan Department of Natural Resources, "Commercial Forests Summary," Tech. Rep. IC4171, Michigan Department of Natural Resources, Mar. 2018.

[188] Western Upper Peninsula Planning & Development Region, "Comprehensive Economic Development Strategy," tech. rep., Western Upper Peninsula Planning & Development Region, Apr. 2017.

[189] E. Dulys-Nusbaum, S. S. Klammer, and S. M. Swinton, "How willing are different types of landowner to supply hardwood timber residues for bioenergy?," *Biomass and Bioenergy*, vol. 122, pp. 45–52, Mar. 2019.

[190] J. R. Schubert and A. L. Mayer, "Peer Influence of Non-Industrial Private Forest Owners in the Western Upper Peninsula of Michigan," *Open Journal of Forestry*, vol. 2, no. 3, pp. 150–158, 2012.

[191] E. S. Huff, J. E. Leahy, D. B. Kittredge, C. L. Noblet, and A. R. Weiskittel, "Psychological distance of timber harvesting for private woodland owners," *Forest sector trade*, vol. 81, pp. 48–56, Aug. 2017.

[192] R. Germain, S. Bick, M. Kelly, J. Benjamin, and W. Farrand, "Case Study of Three High-Performing Contract Loggers with Distinct Harvest Systems: Are They Thriving, Striving, or Just Surviving?," *Forest Products Journal*, vol. 66, pp. 97–105, May 2015.

[193] K. Murphy, "The social pillar of sustainable development: a literature review and framework for policy analysis," *Sustainability: Science, Practice and Policy*, vol. 8, pp. 15–29, Apr. 2012.

[194] OECD, *Society at a Glance 2019: OECD Social Indicators*. Paris: OECD Publishing, 2019.

[195] J. Bliss, "Public Perceptions of Clearcutting," *Journal of Forestry*, vol. 98, pp. 4–9, Dec. 2000.

[196] J. Pâquet and L. Bélanger, "Public Acceptability Thresholds of Clearcutting to Maintain Visual Quality of Boreal Balsam Fir Landscapes," *Forest Science*, vol. 43, pp. 46–55, Feb. 1997.

[197] L. Tahvanainen, L. Tyrväinen, M. Ihalainen, N. Vuorela, and O. Kolehmainen, "Forest management and public perceptions – visual versus verbal information," *Landscape and Urban Planning*, vol. 53, pp. 53–70, Jan. 2001.

[198] F. Zhang, D. M. Johnson, and J. W. Sutherland, "A GIS-based method for identifying the optimal location for a facility to convert forest biomass to biofuel," *Biomass and Bioenergy*, vol. 35, pp. 3951–3961, Oct. 2011.

[199] T. R. Brown and R. C. Brown, "A review of cellulosic biofuel commercial-scale projects in the United States," *Biofuels, Bioproducts and Biorefining*, vol. 7, pp. 235–245, May 2013.

[200] L. A. Leefers and J. M. Vasievich, "Timber Resources and Factors Affecting Timber Availability and Sustainability for Kinross, Michigan," tech. rep., Department of Forestry, Michigan State University, East Lansing, MI, Dec. 2010.

[201] M. C. Hansen, P. V. Potapov, R. Moore, M. Hancher, S. A. Turubanova, A. Tyukavina, D. Thau, S. V. Stehman, S. J. Goetz, T. R. Loveland, A. Kommareddy, A. Egorov, L. Chini, C. O. Justice, and J. R. G. Townshend, "High-Resolution Global Maps of 21st-Century Forest Cover Change," *Science*, vol. 342, p. 850, Nov. 2013.

[202] R. Freeman, "A Theory on the Future of the Rebound Effect in a Resource-Constrained World," *Frontiers in Energy Research*, vol. 6, p. 81, 2018.

[203] T. E. McKone, W. W. Nazaroff, P. Berck, M. Auffhammer, T. Lipman, M. S. Torn, E. Masanet, A. Lobscheid, N. Santero, U. Mishra, A. Barrett, M. Bomberg, K. Fingerman, C. Scown, B. Strogen, and A. Horvath, "Grand Challenges for Life-Cycle Assessment of Biofuels," *Environmental Science & Technology*, vol. 45, pp. 1751–1756, Mar. 2011.

[204] V. Grimm, U. Berger, F. Bastiansen, S. Eliassen, V. Ginot, J. Giske, J. Goss-Custard, T. Grand, S. K. Heinz, G. Huse, A. Huth, J. U. Jepsen, C. Jørgensen, W. M. Mooij, B. Müller, G. Pe′er, C. Piou, S. F. Railsback, A. M. Robbins, M. M. Robbins, E. Rossmanith, N. Rüger, E. Strand, S. Souissi, R. A. Stillman, R. Vabø, U. Visser, and D. L. DeAngelis, "A standard protocol for describing individual-based and agent-based models," *Ecological Modelling*, vol. 198, pp. 115–126, Sept. 2006.

[205] R. Zupko and M. Rouleau, "ForestSim: Spatially explicit agent-based modeling of non-industrial forest owner policies," *SoftwareX*, vol. 9, pp. 117–125, Jan. 2019.

[206] S. A. Pugh, D. C. Heym, B. J. Butler, D. E. Haugen, C. M. Kurtz, W. H. McWilliams, P. D. Miles, R. S. Morin, M. D. Nelson, R. I. Riemann, J. E. Smith, J. A. Westfall, and C. W. Woodall, "Michigan forests 2014," Resour. Bull. NRS-110, U.S. Department of Agriculture, Forest Service, Northern Research Station, Newtown Square, PA, 2017.

[207] M. G. Rollins and C. K. Frame, "The LANDFIRE Prototype Project: nationally consistent and locally relevant geospatial data for wildland fire management," *Gen. Tech. Rep. RMRS-GTR-175. Fort Collins: US Department of Agriculture, Forest Service, Rocky Mountain Research Station. 416 p.*, vol. 175, 2006.

[208] Michigan Department of Natural Resources, "Stumpage Prices Over Time," 2019.

[209] Michigan Department of Natural Resources, "Michigan DNR Forestry Canopy Data," Jan. 2017.

[210] D. G. Chapman, "Statistical problems in dynamics of exploited fisheries populations," in *Proc. 4th Berkeley Symp. on Mathematics, Statistics and Probability*, vol. 4, pp. 153–168, University of California Press Berkeley, 1961.

[211] F. J. Richards, "A Flexible Growth Function for Empirical Use," *Journal of Experimental Botany*, vol. 10, pp. 290–301, June 1959.

[212] U.S. Energy Information Administration, "Weekly Retail Gasoline and Diesel Prices," tech. rep., U.S. Energy Information Administration, Apr. 2019.

[213] Bureau of Labor Statistics, "45-4022 Logging Equipment Operators," occupational Employment and Wages, May 2017, U.S. Department of Labor, Mar. 2018.

[214] Bureau of Labor Statistics, "53-3032 Heavy and Tractor-Trailer Truck Drivers," occupational Employment and Wages, May 2018, U.S. Department of Labor, Mar. 2019.

[215] F. X. Aguilar, Z. Cai, and A. W. D'Amato, "Non-industrial private forest owner's willingness-to-harvest: How higher timber prices influence woody biomass supply," *Biomass and Bioenergy*, vol. 71, pp. 202–215, Dec. 2014.

[216] B. Akinci and M. Fischer, "Factors Affecting Contractors' Risk of Cost Overburden," *Journal of Management in Engineering*, vol. 14, pp. 67–76, Jan. 1998.

[217] U.S. Forest Service, "Cut and Sold: Cumulative FY 2014 Q1 to FY 2014 Q4," tech. rep., United States Department of Agriculture, U.S. Forest Service, Forest Management, Washington, DC, Nov. 2014.

[218] G. E. Dixon and C. E. Keyser, "Lake States (LS) Variant Overview - Forest Vegetation Simulator," internal Rep, U. S. Department of Agriculture, Forest Service, Forest Management Service Center, Fort Collins, CO, Nov. 2018.

[219] J. A. Kershaw, Jr., R. C. Morrissey, D. F. Jacobs, J. R. Seifert, and J. B. McCarter, "Dominant height-based height-diameter equations for trees in southern Indiana," in *Proceedings, 16th Central Hardwood Forest Conference*, (West Lafayette, IN), pp. 341–355, U.S. Department of Agriculture, Forest Service, Northern Research Station, Apr. 2008.

[220] C. Peng, L. Zhang, and J. Liu, "Developing and Validating Nonlinear Height-Diameter Models for Major Tree Species of Ontario's Boreal Forests," *Northern Journal of Applied Forestry*, vol. 18, pp. 87–94, Sept. 2001.

[221] R. M. Burns and H. Barbara, *Silvics of North America: 1. conifers; 2. hardwoods*. No. 654 in Agriculture Handbook, Washington, D.C.: United States Department of Agriculture, Forest Service, 1990.

[222] J. Sullivan, "Betula alleghaniensis," tech. rep., U.S. Department of Agriculture, Forest Service, Rocky Mountain Research Station, Fire Sciences Laboratory, 1994.

[223] Michigan Department of Natural Resources, "Michigan DNR Designated ATV Trails," May 2015.

[224] Michigan Department of Natural Resources, "Michigan DNR Designated Bicycle Trails," May 2015.

[225] Michigan Department of Natural Resources, "Michigan DNR Designated Equestrian Trails," May 2015.

[226] Michigan Department of Natural Resources, "Michigan DNR Designated Hiking Pathways," Jan. 2017.

[227] Michigan Department of Natural Resources, "Michigan DNR Designated Railtrails," May 2015.

[228] Michigan Department of Natural Resources, "Michigan DNR Designated Motorcycle Trails," May 2015.

[229] Michigan Department of Natural Resources, "Michigan DNR Designated Ski Trails," May 2015.

[230] Michigan Department of Natural Resources, "Michigan DNR Designated Snowmobile Trails," Apr. 2017.

[231] Michigan Department of Natural Resources, "Michigan DNR Designated ORV Routes," May 2015.

[232] State of Michigan, "Michigan All Roads," 2016.

[233] S. D. Richardson, "Environmental Mass Spectrometry: Emerging Contaminants and Current Issues," *Analytical Chemistry*, vol. 80, pp. 4373–4402, June 2008.

[234] T. B. Hayes, V. Khoury, A. Narayan, M. Nazir, A. Park, T. Brown, L. Adame, E. Chan, D. Buchholz, T. Stueve, and S. Gallipeau, "Atrazine induces complete feminization and chemical castration in male African clawed frogs (*Xenopus laevis*)," *Proceedings of the National Academy of Sciences*, vol. 107, p. 4612, Mar. 2010.

[235] M. Gavrilescu, K. Demnerová, J. Aamand, S. Agathos, and F. Fava, "Emerging pollutants in the environment: present and future challenges in biomonitoring, ecological risks and bioremediation," *New Biotechnology*, vol. 32, pp. 147–156, Jan. 2015.

[236] S. A. Snyder, E. C. Wert, H. D. Lei, P. Westerhoff, and Y. Yoon, "Removal of EDCs and pharmaceuticals in drinking and reuse treatment processes," tech. rep., Awwa Research Foundation, Denver, CO, 2007.

[237] J. Rice, A. Wutich, and P. Westerhoff, "Assessment of De Facto Wastewater Reuse across the U.S.: Trends between 1980 and 2008," *Environmental Science & Technology*, vol. 47, pp. 11099–11105, Oct. 2013.

[238] National Research Council, *Water Reuse: Potential for Expanding the Nation's Water Supply Through Reuse of Municipal Wastewater*. Washington, DC: The National Academies Press, 2012.

[239] W. H. Glaze, Y. Lay, and J.-W. Kang, "Advanced Oxidation Processes. A Kinetic Model for the Oxidation of 1,2-Dibromo-3-chloropropane in Water by the Combination of Hydrogen Peroxide and UV Radiation," *Industrial & Engineering Chemistry Research*, vol. 34, pp. 2314–2323, July 1995.

[240] C. M. Sharpless and K. G. Linden, "Experimental and Model Comparisons of Low- and Medium-Pressure Hg Lamps for the Direct and H2o2 Assisted UV Photodegradation of N-Nitrosodimethylamine in Simulated Drinking Water," *Environmental Science & Technology*, vol. 37, pp. 1933–1940, May 2003.

[241] H. S. Fogler, *Elements of Chemical Reaction Engineering*. Upper Saddle River, NJ: Prentice Hall PTR, 3rd ed., 1999.

[242] C. D. Yao, W. R. Haag, and T. Mill, "Kinetic features of advanced oxidation processes for treating aqueous chemical mixtures," in *Proceedings of the Second International Symposium on Chemical Oxidation: Technologies for the Nineties*, vol. 2, (Basel, Switzerland), pp. 112–139, Technomic Publishing AG, 1992.

[243] W. Braun, J. T. Herron, and D. K. Kahaner, "Acuchem: A computer program for modeling complex chemical reaction systems," *International Journal of Chemical Kinetics*, vol. 20, pp. 51–62, Jan. 1988.

[244] J. C. Crittenden, S. Hu, D. W. Hand, and S. A. Green, "A kinetic model for H2o2/UV process in a completely mixed batch reactor," *Water Research*, vol. 33, pp. 2315–2328, July 1999.

[245] C. W. Gear, *Numerical Initial Value Problems in Ordinary Differential Equations*. Prentice Hall PTR, 1971.

[246] A. Hindmarsh and R. Gelinas, "GEAR: Ordinary Differential Equation System Solver," tech. rep., California Univ., Livermore. Lawrence Radiation Lab., United States, Jan. 1971.

[247] Y. Lay, *Oxidation of 1, 2-dibromo-3-chloropropane in groundwater using advanced oxidation processes.* Thesis (D. Env), University of California, Los Angeles, CA, 1990.

[248] K. Li, J. Crittenden, D. Hand, and D. Hokanson, "Manual Advanced Oxidation Process Simulation Software (AdOxTM)," 1998.

[249] K. Li, D. R. Hokanson, J. C. Crittenden, R. R. Trussell, and D. Minakata, "Evaluating UV/H2o2 processes for methyl tert-butyl ether and tertiary butyl alcohol removal: Effect of pretreatment options and light sources," *Water Research*, vol. 42, pp. 5045–5053, Dec. 2008.

[250] J. C. Crittenden, R. R. Trussell, D. W. Hand, K. J. Howe, and G. Tchobanoglous, *MWH's water treatment: principles and design.* Hoboken, NJ: John Wiley & Sons, 2012.

[251] B. Wols, D. Harmsen, E. Beerendonk, and C. Hofman-Caris, "Predicting pharmaceutical degradation by UV (LP)/H2o2 processes: A kinetic model," *Chemical Engineering Journal*, vol. 255, pp. 334–343, Nov. 2014.

[252] B. Wols, D. Harmsen, E. Beerendonk, and C. Hofman-Caris, "Predicting pharmaceutical degradation by UV (MP)/H2o2 processes: A kinetic model," *Chemical Engineering Journal*, vol. 263, pp. 336–345, Mar. 2015.

[253] J. A. Bachman and P. Sorger, "New approaches to modeling complex biochemistry," *Nature Methods*, vol. 8, p. 130, Jan. 2011.

[254] M. Pogson, *Modelling the Intracellular NF-kB Signalling Pathway.* PhD Thesis, University of Sheffield, Sheffield, England, Dec. 2006.

[255] H. Samet, "Spatial Data Structures," in *Modern Database Systems, The Object Model, Interoperability and Beyond*, pp. 361–385, New York: ACM Press and Addison-Wesley, 1995.

[256] M. P. Allen and D. J. Tildesley, *Computer Simulation of Liquids.* Oxford, United Kingdom: Oxford University Press, second ed., 2017.

[257] M. Teschner, B. Heidelberger, M. Müller, D. Pomerantes, and M. H. Gross, "Optimized Spatial Hashing for Collision Detection of Deformable Objects.," in *Proceedings of the Vision, Modeling, and Visualization Conference 2003 (VMV 2003), München, Germany, November 19-21, 2003*, pp. 47–54, 2003.

[258] D. Blackman and S. Vigna, "Scrambled Linear Pseudorandom Number Generators," *arXiv e-prints*, p. arXiv:1805.01407, May 2018.

[259] S. Vigna, "DSI utilities," Oct. 2018.

[260] S. Vigna, "fastutil," Sept. 2018.

[261] A. Rohatgi, "WebPlotDigitizer," Apr. 2019. ankitrohatgi@hotmail.com.

[262] D. Kamath, S. P. Mezyk, and D. Minakata, "Elucidating the Elementary Reaction Pathways and Kinetics of Hydroxyl Radical-Induced Acetone Degradation in Aqueous Phase Advanced Oxidation Processes," *Environmental Science & Technology*, vol. 52, pp. 7763–7774, July 2018.

[263] G. V. Buxton, C. L. Greenstock, W. P. Helman, and A. B. Ross, "Critical Review of rate constants for reactions of hydrated electrons, hydrogen atoms and hydroxyl radicals (·OH/·O- in Aqueous Solution," *Journal of Physical and Chemical Reference Data*, vol. 17, pp. 513–886, Apr. 1988.

[264] A. Monod, L. Poulain, S. Grubert, D. Voisin, and H. Wortham, "Kinetics of OH-initiated oxidation of oxygenated organic compounds in the aqueous phase: new rate constants, structure–activity relationships and atmospheric implications," *Atmospheric Environment*, vol. 39, pp. 7667–7688, Dec. 2005.

[265] M. Chin and P. H. Wine, "A Temperature-Dependent Competitive Kinetics Study of the Aqueous-Phase Reactions of OH Radicals with Formate, Formic Acid, Acetate, Acetic Acid, and Hydrated Formaldehyde," in *Aquatic and Surface Photochemistry*, Boca Raton, FL: CRC Press, 1994.

[266] B. Ervens, S. Gligorovski, and H. Herrmann, "Temperature-dependent rate constants for hydroxyl radical reactions with organic compounds in aqueous solutions," *Physical Chemistry Chemical Physics*, vol. 5, no. 9, pp. 1811–1824, 2003.

[267] K. Sehested, N. Getoff, F. Schwoerer, V. Markovic, and S. O. Nielsen, "Pulse radiolysis of oxalic acid and oxalates," *Journal of Physical Chemistry*, vol. 75, no. 6, pp. 749–755, 1971.

[268] M. I. Stefan, A. R. Hoy, and J. R. Bolton, "Kinetics and Mechanism of the Degradation and Mineralization of Acetone in Dilute Aqueous Solution Sensitized by the UV Photolysis of Hydrogen Peroxide," *Environmental Science & Technology*, vol. 30, pp. 2382–2390, June 1996.

[269] M. Klann, H. Koeppl, and M. Reuss, "Spatial Modeling of Vesicle Transport and the Cytoskeleton: The Challenge of Hitting the Right Road," *PLOS ONE*, vol. 7, p. e29645, Jan. 2012.

[270] R. E. Rhoades and V. Nazarea, "Forgotten Futures: Scientific Models vs. Local Visions of Land Use Change," in *Local Science vs. Global Science: Approaches to Indigenous Knowledge in International Development*, vol. 4 of *Studies in Environmental Anthropology and Ethnobiology*, pp. 231–259, New York, NY: Berghan Books, 2009.

[271] Y. Kim, J. W. Kim, Z. Kim, and W. Y. Kim, "Efficient prediction of reaction paths through molecular graph and reaction network analysis," *Chemical Science*, vol. 9, no. 4, pp. 825–835, 2018.

[272] S. Alian and A. Maclean, "Assessing Site Availability of Aspen and Northern Hardwoods for Potential Feedstock Development in Michigan: A Case Study," *Land*, vol. 4, no. 2, 2015.

[273] R. Woods, "U.P. Biofuels Cooperative Strategy," tech. rep., Michigan Technological University, Houghton, Michigan, Oct. 2013.

[274] B. J. Butler, J. H. Hewes, B. J. Dickinson, K. Andrejczyk, S. M. Butler, and M. Markowski-Lindsay, "Family Forest Ownerships of the United States, 2013: Findings from the USDA Forest Service's National Woodland Owner Survey," *Journal of Forestry*, vol. 114, pp. 638–647, Nov. 2016.

[275] ESRI, "ArcGIS 10.5.1 for Desktop," 2017.

[276] V. I. Levenshtein, "Binary Codes Capable of Correcting Deletions, Insertions and Reversals," *Soviet Physics Doklady*, vol. 10, p. 707, Feb. 1966.

[277] B. J. Butler, "Family Forest Owners of the United States, 2006," Tech. Rep. NRS-GTR-27, U.S. Department of Agriculture, Forest Service, Northern Research Station, Newtown Square, PA, 2008.

[278] B. J. Butler, J. H. Hewes, B. J. Dickinson, K. Andrejczyk, S. M. Butler, and M. Markowski-Lindsay, "USDA Forest Service National Woodland Owner Survey: national, regional, and state statistics for family forest and woodland ownerships with 10+ acres, 2011-2013," Research Bulletin NRS-99, U.S. Department of Agriculture, Forest Service, Northern Research Station., Newtown Square, PA, 2016.

COLOPHON

This dissertation was typeset using LaTeX 2_ε and BibTeX. The template developed by Dr. Gowtham, with some adaptations by the author, was used to prepare the document to conform to the standards of Michigan Technological University.